MILITARY HANDBOOK

QUANTITATIVE DESCRIPTION OF OBSCURATION FACTORS FOR ELECTRO-OPTICAL AND MILLIMETER WAVE SYSTEMS

METRIC

NO DELIVERABLE DATA REQUIRED
BY THIS DOCUMENT

AREA MISC

DEPARTMENT OF DEFENSE

WASHINGTON, DC 20301

Quantitative Description of Obscuration Factors for Electro-Optical and Millimeter Wave Systems

1. This standardization handbook was developed by the Atmospheric Sciences Laboratory of the US Army Laboratory Command with the assistance of other organizations within the Department of the Army and industry.

2. This document supplements departmental manuals, directives, military standards, etc., and provides fundamental information on the effects of natural and battlefield-induced obscurants on electro-optical and millimeter wave systems. It contains tables that list the effects as major or minor, equations that allow detailed calculation of effects, and illustrative problems with realistic scenarios. It should provide valuable information to engineers and managers responsible for the design of electro-optical and millimeter wave systems.

3. Beneficial comments (recommendations, additions, deletions) and any pertinent data that may be of use in improving this document should be addressed to Commander/Director, US Army Laboratory Command, Atmospheric Sciences Laboratory, ATTN: SLCAS-AR-A, White Sands Missile Range, NM 88002-5501, by using the self-addressed Standardization Document Improvement Proposal (DD Form 1426) appearing at the end of this document or by letter.

FOREWORD

The general purpose of this handbook is to provide Army design engineers, scientists, and analysts with a method to quantify obscuration factors for electro-optical (EO) and millimeter wave (mmw) systems. The specific purposes are (1) to provide data and methodology for Army design engineers to assess the effects of natural obscurants and battlefield-induced contaminants on EO and mmw systems, (2) to provide the analytical community with information to calculate system performance, and (3) to indicate to the test and evaluation community the effects that should be considered when a system is evaluated.

Chapter 1 is a discussion of the handbook contents and the use of the handbook. Chapter 2 is a qualitative description of EO and mmw sensors and of the natural obscurants and battlefield-contaminants that may de-

grade sensor performance. Chapter 3 provides quantitative information on natural obscurants, while Chapter 4 contains quantitative information on battlefield-induced contaminants. Chapter 5 describes sensor performance measures, discusses sensor performance defeat mechanisms, and illustrates sensor performance calculations using the quantitative data developed in Chapters 3 and 4.

This handbook was developed under the auspices of the Army Materiel Command's Engineering Design Handbook Program, under the direction of the US Army Management Engineering Training Activity. The handbook was written by DCS Corporation as subcontractor to Research Triangle Institute under Contract No. DAAA08-80-C-0247.

QUALITY INSPECTED 4

Accession For

NTIS GRA&I	☑
DTIC TAB	☐
Unannounced	☐
Justification	

By_____
Distribution/

Availability Codes

Dist	Avail and/or Special
A-1	

This page intentionally left blank.

CONTENTS

CHAPTER 1
INTRODUCTION

CHAPTER 2
QUALITATIVE DESCRIPTION OF SENSORS
AND OBSCURATION FACTORS

CONTENTS (cont'd)

CHAPTER 3
PROPERTIES AND FREQUENCY OF OCCURRENCE OF NATURAL OBSCURATION FACTORS

CHAPTER 4
PHYSICAL PROPERTIES OF BATTLEFIELD-INDUCED CONTAMINANTS

CONTENTS (cont'd)

CHAPTER 5
OBSCURATION FACTORS AND SYSTEM DESIGN

CONTENTS (cont'd)

LIST OF ILLUSTRATIONS

LIST OF ILLUSTRATIONS (cont'd)

LIST OF TABLES

LIST OF TABLES (cont'd)

LIST OF ABBREVIATIONS AND ACRONYMS

APC = armored personnel carrier

ASL = US Army Atmospheric Sciences Laboratory

ATGM = antitank guided missile

BICT = battlefield-induced contamination test

CL = concentration path length product

CLIMAT = climatology data in ASL EOSAEL code

CRDC = Chemical Research and Development Center

CSL = Chemical Systems Laboratory

EO = electro-optical

EOSAEL = Electro-Optical Systems Atmospheric Effects Library

ETAC = USAF Environmental Technical Applications Center

FAR = false alarm rate

FLIR = forward-looking infrared sensor (thermal imager)

FM = titanium tetrachloride smoke compound

FO = fog oil

FOV = field of view

FRG = Federal Republic of Germany

FS = chlorosulfonic acid smoke compound

FSTC = US Army Foreign Science and Technology Center

GEOSEM = Global Electro-Optics Systems Environmental Matrix

GMT = Greenwich mean time

HC = hexachloroethane

HE = high explosive

HHTV = handheld thermal viewer

JTCG/ME = Joint Technical Coordination Group/ Munitions Effectiveness

I^2 = image intensifier

IR = infrared

LOS = line of sight

LRF = laser range finder

LST = local standard time

MDT = minimum detectable temperature

MRL = multiple rocket launcher

mmw = millimeter wave

MRC = minimum resolvable contrast

MRT = minimum resolvable temperature

MTF = modulation transfer function

NATO = North Atlantic Treaty Organization

NEP = noise equivalent power

NET = noise equivalent temperature

NV&EOL = US Army Night Vision and Electro-Optics Laboratory

OD = optical depth

PWP = plasticized white phosphorus

RH = relative humidity

rms = root mean square

RP = red phosphorus

SNR = signal-to-noise ratio

TNR = threshold-to-noise ratio

VEESS = vehicle engine exhaust smoke system

WP = white phosphorus

TV = television

EXECUTIVE SUMMARY

Electro-optical (EO) and millimeter wave (mmw) sensors are critical components of current military systems. The applications and importance of these sensors will increase in the years ahead as emphasized in the Airland Battle Concept. All of the battlefield functions must increasingly depend on the incorporation of EO and mmw sensors if the goals set forth for the modern army are to be met.

Command and Control. Effective decision making demands rapid and comprehensive information processing and dissemination.

Close Combat. Forces will be dependent on target acquisition as well as mobility on battlefields obscured by dust and smoke.

Fire Support. Both ground and aerial fire support will depend on sophisticated target acquisition as well as target-seeking or directed projectiles.

Air Defense. The protection of land forces in terms of counter air, preemptive air defense, and point defense has relied and will continue to rely heavily on the integration of EO and mmw systems.

Communications. Systems must be capable of operating in electromagnetic pulse (EMP) and electronic warfare (EW) environments, and of providing real-time information. Systems such as fiber optics will continue to increase field capabilities.

The remaining functional areas—combat support, intelligence and electronic warfare, combat service support, and aviation—also incorporate the use of sensors in performing the mission.

With the battlefield so dependent on EO and mmw sensors, the designers of systems in all of these functional areas must face the problem of sensor performance in the presence of obscurants. These obscurants may be natural weather conditions, such as fog, rain, or snow, or battlefield-induced contaminants, such as smokes, dust, and fire products. Sensors operating in different spectral bands may be affected dif-

ferently by the same obscurant. Systems that depend on the operation of sensors in two spectral bands may be effectively "shut down" if the performance of one sensor is severely degraded, even though the other system sensor continues to operate. As electromagnetic energy is propagated through the atmosphere, it essentially encounters obstacles in the form of

1. Molecules of gases of natural constituents of the air

2. Aerosols, such as fog or haze

3. Rain and snow

4. Smokes and dust.

Each of these "obstacles" diminishes the amount of the energy that reaches its destination. Depending on the wavelength of the energy, the effectiveness of the "obstacles" can be insignificant or total.

This handbook records the effects of the various obscurants on EO and mmw sensors. These effects are given in different levels of detail tailored for the interest level of the reader. There are tables that list the effects simply as major or minor, equations that allow exact computation of effects, and text material that explains the defeat mechanisms. Included are sample scenarios and illustrative problems. These scenarios are realistic situations in which a sensor system might be expected to operate. The sequence of computations is arranged in easily followed steps so that the design engineer can not only understand the example but can transfer the analysis to his own particular systems. Finally, the equations are summarized in an appendix for easy reference.

The current requirement for a comprehensive source of data applicable to military systems is met by this handbook, but updated versions will need to be produced as developments use new spectral bands and as research on obscurant effects makes more information available.

CHAPTER 1
INTRODUCTION

This chapter describes the purpose and scope of the handbook, an engineering design tool for calculating the effects of natural obscurants and battlefield-induced contaminants on electro-optical and millimeter wave systems. It includes a chapter-by-chapter summary of the handbook and a brief discussion of the use of the handbook.

1-1 PURPOSE

Electro-optical (EO) and millimeter wave (mmw) sensors are critical components of many new military systems. The performance of these sensors is determined not only by the sensor design but also by the weather and by battlefield-induced contaminants. It is important to optimize the initial system design, to be able to predict the performance of a system that is still in design or development, and to be able to evaluate design changes that are suggested during the development.

The purposes of this handbook are

1. To provide data and methodology for Army design engineers to assess the effects of natural obscurants and battlefield-induced contaminants on EO and mmw systems

2. To provide the analytical community with information to calculate system performance

3. To indicate to the test and evaluation community the effects that should be considered when a system is evaluated.

1-2 SCOPE

This handbook is intended to be a basic design tool for the Army engineer or scientist. The handbook is structured to provide

1. A basic understanding of the optical properties of natural obscurants and battlefield-induced contaminants

2. A description of type and magnitude of the effect that each obscurant may have on generic EO and mmw systems

3. The data and procedures to enable the engineer to calculate the effects of these obscurants on a user-specified system design as illustrated by sample problems.

The handbook is written to provide information that a scientist or engineer can use to identify potential problems in the performance of a sensor under obscured conditions and to estimate the magnitude of the effects and the frequency of the conditions. Detailed discussions on atmospheric physics, obscurants, sensor design, and sensor performance modeling are beyond the scope

of this handbook. Extensive references are provided at the end of each chapter for the user who needs more detailed information.

1-3 DESCRIPTION AND USE OF THE HANDBOOK

In addition to Chapter 1 this handbook contains four chapters treating obscurants and obscurant effects on sensors, as well as a glossary that is a summary of terminology used to describe obscurant effects on EO and mmw systems. The two appendices contain summaries of the key atmospheric transmittance calculations. This paragraph is an overview of the contents of these chapters and includes a brief summary of the contents of each chapter and a description of the intended use of that chapter.

Chapter 2, "Qualitative Description of Sensors and Obscuration Factors", is a qualitative description of EO and mmw sensors, and the natural obscurants and battlefield-induced contaminants which may degrade sensor performance. It provides the basic material the user needs to comprehend an analysis of atmospheric effects on sensors. The chapter includes a description of generic EO and mmw systems and discusses briefly the differences in active and passive sensor operation for imaging and nonimaging sensors. Atmospheric properties that reduce sensor performance, such as absorption, scattering, clutter, and turbulence, are defined. Brief descriptions of natural obscurants and battlefield-induced contaminants are given. Meteorological measurements used to characterize obscurants and obscurant transport are also discussed.

Chapters 3 and 4 provide quantitative information about the natural and battlefield obscurants described in Chapter 2. Chapter 3, "Properties and Frequency of Occurrence of Natural Obscuration Factors", provides quantitative data to enable the engineer to characterize the natural atmosphere for system performance calculations. It contains information about naturally occurring obscurants, such as atmospheric gases and water vapor, haze, fog, precipitation, and blowing dust. This chapter includes (1) quantitative data permitting the

calculation of atmospheric transmittance through the naturally obscured atmosphere; (2) qualitative descriptions of the climatology of four geographical areas (temperate, tropical, desert, and arctic), and (3) quantitative descriptions of the frequency of occurrence of natural obscurants in those areas.

Chapter 4, "Physical Properties of Battlefield Obscuration Factors", includes a quantitative description of the battlefield-induced contaminants discussed in Chapter 2, including smoke, munition explosions, vehicular-induced contaminants, and battlefield fires. This chapter (1) describes the battlefield-induced contaminants, (2) provides mass extinction coefficients, and (3) gives an assessment of the concentration of those contaminants that might be found in a battlefield environment. Three examples are developed—for artillery fire, obscuring smoke, and tank-generated vehicular dust—to indicate anticipated levels of battlefield-induced contaminants.

Chapter 5, "Obscuration Factors and System Design", discusses sensor performance measures and gives illustrative examples of sensor performance calculations. This chapter (1) introduces system performance measures for the classes of systems described in Chapter 2 and shows how they are used to determine performance, (2) discusses sensor defeat mechanisms in the obscured natural and battlefield environments, and (3) "walks" the user through sample problems illustrating the effects of obscurants on those systems by using the quantitative data developed in Chapters 3 and 4.

Appendix A is a summary guide for calculating atmospheric transmittance; it includes references to the required data and equations in the handbook. Appendix B gives equations for converting between different measures of atmospheric water vapor content. The glossary contains definitions of technical terms used in this handbook.

The handbook is designed so that it can be used to obtain either qualitative or quantitative information. The engineer who needs an overview of factors affecting sensor performance can obtain a general understanding of obscurant effects from Chapter 2 and can refer to the defeat mechanism tables in Chapter 5 to see whether an effect is potentially major or minor. Qualitative descriptions of natural and battlefield-induced contaminants are given in pars. 2-4 and 2-5, respectively. Quantitative estimates of natural obscuration can be developed from the data in Chapter 3. Quantitative estimates of battlefield-induced contaminants can be developed using the data in Chapter 4. Individuals who have a general understanding of the subject may go directly to those chapters for quantitative information. The scientist or engineer who needs to perform systems effects calculations may refer to the descriptions of performance measures in par. 5-2 and to the sample problems in par. 5-4. The sample problems are step-by-step illustrations of how to use the data developed from Chapter 3 and Chapter 4 to calculate the performance of a sensor in an obscured atmosphere.

CHAPTER 2
QUALITATIVE DESCRIPTION OF SENSORS
AND OBSCURATION FACTORS

This chapter contains a qualitative description of electro-optical (EO) and millimeter wave (mmw) sensors, and the natural obscurants and battlefield-induced contaminants which may degrade sensor performance. It provides the background needed to perform an analysis of atmospheric effects on sensors. Par. 2-2 describes generic EO and mmw systems with a brief discussion of the differences between active and passive sensor operation for both imaging and nonimaging sensors. Par. 2-3 defines atmospheric properties that reduce sensor performance—i.e., absorption and scattering, clutter introduction, and turbulence. Pars. 2-4 and 2-5 include brief descriptions of natural obscurants and battlefield-induced contaminants, definitions of the terminology used to describe them, and a discussion of the meteorological measurements used to characterize obscurants and obscurant transport. Quantitative descriptions of these natural obscurants and battlefield-induced contaminants are contained in Chapters 3 and 4.

2-0 LIST OF SYMBOLS

$C(r)$ = concentration at point r, g/m^3

CL = concentration path length product, g/m^2

C_o = inherent contrast, dimensionless

C_o' = apparent contrast, dimensionless

C_n^2 = index structure parameter, $m^{-2/3}$

C_T^2 = temperature structure parameter, $K^2/m^{2/3}$

$dL(\lambda,r)$ = change in spectral radiance, $W/(m^2sr)$

dr = distance, m

E = spectral irradiance, $kW/(m^2\mu m)$

E_f = efficiency with which aerosol is disseminated, dimensionless

h = altitude, m

i = imaginary operator, dimensionless

L = path length through obscurant, m

L_b = background luminance, cd/m^2

L_b' = apparent luminance of background, cd/m^2

L_c = obscurant luminance, cd/m^2

L_h = luminance of horizon sky, cd/m^2

L_o = object luminance, cd/m^2

L_o' = apparent luminance of object, cd/m^2

L_p = atmospheric path radiance, dimensionless

$L(\lambda,r)$ = spectral radiance at point r, $W/(m^2sr)$

l = distance between points r_1 and r_2, m

M = mass of particle, g

M_a = mass of aerosol in munition, g

M_a' = mass of obscurant aerosol disseminated by a munition, g

$m(\lambda)$ = complex index of refraction, dimensionless

$n(\lambda)$ = real part of index of refraction, dimensionless

$n_i(\lambda)$ = imaginary part of index of refraction, dimensionless

P = air pressure, mbar

$P_o(\lambda)$ = emitted power, W

Q = extinction efficiency, dimensionless

$Q(\lambda,r)$ = scattering efficiency, dimensionless

R = path length, km

$R_s(\lambda)$ = sensor spectral responsivity, V/W or A/W

r = particle radius, m

T = temperature, K

T_e = effective atmospheric transmittance, dimensionless

$T(r_1)$ = temperature at point r_1, K

$T(r_2)$ = temperature at point r_2, K

$T(\lambda)$ = atmospheric transmittance, dimensionless

$T_c(\lambda)$ = contrast transmittance, dimensionless

$T_s(\lambda)$ = transmittance through obscurant, dimensionless

Y_f = yield factor, dimensionless

$c(\lambda)$ = mass extinction coefficient, m^2/g

$\alpha(\lambda,r)$ = mass extinction coefficient at point r, m^2/g

$\gamma(\lambda)$ = volume extinction coefficient, m^{-1} or km^{-1}

θ = scattering angle, rad

λ = wavelength, μm

$\rho(r)$ = density of the medium, g/m^3

σ = geometric cross section of particle, m^2

σ_s = scattering cross section, m^2

$\sigma_s(\theta)$ = angular scattering cross section, m^2/sr

2-1 INTRODUCTION

Atmospheric obscurants reduce the performance of EO and mmw sensors by (1) reducing the signal radiation reaching the sensor because of reduced atmospheric transmittance in the sensor wavelength response region, (2) increasing noise at the sensor due to scattering of atmospheric radiation or system illuminator energy into the sensor, (3) introducing clutter, i.e., signals which may resemble the target, and (4) reducing the signal-to-noise ratio through turbulence-induced wave-front degradation. In addition, naturally occurring obscurants such as rain and snow modify the target signature, i.e., they change the appearance of the target to the sensor. The nature and magnitude of the effects also depend on sensor characteristics such as (1) the sensor spectral response, sensitivity, and resolution, (2) whether the sensor is an imaging or nonimaging sensor, and (3) whether the sensor is active—illuminates the target and senses the reflected radiation—or passive—relies on naturally occurring radiation reflected from or emitted by the target.

Par. 2-2 introduces generic EO and mmw systems and discusses how these systems are affected by the atmosphere. The remainder of this chapter is a qualitative description of natural obscurants and battlefield-induced contaminants and is designed as a background discussion for engineers who are not familiar with these areas. Chapters 3 and 4 contain quantitative data on natural and battlefield obscurants, which are used in the illustrative system performance calculations in Chapter 5.

2-2 ELECTRO-OPTICAL AND MILLIMETER WAVE SENSORS

Because system design, target signatures, atmospheric effects, and the impact of obscurants on system performance are determined by the spectral region in which the sensor operates, the discussion is broken down by spectral region into (1) visible (0.4-0.7 μm) and near infrared (IR) (0.7-2.0 μm), (2) thermal systems, mid IR (3-5 μm) and far IR (8-12 μm), and (3) mmw (primarily 35 and 94 GHz). The rationale for discussion of these spectral bands to the exclusion of others (6-7 μm for instance) is that these are the spectral regions in which most systems operate because of the transmittance properties of the natural atmosphere, target signatures, and materials technology.

The generic systems addressed in this handbook are listed in Table 2-1 by mode of operation (passive or active, imaging or nonimaging), spectral response, and application.

The spectral regions in which sensors can perform are limited by the atmosphere; for a sensor to perform, the radiation it senses must be able to pass through the environment from the target to the sensor. The low resolution plot of ground level atmospheric transmittance in Fig. 2-1 indicates the major atmospheric "windows"—i.e., regions with generally good atmospheric transmittance. The regions of poor transmittance in Fig. 2-1 indicate atmospheric absorption, primarily by water vapor and CO_2. The three curves indicate a tropical atmosphere with high water vapor content, a subarctic atmosphere, which has a low water

TABLE 2-1
GENERIC SYSTEMS INCLUDED IN THE HANDBOOK

WAVELENGTH	PASSIVE IMAGING	ACTIVE NONIMAGING	PASSIVE NONIMAGING
Visible and Near IR	Eye and Day Sights* Television (TV) Image Intensifiers (I²)	Rangefinder (Ruby, Nd) Designator (Nd) for Semiactive Homing Beamrider (GaAs)	
Mid IR	Thermal Imager Terminal Guidance		Heat-Seeking Missiles
Far IR	Thermal Imager Terminal Guidance	Rangefinder (CO_2) Beamrider (CO_2) Designator (CO_2) Remote Sensing (CO_2)	Remote Detection
Millimeter Wave 35 GHz		Terminal Guidance	Terminal Guidance
94 GHz		Target Location	

*Direct View Optics
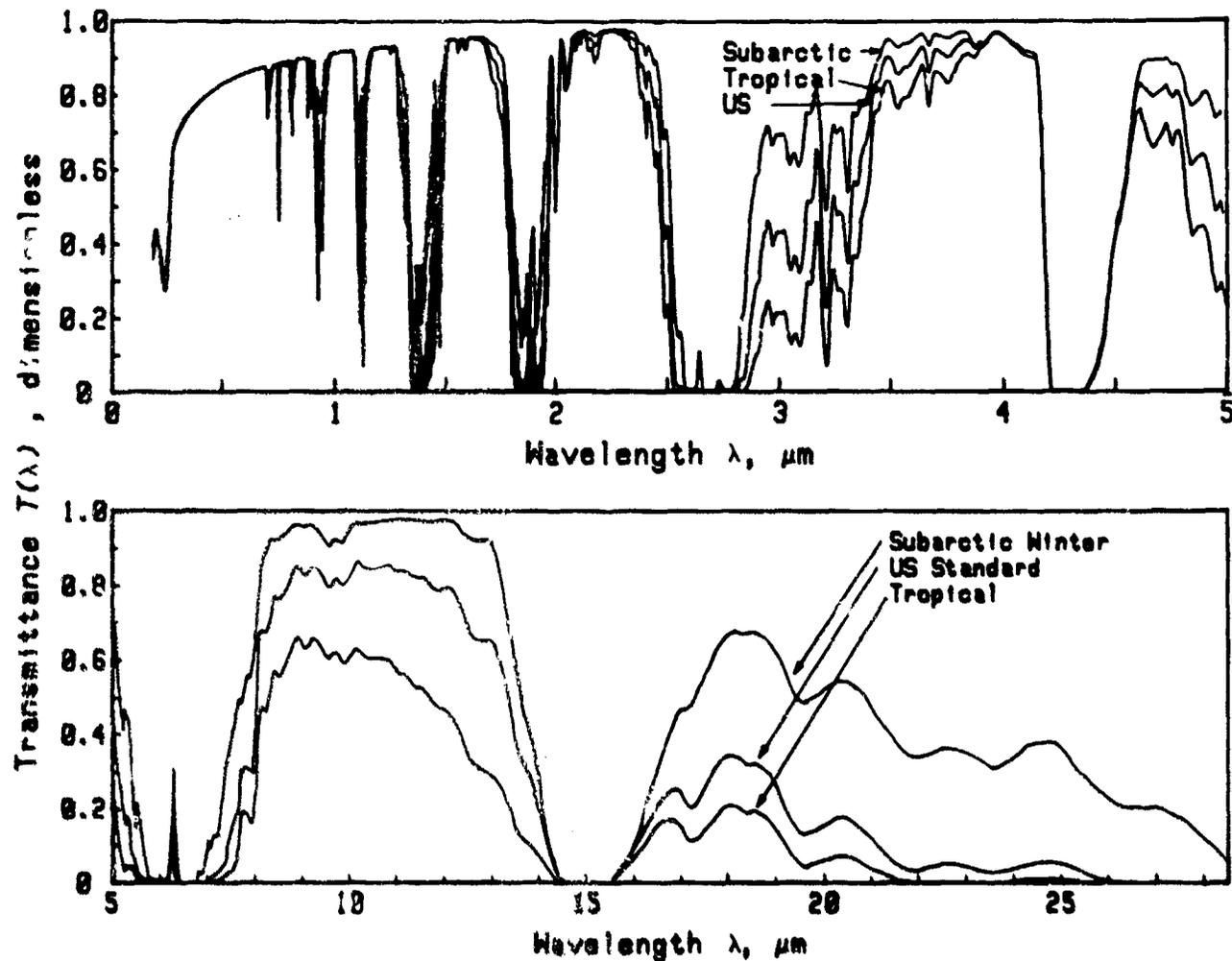
Figure 2-1. Atmospheric Transmittance $T(\lambda)$ vs Wavelength λ (Ref. 1)

vapor content, and a typical US or midlatitude atmosphere, which has a moderate water content. These curves illustrate the effect of water vapor content on thermal transmittance. Millimeter wave transmittance is best in the atmospheric windows at 35 GHz and 94 GHz, with severe water vapor and oxygen absorption limiting the usefulness of other mmw frequencies.* The actual transmittance within the atmospheric windows will be determined by local meteorological conditions.

For EO sensors, obscuration can be caused by the natural atmosphere (including fog, rain, and snow) and battlefield smokes and dust. The major obscurants at 35 GHz and 94 GHz are artillery-produced debris, atmospheric moisture, and precipitation; turbulence sometimes reduces the mmw system signal-to-noise ratio.

The effectiveness of an obscurant against a sensor is dependent not only on the obscurant (and obscurant

concentration) but also on the sensor design. Selection of a sensor spectral operating band within an atmospheric window depends on the target characteristics, the background against which the target must be detected, operational scenarios, sensor design, and materials technology.

Passive systems rely for their operation on differences between the target and background scene. Visible and near IR sensors detect differences in reflected natural illumination—sunlight or moonlight. Passive thermal systems detect the difference in emitted radiation in the scene corresponding to temperature and emissivity differences in the 3-5 or 8-12 μm spectral band. Passive sensors are affected by reduction in atmospheric transmittance, which reduces the signal at the sensor; by scattering of ambient radiation into the sensor field of view (reducing the apparent contrast of the target); and by clutter, or target-like objects in the imagery.

Active target acquisition systems, which use a laser or lamp source to illuminate the target, do not rely on natural illumination or emission. Rather, these spectrally narrow sensors rely on the target reflectance at the

---

*Limited-range covert systems may be designed to operate in regions of poor atmospheric transmittance to limit the possibility of detection.

illuminator wavelength to provide the sensor signal. Active systems generally use coherent sources, such as lasers, rather than broadband (incoherent) sources. Coherent sources are spectrally very narrow and have a narrow spatial beam divergence which concentrates the illuminator energy in a narrow angle (usually 0.1 to 0.5 mrad). The narrow spectral line width permits spectral filtering of the detected signal to reduce background noise. Active systems may be affected by (1) the reduction in atmospheric contrast transmittance, (2) changes in target reflectance at the illumination wavelength, and (3) atmospheric scattering of the illuminator energy back into the system receiver, which may cause false alarms. Multiple scattering of laser radiation by fogs effectively increases background at the illuminator wavelength. Systems that depend on laser sources are also particularly susceptible to (1) atmospheric turbulence effects, which can cause spreading of the illumination, (2) beam wander, which reduces illumination on the target and at the receiver, and (3) beam breakup, which is seen as a "spottiness" in the illuminating beam.

2-2.1 VISII .   ND NEAR IR SENSORS (0.4-2. ᐧ)

The visible spectral region, 0.4-0.7 μm, includes those wavelengths of radiation to which the human eye is sensitive. EO systems operating in this region include direct view optics, TV systems, and ruby laser rangefinders. First and second generation image intensifiers (I^2) operate in the 0.4-0.9 μm spectral region, which includes both the visible spectrum and part of the near IR region; second generation image intensifiers operate in the 0.6-0.9 μm band. TV systems, depending on the photocathode or photoconductor used, may respond to both visible and to near IR radiation. Neodymium laser rangefinders and designators operate at 1.06 μm.

Visible and near IR passive imaging sensors use ambient radiation reflected from the target and target background to form the scene imagery. Daylight systems, including the eye, direct view optics, and day TV, depend on reflected solar radiation. Image intensifiers (I^2) depend on the reflected night sky radiance. The image quality of these systems depends on the level of ambient illumination, the relative reflectance of the target and background scene elements modified by atmospheric contrast reduction, and on the sensor responsivity. Atmospheric contrast reduction has two principal causes: (1) radiation reflected from the scene is attenuated by absorption or scattering and (2) stray radiation is scattered into the sensor. In nonimaging systems, atmospheric absorption and scattering reduce the signal received from the target and increase noise.

The primary natural atmospheric effect in this spectral region is aerosol extinction, the scattering of radia-tion by small haze particles in the atmosphere. The atmospheric transmittance in both the visible and near IR regions scales rather closely with visibility, except in extremely clear weather when absorption and scattering of radiation by gaseous atmospheric molecules are the only remaining factors. Changes in absolute humidity have relatively small effects, except in their contribution to aerosol particle size growth. Rain, snow, and fog reduce the effectiveness of passive imagers by reducing atmospheric contrast transmittance and by reducing the natural illumination level. They scatter active illumination. Snow cover also changes the target contrast. Cloud cover, by itself, reduces the performance of passive visible and near IR systems by reducing the ambient illumination.

2-2.2 THERMAL SYSTEMS (3-5 and 8-12 μm)

Systems operating in the IR spectral regions include passive mid IR (3-5 μm) and far IR (8-12 μm) thermal imagers and terminal guidance systems, some modern missile seekers (4-4.5 μm), and active CO_2 (10.6 μm) rangefinder, designator, beamrider, and remote sensing systems. Active coherent imaging systems using CO_2 laser illuminators are in development. Older missile seekers may operate in the 1.7-3.5 μm spectral region because of detector technology limitations at the time they were designed.

Thermal imaging systems* detect and image the naturally occurring differences in radiation emitted from or reflected by the target and the background scene. The imagery is generally not affected by ambient illumination, except in the presence of IR-reflecting backgrounds, such as water at shallow grazing angles. A thermal signature of a target is usually expressed as the temperature difference in kelvins between the average target temperature and the background temperature referenced to a 300-K background. For ambient temperature targets, the radiation peaks at about 10 μm. For hotter targets the spectral peak shifts to shorter wavelengths. For aircraft engine exhausts, the peak is in the 4-4.5 μm region. For active systems such as CO_2 laser radars and rangefinders, the target signature depends on the target reflectance at the illuminator wavelength rather than the target temperature.

The atmosphere impacts the performance of EO sensors operating in the thermal band by reducing the apparent target signature by transmittance losses and by weather-driven changes in the target signature. Path radiance is not significant except in low visibility conditions or over long distances. Visibility is not in general a good indicator of thermal system performance

---

*Forward-looking infrared (FLIR) systems are thermal imaging systems developed for use in aircraft; the acronym FLIR is often used to indicate any thermal imaging system.

because thermal systems are relatively insensitive to haze. They are, however, affected much more than visible systems by variations in atmospheric water content. The primary mechanisms for atmospheric extinction within the thermal bands are water vapor absorption, CO_2 molecular absorption, and aerosol extinction, including water (fog and clouds). Increases in absolute humidity significantly reduce the transmittance in the thermal bands. Higher humidity conditions may also reduce transmittance by causing aerosol particle size growth, particularly in the salt spray particles of maritime atmospheres.

Aerosol extinction due to rain, snow, and fog significantly degrades thermal sensor performance by attenuating signal radiation and scattering background radiance into the system detector, which increases the noise level. The extent of extinction due to fog depends strongly on the aerosol particle size distribution and cannot be predicted solely from visibility. Aerosols of maritime origin degrade system performance more than aerosols of continental origin; in low visibility conditions (less than 2 km), sensor performance varies strongly with aerosol type. For active systems, backscatter from natural aerosols must be considered because it will increase noise at the illumination wavelength; in moderate to heavy rain, snow, and fogs, multiple scattering effects must also be considered. For nonimaging active sensors, the impact of added in-band noise is a decrease in target acquisition probability and an increase in false alarm rate.

Poor weather also degrades passive thermal imager performance by reducing the target signature. In overcast conditions target and background signatures of passive targets tend to "wash out" to a uniform temperature. Active targets such as exercised tanks may, however, stand out more strongly against this background. Rain and snow cool the targets and backgrounds, which leads to a more uniform temperature distribution across the scene. Rain, snow, and wet fogs also alter active system target signatures by changing the target and background reflectance characteristics.

2-2.3 MILLIMETER WAVE SENSORS (35 and 94 GHz)

Millimeter wave applications currently under development include 35 GHz and 94 GHz terminal guidance sensors, which are active nonimaging systems, and 35 GHz passive nonimaging terminal acquisition sensors.

Atmospheric extinction at mmw and near mmw frequencies is dominated by water vapor, liquid water, and oxygen absorption. The best "windows" in this region are near 35 GHz and 94 GHz. Millimeter wave system performance is generally unaffected by atmospheric haze. Fog, rain, and snow all impair the perfor-

mance of mmw sensors. Fog reduces transmittance because of the increased liquid water content in the atmosphere. Rain and snow scatter and absorb mmw radiation; backscatter from drizzle can cause serious signal-to-noise degradation.

2-3 FACTORS THAT AFFECT EO AND MILLIMETER WAVE SENSOR PERFORMANCE

The atmosphere reduces the amount of signal radiation reaching a sensor from the target. It may also introduce noise in the sensor band and reduce signal quality. The atmospheric parameters used to characterize this signal degradation—atmospheric extinction, transmittance, contrast transmittance, and turbulence—are defined in the paragraphs that follow. Clutter is defined in par. 2-3.5.

2-3.1 EXTINCTION—ABSORPTION AND SCATTERING

Extinction is defined as the reduction, or attenuation, of radiation passing through the atmosphere. Extinction comprises two processes: absorption of energy and scattering of energy. In absorption, a photon of radiation is absorbed by an atmospheric molecule or an aerosol particle. In scattering, the direction of the incident radiation is changed by collisions with atmospheric molecules or aerosol particles. Atmospheric extinction depends on the type, size, and concentration of the atmospheric constituents and the wavelength of the electromagnetic radiation.

Absorption of radiation by atmospheric gases and water vapor causes significant extinction in the IR bands. Absorption is strongly wavelength dependent; the absorption wavelengths must correspond to the energy differences between the different rotational and vibrational states of atmospheric molecules. Absorption by natural atmospheric gases, including water vapor, is described in par. 2-4.1. Absorption usually dominates scattering at IR and mmw wavelengths.

Scattering is the major factor in visible extinction but may also be important at IR wavelengths. Scattering by rain and snow is the major atmospheric mmw attenuation mechanism. The scattering characteristics of a particle are quantified using a scattering cross section. The scattering cross section σ, is defined as that cross section of an incident wave, acted on by the particle, having an area such that all the power flowing across it is equal to the total power scattered in all directions. The effectiveness of an obscurant as a scattering medium depends on the ratio of the obscurant particle size to the radiation wavelength. Scattering effectiveness is given by the scattering efficiency $Q(\lambda, r)$ which is the ratio of the effective scattering cross section of a particle of radius r to its geometric cross section as

$$Q(\lambda,r) = \frac{\sigma_s}{\pi r^2} = \frac{2}{r^2}\int_0^\pi \sigma_s(\theta)\sin\theta d\theta,$$
$$\text{dimensionless (2-1)}$$

where

r = particle radius, m
$\sigma_s(\theta)$ = angular scattering cross section, m^2 sr
θ = scattering angle, rad.

If the particle size is much smaller than the radiation wavelength, Rayleigh scattering results, and scattering efficiency simplifies to the expression

$$Q(\lambda,r) = \frac{8}{3}(2\pi)^4 \frac{r^4[n(\lambda)^2 - 1]^2}{\lambda^4[n(\lambda)^2 + 2]^2},$$
$$\text{dimensionless (2-2)}$$

where

$n(\lambda)$ = real part of index of refraction, dimensionless.

If the particle size is much larger than the radiation wavelength, the scattering efficiency may be calculated using geometric optics. The complex Mie scattering theory must be used for calculations in the scattering resonance region where the particle size and radiation wavelength are of the same order. Fig. 2-2 shows $Q(\lambda,r)$ as a function of the particle size to wavelength ratio for water droplets. There is a λ^{-4} dependence of $Q(\lambda,r)$ in the Rayleigh scattering regime (particle size small compared to wavelength) shown at the left in Fig. 2-2, an increase of $Q(\lambda,r)$ to about 4 when the wavelength and particle size are about the same, and an oscillating value of $Q(\lambda,r)$ converging to about 2 for the geometri-

Figure 2-2. Scattering Efficiency as a Function of Particle Size to Wavelength Ratio for Small Water Droplets (Ref. 2)

cal optics region (shown at the right) in which the particle size is much larger than the radiation wavelength.

The direction in which the radiation is scattered depends on the type of scattering. For Rayleigh scattering, the energy is scattered about equally forward and backward. As the particle size approaches $\lambda/4$, the scattering shifts predominantly to the forward direction. Mie scattering is almost entirely in the forward direction. This is illustrated in Fig. 2-3. Table 2-2 summarizes scattering effects.

Particle sizes for several common obscurants are given in Table 2-3. From the relationships in Table 2-2, it is clear that the atmospheric molecules (10^{-4} μm) will be minor scatterers for visible (0.4-0.7 μm) and thermal systems (3-5 and 8-12 μm). Scattering due to haze and fog oil will primarily affect visible systems; fogs and clouds will scatter both visible and IR radiation. Dust will also scatter visible and thermal radiation. Only rain and snow will be significant scatterers for mmw systems; 94 GHz frequency corresponds to a 3-mm
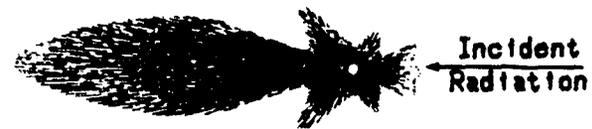
(A) Mie Scattering
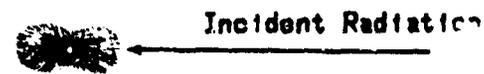
(B) Rayleigh Scattering

Reprinted with permission. Copyright © by John Wiley & Sons, Inc.

Figure 2-3. Scattering Direction for Mie and Rayleigh Scattering (Ref. 3)

wavelength, which is the approximate size of raindrops and snowflakes.

The theoretical Mie curves only apply to monodispersed aerosols. Most practical light-scattering prob-

TABLE 2-2
EFFECT OF PARTICLE SIZE TO WAVELENGTH RATIO ON SCATTERING DIRECTION

PARTICLE RADIUS	SCATTERING THEORY USED	EFFECT
Less than λ 10	Rayleigh scattering	Symmetric scattering; varies as (particle volume)$^2\lambda^{-4}$
Greater than λ 10	Mie scattering	Maximum scattering
About λ 4	Mie scattering	Scattering mostly in forward direction; some spread
Greater than λ	Mie scattering	Almost entirely forward scattering
Greater than 10λ	Geometric optics	Refraction, reflection, or diffraction

TABLE 2-3
PARTICLE SIZE AND SCATTERING EFFECT OF ATMOSPHERIC OBSCURANTS (Ref. 4)

OBSCURANT	APPROXIMATE PARTICLE DIAMETER, μm	SCATTERING* EFFECT		
		VISIBLE	IR	MILLIMETER WAVE
Atmospheric Molecule	10^{-4}	RS	RS	RS
Haze	$10^{-2} - 10^{-1}$	RS-MS	RS	RS
Fog	0.5 - 100	MS-GO	MS	RS
Cloud	2 - 800	MS-GO	MS	RS
Rain	$10^2 - 10^4$	GO	GO	MS
Snow	$5\times10^3 - 5\times10^5$	GO	GO	MS-GO
Fog Oil (mean size)	1	MS-GO	MS	RS
Airborne Dust	1 - 10^7	MS-GO	MS	RS

*RS = Rayleigh scattering

MS = Mie scattering

GO = geometric optics

lens will be related to polydispersed aerosol systems. Since the ligi. -scattering properties depend very strongly on particle size, a mean or effective particle size is of little value in determining the expected scattering result. A statistical description of the aerosol particle size distribution must be found, and an effective efficiency factor determined. It is found that this approach dampens the Mie resonances and results in lower scattering efficiencies, with a smoother shape to the scattering curve.

2-3.2 ATMOSPHERIC TRANSMITTANCE

The atmospheric transmittance $T(\lambda)$, over a specified path length, is defined as the ratio of the received power to the emitted power. It depends on the wavelength of the radiation, the length of the atmospheric path, and the type, size, and concentration of the atmospheric constituents.

For monochromatic (single wavelength) radiation, the change in spectral radiance $dL(\lambda,r)$ across a distance of dr may be expressed in terms of a mass extinction coefficient $\alpha(\lambda,r)$ by

$$dL(\lambda,r) = -\alpha(\lambda,r) \, L(\lambda,r)\rho(r)dr, \text{ W } (\text{m}^2\text{sr}) \quad (2\text{-}3)$$

where

$L(\lambda,r)$ = spectral radiance at point r, W (m²sr)

$\rho(r)$ = density of the medium, g m³

$\alpha(\lambda,r)$ = mass extinction coefficient at point r, m² g.

The mass extinction coefficient is used to calculate extinction by obscurants such as battlefield smoke and airborne dust. These obscurants may have a broad distribution of particle sizes and a nonuniform concentration over the sensor-to-target path.

If the atmosphere is assumed to be uniform, which is the usual assumption over a localized ground level path, then the extinction for a given atmosphere is simply a function of the wavelength of the radiation and its atmospheric path length. It can be expressed in terms of a volume extinction coefficient $\gamma(\lambda)$ as

$$\frac{dL(\lambda,r)}{L(\lambda,r)} = -\gamma(\lambda)dR, \text{ dimensionless} \quad (2\text{-}4)$$

where

R = path length, km.

For monochromatic radiation propagating through the atmosphere, transmittance $T(\lambda)$ for radiation of wavelength λ is given by Beer's Law as

$$T(\lambda) = e^{-\gamma(\lambda)R}, \text{ dimensionless.} \quad (2\text{-}5)$$

Often an "effective atmospheric transmittance" T_e over a sensor spectral band is defined as the ratio of the received power at the sensor to the target signal emitted power $P_o(\lambda)$ in the same spectral region, weighted by the sensor spectral responsivity $R_s(\lambda)$

$$T_e = \frac{\int_{\lambda_1}^{\lambda_2} P_o(\lambda)R_s(\lambda)T(\lambda)d\lambda}{\int_{\lambda_1}^{\lambda_2} P_o(\lambda)R_s(\lambda)d\lambda} \text{ , dimensionless.} \quad (2\text{-}6)$$

This broadband transmittance does not necessarily scale exponentially with range because of the structure in the atmospheric absorption spectrum. To understand this, consider a spectral region for which transmittance at 1 km is 0.1 in half the band and 0.9 in the other half, for a band averaged transmittance of 0.5. At 2 km these transmittances reduce to 0.01 and 0.81, respectively, for a band averaged transmittance of 0.41, instead of 0.25—(0.5)².

The designer should note that systems operating in the same spectral region and the same atmosphere may be affected differently by atmospheric transmittance if the target-sensor geometry differs. Fig. 2-4 shows two direct view geometries: one requiring one-way transmittance through the atmosphere (beamrider) and one requiring a two-way path through the atmosphere (rangefinder). In Fig. 2-4(A) the radiation must be transmitted a distance R to the target from the laser, and transmittance is given by Eq. 2-5.

In the rangefinder application shown in Fig. 2-4(B) the radiation must be propagated to the target, reflected off the target, and be propagated back to the sensor. Thus the path length R is twice the range to the target. The effect of a highly attenuating atmosphere is clearly much more severe in the second case.

A third case occurs if the system must perform over two different atmospheric paths, as in the case of the laser designator shown in Fig. 2-5. Here, the illuminator energy reaches the target over Path 1 and is reflected to the receiver over Path 2. A localized obscurant such as a smoke round in either path prevents proper system operation. If the utility of a system depends on sensors operating at two different wavelengths, the engineering analysis must consider both spectral regions. A forward observer acquires a target visually and designates it, using a Nd:YAG laser designator, for a weapon fired from another position, as in Fig. 2-5. In this case, the operability of the system depends on visual acquisition (passive 0.4-0.7 μm transmittance over Path 1), successful designation (1.06 μm laser transmittance over Path 1 and Path 2), and successful laser tracking (1.06 μm transmittance over Path 2). Interruption of the visual line of sight (LOS) or 1.06 μm LOS on either path for several seconds could result in the missile breaking lock on the target. The visual LOS is necessary for designa-

(A)   Beamrider

(B)   Laser Rangefinder
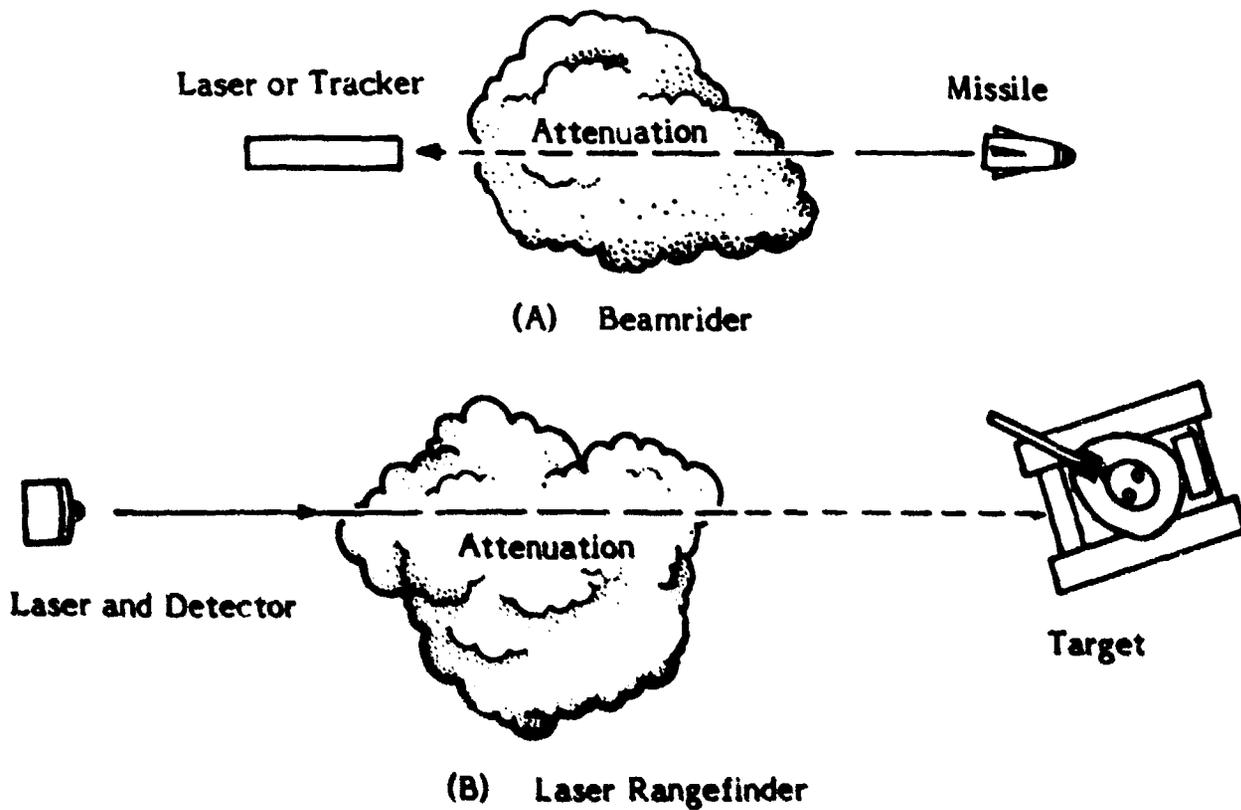
Figure 2-4.   Direct View Geometrics (Ref. 5)

tion; the 1.06-μm LOS is necessary in order that the missile have a signal to track.

2-3.3   CONTRAST TRANSMITTANCE

Atmospheric transmittance losses reduce the target signal at the sensor. Atmospheric scattering of ambient radiation into the sensor may further degrade the sensor signal-to-noise ratio. This atmospheric contrast reduction is particularly important for visible and near IR imaging systems because they are sensitive to natural illumination (sunlight and moonlight) and because

naturally occurring haze is a good scatterer of this energy. The inherent contrast C_o between two objects is defined[*] as

$$C_o = \frac{I_o - I_b}{I_b}, \text{ dimensionless} \quad (2\text{-}7)$$

---

[*] These expressions apply to visible and near IR radiation. Candelas are photopic units normalized to the human eye response curve. For radiometric detection the energy from the object is expressed as radiance in units of W/(m·sr)
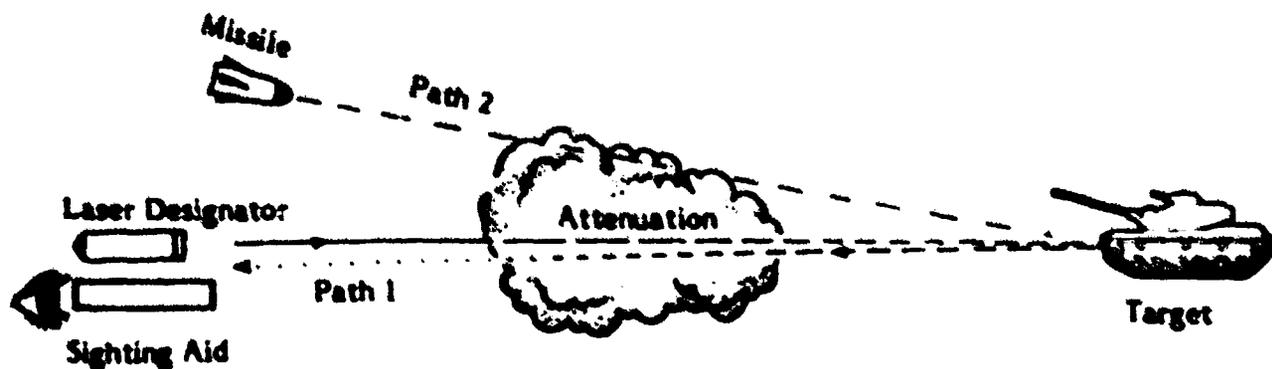
Figure 2.5   Target Acquisition Geometry, Designator not Collocated With Sensor (Ref. 5)

where

L_o = object luminance, cd m²
L_b = background luminance, cd m².

An object at some distance R from the sensor will have an apparent contrast that depends on the object and background luminance as modified by the atmosphere. This atmospheric effect will include both absorption and scattering of the target luminance out of the sensor LOS, scattering of ambient illumination into the LOS, and emissions by atmospheric gas molecules along the path (atmospheric path radiance L_p). Thermal contrast may also be reduced by atmospheric path radiance.

The apparent contrast C_o' of an object at distance R against its background is

$$C_o' = \frac{L_o' - L_b'}{L_b'}, \text{ dimensionless} \quad (2\text{-}8)$$

where

$L_o' = L_o T + L_p$ = apparent luminance of object, cd m²
$L_b' = L_b T + L_p$ = apparent luminance of background, cd m².

Contrast transmittance $T_c(\lambda)$ is the ratio of apparent contrast to inherent contrast and is given by (Ref. 6)

$$T_c(\lambda) = \frac{C_o'}{C_o} = \frac{L_b}{L_b'} T(\lambda), \text{ dimensionless.} \quad (2\text{-}9)$$

If there is no significant scattering of radiation into the sensor by the atmosphere along the path (i.e., if L_b is equal to L_b'), then

$$C_o' = C_o T(\lambda), \text{ dimensionless} \quad (2\text{-}10)$$

If the target contrast depends strongly on the background luminance as in the case of a target against an earth background, then (Ref. 6)

$$C_o' = C_o \left\{ 1 - \frac{L_s}{L_b}[1 - T(\lambda)^{-1}] \right\}^{-1}, \text{ dimensionless} \quad (2\text{-}11)$$

where

L_s = luminance of horizon sky, cd m².

The quantity L_s L_b is called the sky-to-ground ratio. In general, the sky-to-ground ratio decreases with increasing visibility; in Central Europe, it usually falls between 2.0 and 5.0 (Ref. 7). Typical values for the

sky-to-ground ratio for a visual system operating in daylight conditions are given in Table 2-4.

TABLE 2-4
SKY-TO-GROUND RATIO VALUES (Ref. 6)

SKY CONDITION	GROUND CONDITION	SKY-TO-GROUND RATIO
Clear	Fresh Snow	0.2
Clear	Desert	1.4
Clear	Forest	5
Overcast	Fresh Snow	1
Overcast	Desert	7
Overcast	Forest	25

Unlike atmospheric transmittance, contrast transmittance along a path depends on the position of the sun or other light sources relative to the target and observer. In the Mie-scattering regime (forward scattering), contrast transmittance is better with the light source behind the sensor. Additional ambient illumination is scattered into the field of view of a sensor facing in the direction of the sun or up at the night sky. This scattered light reduces the apparent target contrast.

If a localized scatterer such as an obscurant cloud is present between the target and sensor, the contrast equation must include the cloud luminance:

$$C_o' = \frac{T_s(\lambda)(L_o - L_b)}{T_s(\lambda) L_b + L_w}, \text{ dimensionless} \quad (2\text{-}12)$$

where

$T_s(\lambda)$ = transmittance through obscurant, dimensionless
L_w = obscurant luminance, cd m².

2-3.4 OPTICAL TURBULENCE

Optical turbulence is a term used to describe time-varying local fluctuations in the index of refraction of the atmosphere. The nonuniformities are caused by localized temperature fluctuation which results in "cells" of different temperature and refractive index. The intensity of the turbulence is described by the index structure parameter C_n^2 or the temperature structure parameter C_T^2. Turbulence cell size is characterized by two measures, the inner scale and the outer scale. The inner scale of turbulence is the measure of small, local refractive index fluctuations; it is usually on the order of several millimeters. The outer scale of turbulence, for altitudes h within several meters of the ground, is usually about h 2 (Ref. 8).

For ranges between the inner and outer scales of turbulence

$$C_T^2 \approx \frac{\langle [T(r_1) - T(r_2)] \rangle^2}{\ell^{2/3}}, \text{ K}^2/(\text{m}^{2/3}) \quad (2\text{-}13)$$

where

$T(r_1)$ = temperature at point r_1, K
$T(r_2)$ = temperature at point r_2, K
ℓ = distance between r_1 and r_2, m
$\langle \rangle$ = ensemble average.*

C_n^2 and C_T^2 are related by

$$C_n^2 = \left| \frac{\partial n(\lambda)}{\partial T} \right|^2 C_T^2, \text{ m}^{-2/3} \quad (2\text{-}14)$$

where, for dry air and optical wavelengths, the variation of the real part of the index of refraction $n(\lambda)$ with temperature is given by (Ref. 9)

$$\frac{\partial n(\lambda)}{\partial T} = \frac{79P}{T^2} \times 10^{-6}, \text{ K}^{-1} \quad (2\text{-}15)$$

where

P = air pressure, mbar
T = temperature, K.

The effects of turbulence on EO systems are most pronounced for coherent systems (lasers), where the interference with the optical wavefront propagation is most critical. Turbulence-induced beam degradation is manifested in short-term scintillation—i.e., localized high-intensity patches and nulls in the propagated beam—and beam wander—i.e., direction change of the beam centroid—and a longer term beam smear—i.e., spreading of the spot by turbulence-induced direction fluctuations. In imaging systems strong turbulence may result in image smearing—the loss of high spatial frequency information. Turbulence-induced index fluctuations have the strongest effect at visible wavelengths and lesser effect at thermal wavelengths. Millimeter wave systems are insensitive to atmospheric temperature fluctuation but respond to localized fluctuations in absolute humidity, which cause changes in the refractive index at mmw frequencies.

Turbulence is the least pronounced shortly before dawn and after sunset. It is strongest in the middle of the

---

*A statistical ensemble is an assembly of a large group of systems each satisfying a particular set of conditions. An ensemble average is an average value over all systems in the ensemble at a particular time.

day. An excellent summary description of turbulence calculations is included in Ref. 9.

2-3.5 CLUTTER

Clutter is the presence of "target-like" objects in the imagery. Clutter level is a measure of the number of background scene elements that appear to resemble a target on the sensor display or to the sensor signal processor. Clutter occurs in the visible because of differences in the reflectances of naturally occurring objects; in the IR because of differences of temperature among rocks, trees, and the earth; and in the near mmw region because of differences between tree and ground reflectance and because of multipath interference due to multiple reflections off the ground.

The atmosphere reduces the sensor signal-to-noise ratio; this often makes it difficult to discriminate between actual targets and clutter objects. In addition, clutter caused by battlefield-induced contaminants may mask actual targets or result in difficulty in discriminating real targets from clutter. For example, under severe atmospheric attenuation conditions, a thermal sensor cannot resolve high spatial frequency target information, only bright and dark spots. If the attenuating medium also contains exothermic sources, such as white phosphorous (WP), hexachloroethane (HC), or high explosives (HE), the problem of discriminating the obscurant-induced "hot spot" becomes more difficult. The observer either increases target acquisition time, reduces target acquisition probability, or is forced to increase the false alarm rate.

2-4 NATURAL OBSCURANTS

Naturally occurring atmospheric obscurants include atmospheric gas molecules, water vapor, haze, fog, rain, and snow. The extent of extinction due to these obscurants depends on the radiation wavelength as well as the concentration of the obscurants. Sensors are generally designed to operate in atmospheric "windows", spectral regions which exhibit generally good transmittance under clear atmospheric conditions. These windows are determined by absorption and scattering by atmospheric gas molecules. Within each window, daily and seasonal weather fluctuations will change the atmospheric transmittance. The impact of these fluctuations—the distribution of atmospheric transmittance values expected in a given location—and target signature variations will determine the performance of a sensor, i.e., how often the sensor will meet specified requirements, such as target acquisition range. This paragraph qualitatively describes the effects of naturally occurring obscurants on visible, IR, and mmw sensors.
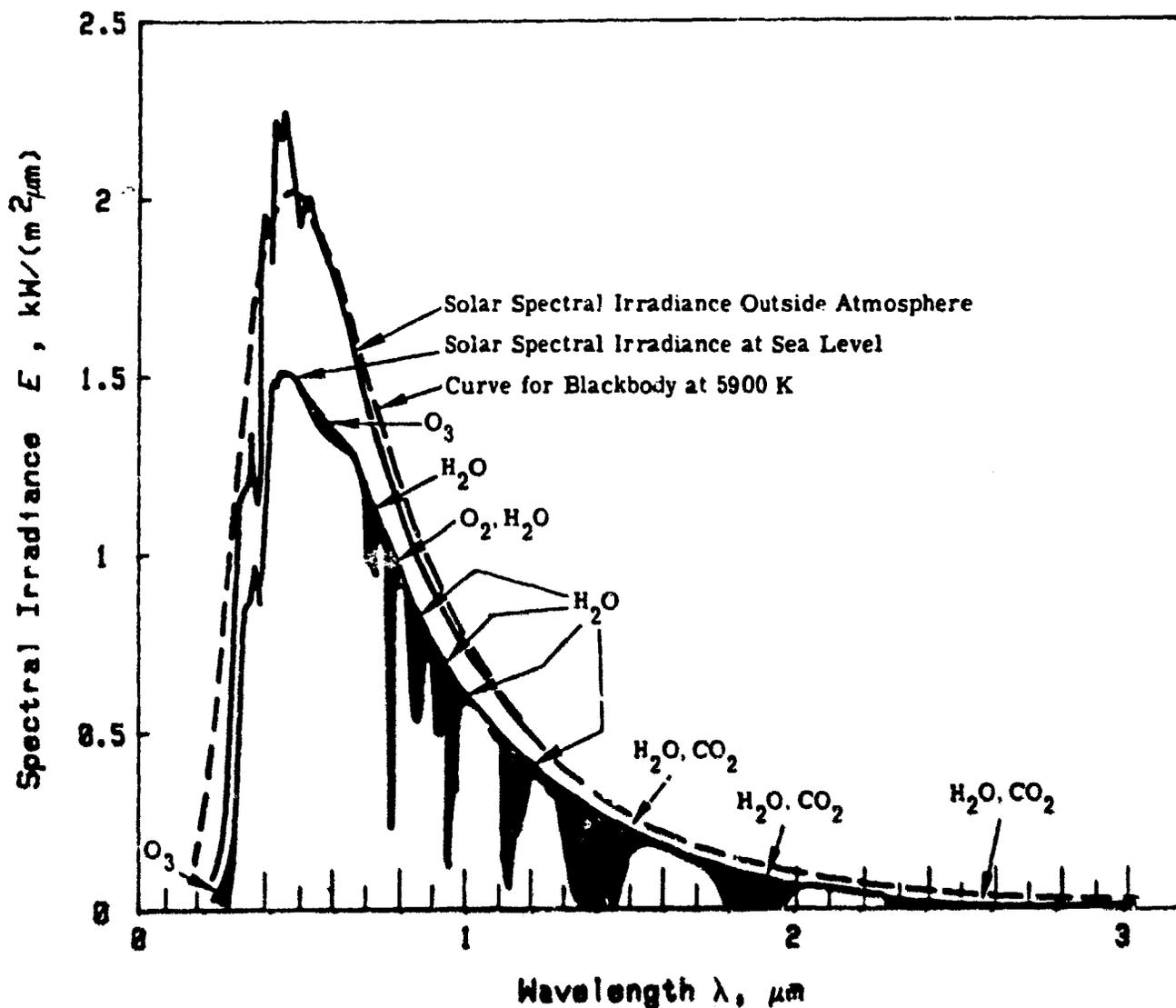
Figure 2-6. Solar Spectrum as Seen Through The Earth's Atmosphere (Ref. 9)

2-4.1 WATER VAPOR AND GASEOUS ABSORPTION

The main extinction effects from atmospheric gases are shown in the observed solar spectrum in Fig. 2-6. This figure shows solar radiation as propagated through the atmosphere and indicates the atmospheric gaseous absorption. Table 2-5 summarizes the major atmospheric attenuators in each spectral region and indicates the local variability in the absorber concentration. Only water vapor shows strong local variations in concentration. The concentrations of other gases have fairly stable profiles with slight local variations. Atmospheric density decreases with altitude; the concentration profiles of atmospheric gases with altitude are well documented for "standard" atmospheres representative of North American, European, tropical, and arctic climates (Ref. 1).

Atmospheric gases do not cause significant absorption in the visual window. In the IR region, water vapor and CO_2 are the most important absorbers. Water vapor content is also the most variable of the gaseous atmospheric constituents. Thus absolute humidity is a strong determinant of thermal system performance. Carbon dioxide is a strong absorber in the infrared regions and strongly affects the line emitters such as CO_2 lasers, but ground level atmospheric CO_2 content is not highly variable. Millimeter wave radiation is strongly attenuated by water vapor and oxygen absorption.

2-4.2 HAZE, FOG, AND CLOUDS

Haze, fog, and clouds are all naturally occurring atmospheric aerosols. Haze refers to small particles suspended in the atmosphere. It may include dust, carbon particles, salt spray, or industrial pollutants. The

TABLE 2-5
MAJOR NATURAL OBSCURATION MECHANISMS FOR VISIBLE, IR, AND
MILLIMETER WAVE RADIATION

SPECTRAL WINDOW	MAIN EXTINCTION MECHANISMS	MAJOR ATMOSPHERIC ATTENUATORS	VARIABILITY
Visible and Near IR	Molecular absorption	O_2	Not highly variable
	Aerosol scattering	Haze, fog, precipitation	Highly variable
	Aerosol absorption	Haze, fog, precipitation	Scales to visibility; highly variable
Mid IR	Molecular absorption	CO_2	Not highly variable
	Water vapor absorption	H_2O (absolute humidity)	Highly variable
	Aerosol scattering	Fog, precipitation (liquid water content)	Highly variable
Far IR	Molecular absorption	CO_2	Not highly variable
	Water vapor absorption	H_2O (absolute humidity)	Highly variable
	Aerosol scattering	Fog, precipitation (liquid water content)	Highly variable
Millimeter Wave 35 GHz, 94 GHz	Molecular absorption	O_2	Not highly variable
	Water vapor absorption	H_2O (absolute humidity)	Highly variable
	Aerosol scattering	Precipitation (liquid water content)	Highly variable
		Snow (rate and liquid water content)	Highly variable

type, size, and number density of these particles will vary with location. Atmospheric aerosol particle sizes may vary from 5×10^{-1} μm up to 10 μm; these small particles scatter atmospheric radiation; the scattering intensity at a given wavelength is determined by particle size, composition (as it affects index of refraction), and concentration. The normal background haze contains particles that peak in size at about 0.01 μm; industrial pollutants in dry to moderate humidity conditions have particle sizes on the order of tenths of micrometers. In the absence of fog or precipitation, scattering from these particles is the principal extinction mechanism for visual radiation. In high humidity cases (relative humidity above 80%), these aerosol particles may hydrate, which causes particle sizes to grow to the order of 1 μm or somewhat larger; these aerosol particles still attenuate visual radiation more than thermal radiation. When the temperature approaches the dew point, these particles act as condensation sites for atmospheric water vapor, which facilitates the formation and growth of fog droplets and cloud droplets, with sizes on the order of 10 μm.

The distinction between fog and haze is somewhat arbitrary. Good working definitions are that "fog" refers to visibilities of one or two kilometers or less and that "haze" is used to describe atmospheres with visibilities greater than one or two kilometers. Hazes usually contain particles in the 1-μm to submicrometer range. Fogs contain droplets in the 1-μm to 10-μm range.

Clouds are also composed of water droplets in the 10-μm size range; the normal working distinction between clouds and fog is one of total droplet number density (liquid water content) and altitude.

Fogs are often categorized by their formation mechanism. A radiation fog is formed by radiative cooling of air to its dew point. Thus radiation fogs usually occur under clear or partly cloudy conditions. The vertical extent of radiation fogs is limited, usually to under about 50 m. Advection fogs are formed by vertical mixing of air at different temperatures often with warm or cold fronts until the air reaches the dew point. An advection fog characterized by a given visibility will be a more severe far IR attenuator than a radiation fog with the same visual transmittance because of the difference in particle size distributions between the fogs.

Clouds and fogs also reduce natural illumination. The lower ambient light level reduces visual and near IR system performance. Cloud cover also reduces solar insolation and thereby causes a "washing out" of passive thermal signatures. Active thermal targets may, however, show up more clearly in these circumstances.

2-4.3 RAIN

Rain is a significant scatterer in the visible, thermal, and mmw wavelength regions. Depending on the rainfall rate, the intensity of a rain can be described as heavy, moderate, or light as shown in Table 2-6. Rain particle sizes range from about 100 μm for drizzle to several mm

in thunderstorms. They are large enough compared to visible and IR wavelengths that scattering due to rain is relatively insensitive to wavelength in the visible and IR regions.

TABLE 2-6
RAIN RATE TABLE (Ref. 4)

RAIN INTENSITY	RAIN RATE
Heavy	More than 7.7 mm per h More than 0.77 mm in 6 min
Moderate	2.5 to 7.7 mm per h 0.25 to 0.77 mm in 6 min
Light	Less than 2.5 mm per h Maximum 0.25 mm in 6 min

Visible and IR attenuation through rain may be calculated using only rain rate and rain particle size distribution (drizzle, widespread rain, or thunderstorm) (Ref. 10). At millimeter wavelengths, rain is an Mie scatterer, and the scattering is strongly dependent on raindrop size distribution. Drizzle produces relatively larger mmw extinction coefficients (for a given rain rate) and the highest backscatter coefficients. Surprisingly, thunderstorms have the smaller relative mmw extinction coefficients with respect to rain rate because of the predominance of large drop sizes.

Rain may also change the apparent target signature by changing the target surface reflectance characteristics (for passive visual sensors or active illuminators) and by "washing out" the temperature differences in a thermal scene.

2-4.4 SNOW

Snow is a significant scatterer for visible, IR, and mmw radiation. In the visible and IR regions, snow particle sizes are much larger than the wavelength, so extinction due to snow can be scaled to visibility through the snow. At high relative humidity (>95%), however, fog may form with the snow. In this case, thermal extinction in snow depends not only on visibility but also on temperature and relative humidity.

Data on mmw extinction and backscatter in snow are very limited. Extinction depends on snow rate and on snow particle size distribution. Current models use rain equivalent snow rate and snow wetness (based on temperature) to establish extinction and backscatter coefficients for snow (Ref. 10).

2-4.5 BLOWING DUST

Blowing dust and sand may become significant in reducing transmittance or denying an LOS in locations

with heavy wind; loose, dry soil; and little or no vegetative cover. Airborne dust scatters visible, near IR, and thermal radiation. The scattering shows little spectral sensitivity in the visible and near IR bands because of the relatively broad particle size distribution; transmittances losses in the termal bands are slightly lower than in the visible and may show some spectral dependence. Blowing dust is not a significant obscurant to mmw systems.

2-5 BATTLEFIELD OBSCURANTS

The sensor used on the battlefield will have to operate in the presence of battlefield-induced contaminants in addition to naturally occurring atmospheric obscurants. These obscurants include countermeasure smokes, vehicle- and munition-generated dust, and fire products. The effect of an obscurant on sensor performance will depend on the obscurant, the sensor, the environmental conditions, and the way it is deployed. Battlefield obscurants cause extinction, contrast reduction, LOS interruptions, and an increase in clutter or false targets.

Battlefield-induced contaminants are described qualitatively in this paragraph. Parameters used for laboratory and field characterization of smoke effectiveness are defined in pars. 2-6 and 2-7. The effects of meteorological conditions and environmental factors on obscurant generation and transport are treated in pars. 2-8 and 2-9.

2-5.1 SMOKES AND OBSCURATION MATERIALS

Smoke may be employed on the battlefield for both offensive and defensive actions. Smoke has five general applications on the battlefield: obscuration, screening, deception, identification, and signaling.

"Obscuration smoke is smoke employed on or against the enemy to degrade his vision both within and beyond his location. Smoke delivered on an enemy antitank guided missile (ATGM) position may prevent the system from acquiring or subsequently tracking targets, thereby reducing its effectiveness. Employment of obscuration smoke on an attacking armored force may cause it to vary its speed, inadvertently change its axis of advance, deploy prematurely, and rely on nonvisual means of command and control.

"Screening smoke is smoke employed in friendly operational areas or in areas between friendly and enemy forces in order to degrade enemy ground and aerial observation, and defeat or degrade enemy electro-optical systems. Screening smoke is employed to conceal ground maneuver, breaching and recovery operations, key assembly areas, and supply routes.

"Deception smoke is smoke used to deceive the enemy regarding intentions of US Army forces. For example,

smoke can be employed on several avenues of approach to deceive the enemy as to the avenue of the main attack.

"Identification and/or signaling smoke is smoke employed to identify targets, supply and evacuation points, friendly unit positions, and to provide for pre-arranged battlefield communications." (Ref. 11).

Table 2-7 summarizes the materiel available for armored vehicle protection, obscuration, and area screening.

TABLE 2-7
SMOKE APPLICATIONS AND MATERIALS

APPLICATION	MATERIEL	SMOKE MATERIALS
Armored Vehicle Protection	Grenades VEESS*	HC, WP, RP** Diesel Oil
Obscuration	Artillery Mortars Rockets	WP, HC WP, RP WP
Screening	Generators Pots	Fog Oil HC, Fog Oil

*Vehicle Engine Exhaust Smoke System

**Red Phosphorous

Threat concepts, materiel, and materials are similar to those of the US inventory. Soviet doctrine refers to camouflage and blinding smoke in place of our terms of area screening and obscuration.

Smoke clouds last from minutes to hours depending upon the material used for dissemination. Submunitioned WP projectiles, such as the M825 155-mm artillery round and the M259 2.75-in. rocket, spread the smoke-producing submunitions over an impact area; they burn for several minutes.

Dense clouds of phosphorous smoke are produced for self-protection by grenades discharged from an armament subsystem integrated into armored fighting vehicles. These rapidly generated clouds, which may last for several minutes, may be supplemented by diesel oil smoke produced from the integral Vehicle Engine Exhaust Smoke System (VEESS). The VEESS may be operated as long as the vehicle has fuel.

Materiel designed to produce smoke coverage in friendly areas include smoke pots and generators. Depending on their size and local conditions, smoke pots produce HC (M5, M1) or fog oil (M7) smoke for up to 20 min and provide downwind coverages of up to 500 m. Large area generators (M3A3) can be run as long as smoke-producing material is provided, and they provide downwind coverages of several kilometers.

The development, transport, and dissipation of a smoke cloud is strongly affected by the munition, the placement of it, and environmental conditions. Explosively disseminated smokes evolve in the same phases as HE-dust (see par. 2-5.2). This development is illustrated in Fig. 2-7. Nonexplosively disseminated smoke clouds evolve in three phases: the streamer and buildup phase, uniform phase, and terminal phase. In the first phase, a streamer of smoke is formed from the smoke source and
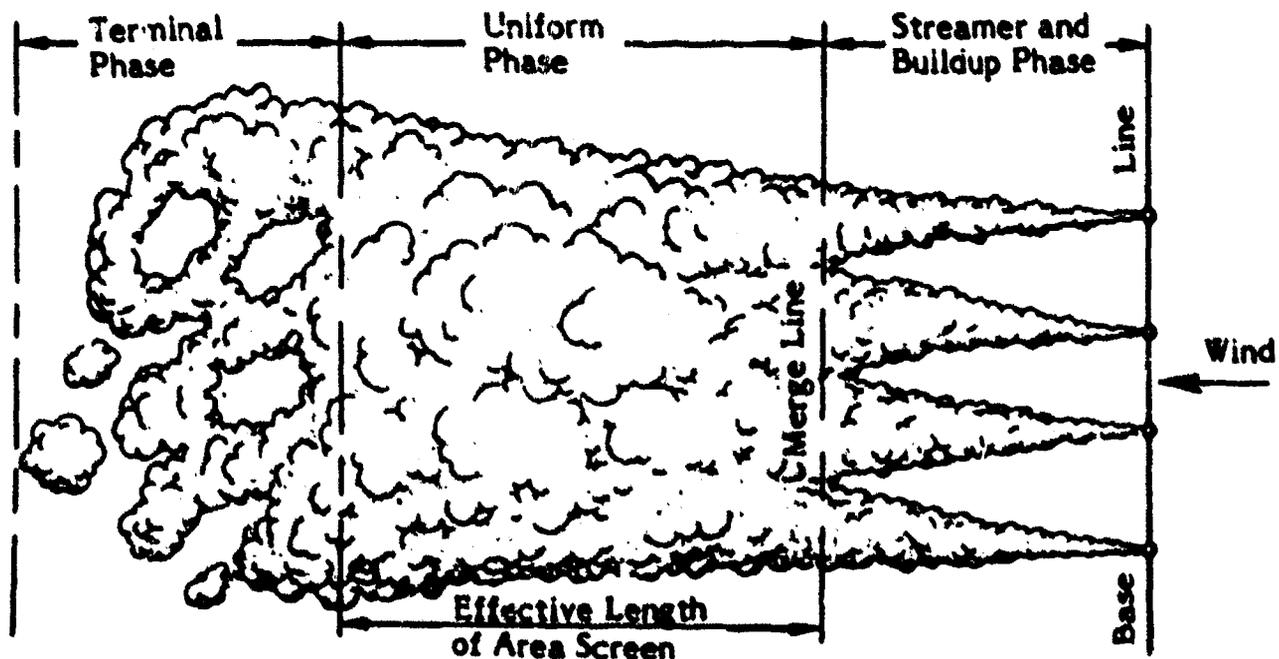
Figure 2-7. Smoke Screen—Effective Length and Smoke Phases (Ref. 5)

exists alone before diffusing to merge with other streamers. The diffusion depends on atmospheric stability and wind speed. Buildup occurs when streamers overlap, but the smoke is not uniformly distributed. In the uniform phase the size of the screened area is determined by the smoke output of each source, the relative placement, and local meteorological conditions. Finally, in the terminal phase the smoke is diffused so much that it is not an effective screen.

The effectiveness of a smoke cloud in screening a particular position will depend not only on the amount of smoke between the sensor and the target but also on the extinction characteristics of that smoke in the sensor spectral band. Current inventory smokes are more effective in the visible than in the IR bands; they have negligible impact on mmw sensors.

The discussion on smoke has addressed primarily the use of smokes in reducing atmospheric transmittance. Smokes may also contribute to sensor performance degradation through contrast reduction from scattering of ambient light by the smoke particles or backscattering of laser illuminator radiation. Exothermic smokes also reduce thermal contrast, increase thermal clutter, and may appear as false targets.

2-5.2 DUST (MUNITION AND VEHICLE PRODUCED)

Airborne battlefield dust may be produced by vehicular traffic or by dirt raised by munitions impact. The amount of dirt raised by vehicular traffic will depend on the soil dryness and vegetative cover, the type of vehicle, and the vehicular speed. The amount of dust produced by munition firings will be determined by the type of soil, soil moisture, and vegetative cover, as well as by the munition type, fill weight, and point of detonation. The spread of the dust will depend on local meteorological conditions, particularly on wind speed and atmospheric stability. The persistence of the dust will be determined in part by the dust particle size. Gravitational settling will limit the duration of dust clouds composed of larger particles, but very small dust particles may stay aloft for long periods of time.

The HE-produced dust cloud develops and dissipates in three stages: impact phase, rise phase, and drift and dissipation phase. The generation, diffusion, and transport of a munition-generated dust cloud are shown in Fig. 2-8. In the initial phase, a crater is formed by the munition impact, and both dust and large chunks of debris may be lofted. A hot dust-and-fire ball several meters across, containing most of the dust and debris, is formed close to the surface. A dust skirt 6-10 m wide and 1-3 m high* is also formed. In the rise phase, the dust-and-fire ball expands and rises quickly to 10-30 m in

(A) Impact Phase

(B) Rise Phase
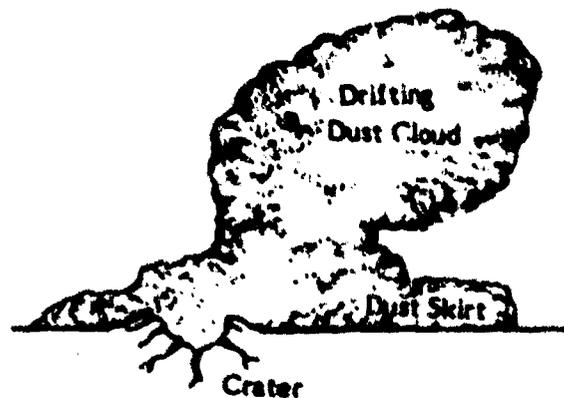
(C) Drift and Dissipation Phase

Figure 2-8. Munition Dust Cloud Impact, Rise, and Drift and Dissipation Phase (Ref. 5)

---

* The size will vary with munition type. These values are for 155-mm munitions.

2-16

height because of its thermal buoyancy. The large debris settles out quickly. The dust skirt diffuses but does not rise. Finally, the dust cloud, blown by the wind, drifts and dissipates. The dust skirt usually drifts more slowly than the cloud because wind speed tends to be lower near the ground (Ref. 5).

Airborne dust scatters visible and IR radiation; generally, the extinction is not spectrally dependent because of the wide distribution of particle sizes. Battlefield vehicular dust may indicate troop movement while obscuring the details of that movement. Vehicular dust can sometimes greatly enhance detection of vehicular traffic by cuing the target location. However, dust can obscure detection and recognition of targets within the dust clouds. Vehicular and HE-generated dust may thus degrade the performance of EO sensors and may deny continued lock-on of precision guided munitions. Munitions salvos may be used deliberately to blind artillery observation points. HE-generated fireballs also introduce visible and thermal clutter. The large, lofted debris may obscure the LOS for mmw systems for several seconds; the smaller airborne dust particles do not obscure mmw sensors.

2-5.3 FIRES AND FIRE PRODUCTS

Fires on the battlefield may be deliberately set or may be the result of burning vehicles or burning vegetation. Fire product constituents include burning gases and carbon particles. These fire products may cause transmittance losses, scattering, and sensor LOS interruptions. Carbon, in particular, is an excellent attenuator of electromagnetic radiation. The illumination from fires may temporarily blind image intensifiers. In the thermal band, fires introduce thermal clutter and false targets. Thermal gradients due to heating by the fire also cause turbulence. Fire-induced turbulence may affect the image quality of visible and thermal systems and may diffuse radiation from active laser and mmw systems.

2-6 AEROSOL PARAMETERS

Battlefield-induced contaminants are described by two sets of parameters. The aerosol parameters defined in this paragraph are used as a baseline for predicting the effects of an obscurant in the battlefield atmosphere. Battlefield-induced obscuration parameters are described in par. 2-7.

2-6.1 SIZE DISTRIBUTION AND CONCENTRATION

The particle size distribution of an aerosol is the number density or mass density of aerosol particles as a function of particle radius. The particle size of an aerosol is critical in determining its spectral efficiency as a scatterer as discussed in par. 2-5.1. A spherical aerosol

has the highest scattering efficiency (Mie cross section about four times the geometric cross section) if the particle radius is approximately the same as the wavelength of the radiation. The scattering efficiency drops to 2 if the wavelength is much smaller than the particle size; it drops as (particle volume)$^2\lambda^{-4}$ if the particle size is much smaller than the wavelength.

The mass concentration of an obscurant is simply a measure of the mass of an obscurant in a given volume. An aerosol is the most effective scatterer at a given wavelength if it is present in high concentration and if most of its mass is in particles with a radius approximately the same as the radiation wavelength.

2-6.2 COMPOSITION, SHAPE, AND INDEX OF REFRACTION

The effectiveness of an aerosol as an attenuator is determined in part by the index of refraction of the aerosol. The complex index of refraction $m(\lambda)$ of an obscurant at wavelength λ may be represented by real and imaginary parts

$$m(\lambda) = n(\lambda) - in_i(\lambda), \text{ dimensionless} \quad (2\text{-}16)$$

where

$n(\lambda)$ = real part of the index of refraction, dimensionless

$n_i(\lambda)$ = imaginary part of the index of refraction, dimensionless.

The index of refraction of an aerosol is determined by its composition. The effectiveness of an aerosol as a scatterer is determined by the magnitude of the real part of the index of refraction. Its effectiveness as an absorber is determined by the magnitude of the imaginary part of the refractive index.

The shape of a particle will determine its effectiveness as a broadband attenuator. The best broadband attenuators are conducting particles with high aspect (length-to-width) ratios (Ref. 12).

2-7 BATTLEFIELD-INDUCED CONTAMINANT PARAMETERS

This paragraph defines and discusses parameters used to specify the amount of obscurant in the battlefield atmosphere and to calculate the transmittance of radiation through the obscurant. These parameters are mass extinction coefficient, concentration path length product, yield factor, and burn rate.

2-7.1 MASS EXTINCTION COEFFICIENT AND CONCENTRATION PATH LENGTH

The mass extinction coefficient $\alpha(\lambda)$ is defined as

$$\alpha(\lambda) = \ll \frac{Q\sigma}{M} \gg, \text{ m}^2/\text{g} \qquad (2\text{-}17)$$

where

σ = geometric cross section of particle, m²
Q = extinction efficiency, dimensionless
M = mass of the particle, g.

The inner brackets represent an average over solid angle, and the outer brackets represent an average over the particle mass size distribution. Obscurant mass extinction coefficients may exhibit a strong spectral dependence. The concentration path length product (CL) of an obscurant is the amount of obscurant contained in a path of length L through an obscurant of known concentration. For nonuniform obscurants distributed over a path from r_1 to r_2

$$CL = \int_{r_1}^{r_2} c(r)\, dl, \text{ g} \cdot \text{m}^2 \qquad (2\text{-}18)$$

where

$C(r)$ = concentration at point r, g·m³.

Transmittance $T_s(\lambda)$ through the obscurant is calculated by

$$T_s(\lambda) = e^{-\alpha(\lambda)CL}, \text{ dimensionless.} \qquad (2\text{-}19)$$

2-7.2 YIELD FACTOR AND BURN RATE

The mass of obscurant aerosol M_a' disseminated by a munition is determined from

$$M_a' = Y_f M_a E_f, \text{ g} \qquad (2\text{-}20)$$

where

M_a = mass of aerosol in munition, g
E_f = efficiency with which aerosol is disseminated, dimensionless
Y_f = yield factor, dimensionless.

The yield factor is used to account for the growth of hygroscopic aerosol particles in the atmosphere by absorption of atmospheric water vapor. For these smokes the yield factor increases with increasing relative humidity. For HC smokes the yield factor at 10% relative humidity is 1.5 and increases to 3.5 at 90% relative humidity. The yield factor for WP goes from 3.5 to about 8 over the same range. The yield factor for fog oil is 1.0 (Ref. 10).

The burn rate, or mass production rate, of obscurant smokes is the rate of delivery of the munition fill mass into the atmosphere. Munitions with lower burn rates usually result in cooler smokes with less buoyant rise:

these smokes stay closer to the ground and provide better protection to ground targets.

2-8 METEOROLOGICAL PARAMETERS

Meteorological measurements are routinely made at military and civilian weather stations. Hourly records of meteorological data, taken over a period of several years, are available for many locations. Standard meteorological measurables are defined in par. 2-8.1. Atmospheric stability and turbulence—parameters derived from meteorological data—are discussed in par. 2-8.2.

2-8.1 METEOROLOGICAL MEASURABLES

Standard meteorological measurables include air temperature, dew point, depression, visibility, atmospheric pressure, wind speed, wind direction, precipitation, and cloud cover.

Air temperature is the ground level dry bulb air temperature. Dew point is the temperature to which a given parcel of air must be cooled at constant pressure and water vapor content in order for saturation to occur; any further cooling results in the formation of dew or frost. Dew point depression is the difference between air temperature and dew point. Ground level atmospheric pressure is the force per unit area applied at the ground by the column of air above it. It is reported in mbar. Visibility is the distance at which it is just possible to distinguish a high contrast object against the background with the unaided eye; it is usually taken as the distance over which the 0.4-0.7 μm atmospheric transmittance is 0.02. Visibility is estimated by sighting to landmarks at known distances. Relative humidity, required to establish the yield factor of hygroscopic smokes, is established from air temperature and dew point.

Atmospheric transmittance at wavelengths from ultraviolet to mmw may be calculated directly from meteorological observables using standard atmospheric codes, such as those developed by the Air Force Geophysics Laboratory (Refs. 1 and 13). These codes require as input the air temperature, pressure, dew point or relative humidity, and visibility, as well as parameters defining the atmospheric path geometry.

At specialized meteorological stations, atmospheric transmittance has been measured at selected wavelengths. The atmospheric extinction coefficient at these selected wavelengths may be derived directly as shown in par. 2-3.3.

2-8.2 STABILITY CATEGORY

Pasquill category, or atmospheric stability category, is a measure of the rate of vertical spread from an obscurant source. The atmosphere is characterized as unstable (Pasquill Categories A and B), neutral (C and D), or

stable (E and F). Pasquill category may be estimated from cloud cover, wind speed, and sun angle (Ref. 14).

Unstable (lapse) conditions are characterized by significant turbulence and a decrease in air temperature with height. Lapse conditions occur with high insolation and light winds, such as exist at midday on a clear, sunny day with light winds. Stable (inversion) conditions are present when there is an increase of temperature with increasing height. Inversions occur on clear nights or on cloudy days when wind speed is low and the air at ground level has been cooled by contact with the cooler earth. Increasing winds drive the atmosphere toward neutral conditions, with no vertical temperature gradient near ground level. Neutral conditions are usually found near sunrise or sunset.

2-8.3 MECHANICAL TURBULENCE

Atmospheric turbulence causes small local fluctuations in wind speed and wind direction, which in turn cause the entrainment of air in the obscurant cloud. After the initial buoyant rise of a smoke or munition cloud, dilution and dissipation of the obscurant are due almost entirely to local turbulence effects. The time-varying nature of this turbulence may cause local non-uniformities in the cloud, and in some cases it results in the appearance of thin areas or "holes", which permit a temporary LOS through an obscuring cloud. The effect is particularly strong in HE-generated dust clouds, which also have a turbulent contribution from the initial explosion. Strong turbulence in an HE cloud can degrade mmw signals even though the dust itself has only a minor effect on the mmw radiation.

2-9 EFFECTS OF ENVIRONMENTAL FACTORS ON BATTLEFIELD-INDUCED CONTAMINANTS

The transport and diffusion of obscurant clouds depend strongly on local environmental conditions, including atmospheric stability (Pasquill category), wind speed, wind direction, humidity and temperature, and terrain. These effects are described qualitatively in the paragraphs that follow.

2-9.1 TRANSPORT AND DIFFUSION

Atmospheric stability, wind speed, and wind direction are strong influences on dust and smoke cloud development, diffusion, and dissipation. In turbulent, unstable conditions, obscurant clouds will rise rapidly because of the thermal gradient with altitude and will diffuse rapidly because of turbulence-induced air entrainment. In very stable conditions obscurant clouds will tend to remain at the same altitude and dissipate slowly, although exothermic smokes and munition-generated clouds will exhibit an initial buoyant rise. In

neutral conditions, the obscurant cloud will rise slowly. Fig. 2-9 shows the effect of atmospheric stability in the development of a smoke cloud. Dust cloud development in lapse and stable atmospheric conditions is illustrated in Fig. 2-10. Stable to neutral conditions are most favorable for the production of area smoke screens. Neutral to lapse conditions are favorable for the production of smoke curtains.

Obscurant clouds move in the direction of the wind at the prevailing wind speed while diffusing in altitude and width. The top portion of the cloud will tend to drift slightly faster than the skirt because of a wind gradient with altitude. High wind speeds cause the obscurant to drift rapidly and diffuse more quickly; this
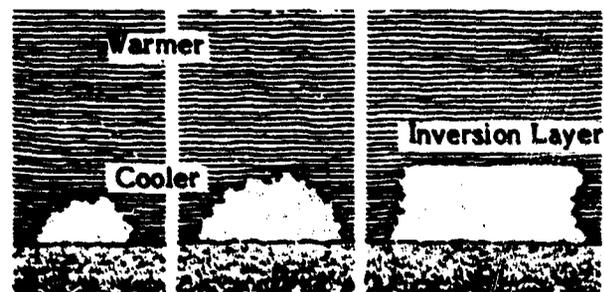
(A)　Stable Conditions
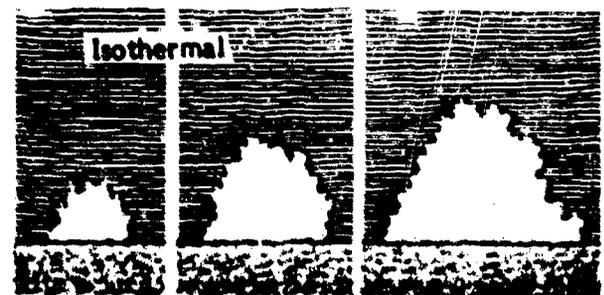
(B)　Neutral Conditions
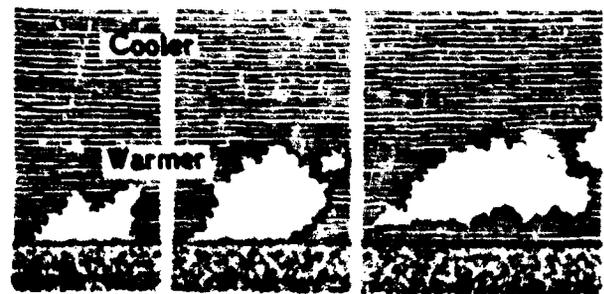
(C)　Lapse Conditions

Figure 2-9.　Atmospheric Stability Effect on Smoke Cloud Development (Ref. 5)

(A)   Lapse Conditions

Low-Lying Inversion

(B)   Stable Conditions
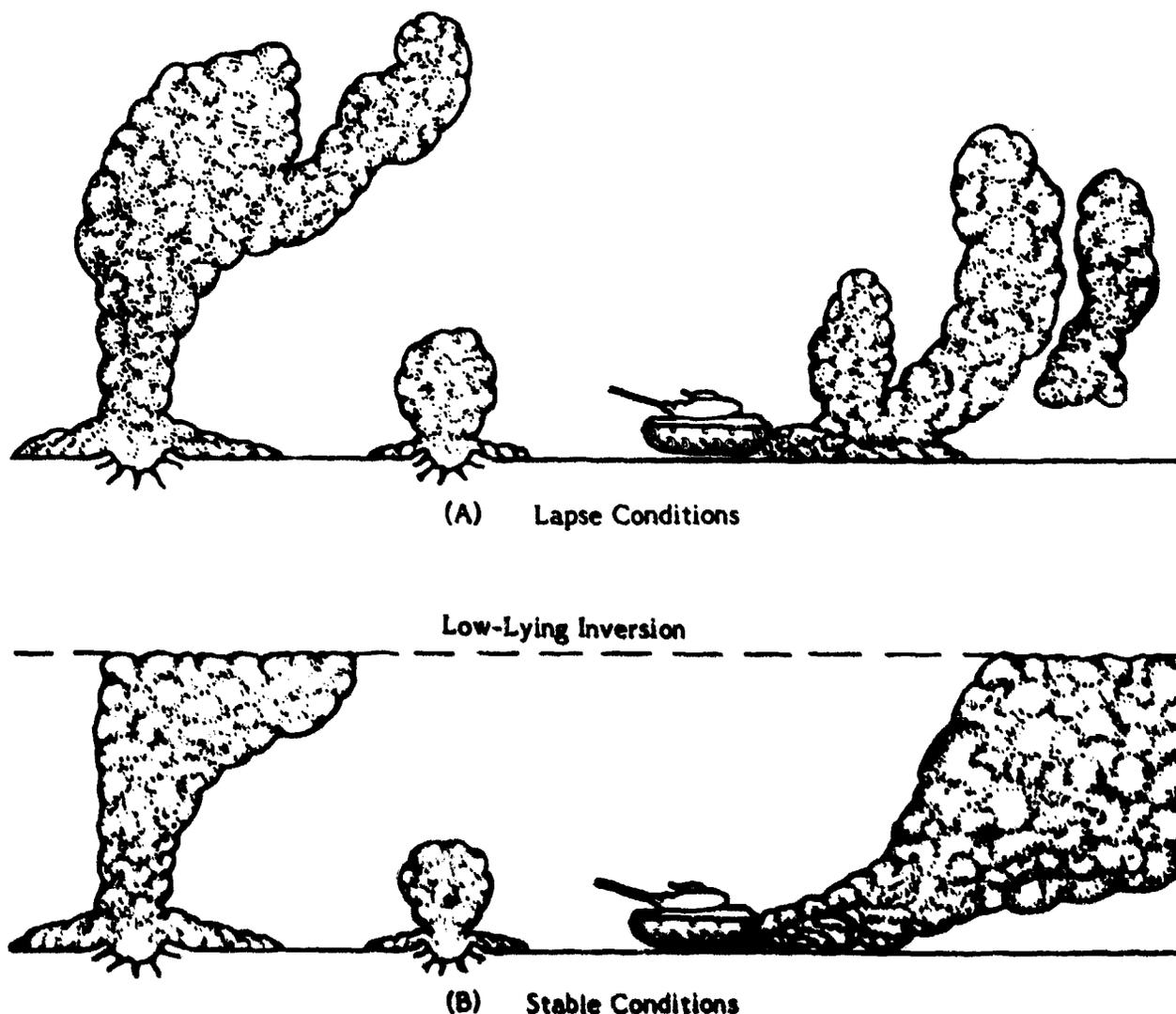
Figure 2-10.   Atmospheric Stability Effect on HE-Generated Dust Cloud Development (Ref. 5)

reduces obscuration time. Mechanical turbulence created by local wind speed fluctuation will cause temporal and spatial variations in obscurant density, such as eddies and holes in the cloud. Wind direction and wind speed must be considered in determining the placement of an obscurant cloud to make sure that the windblown obscurant will screen the target and not be blown out of the LOS. This is indicated in Fig. 2-11.

2-9.2   HUMIDITY AND TEMPERATURE

Humidity and temperature effects on obscurant cloud development and dissipation have been mentioned briefly. The yield factor of hygroscopic smokes is a strong function of relative humidity as discussed in par. 2-7.2. The increased size of these smoke particles in high humidity environments increases their scattering effectiveness. However, the mass extinction coefficient

is slightly reduced because the index of refraction of the smoke changes as the water content of the smoke is increased.

Atmospheric temperature profiles are strong determinants of smoke cloud development and transport because of their impact on atmospheric stability as discussed in pars. 2-8.2 and 2-9.1. In addition, the turbulence induced by local temperature fluctuations increases mixing and dissipation of the obscurant.

2-9.3   TERRAIN

The effects of terrain are similar for HE-generated dust, vehicular dust, and smoke clouds. However, terrain-induced variations in wind speed and direction will clearly affect obscurant cloud transport. The impact of terrain on smoke is small although rough vegetative growth will slow the transport of the base of

(A) Wind Across Maneuver-Target Line

(B) Wind Along Maneuver-Target Line
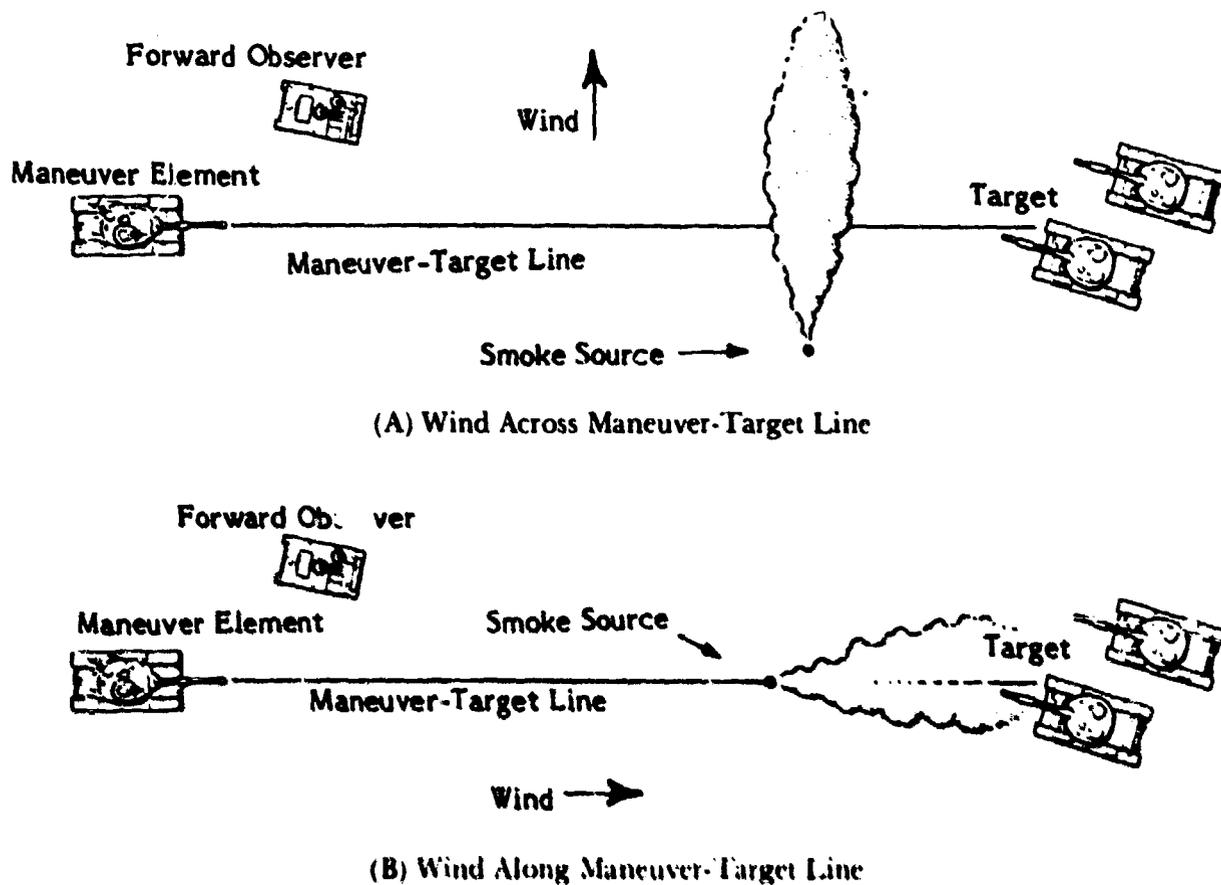
Figure 2-11. Effect of Prevailing Wind on Smoke Placement and Diffusion (Ref. 5)

the cloud. Soil type, moisture content, and vegetative cover are much more important in dust cloud generation. Dry clay and silty soils will produce more airborne dust than sandy soils; wet soils produce less dust than dry ones. Vegetative cover or heavy sod reduces the amount of dust produced. In general, dust from dry silty a clay soils obscures more in the visible region than the IR region, whereas sandy or wet soil particles may be better IR obscurants. Millimeter wave sensor LOS may be interrupted for several seconds by the debris generated by HE munitions; wet soil chunks are more effective than dry ones against mmw sensors.

REFERENCES

1. F. X. Kneizys, et al., *Atmospheric Transmittance Radiance: Computer Code LOWTRAN 5*, AFCRL-80-0067, US Air Force Geophysics Laboratory, Hanscomb AFB, MA, 1980.

2. R. J. List, *Smithsonian Meteorological Tables*, Smithsonian Institution, Washington, DC, 1966.

3. Earl J. McCartney, *Optics of the Atmosphere*, John Wiley and Sons, New York, NY, 1976.

4. Marvin D. Kays, et al., *Qualitative Description of Obscuration Factors in Central Europe*, ASL Monograph No. 4, US Army Atmospheric Sciences Laboratory, White Sands Missile Range, NM, 1980.

5. *Smoke, An Obscuration Primer*, 61 JTCG-ME-77-15, Joint Technical Coordination Group for Munitions Effectiveness, Aberdeen Proving Ground, MD, 1978.

6. W. E. K. Middleton, *Vision Through the Atmosphere*, University of Toronto Press, Toronto, Canada, 1952.

7. R. E. Huschke, *Atmospheric Visual and Infrared Transmission Deduced from Surface Weather Observations: Weather and Warplanes II*, Rand Corporation, Santa Monica, CA, 1976.

8. Frederick Gebhardt, *Development of Turbulence Effects Models*, Science Applications, Inc., Ann Arbor, MI, 1980.

9. William Wolfe and George Zissis, Eds., *The Infrared Handbook*, Environmental Research Institute of Michigan, Ann Arbor, MI, 1978.

10. Louis D. Duncan, et al., *EOSAEL 82*, ASL-TR-0122, US Army Atmospheric Sciences Laboratory, White Sands Missile Range, NM, 1982.

11. TRADOC Pamphlet 525-3, *Employment of Smoke*, 1980.

12. Gerald C. Holst and Janon F. Embury, *Design Criteria for Smokes and Obscurants*, ARCSL-TR-82024, US Army Chemical Systems Laboratory, Aberdeen Proving Ground, MD, 1982.

13. H. J. P. Smith, et al., *FASCODE—Fast Atmospheric Signature Code (Spectral Transmittance and Radiance)*, US Air Force Geophysics Laboratory, Hanscomb AFB, MA, 1978.

14. D. Bruce Turner, "A Diffusion Model for an Urban Area", *Journal of Applied Meteorology*, 83-91 (February 1964).

BIBLIOGRAPHY

Visible and Near-IR Systems

Electro-Optics Handbook, RCA Corporation, Lancaster, PA, 1974.

L. P. Obert, J. T. Wood, and C. J. Nash, *Visionics Handbook of EO Sensor Performance, Volume I (Natural European Environment)* (U), US Army Night Vision and Electro-Optics Laboratory, Fort Belvoir, VA, 1981 (THIS DOCUMENT IS CLASSIFIED CONFIDENTIAL).

Infrared Systems

Christopher Due and Lauren Peterson, *Optical-Mechanical, Active, Passive Imaging Systems* Environmental Research Institute of Michigan, Ann Arbor, MI, 1982.

J. M. Lloyd, *Thermal Imaging Systems*, Plenum Press, New York, NY, 1975.

L. P. Obert, J. T. Wood, and C. J. Nash, *Visionics Handbook of EO Sensor Performance, Volume I (Natural European Environment)* (U), US Army Night Vision and Electro-Optics Laboratory, Fort Belvoir, VA, 1981 (THIS DOCUMENT IS CLASSIFIED CONFIDENTIAL).

J. A. Ratches, "Static Performance for Thermal Imaging Systems", *Optical Engineering* 15, 525 (1976).

William Wolfe and George Zissis, Eds., *The Infrared Handbook*, Environmental Research Institute of Michigan, Ann Arbor, MI, 1978.

Millimeter Wave Systems

K. J. Brandt, et al., *Millimeter Wave Systems and Components*, ARCSL-CR-83008, IIT Research Institute, Chicago, IL, 1983.

Optical Propagation and Scattering

Max Born and Emil Wolf, *Principles of Optics*, Pergamon Press, Oxford, Great Britain, 1975.

F. X. Kneizys, et al., *Atmospheric Transmittance Radiance Computer Code LOWTRAN 5*, AFGL-TR-80-0067, US Air Force Geophysics Laboratory, Hanscomb AFB, MA, 1980.

Earl J. McCartney, *Optics of the Atmosphere*, John Wiley & Sons, New York, NY, 1976.

V. I. Tatarski, *The Effects of the Turbulent Atmosphere on Wave Propagation*, Israel Program for Scientific Translations, Jerusalem, Israel, 1971.

Obscurants

Louis D. Duncan, et al., *EOSAEL 82*, ASL-TR-0122, US Army Atmospheric Sciences Laboratory, White Sands Missile Range, NM, 1982.

Gerald C. Holst and Janon F. Embury, *Design Criteria for Smokes and Obscurants*, ARCSL-TR-82024, US Army Chemical Systems Laboratory, Aberdeen Proving Ground, MD, 1982.

Marvin D. Kays, et al., *Qualitative Description of Obscuration Factors in Central Europe*, ASL, Monograph No. 4, US Army Atmospheric Sciences Laboratory, White Sands Missile Range, NM, 1980.

Limited Visibility Battlefield Conditions, The Technical Coordination Group, Joint Action Group (JAG) 10, 1983.

Smoke, An Obscuration Primer, 61 JTCG ME-77-13, Joint Technical Coordination Group/Munition Effectiveness, Aberdeen Proving Ground, MD, 1978.

TRADOC Pamphlet 525-3, *Employment of Smoke*, 1980.

CHAPTER 3
PROPERTIES AND FREQUENCY OF OCCURRENCE OF NATURAL OBSCURATION FACTORS

This chapter explains how to estimate natural obscuration factors, such as atmospheric transmittance and extinction coefficients. It also provides data that enable the user to characterize quantitatively the natural atmosphere for systems performance calculations. This information is provided for four different types of climate—temperate, tropical, desert, and northern—as represented by the European highlands, Central America, the Mideast desert, and Scandinavia, respectively.

3-0 LIST OF SYMBOLS

a,b = rain extinction parameters, dimensionless

CL = concentration path length product, g/m²

C_n^2 = index of refraction structure constant, m$^{-2/3}$

c,d = snow extinction parameters, dimensionless

D = effective laser aperture diameter, m

D_w = beam wander, m

D_{w1} = beam wander when $D/r_0 \leq 3$, m

D_{w2} = beam wander when $D/r_0 > 3$, m

E = illuminance, lm/m²

F = focal length, m

Im = imaginary part of bracketed expression, dimensionless

$m(\lambda)$ = complex index of refraction, dimensionless

R = path length, m or km

RH = relative humidity, %

r = rain rate, mm/h

r_0 = coherence length, m

r_s = rain equivalent snow rate, mm/h

S_L = long-term Strehl ratio, dimensionless

S_s = short-term Strehl ratio, dimensionless

S_{s1} = short-term Strehl ratio when $D/r_0 \leq 3$, dimensionless

S_{s2} = short-term Strehl ratio when $D/r_0 > 3$, dimensionless

T = temperature, °C

$T(\lambda)$ = transmittance, dimensionless

$T_a(\lambda)$ = atmospheric transmittance considering only aerosol extinction, dimensionless

$T_d(\lambda)$ = transmittance through dust, dimensionless

$T_m(\lambda)$ = atmospheric transmittance considering only molecular extinction, dimensionless

$T_p(\lambda)$ = atmospheric transmittance considering only precipitation, dimensionless

$T_s(\lambda)$ = transmittance through smoke, dimensionless

V = visibility, km

w = liquid water content, g/m³

Z = mass loading, g/m³

$\alpha_d(\lambda)$ = dust mass extinction coefficient for any wavelength λ, m²/g

$\gamma_a(\lambda)$ = aerosol volume extinction coefficient for any wavelength λ, km^{-1}

$\gamma_{a1}(1.06)$ = aerosol extinction coefficient when $V > 0.6$ km, km^{-1}

$\gamma_{a2}(1.06)$ = aerosol extinction coefficient when $V \leq 0.6$ km, km^{-1}

$\gamma_m(\lambda)$ = molecular volume extinction coefficient for any wavelength λ, km^{-1}

$\gamma_p(\lambda)$ = precipitation volume extinction coefficient for any wavelength λ, km^{-1}

$\gamma_{pr}(\lambda)$ = precipitation volume extinction coefficient for rain at any wavelength λ, km^{-1}

$\gamma_{pd}(\lambda)$ = precipitation volume extinction coefficient for drizzle at any wavelength λ, km^{-1}

$\gamma_{pt}(\lambda)$ = precipitation volume extinction coefficient for thunderstorms at any wavelength λ, km^{-1}

$\gamma_{pw}(\lambda)$ = precipitation volume extinction coefficient for widespread rain at any wavelength λ, km^{-1}

$\gamma_{ps}(\lambda)$ = precipitation volume extinction coefficient for snow at any wavelength λ, km^{-1}

λ = wavelength, μm

ρ = absolute humidity, g/m³

σ = standard deviation, dimensionless

σ_I^2 = variance in average irradiance, W²

σ_c^2 = centroid wander single axis variance, m²

3-1 INTRODUCTION

This chapter provides quantitative data on natural atmospheric extinction to enable the user to characterize this atmosphere for systems performance calculations. It also gives weather data for four different types of climate—temperate, tropical, desert, and northern.

Par. 3-2 is designed to provide atmospheric data for user-specified weather conditions. It contains tables and equations designed for use in the calculation of atmospheric extinction by water vapor and other gaseous molecules, and aerosol extinction due to haze, fog, clouds, rain, snow, or blowing dust. Data are provided for the visible (0.4-0.7μm) and near infrared (IR) (0.7-1.1μm) spectral bands, the thermal bands (3-5 and 8-12μm), the Nd:YAG (1.06μm) and CO_2 (10.591μm) laser lines, and at 35 GHz and 94 GHz millimeter wave (mmw) frequencies.

Four types of climate are described briefly in par. 3-3: a temperate region, represented by the central European highlands; a tropical climate, represented by Central America; a desert climate, represented by the Mideast desert region; and a high-latitude northern climate, represented by eastern Scandinavia. The specific locales were selected both because of the range of weather types they include and because of the availability of complete, reliable meteorological records. Par. 3-3 also contains seasonal average meteorological observations for these locations, designed to familiarize the engineer with the variety of weather conditions in which a system design will have to operate.

More detailed information about the frequency of occurrence of naturally obscured weather for these locations is included in pars. 3-4 through 3-7. This detailed information will give the engineer a clearer picture of the types of weather under which a system must operate and the relative frequency of these conditions. Illustrations of the variation in atmospheric transmittance are included for representative European and Mideast locations in plots of cumulative frequency of atmospheric transmittance in the visible, thermal, and mmw spectral regions.

3-2 OPTICAL PROPERTIES OF NATURAL OBSCURATION FACTORS

The tables and equations in this paragraph are used to obtain values for atmospheric transmittance through the natural atmosphere for user-specified weather conditions. Par. 3-2.1 treats molecular absorption and scattering by the clear natural atmosphere. Additional transmittance losses due to atmospheric aerosol absorption and scattering, rain, snow, and blowing dust are treated in pars. 3-2.2 through 3-2.5.

The total atmospheric transmittance $T(\lambda)$ for a given path length (range to target) is the product of the clear

atmosphere molecular transmittance term $T_m(\lambda)$, the atmospheric aerosol transmittance term $T_a(\lambda)$ or atmospheric precipitation transmittance term $T_p(\lambda)$, and the dust transmittance term $T_d(\lambda)$ or smoke transmittance term $T_s(\lambda)$. In the absence of precipitation

$$T(\lambda) = T_m(\lambda)T_a(\lambda)T_s(\lambda)T_d(\lambda), \quad (3-1)$$
dimensionless

where

λ = wavelength, μm

$T_m(\lambda)$ = atmospheric transmittance considering only molecular extinction, dimensionless

$T_a(\lambda)$ = atmospheric transmittance considering only aerosol extinction, dimensionless

$T_s(\lambda)$ = transmittance through smoke, dimensionless

$T_d(\lambda)$ = transmittance through dust, dimensionless.

If it is raining or snowing,

$$T(\lambda) = T_m(\lambda)T_p(\lambda)T_s(\lambda)T_d(\lambda), \quad (3-2)$$
dimensionless

where

$T_p(\lambda)$ = atmospheric transmittance considering only precipitation, dimensionless.

If there is no smoke, $T_s(\lambda) = 1.0$.

If there is no dust, $T_d(\lambda) = 1.0$.

This chapter characterizes transmittance through the natural atmosphere, which includes precipitation and blowing dust. The information in Chapter 4 addresses transmittance calculations through battlefield-induced contaminants including smokes, high explosive (HE) generated dust, dust raised by vehicular traffic, and fire products.

Values are tabulated in this chapter for the visible (0.4-0.7μm), near IR (0.7-1.1μm), and thermal spectral bands (3-5μm and 8-12μm) as well as for discrete wavelengths at the 1.06μm (Nd:YAG laser) and 10.591 μm (CO_2 laser) laser lines, and the 35 GHz and 94 GHz mmw lines. When using values from different subparagraphs for molecular absorption and scattering, the engineer must make sure the meteorological conditions used to calculate each transmittance term are compatible. For instance, rain should occur only at temperatures above freezing; it will be accompanied by high relative humidity and limited visibility.

The equations in this paragraph may require a conversion among relative humidity, absolute humidity, and dew point, depending on the data available to the

engineer. The conversion may be performed using the relationships in Appendix B.

3-2.1 WATER VAPOR AND GASEOUS ABSORPTION

This paragraph provides equations and tables to determine atmospheric transmittance $T_m(\lambda)$ for water vapor and gaseous absorption. For the broadband thermal spectral regions (3-5μm and 8-12μm), $T_m(\lambda)$ is tabulated. For visible, near IR, laser, and mmw wavelengths, $T_m(\lambda)$ is calculated from

$$T_m(\lambda) = e^{-\gamma_m(\lambda)R}, \text{dimensionless} \quad (3-3)$$

where

$R =$ path length, km

$\gamma_m(\lambda) =$ molecular volume extinction coefficient for any wavelength λ, km^{-1}.

3-2.1.1 Visible

Molecular extinction and water vapor absorption have a minor effect in the visible spectral region; visible transmittance is dominated by aerosol absorption and scattering.

A representative value for $\gamma_m(\lambda)$ in the visible region is 0.02 km^{-1} for both a low humidity environment (3.5 g/m^3 water vapor) and for a high humidity environment (14 g/m^3 water vapor).

3-2.1.2 Near IR (0.7-1.1μm and 1.06μm)

Gaseous and water vapor absorption have a negligible effect at the 1.06μm Nd:YAG laser line. The molecular transmittance term $T_m(\lambda)$ is equal to 1.0 at 1.06μm. Gaseous and water vapor absorption have a minor effect in the near IR band out to 1.1μm. The magnitude can be calculated using Eq. 3-3, with

$\gamma_m(0.7-1.1\mu m) = 0.02$ km^{-1} (low humidity) and
$\qquad\qquad\qquad 0.03$ km^{-1} (high humidity).

These numbers represent typical values for a ground level midlatitude (European) atmosphere. Actual transmittance in the near IR is somewhat wavelength dependent; absorption increases as one moves from the 0.7-0.9 μm region to the 0.9-1.1 μm region. More detailed data may be obtained by using atmospheric transmittance codes such as LOWTRAN or FASCODE* (Refs. 1 and 2).

3-2.1.3 Thermal (3-5 and 8-12μm)

Thermal band transmittance is sensitive to water vapor content and thus to relative humidity (RH) and temperature. Band-averaged transmittance in the 3-5 and 8-12 μm spectral regions does not scale exponentially with range for the reasons discussed in par. 2-3.2. Thus the thermal molecular transmittance term $T_m(\lambda)$ is provided in tabular form. Table 3-1 contains $T_m(3-5\mu m)$; Table 3-2 contains $T_m(8-12\mu m)$. These tables give transmittance for a range of values of temperature and relative humidity over six ground level path lengths between one and 20 km. Transmittance over path lengths between these values may be estimated by interpolation. The tables were derived using LOWTRAN 5 with no aerosol contribution.

3-2.1.4 CO₂ Laser (10,591μm) and Millimeter Wave (35 GHz and 94 GHz)

The atmospheric molecular transmittance term $T_m(\lambda)$ at CO_2 laser and mmw wavelengths is calculated using Eq. 3-3. The volume molecular extinction coefficient $\gamma_m(\lambda)$ depends on atmospheric water vapor content. Table 3-3 gives values of $\gamma_m(\lambda)$ at the 10.591μm CO_2 laser line, 35 GHz, and 94 GHz; these values were generated using Electro-Optical Systems Atmospheric Effects Library (EOSAEL) 82 (Ref. 3).

3-2.2 HAZE, FOG, AND CLOUDS

Extinction of radiation by haze, fog, and clouds varies slowly with wavelength. The aerosol transmittance term $T_a(\lambda)$ can be expressed using an equation of the same form as Eq. 3-3:

$$T_a(\lambda) = e^{-\gamma_a(\lambda)R}, \text{dimensionless} \quad (3-4)$$

where

$\gamma_a(\lambda) =$ aerosol volume extinction coefficient for any wavelength λ, km^{-1}.

3-2.2.1 Visible (0.4-0.7μm)

Aerosol extinction in the visible region is scaled to visibility. In this handbook the definition of meteorological range is used for visibility. Meteorological range is the range at which an object with a contrast of 1.0 can just be perceived visually against the background with the visual contrast threshold set at 0.02 * The expression for visual aerosol extinction coefficient then becomes

---

*The LOWTRAN code is used to calculate atmospheric transmittance and path radiance with low spectral resolution (20 cm^{-1}) and is used for broadband calculations. FASCODE is used to calculate atmospheric transmittance with high spectral resolution and can be used for laser and mmw line calculations.

*In practice, observations of visibility are not precise because they rely on the judgement of a human observer. In addition, the visibility is not precisely defined; the World Meteorological Organization, for example, uses a 5% transmittance standard in its field equipment.

TABLE 3-1
3-5μm BAND-AVERAGED ATMOSPHERIC TRANSMITTANCE (No Aerosols)

		Transmittance $T_m(\lambda)$, dimensionless						
Relative Humidity RH, %	Temperature T, °C	Path Length R, km						
		1	3	5	7	10	15	20
10	0	0.77	0.68	0.62	0.58	0.53	0.47	0.43
	10	0.74	0.64	0.58	0.53	0.48	0.42	0.38
	20	0.71	0.60	0.53	0.49	0.44	0.38	0.33
	30	0.67	0.55	0.48	0.44	0.39	0.33	0.29
40	0	0.70	0.58	0.51	0.47	0.41	0.35	0.31
	10	0.66	0.53	0.46	0.41	0.36	0.30	0.25
	20	0.61	0.47	0.40	0.35	0.30	0.24	0.20
	30	0.56	0.42	0.35	0.30	0.25	0.19	0.15
70	0	0.65	0.53	0.46	0.41	0.36	0.30	0.25
	10	0.61	0.47	0.40	0.35	0.30	0.24	0.20
	20	0.56	0.41	0.34	0.29	0.24	0.18	0.14
	30	0.50	0.36	0.28	0.23	0.18	0.13	0.09
90	0	0.64	0.51	0.44	0.39	0.33	0.27	0.23
	10	0.59	0.45	0.37	0.33	0.27	0.21	0.17
	20	0.53	0.39	0.31	0.26	0.21	0.15	0.12
	30	0.48	0.33	0.25	0.20	0.15	0.10	0.07

TABLE 3-2
8-12μm BAND-AVERAGED ATMOSPHERIC TRANSMITTANCE (No Aerosols)

		Transmittance $T_m(\lambda)$, dimensionless						
Relative Humidity RH, %	Temperature T, °C	Path Length R, km						
		1	3	5	7	10	15	20
10	0	0.97	0.95	0.93	0.91	0.89	0.86	0.84
	10	0.97	0.95	0.91	0.89	0.86	0.82	0.79
	20	0.95	0.91	0.87	0.85	0.81	0.76	0.71
	30	0.94	0.87	0.82	0.78	0.72	0.65	0.59
40	0	0.95	0.89	0.86	0.82	0.78	0.72	0.67
	10	0.92	0.84	0.77	0.72	0.65	0.55	0.48
	20	0.87	0.73	0.62	0.54	0.43	0.31	0.22
	30	0.78	0.54	0.39	0.28	0.18	0.09	0.04
70	0	0.93	0.84	0.78	0.73	0.66	0.56	0.49
	10	0.87	0.73	0.62	0.53	0.42	0.30	0.22
	20	0.77	0.52	0.36	0.26	0.15	0.07	0.03
	30	0.59	0.25	0.11	0.05	0.02	0.0	0.0
90	0	0.91	0.80	0.72	0.66	0.57	0.46	0.38
	10	0.83	0.64	0.51	0.41	0.30	0.18	0.11
	20	0.69	0.39	0.23	0.13	0.06	0.02	0.01
	30	0.46	0.12	0.04	0.01	0.0	0.0	0.0

TABLE 3-3
GASEOUS AND WATER VAPOR EXTINCTION COEFFICIENTS FOR
CO₂ LASER AND MILLIMETER WAVE WAVELENGTHS

ABSOLUTE HUMIDITY, ρ, g/m³	EXTINCTION COEFFICIENT $\gamma_m(\lambda)$, km⁻¹		
	10.591 μm	55 GHz	94 GHz
1	0.083	0.018	0.025
3	0.091	0.021	0.043
5	0.109	0.024	0.067
10	0.185	0.032	0.108
15	0.311	0.041	0.154
20	0.383	0.049	0.201

$$\gamma_a(0.4\text{-}0.7\mu m) = 3.912/V, \quad km^{-1} \quad (3\text{-}5)$$

where

V = visibility, km.

The value $3.912/V$, used as the extinction coefficient, gives a visual transmittance of 0.02 if the path length and the visual range are equal.

3-2.2.2 Near IR (0.7-1.1 μm and 1.06 μm)

Aerosol extinction in the near IR also may be scaled to visibility. For the 1.06 μm Nd:YAG laser line, the aerosol extinction coefficient used in Eq. 3-4 is (Ref. 3)

1. V greater than 0.6 km

$$\gamma_{a1}(1.06) = 10^{[0.146 + 1.16 \log_{10}(3.912/V)]}, \quad km^{-1} \quad (3\text{-}6)$$

2. V less than or equal to 0.6 km

$$\gamma_{a2}(1.06) = 3.912/V, \quad km^{-1} \quad (3\text{-}7)$$

In haze the broadband 0.7-1.1 μm extinction coefficient can be estimated using Eq. 3-8, which was derived from LOWTRAN 5 calculations.

$$\gamma_a(0.7\text{-}1.0) = 0.6\,(3.912/V), \quad km^{-1} \quad (3\text{-}8)$$

In fogs the visible aerosol extinction coefficient may be used to calculate near IR extinction.

3-2.2.3 Thermal Bands (3-5 and 8-12 μm) and the CO₂ Laser Line (10.591 μm)

Thermal transmittance is decreased only slightly by haze. Transmittance through fog depends strongly on water vapor, liquid water content, and particle size distribution. Table 3-4 gives aerosol extinction coefficients in the thermal bands for three representative conditions: an urban haze, with a 2-, 5-, or 15-km visibility; a radiation fog, with 0.5-km and 1.0-km visibility; and an advection fog, with 0.5-km and 1.0-km visibility.

TABLE 3-4
AEROSOL EXTINCTION COEFFICIENTS FOR THERMAL RADIATION

AEROSOL	AEROSOL EXTINCTION COEFFICIENT $\gamma_a(\lambda)$, km⁻¹		
	3-5 μm	8-12 μm	10.591 μm
Urban Haze			
2 km visibility	0.29	0.18	0.10
5 km visibility	0.11	0.07	0.06
10 km visibility	0.06	0.04	0.03
15 km visibility	0.04	0.02	0.02
Radiation Fog*			
0.5 km visibility	10.1	2.4	1.7
1.0 km visibility	5.1	1.2	0.9
Advection Fog*			
0.5 km visibility	8.4	9.0	8.9
1.0 km visibility	4.2	4.5	4.5

*Radiation and advection fogs are discussed in par. 2-4.2.

Thermal transmittance through clouds will generally be as poor as visual transmittance. The transmittance of thermal radiation through clouds depends on the liquid water content of the cloud and the radiation wavelength. The extinction coefficient at $10.591\mu m$ can be estimated by

$$\gamma_a (10.591\mu m) = 159\, w, \quad km^{-1} \quad (3\text{-}9)$$

where

w = liquid water content, g/m^3.

The extinction coefficient in the 8-12μm band varies from $300w$ at 8μm to $130w$ at 11μm. In the 3-5μm band the extinction coefficient varies from $1330w$ at 3μm to $530w$ at 5μm (Ref. 4).

Liquid water content in clouds depends on the type of cloud. The water content ranges from 0.02 to 1.5 g/m^3 for cumulus clouds to 0.02 to 0.60 g/m^3 for stratus clouds (Ref. 5). If the value of w is not known, it may be estimated from (Ref. 3)

$$w = 5.95 \times 10^{-3} V^{-1.33}, g/m^3. \quad (3\text{-}10)$$

This expression is valid only in clouds.

3-2.2.4 Millimeter Wave (35 GHz and 94 GHz)

Millimeter wave radiation is not seriously attenuated by haze. Millimeter wave extinction through fogs and clouds depends on the liquid water content of the aerosol and the index of refraction, which is temperature dependent. Aerosol extinction coefficients for fog and clouds are calculated from liquid water content using

$$\gamma_a(mmw) = \frac{6w\pi}{10^3\lambda} Im\left[-\frac{(m^2(\lambda) - 1)}{(m^2(\lambda) + 2)}\right] \quad (3\text{-}11)$$

where

$m(\lambda)$ = complex index of refraction, dimensionless

Im = imaginary part of bracketed expression, dimensionless.

Values for the extinction coefficient at 35 GHz and 94 GHz, calculated using EOSAEL algorithms (Ref. 3), are listed in Table 3-5.

3-2.3 RAIN

The transmittance through precipitation $T_p(\lambda)$ is

$$T_p(\lambda) = e^{-\gamma_p(\lambda)R}, \text{ dimensionless} \quad (3\text{-}12)$$

where

$\gamma_p(\lambda)$ = precipitation volume extinction coefficient for any wavelength λ, km^{-1}.

The value of the precipitation volume extinction coefficient depends on the type of precipitation—rain or snow—and on wavelength.

TABLE 3-5
VALUES OF THE AEROSOL EXTINCTION COEFFICIENT FOR WATER AT 35 GHz AND 94 GHZ

AEROSOL EXTINCTION COEFFICIENT $\gamma_a(\lambda)$, km^{-1}		
Temperature T, °C	35 GHz	94 GHz
0	0.24 w	1.11 w
10	0.19 w	1.01 w
20	0.15 w	0.88 w
30	0.12 w	0.76 w

At visible and thermal wavelengths, rain droplet sizes are large with respect to the radiation wavelength, so the scattering efficiency factor may be assumed to be 2.0. In these regions, then, the extinction due to scattering from rain will depend only on particle size distribution, not on wavelength. Empirical relationships developed by Laws and Parsons (Ref. 6) for widespread rain (Eq. 3-14) and equations developed by Joss and Waldvogel (Ref. 7) for drizzle and thunderstorms (Eqs. 3-13 and 3-15) are used to estimate the precipitation volume extinction coefficient $\gamma_p(\lambda)$ due to rain. The equations used for visible through thermal wavelengths are

1. Drizzle

$$\gamma_{prd}(vis, thermal) = 0.51r^{0.63}, km^{-1} \quad (3\text{-}13)$$

2. Widespread rain

$$\gamma_{prw}(vis, thermal) = 0.36r^{0.63}, km^{-1} \quad (3\text{-}14)$$

3. Thunderstorms

$$\gamma_{prt}(vis, thermal) = 0.16r^{0.63}, km^{-1} \quad (3\text{-}15)$$

where

r = rain rate, mm/h.

At mmw wavelengths, extinction due to rain would properly be treated using a full Mie* scattering calculation over the rain particle size distribution. Because of the complexity of this approach, a power law approximation based on rain rate is used to calculate the mmw precipitation coefficient for rain (Ref. 3):

$$\gamma_{pr}(mmw) = ar^b, km^{-1} \quad (3\text{-}16)$$

where

a,b = rain extinction parameters, dimensionless

and a and b vary with rain rate, mmw frequency, and temperature, as shown in Table 3-6.

*Mie scattering is discussed in par. 2-3.1.

TABLE 3-6
MILLIMETER WAVE RAIN EXTINCTION PARAMETERS

Rain	Temperature T, °C	a (35 GHz)	b (35 GHz)	a (94 GHz)	b (94 GHz)
Drizzle	0	0.0040	1.085	0.294	0.870
	20	0.0039	1.106	0.309	0.859
Widespread	0	0.062	0.951	0.335	0.638
	20	0.063	0.945	0.345	0.634
Thunderstorm	0	0.084	0.775	0.230	0.617
	20	0.082	0.771	0.230	0.614

3-2.4 SNOW

The transmittance $T_p(\lambda)$ through snow may be estimated using Eq. 3-12. For visible and near IR radiation, the precipitation extinction coefficient $\gamma_{ps}(\lambda)$ for snow may be calculated from visibility:

$$\gamma_{ps} \text{ (vis, near IR)} = \frac{3.912}{V}, \text{ km}^{-1}. \quad (3\text{-}17)$$

At low relative humidities the snow extinction coefficient for the 3-5 and 8-12μm spectral bands also scales to visibility. For relative humidities greater than 94%, there is usually fog mixed with the snow. In this case, the thermal extinction coefficient of snow also depends on temperature. For both the 3-5 and 8-12 μm thermal bands at low relative humidities, the visual scattering coefficient in the presence of snow may be used with the assumption that the scattering is in the geometric optics regions, and the Mie scattering coefficient is 2.0 for both visual and thermal radiation. However, visual scattering is strongly peaked in the forward direction; thermal radiation is scattered over a wider angle. Thus the measured thermal extinction (and that seen by a wide-aperture thermal sensor) may be much higher.

The thermal precipitation extinction coefficient in snow may be estimated by

$$\gamma_{ps} \text{ (thermal)} = \frac{3.912}{V}, \text{ km}^{-1}. \quad (3\text{-}18)$$

Data on mmw extinction by snow is extremely scarce. Extinction of mmw radiation by snow may be approximated using a power law relationship (Ref. 8):

$$\gamma_{ps} \text{(mmw)} = c r_s^d, \text{ km}^{-1} \quad (3\text{-}19)$$

where

    c, d = snow extinction parameters, dimensionless

    r_s = rain equivalent snow rate, mm/h.

The values of c and d depend on the wetness of the snow and the mmw wavelength. Values for c and d are listed in Table 3-7.

TABLE 3-7
MILLIMETER WAVE SNOW EXTINCTION PARAMETERS

Snow Type	c (35 GHz)	d (35 GHz)	c (94 GHz)	d (94 GHz)
Dry	0.0125	1.60	0.08	1.26
Moist	0.160	0.95	0.31	0.75
Wet	0.235	0.95	0.61	0.75

3-2.5 BLOWING DUST

The transmittance through blowing dust $T_d(\lambda)$ is calculated using the spectral mass extinction coefficient for dust and the concentration path length product (CL) of dust in the atmosphere:

$$T_d(\lambda) = e^{-\alpha_d(\lambda) \, CL}, \text{ dimensionless} \quad (3\text{-}20)$$

where

    $\alpha_d(\lambda)$ = dust mass extinction coefficient for any wavelength λ, m²/g

    CL = concentration path length product of dust, g/m².

The CL product of dust in the path is found by multiplying the mass loading Z by the path length R. Mass extinction coefficients for dust are given in Table 3-8.* Mass loading of dust into the atmosphere may be estimated from the visibility through dust by using the values given in Table 3-9.

In the absence of blowing dust or dust storms, values of ambient dust concentration range from 1-2×10^{-5} g/m³ for rural regions to 4-15×10^{-4} g/m³ for industrial areas.

3-2.6 OPTICAL TURBULENCE

The effects of turbulence are most pronounced on active systems using laser sources and least important

*Transmittance through dust exhibits some spectral dependence. The spectral mass extinction coefficient depends on the composition of the dust, e.g., clay or quartz. Detailed spectral transmittance plots for different soils are found in Ref. 10.

TABLE 3-8
MASS EXTINCTION COEFFICIENTS
FOR DUST (Ref. 3)

WAVELENGTH λ	MASS EXTINCTION COEFFICIENT $\alpha_d(\lambda)$, m^2/g
visi 'e (0.4-0.7μm)	0.32
near IR (0.7-1.1μm)	0.30
1.06μm	0.29
3-5μm	0.27
8-12μm	0.25
10.6μm	0.25
33, 94 GHz	0.001

TABLE 3-9
MASS LOADING
FROM VISIBILITY (Ref. 9)

VISIBILITY V, km	MASS LOADING Z, g m^3
0.2	1.1×10^{-1}
0.47	6.9×10^{-2}
1.0	2.1×10^{-2}
3.2	5.2×10^{-3}
8.0	2.0×10^{-3}

for passive imagers. The effect of turbulence decreases with increasing wavelength. Turbulence causes beam spreading, beam wander, and scintillation (fluctuations) in laser illumination. These effects are characterized by the beam radius, beam centroid displacement, and the variance or covariance of the irradiance. The effect of scintillation on system performance is decreased by averaging the power fluctuations over the receiver aperture (aperture averaging); the larger the receiver aperture, the smaller the effect of scintillation. Imaging system degradation by turbulence-induced blur or image motion is characterized by the optical transfer function (or coherence length r_0) and the wave front tilt.

The effects of turbulence on laser and imaging systems are summarized in Table 3-10. The appropriate measure of turbulence effect is given in the right column. The equations for calculating these quantities are explained in this paragraph. More detailed treatments of turbulence can be found in Refs. 11, 12, and 13.

Laser beam spread can be expressed in terms of the Strehl ratio, which is the ratio of the average on-axis irradiance with turbulence to the average on-axis irradiance without turbulence. The Strehl ratio is given by (Ref. 12)

1. Long-Term

$$S_l = [1 + (D/r_0)^2]^{-1}, \text{ dimensionless} \quad (3\text{-}21)$$

TABLE 3-10
OPTICAL TURBULENCE EFFECTS

Laser Systems	Descriptor
Beam Spread	
Short-Term	Strehl Ratio
Long-Term	Strehl Ratio
Beam Wander	Centroid Movement
Imaging Systems	**Descriptor**
Short-Term Blur	Optical Transfer Function Loss
Long-Term Blur	Optical Transfer Function Loss
Image Motion	Centroid Movement

2. Short-Term

a. $D/r_0 \leq 3$

$$S_{s1} = [1 + 0.182 (D/r_0)^2]^{-1}, \text{ dimensionless} \quad (3\text{-}22)$$

b. $D/r_0 > 3$

$$S_{s2} = [1 + (D/r_0)^2 - 1.18 (D/r_0)^{5/3}]^{-1}, \quad (3\text{-}23)$$
$$\text{dimensionless}$$

where

D = effective laser aperture diameter, m

S_l = long-term Strehl ratio, dimensionless

S_s = short-term Strehl ratio, dimensionless.

The ratio of the beam diameter with turbulence to the beam diameter without turbulence is equal to (Strehl ratio)$^{-1/2}$. If the turbulence is uniform, the coherence length r_0 is (Ref. 12)

$$r_0 = 0.3325(10^{-6}\lambda)^{6/5} (10^3 C_n^2 R)^{-3/5}, \text{ m} \quad (3\text{-}24)$$

where

C_n^2 = index of refraction structure constant, $m^{-2/3}$.

This expression for r_0 applies for ranges of tactical interest. If turbulence is not uniform, the turbulence closest to the laser source will have the strongest effect. Daytime values of turbulence may range from C_n^2 of 10^{-14} $m^{-2/3}$ (weak) to 6×10^{-14} $m^{-2/3}$ (moderate) to 6×10^{-13} $m^{-2/3}$ (strong).

For homogeneous turbulence, the root mean square (rms) full width beam wander D_w is (Ref. 13)

1. $D/r_0 \leq 3$

$$D_{w1} = 0.245 \, \lambda^{-1/5} \, C_n^{6/5} \, (10^3 R)^{8/5}, \text{ m} \quad (3\text{-}25)$$

2. $D/r_0 > 3$

$$D_{w2} = 0.245 \, C_n \, (10^3 R)^{1/2} \, D^{-1/6}, \text{ m}. \quad (3\text{-}26)$$

Scintillation may be approximated by (Ref. 13)

$$\sigma_I^2 = 1.24 \, C_n^2 \, (2\pi/\lambda)^{7/6} \, (10^3 R)^{11/6}, \, W^2 \quad (3\text{-}27)$$

where

σ_I^2 = variance in average irradiance, W^2.

The effects of turbulence saturate at long ranges or in strong turbulence; in general, σ_I^2 does not exceed 0.5.

Turbulence effects on imaging systems are generally minor. For an ideal diffraction-limited system, as the aperture is increased above r_0, the limiting resolution becomes equal to that of a diffraction-limited system with a diameter r_0.

The image centroid wander for an imaging system in homogeneous turbulence is characterized by its single-axis variance σ_x^2 (Ref. 13):

$$\sigma_x^2 = 1.093 \, F^2 \, D^{-1/3} \, C_n^2 \, 10^3 \, R \, , \, m^2 \quad (3\text{-}28)$$

where

F = focal length, m.

3-2.7 ILLUMINATION

The performance of visual and near IR systems depends on reflected natural illumination (ambient light level), i.e., on daylight and the reflected night sky radiance. Passive thermal signatures are influenced by solar heating or insolation. There is a wide variation in the available light level and insolation. The daytime ambient light level and insolation are determined by location, season, time of day, and cloud cover. Night-time ambient light level is determined by starlight, phase of the moon, and cloud cover, as well as by scattered man-made illumination.

The variation of natural light level is shown in Table 3-11, which gives illumination values for day and night conditions. Daytime light level is affected by cloud cover and solar angle (time of day, location, and season). Night light levels change with lunar phase and cloud cover. The range of naturally occurring light levels with season is illustrated by Fig. 3-1, which shows typical light levels for day and night conditions as a function of sun or moon angle. The shaded band is the night sky illuminance. Frequency of occurrence of light level for Germany at night is tabulated, by season, in Ref. 15. Seasonal solar insolation variations are available in Ref. 16 as world maps with insolation contour overlays. Fig. 3-2 is a sample of these data. Mean monthly cloud cover variations are available in similar form in Ref. 17 as illustrated in Fig. 3-3. A comprehensive procedure for scaling insolation using cloud cover observations is described in Ref. 18.

TABLE 3-11
NATURALLY OCCURRING LIGHT
LEVEL (Ref. 14)

Ambient Light	Light Level (lm/m²)
Overcast Night Sky	5×10^{-4}
Clear Night Sky	1×10^{-3}
¼ Moon	2×10^{-2}
Full Moon	1×10^{-1}
Overcast Day	5×10^{3}
Bright Day	5×10^{4}

3-3 DESCRIPTION OF SELECTED NATURAL ENVIRONMENTS

The natural environments selected for inclusion in this handbook represent temperate, tropical, desert, and high-latitude northern climates. The temperate northern European highland region includes the southern part of the Federal Republic of Germany, excluding the Rhine Valley, and portions of France, Switzerland, Czechoslovakia, and East Germany. The tropical Central American region includes the interior of Central America. The Mideast desert region includes most of Iran, Iraq, Syria, Jordan, the Saudi peninsula, Egypt, and Sudan, except for the region surrounding the Persian Gulf, Mediterranean Sea, and Red Sea. The high-
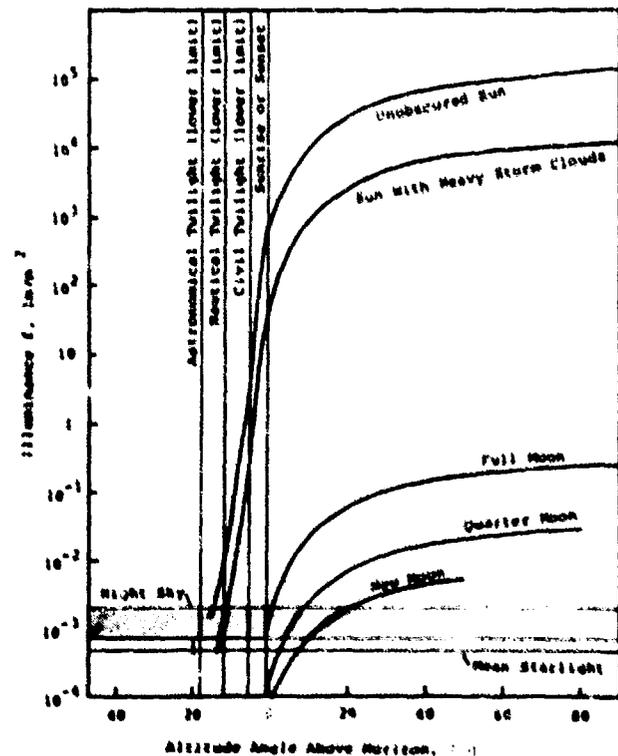
Figure 3-1. Light Level Under Various Atmospheric Conditions

Mean Solar Radiation, g-cal/(cm²/day)
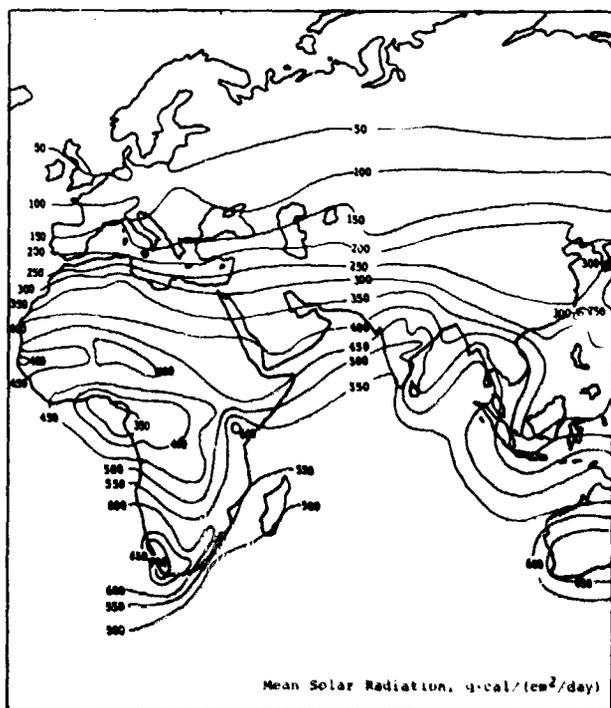
George O. Lof, et al., *World Distribution of Solar Radiation*, Solar Energy Laboratory, Report 21, University of Wisconsin, Madison, WI, 1966.

Figure 3-2. Solar Insolation, January (Ref. 16)

latitude region includes eastern Scandinavia but excludes the western coastal regions and the northern tundra.

A brief climatological description of these four locations is included in pars. 3-3.1 through 3-3.4. The paragraphs also contain summary weather charts for each region, which are broken down by season and time of day. These indicate the expected values of temperature, relative humidity, absolute humidity, wind speed, cloud cover, and Pasquill stability category. For a discussion of Pasquill category see par. 2-8.2.

Detailed information on the causes and frequency of naturally obscured weather in these regions is included in pars. 3-4 through 3-7. Frequency of occurrence of transmittance data in the visible, IR, and mmw spectral regions is included for cities in the European and Mideast desert regions. These transmittance data permit the system designer to gauge the variation of atmospheric transmittance conditions and to estimate how often the system may encounter marginal transmittance conditions.

The weather data and transmittance data in pars. 3-3 through 3-7 were provided by the US Army Atmospheric Sciences Laboratory (ASL) and are based on the USAF Air Weather Service meteorological data base, the ASL EOSAEL computer code (Ref. 3), and the Glo-
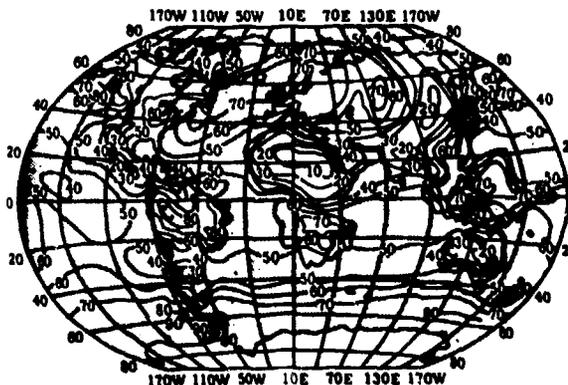
Figure 3-3. Mean Cloudiness in Percentage of Sky Cover, January (Ref. 17)

bal Electro-Optics Systems Environment Matrix (GEOSEM) data base (Ref. 19).

3-3.1 TEMPERATE ZONE (EUROPEAN HIGHLANDS)

The area included in the European highlands region is shown in the shaded area of Fig. 3-4. "The climate of the highlands is continental in nature, but topography plays an important part in the occurrence of adverse weather. The diversified topography is characterized by low rolling mountains interspersed with long, winding river valleys. This area represents a transition between the mild, wet winters to the northwest and very cold, dry Soviet winters. This region is influenced by both weather regimes. Precipitation decreases from the west to the east. More precipitation occurs in the summer than in the winter." (Ref. 3). Summary weather statistics for the highlands are shown in Table 3-12.

3-3.2 TROPICS (CENTRAL AMERICA)

Central America has a tropical climate strongly affected by the trade winds. The climate has two distinct
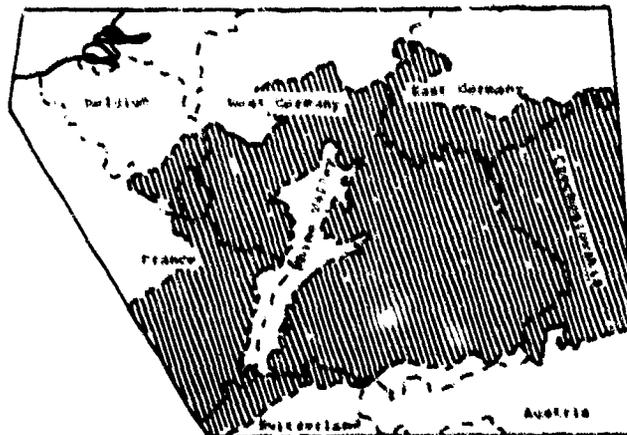
Figure 3-4. European Highlands Region (Ref. 3)

TABLE 3-12
EUROPEAN HIGHLANDS WEATHER SUMMARY CHART
(Mean value of observations reported over a 10-year period)

	Temper- ature T, °C	Absolute Humidity ρ, g/m³	Visibility V, km	Wind Velocity* Mean/σ, m/s	Cloud Height, km	Cloud Cover* Mean/σ, %	Pasquill Category** (% of observations in each category)					
							A	B	C	D	E	F
Spring Hours												
20-02	5.8	5.9	11.5	3.1/3.5	1.9	54/40	0.0	0.0	0.0	41.2	16.2	42.6
03-09	4.3	5.8	9.6	3.1/3.5	1.8	63/39	0.0	4.2	14.3	55.1	6.9	19.5
10-14	9.0	6.0	12.9	4.2/3.3	2.1	68/33	2.4	19.8	17.6	60.3	0.0	0.0
15-19	10.1	5.9	14.8	4.1/3.2	2.5	67/32	0.3	5.1	16.2	66.2	5.0	7.1
Summer Hours												
20-02	14.2	10.0	12.2	2.3/2.8	2.2	51/39	0.0	0.0	0.0	27.7	16.0	56.3
03-09	12.6	9.8	9.7	2.3/2.9	2.0	56/39	0.0	13.5	15.8	38.5	6.4	25.9
10-14	18.3	10.1	13.9	3.6/2.7	2.1	61/33	8.7	27.9	21.4	42.0	0.0	0.0
15-19	19.3	9.9	16.1	3.5/2.7	2.7	61/32	0.7	10.7	24.3	64.3	0.0	0.0
Fall Hours												
20-02	9.1	8.0	9.7	2.6/3.4	1.6	54/42	0.0	0.0	0.0	37.4	13.4	49.2
03-09	7.8	7.7	7.9	2.6/3.3	1.6	63/39	0.0	0.0	12.6	53.3	7.6	26.4
10-14	12.3	8.3	11.3	3.6/3.3	2.1	65/34	1.6	18.4	22.7	57.4	0.0	0.0
15-19	12.9	8.3	12.9	3.3/3.2	2.6	62/35	0.0	3.7	14.5	49.9	8.7	23.2
Winter Hours												
20-02	0.4	4.6	8.1	3.7/4.0	1.2	73/37	0.0	0.0	0.0	63.7	11.2	25.1
03-09	-0.2	4.5	7.7	3.7/4.2	1.1	76/35	0.0	0.0	0.0	67.3	10.3	22.4
10-14	1.4	4.7	8.6	4.1/4.0	1.6	78/31	0.0	5.7	17.7	76.5	0.0	0.0
15-19	1.8	4.7	9.2	3.9/3.9	1.7	75/33	0.0	0.0	7.2	73.9	6.6	12.3

*Entries are mean/standard deviation.

**For a discussion of Pasquill category see par. 2-8.2.

phases: a dry season extending from January through April and a wet season from June to October with transitional seasons between. Rain is heavier on the Atlantic side than on the Pacific side or in the interior mountains. Fog seldom occurs on the coast; the interior stations occasionally have shallow morning fogs, which dissipate quickly. Dust storms may be stirred up by northers in the dry season; these cause limited visibility (Ref. 19).

The area included in the Central American climatology is shown in the shaded area of Fig. 3-5. Summary weather statistics for the Central American interior region are shown in Table 3-13.

3-3.3 DESERT (MIDEAST DESERT)

The areas included in the Mideast desert climatology are shown in the shaded area of Fig. 3-6. "The desert regions comprise the greatest climatic classification in
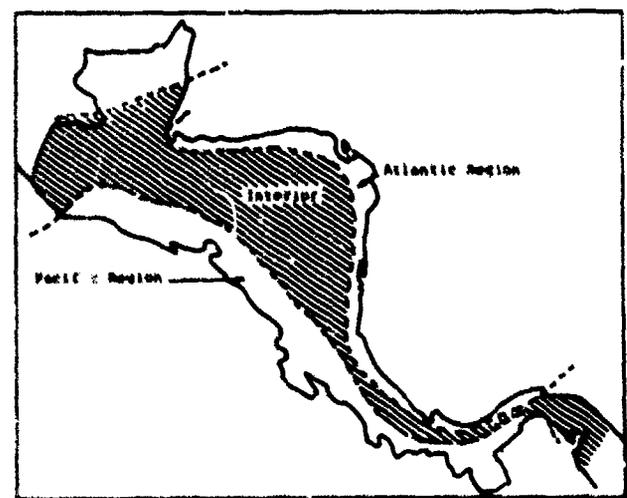
Figure 3-5. Central American Region (Ref. 19)

TABLE 3-13
CENTRAL AMERICAN INTERIOR WEATHER SUMMARY CHART
(Mean value of observations reported over a 10-year period)

	Temperature T, °C	Absolute Humidity ρ, g/m³	Visibility V, km	Wind Velocity* Mean/σ, m/s	Cloud Height, km	Cloud Cover* Mean/σ, %	Pasquill Category** (% of observations in each category)					
							A	B	C	D	E	F
Spring Hours												
20-02	22.7	12.1	14.5	2.2/1.7	5.8	64/35	0.0	0.0	0.0	25.8	27.2	47.0
03-09	22.2	12.4	14.4	1.5/1.8	6.7	66/27	6.9	18.6	37.5	21.5	3.5	11.9
10-14	28.6	12.1	18.2	3.0/2.0	6.9	66/20	32.8	27.6	29.4	10.2	0.0	0.0
15-19	28.0	12.1	16.8	3.3/2.1	9.8	70/23	3.3	17.4	27.5	51.8	0.0	0.0
Summer Hours												
20-02	21.0	14.9	17.1	1.6/1.9	6.8	73/27	0.0	0.0	0.0	21.3	23.3	55.4
03-09	21.0	15.1	16.6	1.6/1.8	8.3	74/21	7.5	16.6	34.3	26.3	3.5	11.8
10-14	26.4	14.0	21.0	3.2/2.1	9.4	74/17	31.2	22.0	32.3	14.4	0.0	0.0
15-19	25.6	14.2	19.5	3.0/2.3	11.3	77/18	4.0	16.8	21.6	41.1	6.2	10.2
Fall Hours												
20-02	19.1	15.3	18.6	2.2/2.0	4.7	59/34	0.0	0.0	0.0	27.1	19.8	53.1
03-09	18.9	15.2	17.5	2.1/2.2	6.9	65/27	5.2	13.9	11.6	29.5	8.6	31.3
10-14	24.5	15.3	21.5	3.7/2.9	7.6	69/22	5.9	28.5	19.5	46.1	0.0	0.0
15-19	23.9	15.4	20.9	3.1/2.2	8.3	69/23	0.0	8.1	15.5	43.6	12.5	20.3
Winter Hours												
20-02	20.1	13.8	19.5	2.7/2.7	4.3	44/35	0.0	0.0	0.0	24.0	22.2	53.8
03-09	19.1	13.6	18.5	2.1/2.3	4.8	53/30	8.1	16.5	23.0	25.4	6.5	20.4
10-14	25.8	14.2	22.0	4.0/2.5	5.0	59/25	18.5	22.7	33.2	25.6	0.0	0.0
15-19	26.0	14.3	21.8	4.0/2.5	5.7	57/26	0.8	9.5	14.2	47.4	14.5	13.6

*Entries are mean/standard deviation.
**For a discussion of Pasquill category see par. 2-8.2.
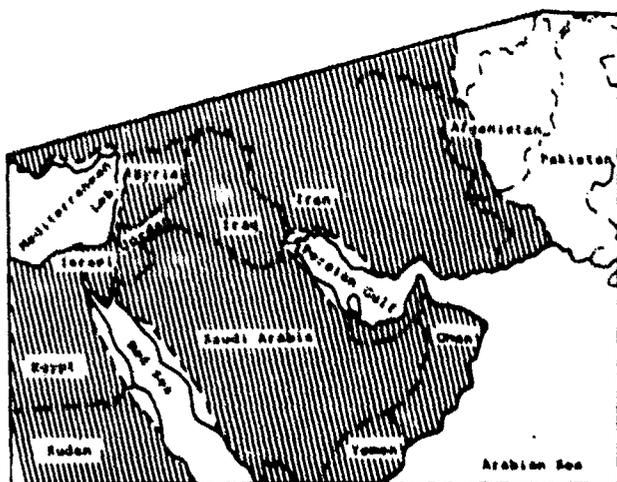
Figure 3-6. Mideast Desert Region (Ref. 3)

the Mideast area. However, one cannot ignore the difference between the deserts of the Arabian Peninsula, the high deserts of Iran and Afghanistan, the Mesopo-

tamian Plain, and the Trans-Jordan. The main differences are the temperature regimes and the frequency of occurrence of dust. Mean daily maximum and minimum temperatures in summer range between 38° to 46°C and 20° to 28°C. In the coldest winter month, usually January, afternoon temperatures range from the mid-teens to the mid-20's. However they drop to about 10°C in the higher elevations. Early morning temperatures in January range from 5°C to the low teens except in the higher elevations where somewhat lower values prevail. In general, diurnal variations in temperature are greatest in the summer. Predominantly clear skies promote intense solar heating by day and rapid radiational cooling by night, resulting in diurnal temperature ranges of 20° to 25°C. Temperatures of 38°C or higher have been observed as early as February and as late as November. Many lowland locations have recorded temperatures between 45° and 50°C, and temperatures are estimated to reach as high as 57°C in portions of Saudi Arabia. Sandstorms and duststorms are important climatic features of the desert regions.

TABLE 3-14
MIDEAST DESERT WEATHER SUMMARY CHART
(Mean value of observations reported over a 10-year period)

	Temper-ature T, °C	Absolute Humidity ρ, g/m³	Visibility V, km	Wind Velocity* Mean/σ, m/s	Cloud Height, km	Cloud Cover* Mean/σ, %	Pasquill Category** (% of observations in each category)					
							A	B	C	D	E	F
Spring												
Hours												
20-02	15.9	7.1	15.7	3.2/3.2	1.3	32/36	0.0	0.0	0.0	27.2	21.9	51.0
03-09	14.9	7.2	14.4	2.9/3.1	1.6	35/36	3.0	14.7	21.9	33.0	6.6	20.8
10-14	21.9	7.0	15.4	4.0/3.5	1.7	42/35	18.0	25.5	25.3	31.2	0.0	0.0
15-19	23.5	6.7	14.5	4.5/3.7	1.9	47/35	1.7	8.8	20.2	61.8	2.5	5.0
Summer												
Hours												
20-02	25.2	9.5	16.6	3.5/3.3	0.5	10/22	0.0	0.0	0.0	23.6	23.8	52.6
03-09	24.3	9.4	15.1	3.1/3.2	0.6	11/23	5.7	18.8	23.3	31.2	5.1	16.0
10-14	32.1	9.3	16.0	4.1/3.3	0.7	13/23	27.1	28.0	32.1	12.8	0.0	0.0
15-19	34.9	8.4	14.7	4.7/3.5	0.7	14/23	3.6	13.4	26.0	53.7	0.9	2.3
Fall												
Hours												
20-02	17.4	7.9	16.4	2.5/2.7	0.8	19/30	0.0	0.0	0.0	14.9	18.8	66.3
03-09	16.0	7.6	15.0	2.2/2.6	1.0	21/31	1.1	15.8	21.2	19.4	7.0	35.5
10-14	23.8	7.6	16.2	3.1/3.0	1.2	26/31	14.4	37.2	24.7	23.8	0.0	0.0
15-19	25.4	7.0	15.3	3.2/3.2	1.2	26/31	0.9	10.8	22.8	41.3	5.2	18.9
Winter												
Hours												
20-02	6.6	5.4	14.9	2.7/2.9	1.2	38/39	0.0	0.0	0.0	26.7	19.0	54.4
03-09	5.1	5.2	13.3	2.5/3.0	1.5	42/39	0.0	7.8	19.3	34.6	7.6	30.6
10-14	10.9	5.4	14.7	3.3/3.4	1.7	48/37	5.0	24.9	27.1	43.0	0.0	0.0
15-19	11.7	5.3	14.3	3.2/3.3	1.8	48/37	0.0	5.4	16.7	47.0	8.8	22.0

*Entries are mean/standard deviation.
**For a discussion of Pasquill category see par. 2-8.2.

Because of the vast area of the desert, the effects of these storms are felt in the other climatic regions. Visibilities are greatly reduced at times. Duststorms are most frequent in the summer and especially in the deep silt areas of the Tigris-Euphrates basin. With the intense heat of summer, strong convective currents over the area lift dust to great heights, and if the winds aloft are strong, the dust is carried great distances. The top of the dust layer could extend above 4500 m and remain suspended for days. A hazard to aircraft operations occurs when surface visibility improves but the dust layer still prevents the aircraft from seeing the ground until the aircraft descends below 200 m." (Ref. 3). Summary weather statistics for the Mideast desert region are given in Table 3-14.

3-3.4 HIGH-LATITUDE NORTHERN ENVIRONMENT (SCANDINAVIA)

The Scandinavian climate is strongly controlled by topography and air circulation patterns. The actual weather varies widely from one region to another because of the intensity and paths of low pressure centers. The Scandinavian mountain chain provides a barrier to weather systems moving from the southwest. Scandinavia is very cloudy with cloud cover averaging 65-80% of the time on the coasts. Fog occurs often in the mountains and in regions of southern Sweden (Ref. 19). The Scandinavian region is shown in the shaded area of Fig. 3-7. Summary weather statistics for the eastern Scandinavian region are included in Table 3-15.

3-4 FREQUENCY OF OCCURRENCE OF NATURAL OBSCURATION FACTORS IN THE EUROPEAN HIGHLANDS

The frequency of occurrence data presented in this paragraph for the European highlands are from the GEOSEM meteorological data base developed by the US Army ASL using data from USAF Air Weather Service Environmental Technical Applications Center

TABLE 3-15
EASTERN SCANDINAVIA WEATHER SUMMARY CHART
(Mean value of observations reported over a 10-year period)

	Temper-ature T, °C	Absolute Humidity ρ, g/m³	Visibility V, km	Wind Velocity* Mean/σ, m/s	Cloud Height, km	Cloud Cover* Mean/σ, %	Pasquill Category** (% of observations in each category)					
							A	B	C	D	E	F
Spring												
Hours												
20-02	0.2	4.1	27.0	3.0/2.6	1.5	61/40	0.0	0.0	0.0	44.5	18.4	37.1
03-09	-0.8	4.1	24.1	3.1/2.3	1.5	67/40	0.0	6.3	14.7	58.7	7.5	12.8
10-14	4.0	4.1	30.2	4.5/2.3	1.6	70/32	0.8	13.0	17.0	69.1	0.0	0.0
15-19	4.9	4.1	32.7	4.3/2.0	2.2	68/32	0.0	1.9	18.2	69.0	6.2	5.2
Summer												
Hours												
20-02	10.6	8.0	31.2	2.7/1.9	1.9	57/36	0.0	0.0	5.1	45.5	14.6	34.8
03-09	10.0	8.1	28.1	2.8/2.0	1.9	62/36	0.0	5.2	28.4	59.5	1.9	5.1
10-14	15.0	7.9	35.5	4.3/2.0	2.0	67/31	0.3	14.5	19.9	65.3	0.0	0.0
15-19	15.6	7.9	38.1	4.2/2.2	2.9	63/31	0.0	1.7	21.2	74.9	0.7	1.5
Fall												
Hours												
20-02	2.0	5.3	24.0	3.2/2.1	1.1	69/39	0.0	0.0	0.0	59.1	16.2	24.7
03-09	1.7	5.3	21.5	3.2/2.2	1.1	74/36	0.0	0.0	7.9	73.3	6.9	12.0
10-14	4.4	5.5	26.2	4.0/2.2	1.3	76/30	0.0	2.8	17.0	80.2	0.0	0.0
15-19	4.7	5.6	28.1	3.6/2.2	1.8	74/32	0.0	0.0	5.6	77.2	6.7	10.5
Winter												
Hours												
20-02	-5.8	3.3	18.9	3.5/2.7	1.0	73/39	0.0	0.0	0.0	65.6	11.8	22.6
03-09	-6.0	3.3	16.7	3.4/2.4	1.0	76/37	0.0	0.0	2.1	69.1	9.5	19.3
10-14	-4.2	3.4	19.3	3.8/2.4	1.2	76/33	0.0	1.4	14.8	80.9	0.7	2.2
15-19	-3.3	3.6	20.6	3.7/2.4	1.4	74/35	0.0	0.0	1.5	71.4	10.4	16.7

*Entries are mean/standard deviation.

**For a discussion of Pasquill category see par. 2-8.2.
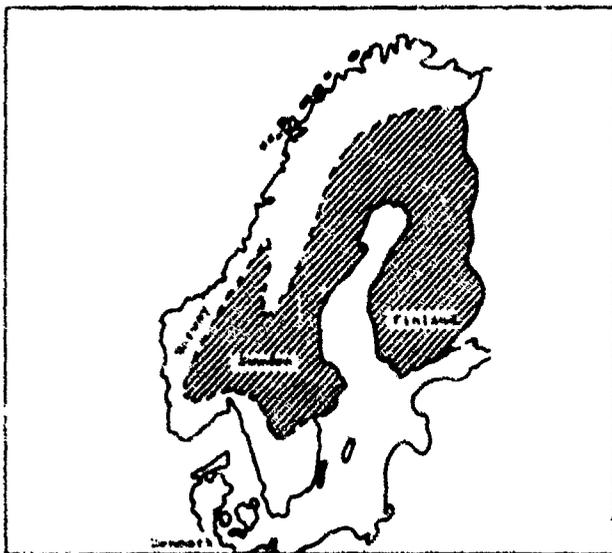
Figure 3-7. Eastern Scandinavian Region (Ref. 19)

(ETAC) meteorological observations. Atmospheric transmittance data were developed by ASL using ETAC data for individual meteorological stations within a larger climate region; the data represent frequency of occurrence for that station location and not necessarily for the larger climatic area.

Fig. 3-8 presents frequency of occurrence of obscuration as a function of season, time of day (4 time periods), and visibility class (less than 1 km, 1 to 3 km, 3 to 7 km, and 7 km or higher). Table 3-16 gives a breakdown of the frequencies of occurrence by categories: (I) fog, haze, or mist, (II) dust, (III) drizzle, rain, or thunderstorms, (IV) snow, (V) clear weather with humidity less than 10 g/m³, (VI) clear weather with humidity equal to or exceeding 10 g/m³, (VII) ceiling less than 300 m, and (VIII) ceiling less than 300 m with visibility less than 1 km.

In addition, representative frequency of occurrence of transmittance graphs generated by ASL are included for the Fulda gap region within the highlands region. The

(A) Visibility Less Than 1 km

(B) Visibility At Least 1km, But Less Than 3 km
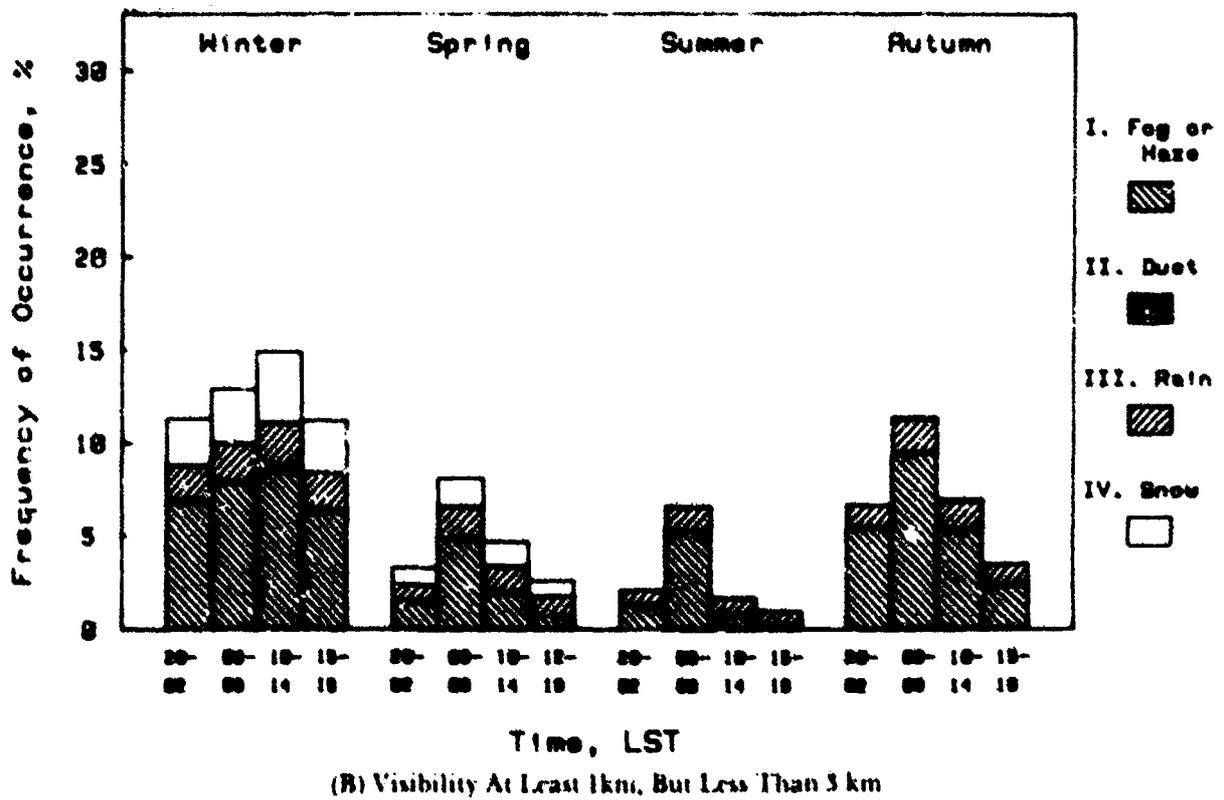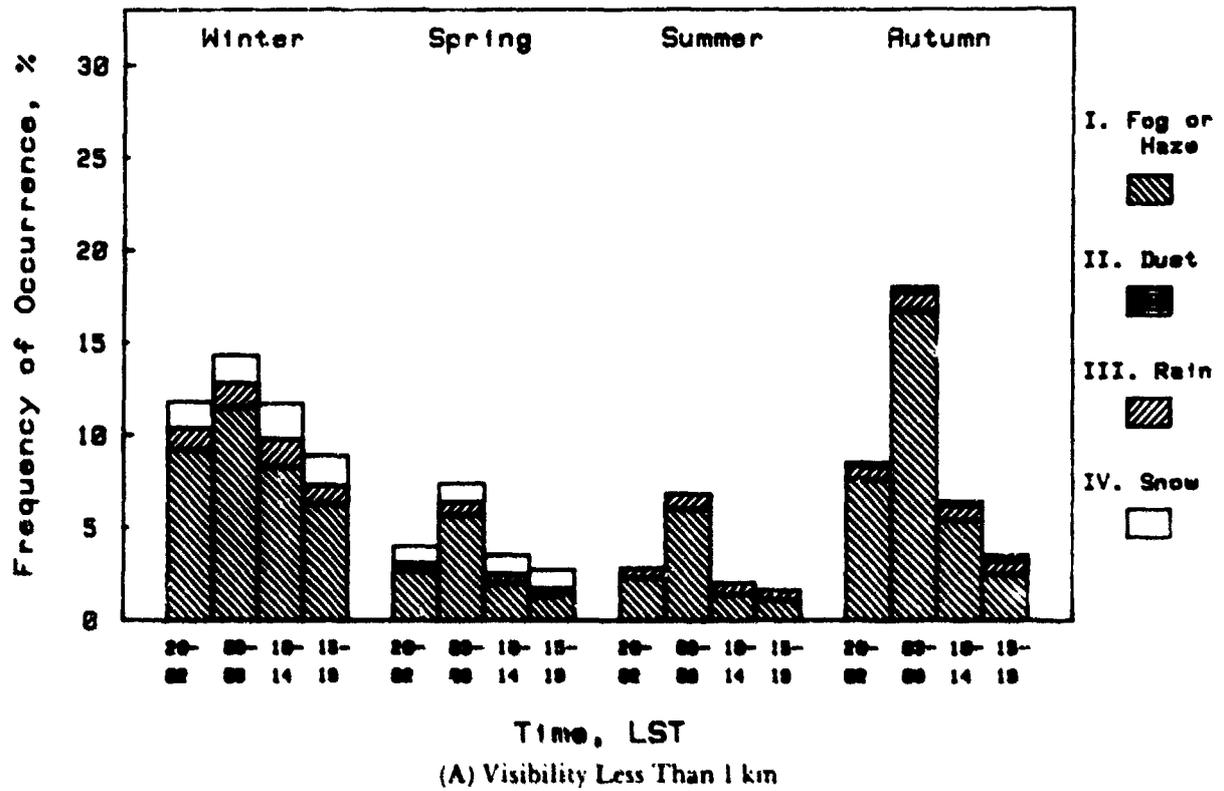
Figure 3-8.　European Highlands, Frequency of Natural Obscuration

(C) Visibility At Least 3 km, But Less Than 7 km

(D) Visibility 7 km or Greater
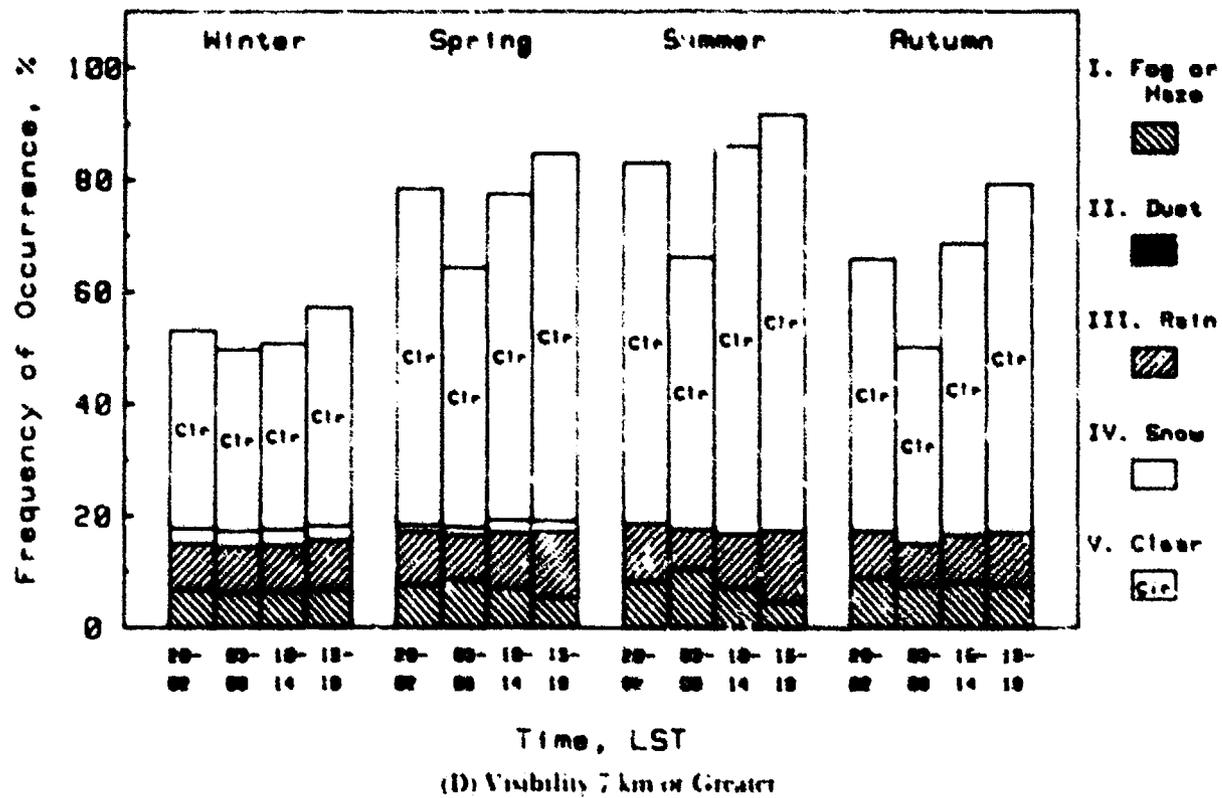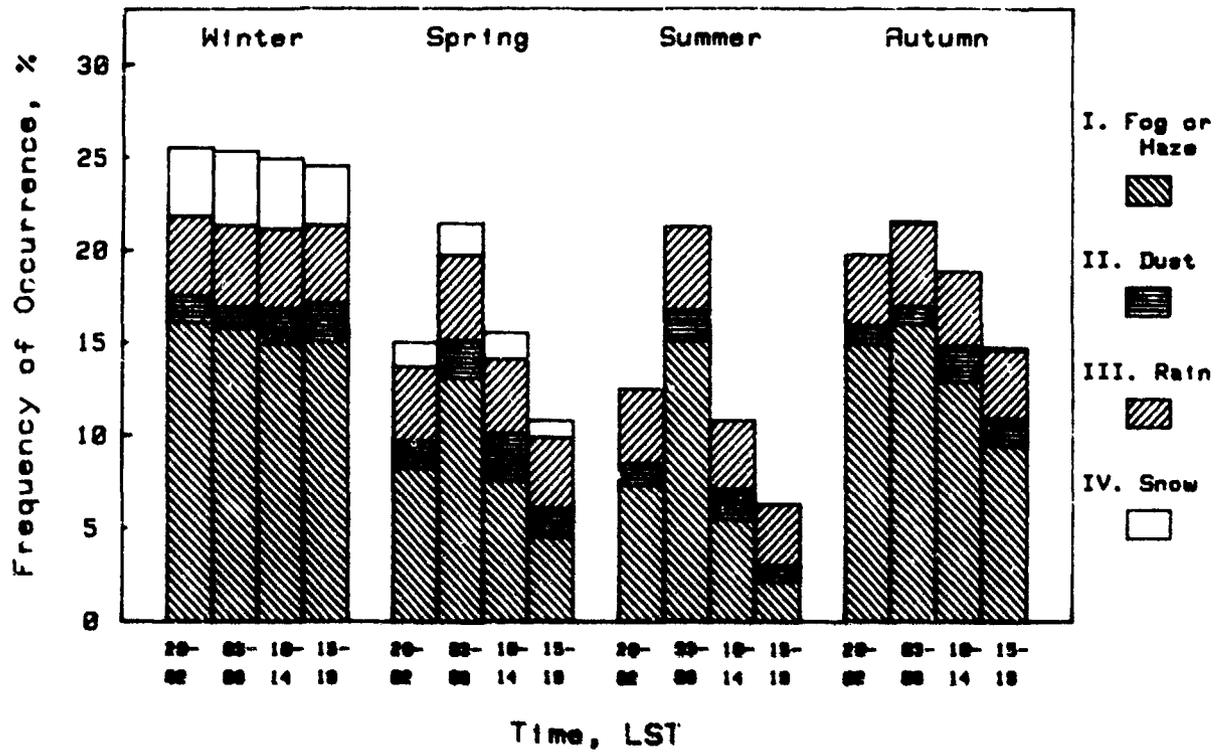
Figure 3-8. (cont'd)

TABLE 3-16
EUROPEAN HIGHLANDS OBSCURATION STATISTICS
Total Percentage of Occurrences*
(% to nearest tenth)

	Winter					Spring			
	Time					Time			
Category	20-02	03-09	10-14	15-19	Category	20-02	03-09	10-14	15-19
I	39.0	41.4	38.3	34.4	I	20.0	34.1	18.5	12.0
II	1.4	1.1	1.9	2.1	II	1.4	2.0	2.5	1.5
III	15.6	16.0	16.5	16.0	III	14.9	15.1	15.9	17.0
IV	10.3	11.2	12.3	10.2	IV	4.3	5.6	5.9	4.6
V	35.4	32.5	33.3	39.1	V	58.8	45.7	56.3	63.8
VI	0.0	0.0	0.0	0.0	VI	1.3	0.7	2.0	1.9
VII	26.1	30.6	28.6	23.1	VII	9.1	14.1	11.5	8.3
VIII	9.1	10.8	9.2	7.1	VIII	3.0	4.8	2.9	2.4

	Summer					Autumn			
	Time					Time			
Category	20-02	03-09	10-14	15-19	Category	20-02	03-09	10-14	15-19
I	19.2	36.8	14.8	8.2	I	36.9	49.8	31.8	21.9
II	1.1	1.6	1.6	0.8	II	1.0	0.9	1.9	1.4
III	15.7	13.7	14.8	17.2	III	14.0	14.5	14.7	14.9
IV	0.0	0.0	0.0	0.0	IV	0.3	0.6	0.4	0.5
V	38.5	31.4	39.0	43.3	V	40.6	30.9	41.0	48.0
VI	26.0	17.1	30.3	31.0	VI	7.8	4.1	10.9	13.6
VII	6.2	11.4	8.8	5.7	VII	12.3	21.8	16.9	9.1
VIII	2.1	4.2	1.8	1.5	VIII	5.6	11.5	5.4	2.9

*Sum totals may be more than 100% as coexisting phenomena were counted in their proper category; therefore, some observations were counted twice.

graphs, in Fig. 3-9, show cumulative transmittance frequency for 0.55, 1.06, 3-5, 10.6, and 8-12μm, and 35 and 94 GHz. These graphs show transmittance over a range of 2 km between the ground and a point at an angle of 20 deg above ground (20-deg look angle) for four times of day, local standard time (LST). The curves for each spectral band plot transmittance in that spectral band against cumulative frequency of transmittance—the percentage of the time that the transmittance is the indicated value or lower. For an interpretation of how to use the charts, consider the figure for Fulda at 2400 hours. The 3-5 μm transmittance curve (dotted line) indicates a cumulative frequency of 25% for a transmittance of 0.1, and a cumulative frequency of 100% for a transmittance of 0.45. This means that the transmittance is 10% or lower one fourth of the time, and rarely exceeds 45%, at midnight in Fulda, over this 2-km path.

3-5 FREQUENCY OF OCCURRENCE OF NATURAL OBSCURATION FACTORS IN CENTRAL AMERICA (INTERIOR REGION)

This paragraph contains the same formats for Central America as par. 3-4 contained for Europe, except

for the lack of frequency of occurrence of transmittance data.

Fig. 3-10 presents frequency of occurrence as a function of season, time of day, and visibility class. Table 3-17 gives a breakdown of the frequencies of occurrence by categories: (I) fog, haze, or mist, (II) dust, (III) drizzle, rain, or thunderstorms, (IV) snow, (V) clear weather with humidity less than 10 g m³, (VI) clear weather with humidity equal to or exceeding 10 g m³, (VII) ceiling less than 300 m, and (VIII) ceiling less than 500 m with visibility less than 1 km.

3-6 FREQUENCY OF OCCURRENCE OF NATURAL OBSCURATION FACTORS IN THE MIDEAST DESERT

This paragraph contains the obscuration frequency data for the Mideast desert area. Fig. 3-11 presents frequency of occurrence as a function of season, time of day, and visibility class (less than 1 km, 1 to 3 km, 3 to 7 km, and 7 km or higher). Table 3-18 gives a breakdown of the frequencies of occurrence by categories: (I) fog, haze, or mist, (II) dust, (III) drizzle, rain, or thunderstorms, (IV) snow, (V) clear weather with humidity less
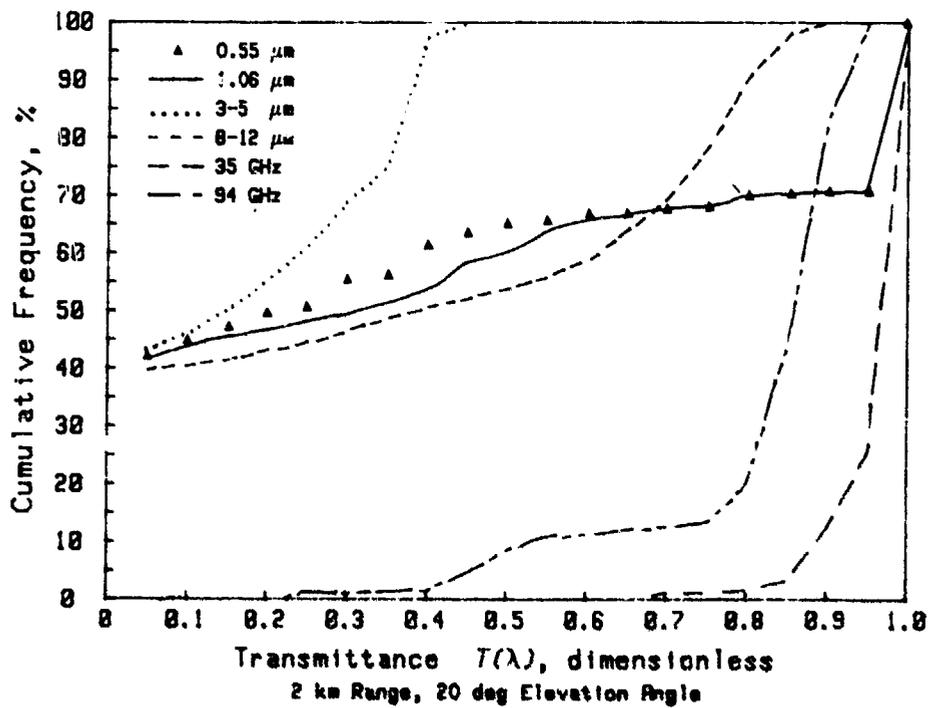
(A) Morning Nautical Twilight
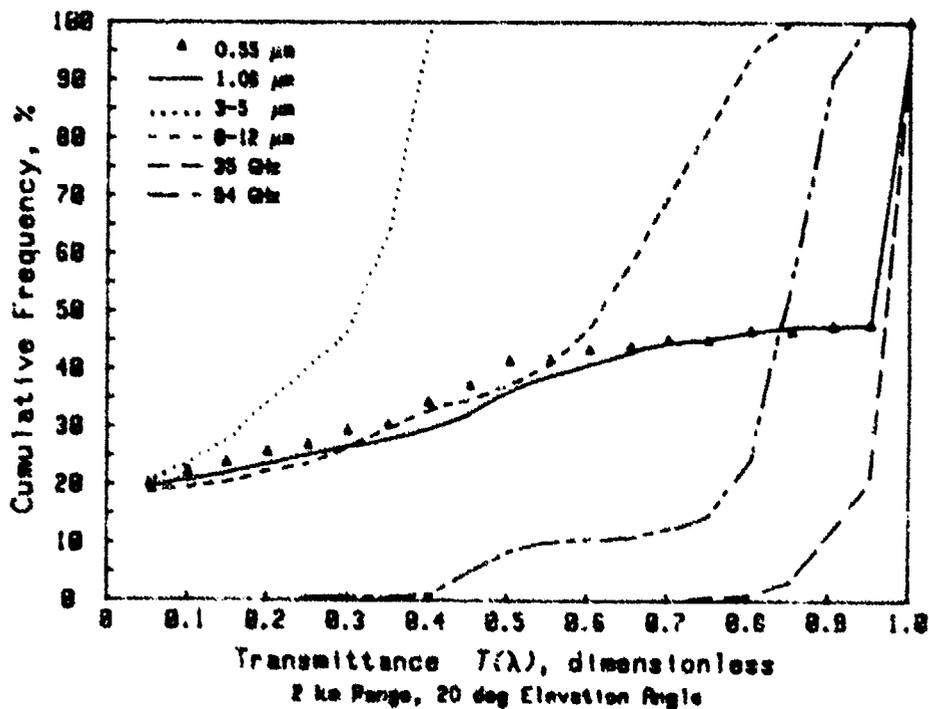
(B) 1300 hours

Figure 3-9.   Frequency of Occurrence of Transmittance at Fulda, FRG (Ref. 20)
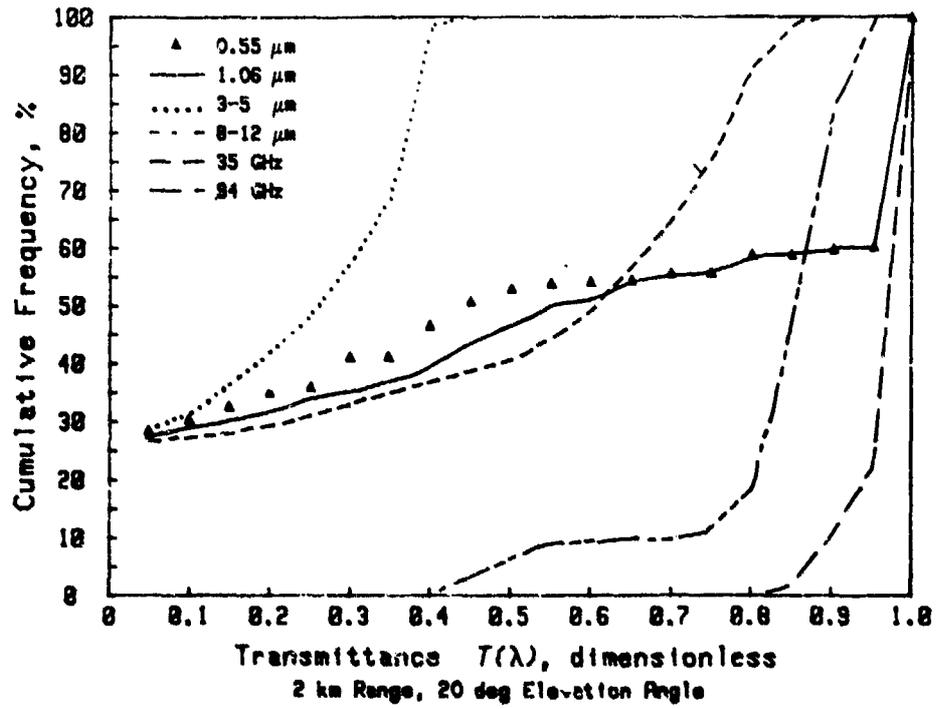
(C) Evening Nautical Twilight
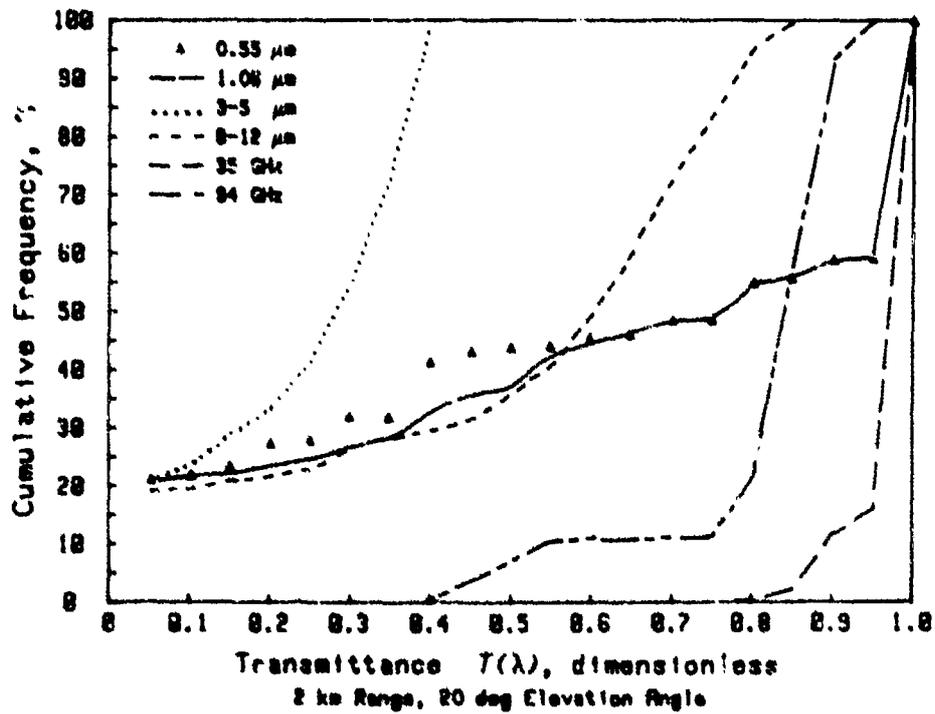
(D) 2400 Hours

Figure 3-9   (cont'd)
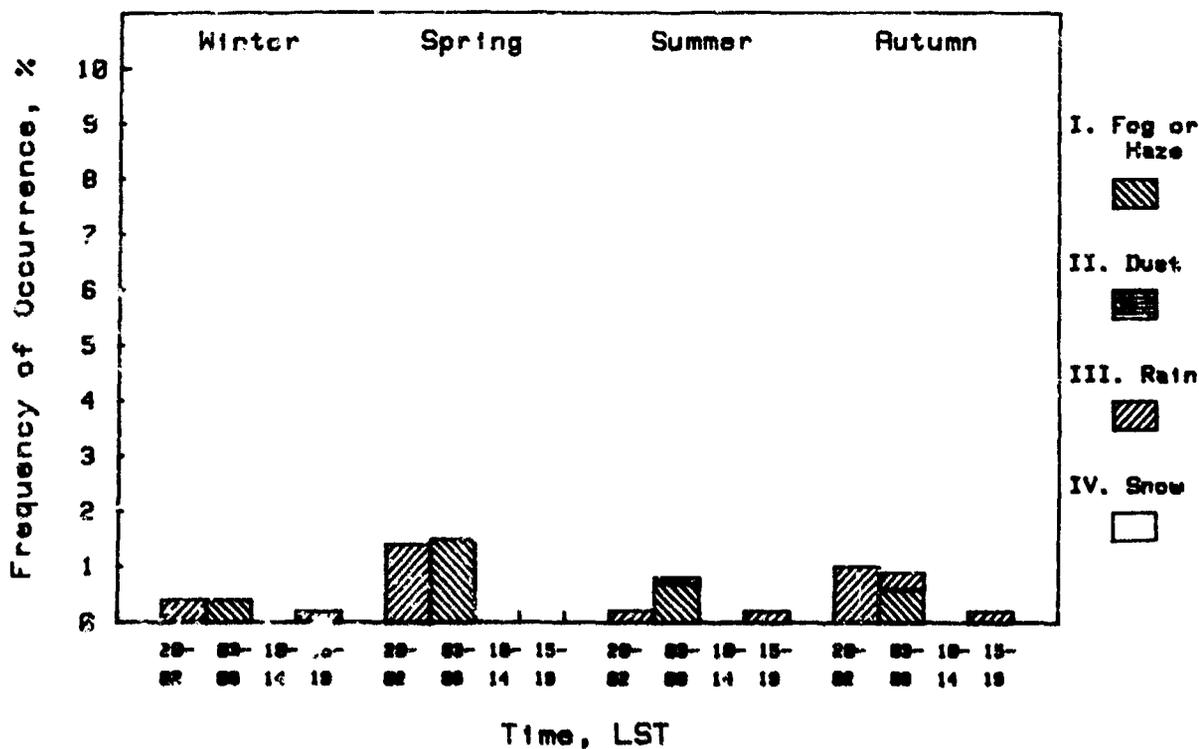
(A) Visbility Less Than 1 km
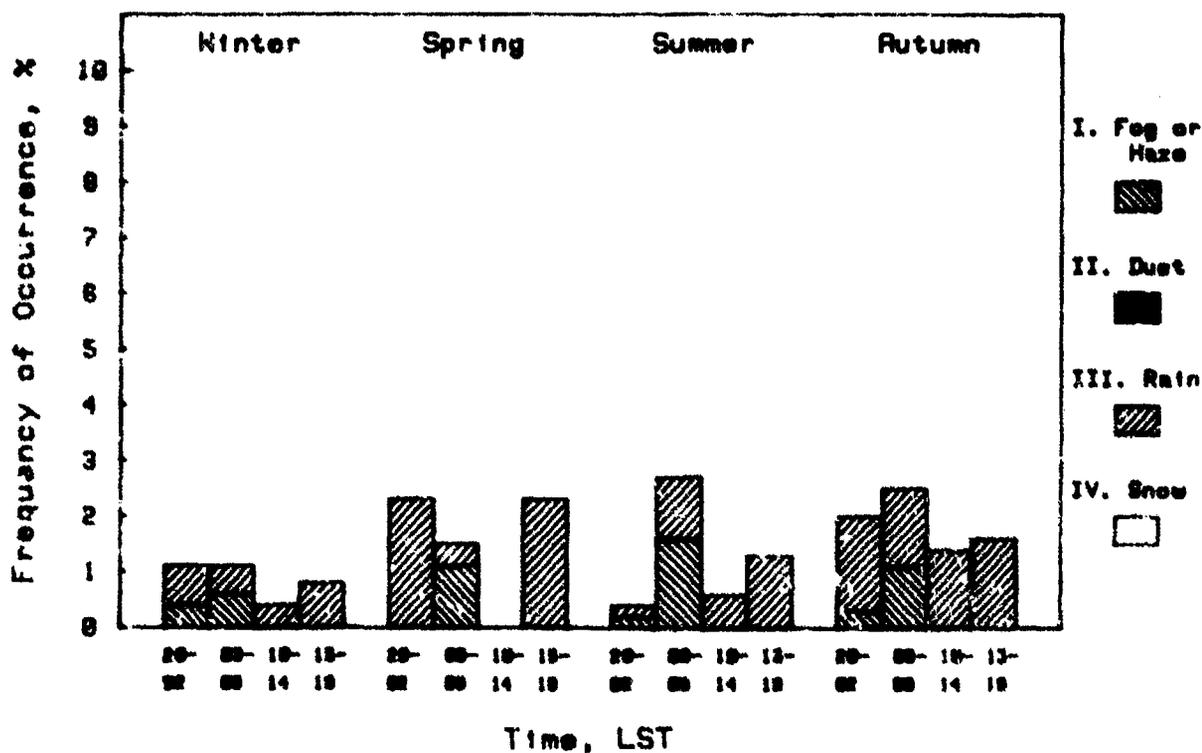
(B) Visibility At Least 1 km, But Less Than 3 km

Figure 3-10.   Central America, Frequency of Natural Obscuration
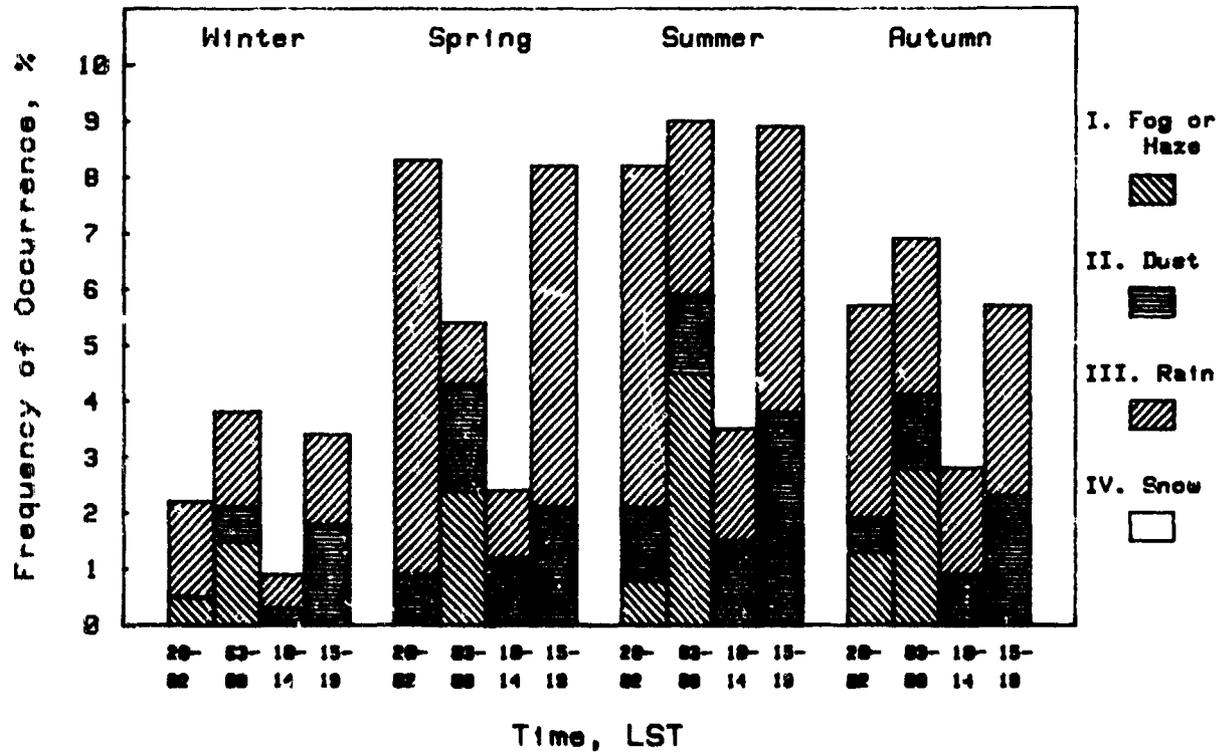
(C) Visibility At Least 3 km, But Less Than 7 km
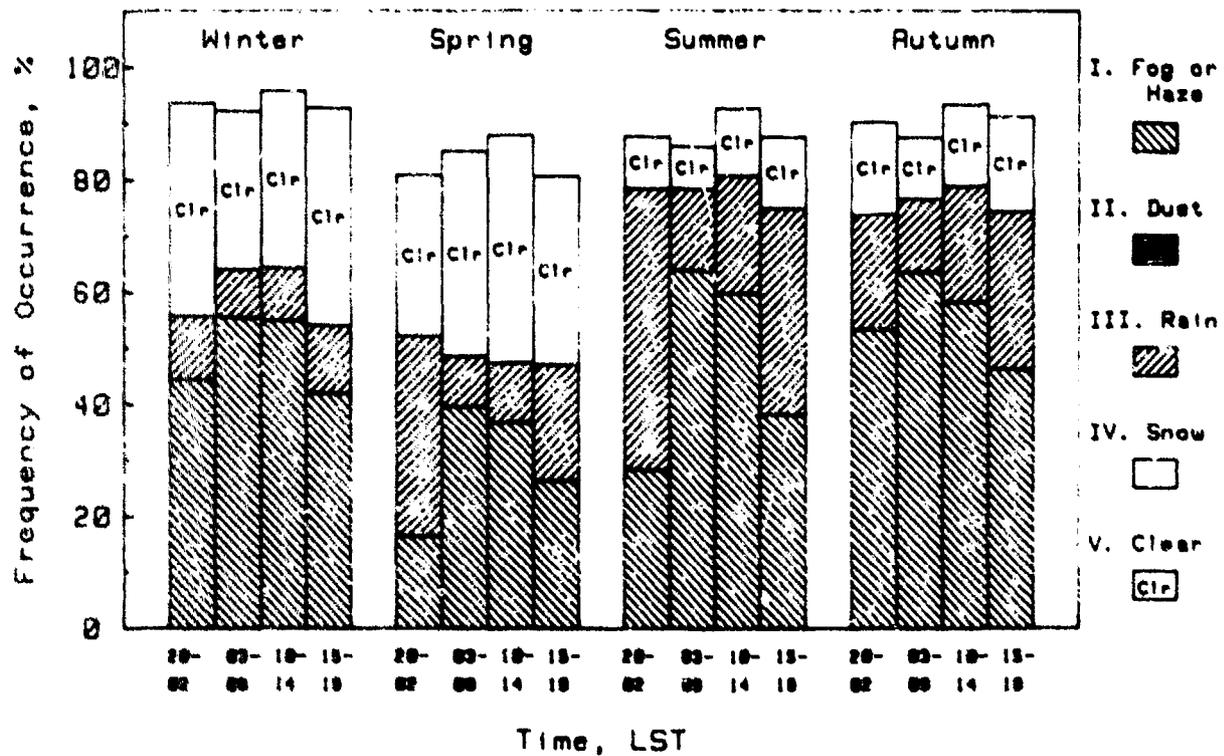
(D) Visibility 7 km or Greater

Figure 3-10.   (cont'd)

TABLE 3-17
CENTRAL AMERICAN INTERIOR OBSCURATION STATISTICS
Total Percentage of Occurrences*
(% to nearest tenth)

	Winter					Spring			
	Time					Time			
Category	20-02	03-09	10-14	15-19	Category	20-02	03-09	10-14	15-19
I	45.4	58.0	54.9	42.0	I	16.5	44.7	36.8	26.5
II	0.0	0.6	0.3	1.8	II	0.9	1.9	1.2	2.1
III	14.1	10.8	10.4	14.7	III	46.8	10.4	11.8	29.0
IV	0.0	0.0	0.0	0.0	IV	0.0	0.0	0.0	0.0
V	5.3	2.9	9.3	12.9	V	2.0	1.1	2.4	5.4
VI	32.5	25.2	22.1	25.7	VI	26.6	35.3	38.0	28.1
VII	1.7	1.7	0.0	0.7	VII	1.1	0.9	0.0	0.6
VII	0.4	0.2	0.0	0.1	VIII	0.0	0.0	0.0	0.0

	Summer					Autumn			
	Time					Time			
Category	20-02	03-09	10-14	15-19	Category	20-02	03-09	10-14	15-19
I	29.4	70.7	59.8	38.2	I	54.9	68.0	58.2	46.2
II	1.3	1.4	1.5	3.7	II	0.6	1.3	0.9	2.3
III	58.3	18.8	23.5	43.4	III	27.1	17.5	24.0	33.3
IV	0.0	0.0	0.0	0.1	IV	0.0	0.0	0.0	0.0
V	0.1	0.2	0.4	0.7	V	1.2	0.7	2.4	2.0
VI	9.1	7.3	11.5	11.9	VI	15.1	10.3	12.0	14.9
VII	1.5	2.5	0.5	0.8	VII	3.2	3.2	2.2	1.1
VIII	0.1	0.2	0.0	0.1	VIII	1.0	0.5	0.0	0.0

*Sum totals may be more than 100% as coexisting phenomena were counted in their proper category; therefore, some observations were counted twice.

than 10 g m³, (VI) clear weather with humidity equal to or exceeding 10 g m³, (VII) ceiling less than 300 m, and (VIII) ceiling less than 300 m with visibility less than 1 km.

In addition, frequency of occurrence of transmittance graphs generated by ASL are included for Kheshan, a Mideast city in the high desert plateau of Iran. The graphs in Fig. 3-12 show transmittance frequency for 0.55, 1.06, 3-5, 10.6, and 8-12μm, and 35 and 94 GHz.

3-7 FREQUENCY OF OCCURRENCE OF NATURAL OBSCURATION FACTORS IN SCANDINAVIA (EASTERN REGION)

This paragraph contains the obscuration frequency data for northern Scandinavia. Fig. 3-13 presents frequency of occurrence as a function of season, time of day, and visibility class (less than 1 km, 1 to 3 km, 3 to 7 km, and 7 km or higher). Table 3-19 summarizes the frequency of occurrence by categories: (I) fog, haze, or mist, (II) dust, (III) drizzle, rain, or thunderstorms, (IV) snow, (V) clear weather with humidity less than 10 g m³, (VI) clear weather with humidity equal to or exceeding 10 g m³, (VII) ceiling less than 300 m, and (VIII) ceiling less than 300 m with visibility less than 1 km.

TABLE 3-18
EUROPEAN HIGHLANDS OBSCURATION STATISTICS
Total Percentage of Occurrences*
(% to nearest tenth)

| Winter					Spring			
	Time					Time		
Category	20-02	03-09	10-14	15-19	Category	20-02	03-09	10-14	15-19
I	5.8	13.2	9.0	4.9	I	2.0	7.1	4.4	2.9
II	2.0	3.0	4.5	5.0	II	4.6	6.2	8.5	8.1
III	6.3	5.5	5.0	5.4	III	5.9	4.4	4.4	5.5
IV	2.0	2.0	2.1	1.7	IV	0.4	0.4	0.4	0.2
V	81.7	74 ˉ	76.4	81.5	V	75.5	70.6	72.0	74.3
VI	2.2	1.8	2.9	2.6	VI	11.8	11.4	10.5	9.0
VII	2.7	4.2	4.2	3.4	VII	1.0	1.5	1.8	2.0
VIII	0.9	1.8	0.9	0.6	VIII	0.2	0.3	0.3	0.3

Summer					Autumn			
	Time					Time		
Category	20-02	03-09	10-14	15-19	Category	20-02	03-09	10-14	15-19
I	1.9	7.4	5.4	3.8	I	2.0	8.2	5.6	3.0
II	2.7	4.9	7.1	7.3	II	1.5	2.8	4.0	3.3
III	1.8	0.8	0.8	1.0	III	3.8	2.4	2.3	2.6
IV	0.0	0.0	0.0	0.0	IV	0.1	0.1	0.0	0.0
V	60.0	58.2	59.9	69.8	V	69.9	68.9	70.5	78.8
VI	33.6	28.8	26.7	18.0	VI	22.4	17.6	17.5	12.2
VII	0.3	0.5	0.3	0.4	VII	0.5	0.7	0.7	0.7
VIII	0.1	0.1	0.1	0.1	VIII	0.1	0.2	0.1	0.1

*Sum totals may be more than 100% as coexisting phenomena were counted in their proper category; therefore, some observations were counted twice.
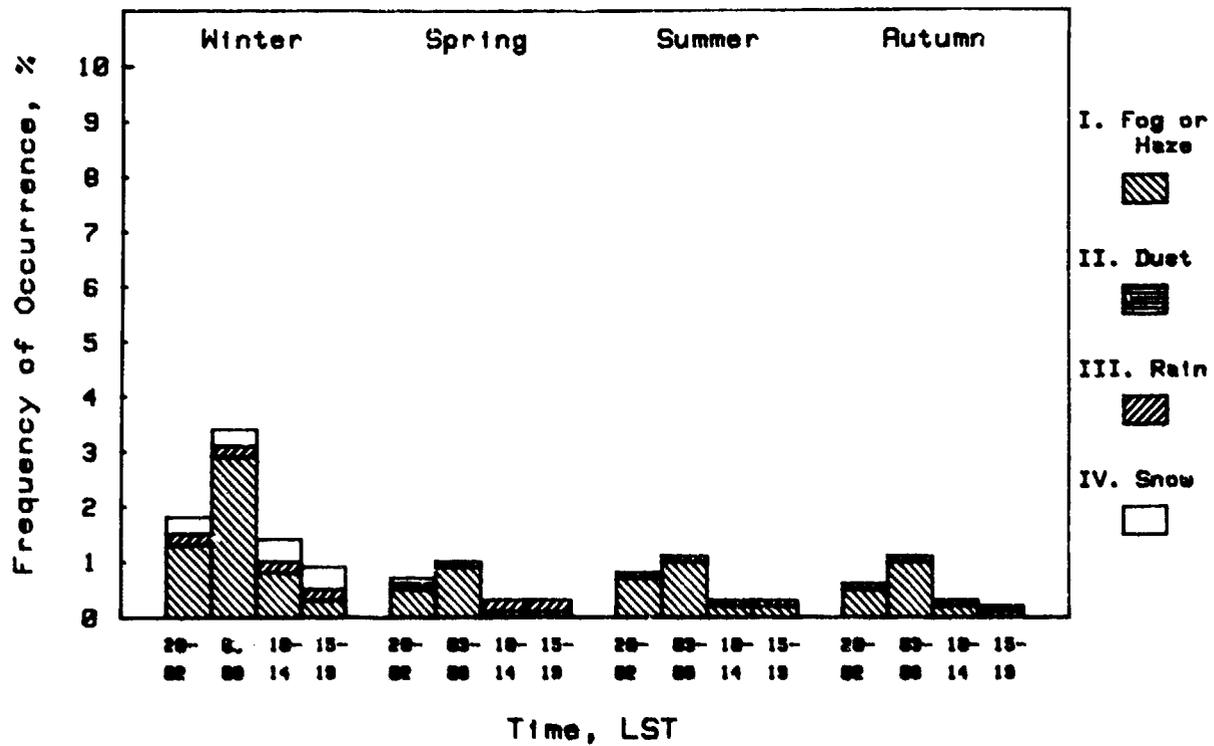
(A) Visibility Less Than 1 km
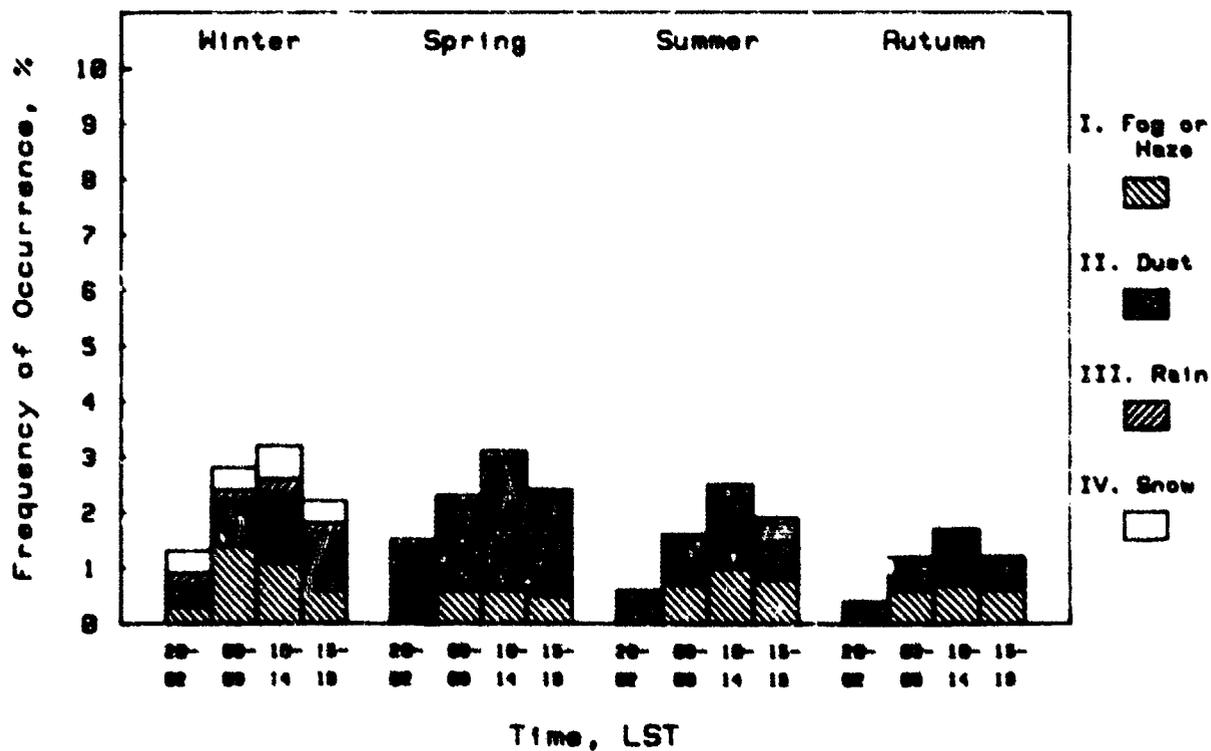
(B) Visibility At Least 1 km, But Less Than 5 km

Figure 3-11.   Mideast Desert, Frequency of Natural Obscuration.
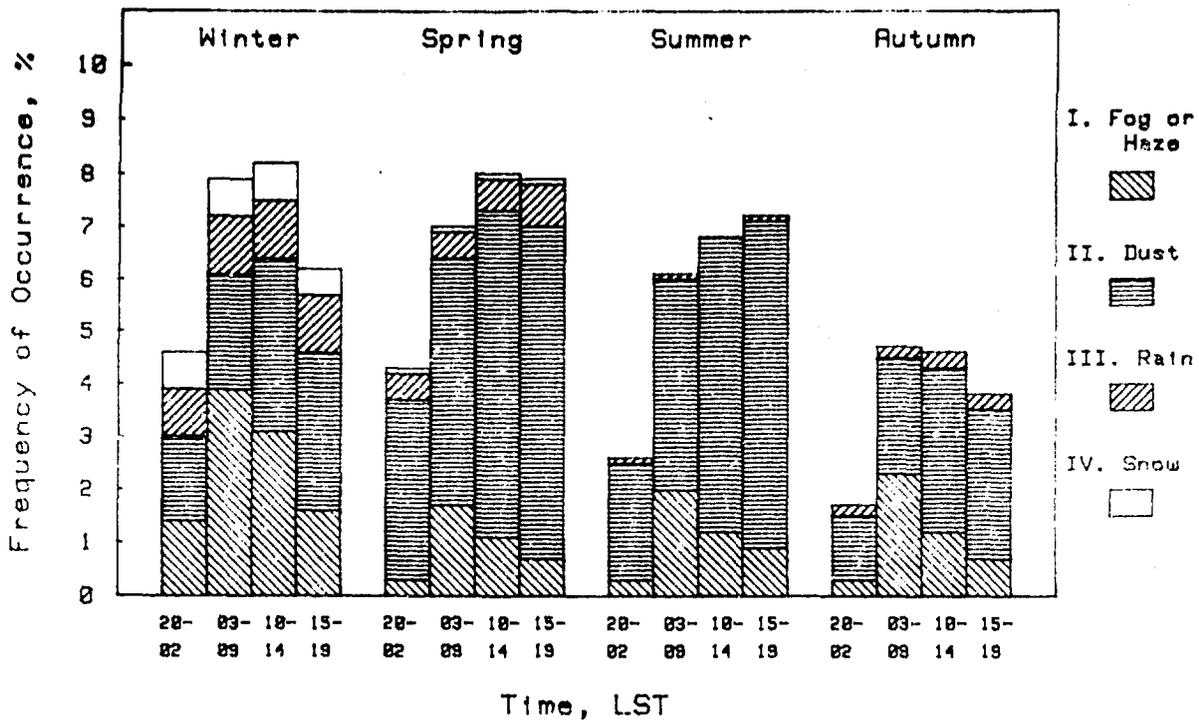
(C) Visibility At Least 3 km, But Less Than 7 km
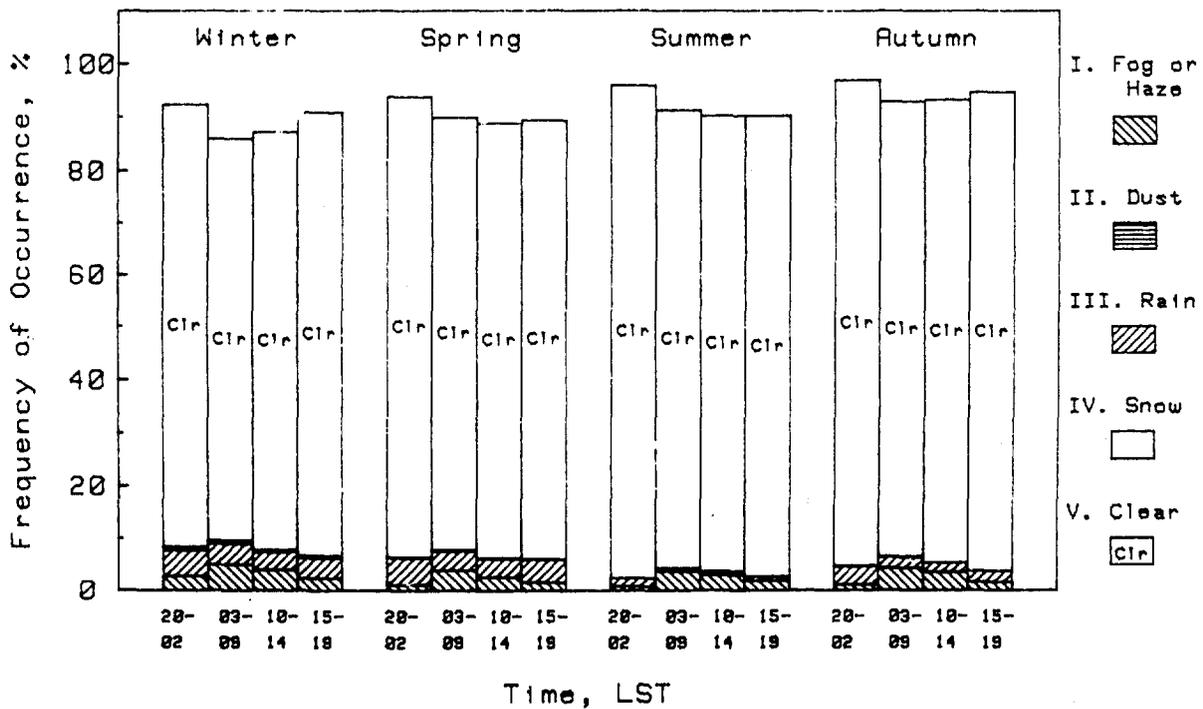
(D) Visibility 7 km or Greater

Figure 3-11. (cont'd)
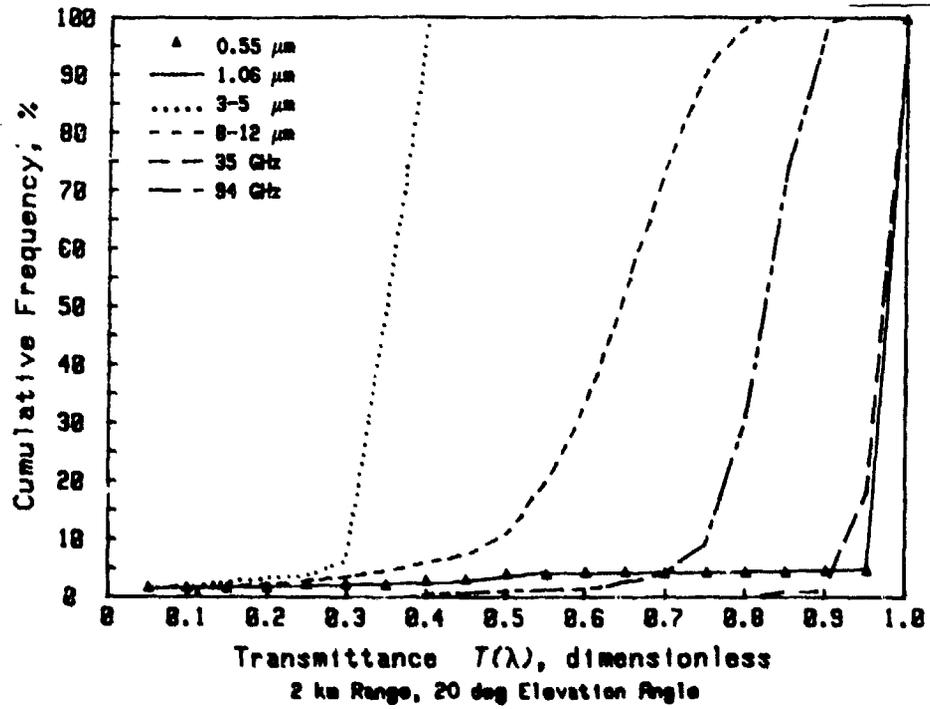
(A) Efsahan, Iran, Morning Nautical Twilight
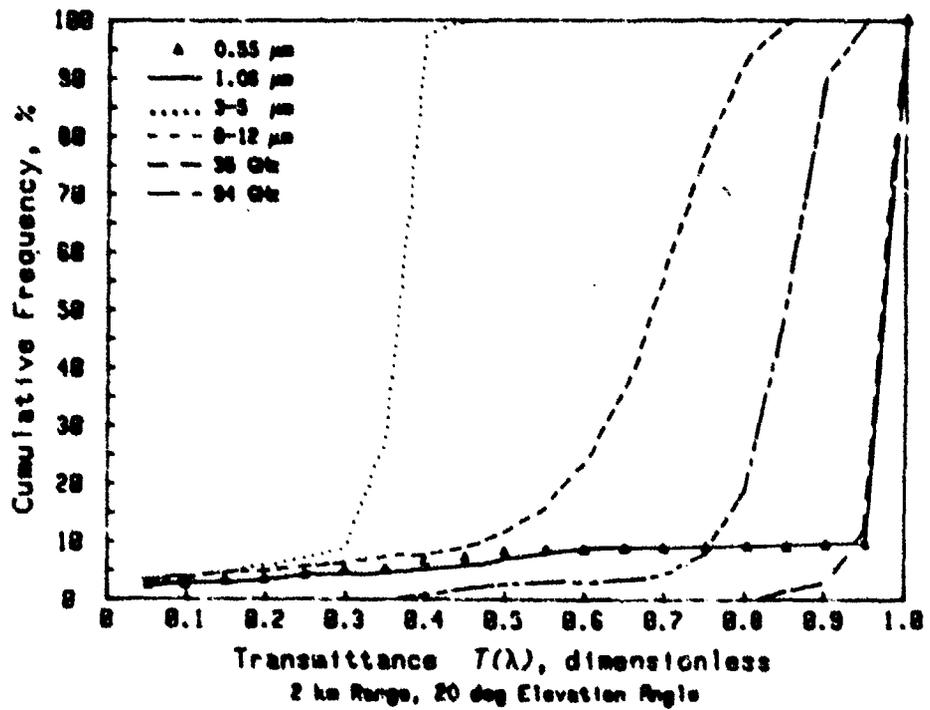
(B) Efsahan, Iran, 1300 Hours

Figure 3-12.   Frequency of Occurrence of Transmittance, Mideast Desert (Ref. 20)
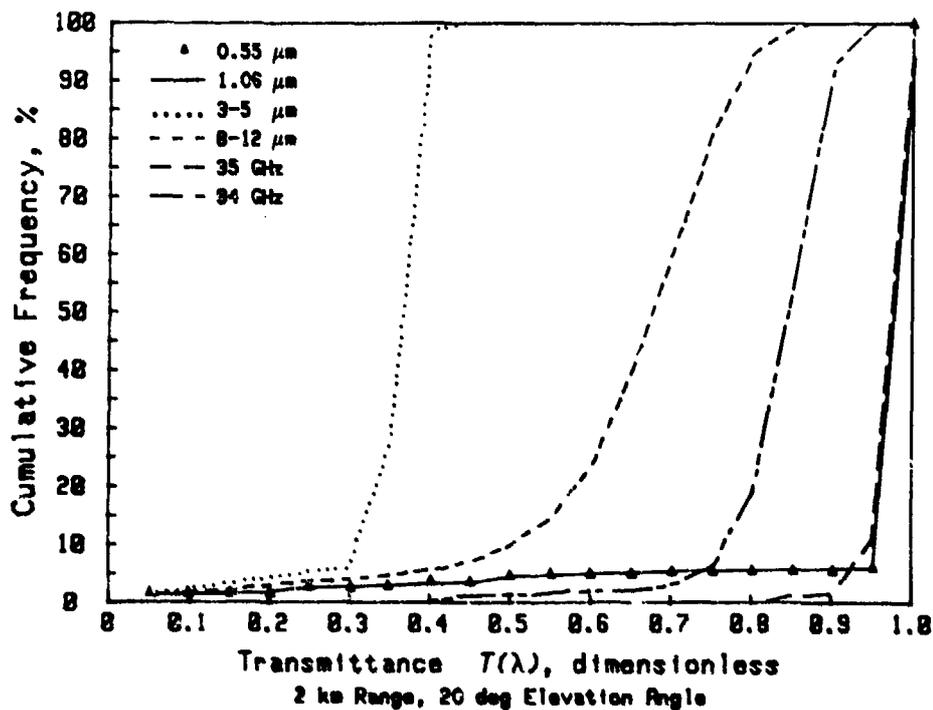
(C) Efsahan, Iran, Evening Nautical Twilight
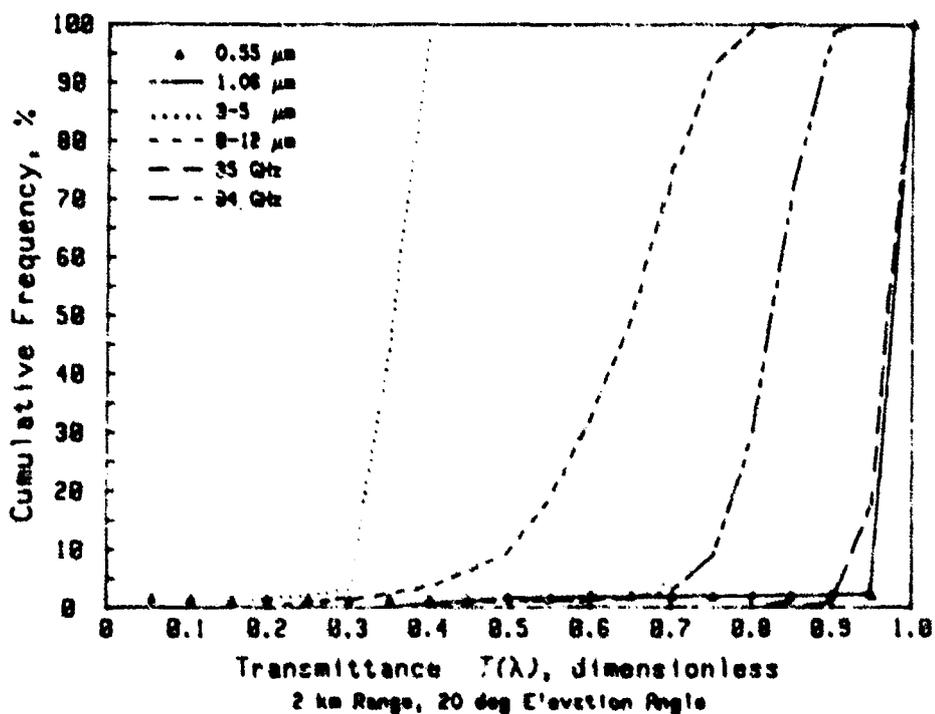
(D) Efsahan, Iran, 2400 Hours

**Figure 3-12   (cont'd)**
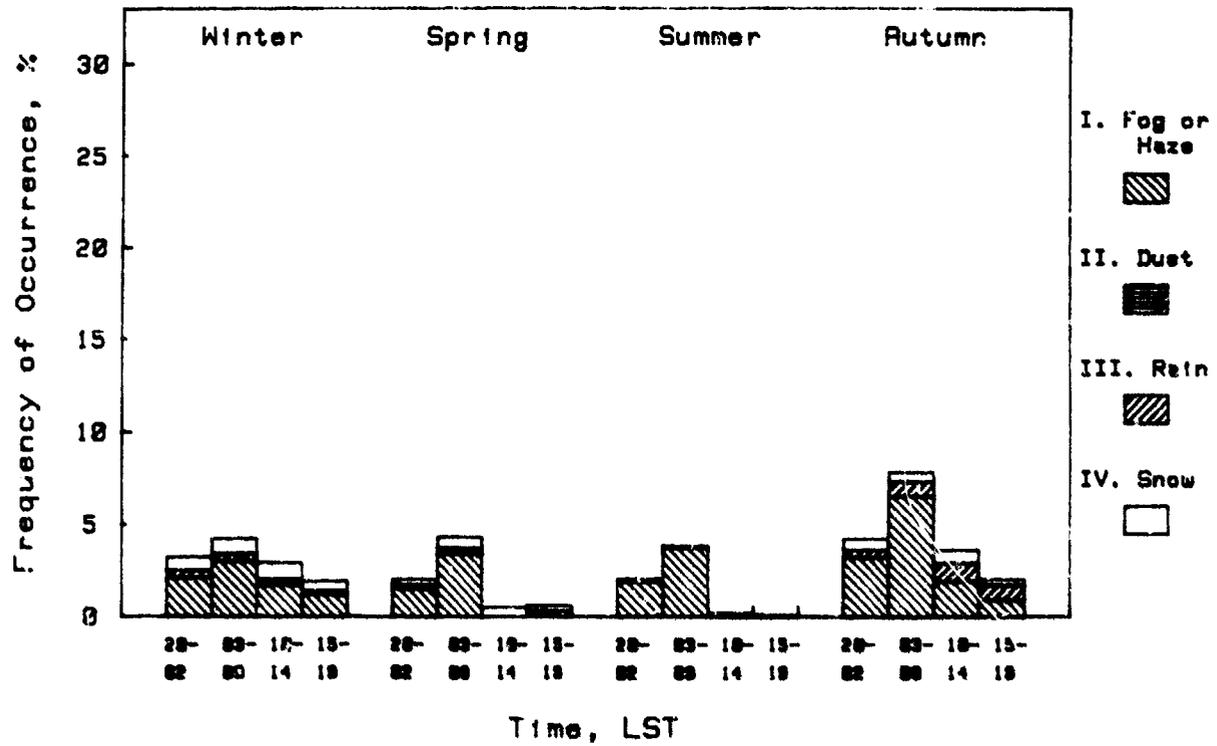
(A) Visibility Less Than 1 km
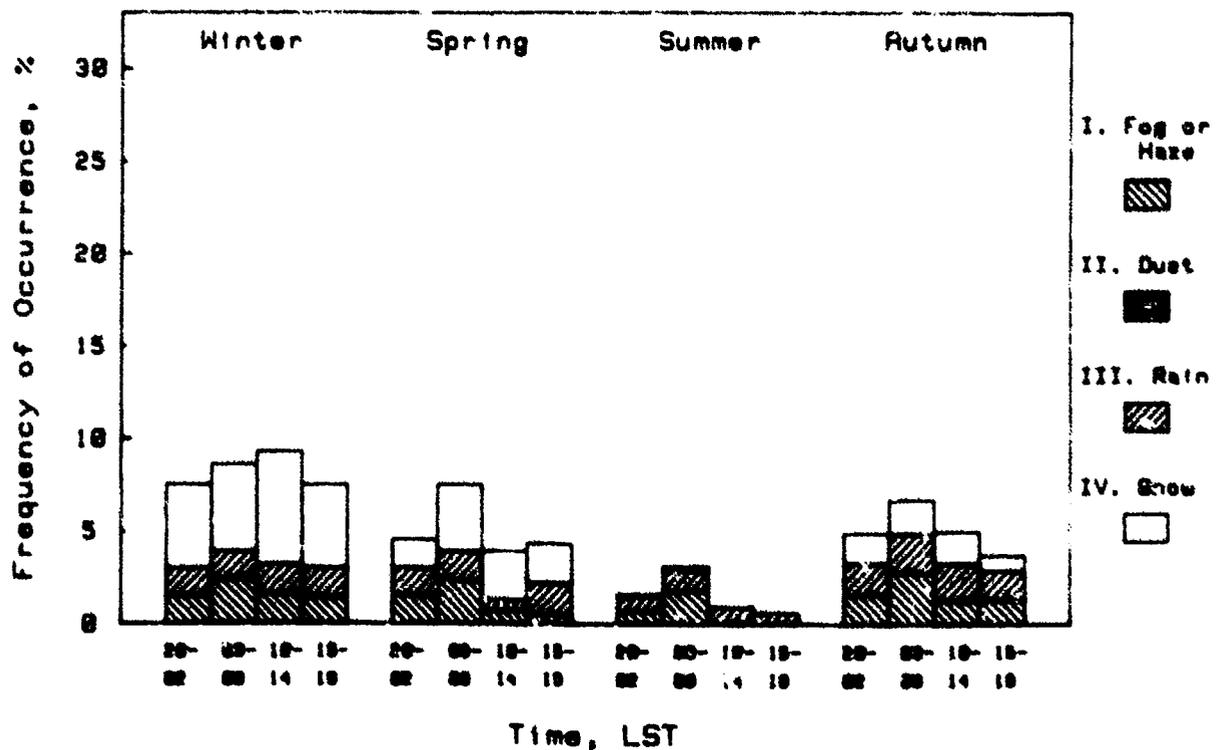
(B) Visibility At Least 1 km But Less Than 3 km

Figure 3-13.   Eastern Scandinavia, Frequency of Natural Obscuration
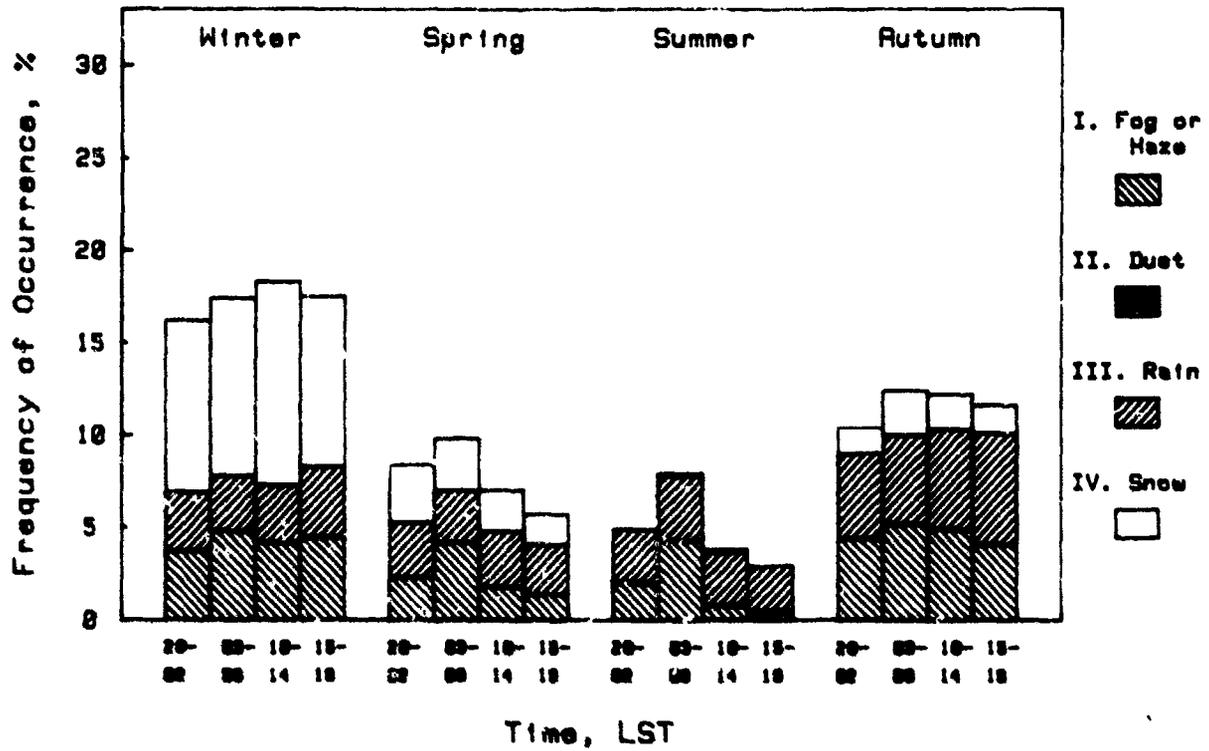
(C) Visibility At Least 3 km, But Less Than 7 km
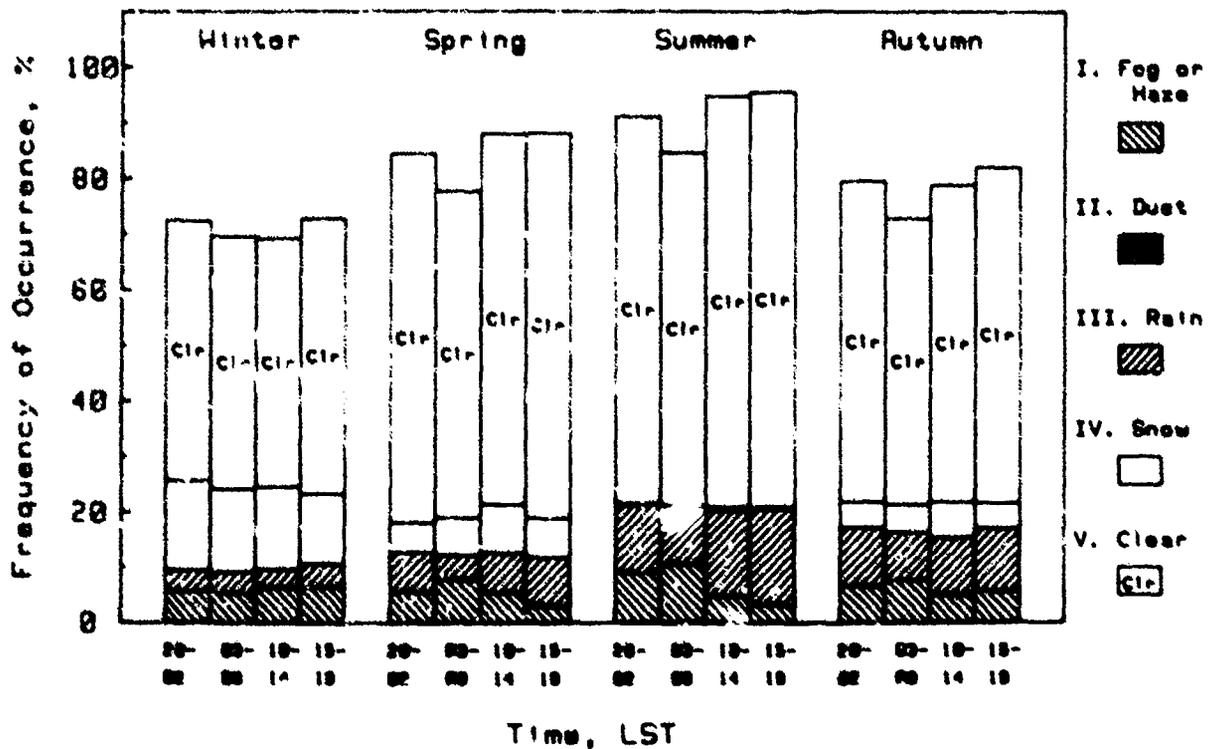
(D) Visibility 7 km or Greater

Figure 3-13   (cont'd)

TABLE 3-19
EASTERN SCANDINAVIA OBSCURATION STATISTICS
Total Percentage of Occurrences*
(% to nearest tenth)

	Winter					Spring			
	Time					Time			
Category	20-02	03-09	10-14	15-19	Category	20-02	03-09	10-14	15-19
I	13.1	15.5	13.8	13.5	I	10.8	17.6	7.9	5.2
II	0.0	0.0	0.0	0.0	II	0.0	0.0	0.0	0.0
III	8.9	8.8	8.3	9.8	III	11.9	9.2	10.8	13.2
IV	30.6	30.0	32.9	26.8	IV	10.2	13.7	14.0	11.1
V	46.7	45.4	44.6	49.5	V	66.4	58.8	66.7	69.3
VI	0.0	0.0	0.0	0.0	VI	0.0	0.0	0.0	0.0
VII	36.8	40.2	33.1	29.5	VII	18.2	25.3	14.2	10.3
VIII	2.7	3.8	2.5	1.6	VIII	1.7	4.1	0.4	0.3

	Summer					Autumn			
	Time					Time			
Category	20-02	03-09	10-14	15-19	Category	20-02	03-09	10-14	15-19
I	13.7	29.5	5.8	3.7	I	15.8	22.2	13.1	12.0
II	0.1	0.0	0.0	0.1	II	0.0	0.0	0.0	0.0
III	15.9	14.8	19.3	20.4	III	17.4	16.4	18.8	19.8
IV	0.4	0.8	0.7	0.4	IV	8.8	9.7	10.7	7.1
V	57.2	52.4	61.8	62.3	V	57.7	51.5	57.1	60.5
VI	12.4	11.0	12.1	12.3	VI	0.0	0.0	0.0	0.0
VII	8.7	16.1	7.1	4.1	VII	28.5	35.6	27.8	20.9
VIII	0.5	1.9	0.1	0.1	VIII	3.1	5.9	3.3	2.6

*Sum totals may be more than 100% as coexisting phenomena were counted in their proper category; therefore, some observations were counted twice.

REFERENCES

1. F. X. Kneizys, et al., *Atmospheric Transmittance Radiance Computer Code LOWTRAN 5*, AFGL-TR-80-0067, US Air Force Geophysics Laboratory, Hanscomb AFB, MA, 1980.

2. H. J. P. Smith, et al., *FASCODE--Fast Atmospheric Signature Code (Spectral Transmittance and Radiance)*, AFGL-TR-0067, US Air Force Geophysics Laboratory, Hanscomb AFB, MA, 1978.

3. Louis D. Duncan, et al., *EOSAEL 82*, ASL-TR-0122, US Army Atmospheric Sciences Laboratory, White Sands Missile Range, NM, 1982.

4. R. Pinnick, et al., *Relationships Between IR Extinction, Absorption, and Liquid Water Content of Fogs*, ASL-TR-0037, US Army Atmospheric Sciences Laboratory, White Sands Missile Range, NM, 1979.

5. Marvin D. Kays, et al., *Qualitative Description of Obscuration Factors in Central Europe*, ASL Monograph No. 4, US Army Atmospheric Sciences Laboratory, White Sands Missile Range, NM, 1980.

6. J. O. Laws and D. A. Parsons, "The Relation of Raindrops to Intensity", Trans. AM. Geophys. Union 24, 452 (1943).

7. S. Joss and A. Waldvogel, "Raindrop Size Distribution and Sampling Size Errors", J. Atmos. Sci. 26, 566 (1969).

8. D. R. Brown, "An Empirical Model for Near Millimeter Wave Snow Extinction and Backscatter", *Proceedings of 1982 Army Science Conference*, West Point, NY, 1983.

9. E. M. Patterson and D. A. Gillette, *Measurements of Visibility vs. Mass-Concentration for Airborne Soil Particles, Vol. 11*, National Center for Atmospheric Research, Boulder, CO, 1978.

10. G. B. Hoidale, et al., *A Study of Atmospheric Dust*, ECOM-5067, Atmospheric Sciences Laboratory, White Sands Missile Range, NM, 1967.

11. William L. Wolfe and George J. Zissis, Eds., *The Infrared Handbook*, Office of Naval Research, Arlington, VA, 1978.

12. M. B. Richardson, *A General Algorithm for the Calculation of Laser Beam Spreading*, ASL-TR-0116, US Army Atmospheric Sciences Laboratory, White Sands Missile Range, NM, 1981.

13. Frederick G. Gebhardt, *Development of Turbulence Effects Models*, Science Applications, Inc., Ann Arbor, MI, 1980.

14. D. S. Bond and F. P. Henderson, *The Conquest of Darkness*, David Sarnoff Research Center, Princeton, NJ, 1963.

15. T. J. V. Schie, *Nocturnal Illumination and Decrease of Contrast in the Atmosphere*, TNO, Amsterdam, Netherlands, 1969.

16. George O. Lof, et al., *Worldwide Distribution of Solar Radiation*, Solar Energy Laboratory, University of Wisconsin, Madison, WI, 1966.

17. William L. Wolfe, Ed., *Handbook of Military Infrared Technology*, Office of Naval Research, Washington, DC, 1965.

18. Ralph Shapiro, *Solar Radiative Flux Calculations from Standard Surface Meteorological Observations*, AFGL-TR-82-0039, US Air Force Geophysics Laboratory, Hanscomb AFB, MA, 1982.

19. Bruce Miers, *Geosem Worldwide Data Base*, US Army Atmospheric Sciences Laboratory, White Sands Missile Range, NM, 1984.

20. E. M. D'Arcy and E. P. Avara, *Slant Path Atmospheric Transmission Statistics for Visible Through Millimeter Wavelengths*, ASL-TR-0154, US Army Atmospheric Sciences Laboratory, White Sands Missile Range, NM, 1984.

BIBLIOGRAPHY

Meteorology and Climatology

R. E. Huschke, *Atmospheric Visual and Infrared Transmission Deduced from Surface Weather Observations: Weather and Warplanes VI*, Rand Corporation, Santa Monica, CA, 1976.

Marvin D. Kays, et al., *Qualitative Description of Obscuration Factors in Central Europe*, ASL Monograph No. 4, US Army Atmospheric Sciences Laboratory, White Sands Missile Range, NM, 1980.

R. J. List, *Smithsonian Meteorological Tables*, Smithsonian Institution, Washington, DC, 1966.

George O. Lof, et al., *Worldwide Distribution of Solar Radiation*, Solar Energy Laboratory, University of Wisconsin, Madison, WI, 1966.

Bruce Miers, *Geosem Worldwide Data Base*, US Army Atmospheric Sciences Laboratory, White Sands Missile Range, NM, 1984.

Ralph Shapiro, *Solar Radiative Flux Calculations from Standard Surface Meteorological Observations*, AFGL-TR 82-0039, US Air Force Geophysics Laboratory, Hanscomb AFB, MA, 1982.

William Wolfe, Ed., *Handbook of Military Infrared Technology*, Office of Naval Research, Arlington, VA, 1965.

Optical Propagation

Louis D. Duncan, et al., *EOSAEL 82*, ASL-TR-0122, US Army Atmospheric Sciences Laboratory, White Sands Missile Range, NM, 1982.

Marvin D. Kays, et al., *Qualitative Description of Obscuration Factors in Central Europe*, ASL Monograph No. 4, US Army Atmospheric Sciences Laboratory, White Sands Missile Range, NM, 1980.

F. X. Kneizys, et al., *Atmospheric Transmittance Radiance Computer Code LOWTRAN 5*, AFGL-TR-80-0067, US Air Force Geophysics Laboratory, Hanscomb AFB, MA, 1980.

Earl J. McCartney, *Optics of the Atmosphere*, John Wiley & Sons, New York, NY, 1976.

W. F. K. Middleton, *Vision Through the Atmosphere*, University of Toronto Press, Toronto, Canada, 1952.

T. J. V. Schie, *Nocturnal Illumination and Decrease of Contrast in the Atmosphere*, TNO, Amsterdam, Netherlands, 1969.

H. J. P. Smith, et al., *FASCODE—Fast Atmospheric Signature Code (Spectral Transmittance and Radiance)*, AFGL-TR-0067, US Air Force Geophysics Laboratory, Hanscomb AFB, MA, 1978.

D. Bruce Turner, "A Diffusion Model for an Urban Area", *Journal of Applied Meteorology*, 83-91 (February 1964).

William L. Wolfe and George J. Zissis, Eds., *The Infrared Handbook*, Office of Naval Research, Arlington, VA, 1978.

Limited Visibility Battlefield Conditions, The Technical Coordination Group, Joint Action Group (JAG) 10, 1983.

Status Report on Linear Atmospheric Transmission, The Technical Coordination Group, Joint Action Group (JAG) 5, 1977.

Turbulence

Louis D. Duncan, et al., *EOSAEL 82*, ASL-TR-0122, US Army Atmospheric Sciences Laboratory, White Sands Missile Range, NM, 1982.

Frederick Gebhardt, *Development of Turbulence Effects Models*, Science Applications, Inc., Ann Arbor, MI, 1980.

R. F. Lutomirski, et al., *Degradation of Laser Systems by Atmospheric Turbulence*, Rand Corporation, Santa Monica, CA, 1973.

V. I. Tatarski, *The Effects of Turbulent Atmosphere on Wave Propagation*, Israel Program for Scientific Translations, Jerusalem, Israel, 1971.

William Wolfe and George Zissis, Eds., *The Infrared Handbook*, Environmental Research Institute of Michigan, Ann Arbor, MI, 1978.

Other Relevant Literature

G. B. Hoidale, et al., *A Study of Atmospheric Dust*, ECOM-5067, Atmospheric Sciences Laboratory, White Sands Missile Range, NM, 1967.

AMCP 706-117, Engineering Design Handbook, *Environmental Series, Part Three, Induced Environmental Factors*, 1976.

Combat Environment Obscuration Handbook (Draft), Smoke and Aerosol Working Group, Joint Technical Coordination Group/Munition Effectiveness, Aberdeen Proving Ground, MD, 1984.

CHAPTER 4
PHYSICAL PROPERTIES OF
BATTLEFIELD-INDUCED CONTAMINANTS

This chapter is a quantitative description of battlefield-induced contaminants, including smokes and obscuration materials; it includes a discussion of munition explosions, launcher-associated obscuration, vehicular factors, and battlefield fires. It also contains sample illustrations of artillery, smoke, and vehicle usage, which indicate reasonable levels of battlefield obscurants. These combat examples will be used in the sample system performance calculations in Chapter 5.

4-0 LIST OF SYMBOLS

C_n^2 = index of refraction structure constant, $m^{-2/3}$

CL = concentration path length product, g/m^2

D = number of helicopter rotor diameters, dimensionless

h = height, m

h_p = height above source expressed in source radii, dimensionless

I' = apparent radiant intensity, kW/sr

OD = optical depth, dimensionless

r = hot spot radius, m

T = temperature, K or °C

δT_c = plume centerline temperature above ambient, deg C

T_F = measured peak fireball temperature, K

T_P = predicted volume averaged temperature, K

δT_s = source temperature above ambient, deg C

T_V = measured volume averaged temperature, K

$T(\lambda)$ = transmittance, dimensionless

$T_a(\lambda)$ = atmospheric transmittance considering only aerosol extinction, dimensionless

$T_d(\lambda)$ = transmittance through HE dust or vehicular dust, dimensionless

$T_d'(\lambda)$ = transmittance through lofted snow, dimensionless

$T_m(\lambda)$ = atmospheric transmittance considering only molecular extinction, dimensionless

$T_s(\lambda)$ = transmittance through smoke, dimensionless

t = time, s or ms

Y_f = yield factor, dimensionless

$\alpha(\lambda)$ = obscurant mass extinction coefficient for any wavelength λ, m^2/g

$\alpha_d(\lambda)$ = dust mass extinction coefficient for any wavelength λ, m^2/g

$\alpha_d'(\lambda)$ = mass extinction coefficient for lofted snow for any wavelength λ, m^2/g

$\alpha_s(\lambda)$ = smoke mass extinction coefficient for any wavelength λ, m^2/g

λ = wavelength, μm

4-1 INTRODUCTION

This chapter provides the basis for the calculations of battlefield-induced contaminant effects on sensor performance by describing the battlefield-induced contaminants; by providing mass extinction coefficients for these contaminants; by giving an assessment of the expected concentration, or mass loading, of these contaminants on the battlefield; and by developing combat examples that illustrate possible obscurant concentrations on the battlefield. The combat examples will be

used with the quantitative obscuration data to calculate obscurant effects on system performance.

Inventory smokes, including phosphorus, hexachloroethane (HC), and fog oil smokes, are described in par. 4-2. Brief discussions of developmental smokes and threat smokes are included, but the data are limited to keep the discussion at an unclassified level. Literature references to documentation on threat smokes, candidate smokes, and developmental smokes are included in the bibliography. Par. 4-3 treats munitions explosions and includes munition-generated dust and debris, as well as a discussion of dust cloud temperature and gaseous emissions. Launcher-associated obscuration, vehicular factors, and battlefield fires are characterized in pars. 4-4 through 4-6. Battlefield contaminant usage levels are developed in par. 4-7 by using examples of artillery barrage-generated dust and debris, obscuring smoke, and vehicular dust.

The mass extinction coefficients given in this chapter permit the calculation of transmittance through smoke $T_s(\lambda)$ and transmittance $T_d(\lambda)$ through high explosive (HE) dust or vehicular dust ($T_d'(\lambda)$ for lofted snow) which are used with the molecular transmittance term $T_m(\lambda)$ and the aerosol transmittance term $T_a(\lambda)$ in Eq. 3-1 to calculate transmittance $T(\lambda)$

$$T(\lambda) = T_m(\lambda) \ T_a(\lambda) \ T_s(\lambda) \ T_d(\lambda), \atop \text{dimensionless} \quad (4\text{-}1)$$

4-2 SMOKES AND OBSCURATION MATERIAL

There are four well-established methods of smoke production: burning phosphorus in air, burning pyrotechnic compositions, vaporization and recondensation of oils, and the dispersion of reactive liquids (Ref. 1). Phosphorus smokes are formed by burning phosphorus in air to form phosphorus oxides, which absorb atmospheric moisture to form aerosols of dilute phosphoric acid, and they may be delivered as bulk-filled white phosphorus (WP), plasticized white phosphorus (PWP), or red phosphorus (RP), or as WP or RP submunitions. The optical properties of the smokes are identical (Ref. 1). Most modern armies have phosphorus smokes.

Aerosols generated by burning pyrotechnic compositions, primarily HC and the Yershov compositions, are the second most common military smokes. HC and the Yershov compositions form hydrated aerosols with similar extinction coefficients. The HC smokes used by the United States and western European countries produce zinc chloride aerosols, whereas the Yershov compositions used by Warsaw Pact countries produce ammonium chloride aerosols (Ref. 1).

Oil-based aerosols are commonly used for smoke screening. They are formed by spraying diesel oil on the engine manifold or by vaporizing fog oil with pyrotechnic or mechanical generators. The spectral characteristics of the two oil smokes are similar. The U.S. has fog oil generators and uses vehicle engine exhaust smoke systems (VEESS) for armored vehicle protection. The Warsaw Pact countries have an extensive oil smoke generation capability.

The most common reactive smokes are chlorosulfonic acid (FS), which produces sulfuric acid smoke, and titanium tetrachloride (FM), which produces dilute titanium hydroxide and hydrochloric acid aerosols. Both are similar to phosphorus in extinction properties. The reactive liquids are obsolete in US inventories because they are highly corrosive and dangerous (Ref. 1).

Representative spectral extinction coefficients of these smokes, measured by the US Army Chemical Research and Development Center (CRDC)*, are shown in Fig. 4-1. All of these smokes are effective in the visible and are less effective in the infrared (IR). Phosphorous smokes have the highest far IR extinction. None of these smokes is effective at millimeter wave (mmw) wavelengths.

Smokes currently in the US Army inventory include phosphorus (munitions and grenades), HC munitions and smoke pots, and fog oil for generators. All of these generate white smokes, which attenuate by diffusing or scattering radiation. They are listed in Table 4-1 with several foreign smokes and developmental smokes.

Developmental smokes and threat smokes are discussed briefly at an unclassified level in pars. 4-2.4 and 4-2.5, respectively, and references to more detailed information are provided.

Spectral mass extinction coefficients for fog oil, diesel oil, phosphorus, HC, and anthracene smokes are given in Table 4-2. The tabulated values are for 50%

*Formerly Chemical Systems Laboratory (CSL).
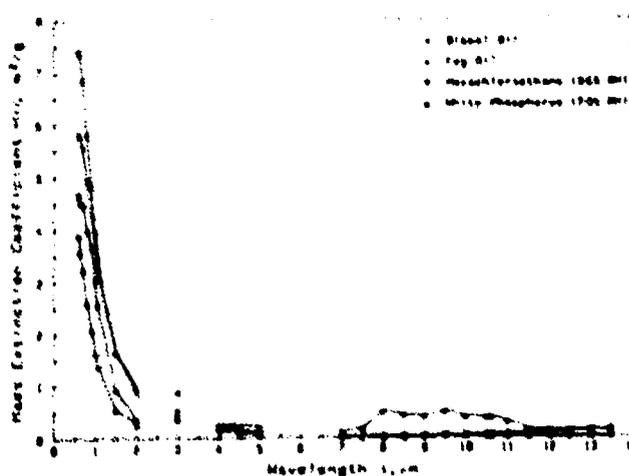
Figure 4-1. Mass Extinction Coefficient of Standard Screening Smokes (Refs. 1 and 2)

TABLE 4-1. INVENTORY AND DEVELOPMENTAL SMOKES
(Refs. 2 and 3)

MUNITION	FILL WEIGHT, kg	BURN DURATION, s	EFFICIENCY, %
155-mm HC M116B1 projectile	8.61	100	70
105-mm HC M84A1 projectile	2.15	120	70
Smoke pot, HC M5	14.06	900	70
81-mm WP M375A2	0.73	45	100
4.2-in. WP M328A1	3.70	45	100
155-mm WP M110E2	7.09	60	100
155-mm WP M825	7.45	720	77
105-mm WP M60A2	1.74	75	100
60-mm WP M302A1	0.34	45	100
4.2-in. PWP M328A1	3.70	180	60
5-in. PWP Zuni Mk4	6.15	180	60
Oil generator, M3A3	151.2 L h	900	100
2.75-in. WP rocket M156	0.96	120	—
L8A1 RP	0.36	100	—
Grenade, hand M8	0.55	120	—
Smoke pot, SGFZ, M7	5.91	600	—
VEESS M60	181.4 L h	N/A	—
VEESS M1	317.5 L h	N/A	—
Developmental Items			
81-mm XM819	1.37	300	—
XM76 grenade	—	—	—
Oil generator, XM52	227 L h	N/A	—
Foreign Munitions*			
155-mm WP projectile	7.09	126	100
122-, 132-mm WP projectile	3.59	80	100
120-mm WP projectile	1.95	51	100
82-mm WP projectile	0.34	17	100
122-mm PWP projectile	3.59	180	100

*European

TABLE 4-2. COMPARISON OF SPECTRAL MASS EXTINCTION COEFFICIENTS $\alpha(\lambda)$
(Refs. 3 and 4)

Obscurant	Mass Extinction Coefficient $\alpha(\lambda)$, m²/g Wavelength λ, μm						
	0.4 to 0.7	0.7 to 1.2	1.06	3 to 5	8 to 12	10.6	35 GHz 94 GHz
Fog Oil	6.85	4.59	3.48	0.25	0.02	0.02	0.001*
Diesel Oil	5.65	4.08	3.25	0.25	0.02	0.03	0.001*
Phosphorus	1.08	1.77	1.37	0.29	0.38	0.38	0.001*
HC	3.66	2.67	2.28	0.19	0.03	0.04	0.001*
Anthracene	6.00	3.50	2.00	0.23	0.06	0.05	0.001*

*Or lower

relative humidity at 10°C. The hygroscopic smokes, e.g., WP and HC, show some dependence on relative humidity due to both change in refractive index and the change in particle size as droplets take up water from the air. The change in extinction coefficient of WP and HC with relative humidity is discussed in pars. 4-2.1 and 4-2.2.

Transmittance $T_s(\lambda)$ through smoke is calculated from the extinction coefficient $\alpha_s(\lambda)$ and the CL product of obscurant:

$$T_s(\lambda) = e^{-\alpha_s(\lambda) CL}, \text{ dimensionless} \quad (4-2)$$

where

CL = concentration path length product, g $\cdot$ m²

$\alpha_s(\lambda)$ = smoke mass extinction coefficient for any wavelength λ, m² g.

Smoke concentration is discussed in pars. 4-2.1 through 4-2.3; representative CL products of smoke may be developed from the combat usage levels in par. 4-7.1.

4-2.1 PHOSPHORUS SMOKES

Phosphorus smoke is formed by burning elemental phosphorus in air. It hydrates rapidly to form a phosphoric acid aerosol. The burning phosphorus is very bright visually; the smoke radiance also is apparent in thermal imagers. Phosphorus smokes are not generally used over friendly positions because of the danger from the hot, burning phosphorus and the acidity of the smoke.

Bulk phosphorus burns very rapidly, and the resulting aerosol rises quickly. Plasticized white phosphorus, phosphorus impregnated felt wedges, and red phosphorus compositions are designed to burn more slowly and with increased burn uniformity. The fill weight

and burn time for standard phosphorus munitions are given in Table 4-1.

Phosphorus smoke particles grow rapidly; they pull moisture from the air and dilute the acid concentration. The particle size, refractive index, and mass extinction coefficient change as this happens. The expected size of phosphorus aerosol particles depends on the atmospheric relative humidity (RH). The effective extinction coefficient and yield factor of WP smoke as a function of relative humidity is shown in Table 4-3.

WP cloud temperature vs time for a bulk-filled 155-mm projectile is given in Table 4-4. The right column gives predicted average cloud temperature in neutral atmospheric conditions developed using the Electro-Optical Systems Atmospheric Effects Library (EOSAEL) code (Ref. 3). The measured peak cloud temperature and average cloud temperature data are shown in the left and center columns, respectively. These temperature differences within the cloud appear as clutter or false targets when viewed through thermal imaging systems.

It is difficult to predict the level of phosphorus smoke to be expected in a battlefield environment. The amount of phosphorus smoke in the sensor line of sight depends on many factors including the atmospheric conditions, the placement of the smoke relative to the sensor, the quantity of smoke placed, and the frequency with which it is placed. Indications of reasonable levels of WP are developed in the smoke usage illustration in par. 4-7.2. The WP concentration path length plot for a volley of six bulk-filled 155-mm munitions, shown in Fig. 4-2, indicates a typical shape for the WP concentration vs time across a sensor line of sight (LOS), showing a rapid buildup, then a gradual falloff as the cloud is blown past. Turbulence in the smoke and local shifts in

TABLE 4-3. YIELD FACTOR AND MASS EXTINCTION COEFFICIENT FOR WP SMOKE AS A FUNCTION OF RELATIVE HUMIDITY
(Ref. 5)

		Mass Extinction Coefficient $\alpha_s(\lambda)$, m² g						
		Wavelength λ, μm						
RH, %	Yield Factor Y_s,* dimensionless	0.4 to 0.7	0.7 to 1.2	1.06	3 to 5	8 to 12	10.6	35 GHz 94 GHz
5	3.39	2.66	1.50	1.34	0.26	0.38	0.35	0.001⁺
10	3.53	2.94	1.51	1.30	0.29	0.38	0.36	0.001
30	3.91	3.76	1.60	1.26	0.33	0.38	0.39	.0.001
50	4.34	4.08	1.77	1.37	0.29	0.38	0.38	0.001
70	5.10	3.90	2.03	1.66	0.29	0.36	0.35	0.001
90	7.85	3.23	2.36	2.11	0.41	0.30	0.28	0.001
95	11.70	2.98	2.16	2.25	0.48	0.27	0.26	0.001

*Yield factor is discussed in par. 2-7.2
⁺Nominal low value

TABLE 4-4. WP CLOUD TEMPERATURE vs TIME (155-mm BULK-FILLED PROJECTILE) UNDER NEUTRAL ATMOSPHERIC CONDITIONS (Refs. 5 and 6)

	Measu.		Predicted*
Time t, s	Peak Fireball Temperature T_F, K	Volume Averaged Temperature T_V, K	Volume Averaged Temperature T_P, K
0	≥450	336	339
2	413-424	327-330	320
5	377-388	318-321	303
10	314-323	297-300	295
15	305-310	294-296	294
20	300-301	292-293	293

*EOSAEL dust model (Conditions: temperature 16.9°C, 50% RH, Pasquill Category C, wind 3.1 m/s).
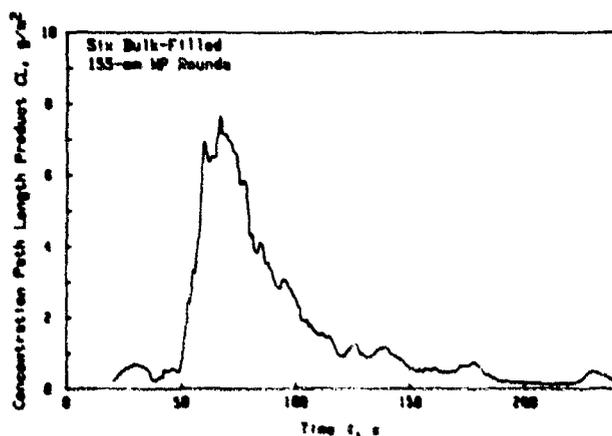
Figure 4-2. Integrated WP Smoke Concentration vs Time (Ref. 7)

wind velocity and direction will cause rapid local fluctuations in the concentration.

WP smoke is a good visual screener, a marginal screener in the thermal bands, and ineffective at mmw wavelengths.

4-2.2 HEXACHLOROETHANE (HC)

HC smoke is a pyrotechnic smoke generated by the burning of the HC composition of aluminium, zinc oxide, and hexachloroethane. Zinc chloride is the resulting hygroscopic aerosol. HC burns more slowly than phosphorus and releases about one-ninth the thermal energy per unit rate; thus it rises less and is not dissipated as quickly. The standard HC munition is the 155-mm artillery-delivered M116B1 round with a fill weight of 8.61 kg and a burn time of 100 s.

Thermal cloud radiance effects are generally not significant for HC munitions. Changes in HC smoke extinction with RH are less pronounced than with WP smokes, but they are important. HC smoke yield factor and extinction coefficient, as a function of relative humidity, are shown in Table 4-5.

TABLE 4-5. YIELD FACTOR AND MASS EXTINCTION COEFFICIENT FOR HC SMOKE AS A FUNCTION OF RELATIVE HUMIDITY (Ref. 5)

		Mass Extinction Coefficient $\alpha_e(\lambda)$, m²/g						
		Wavelength λ, μm						
RH, %	Yield Factor Y_s,* dimensionless	0.4 to 0.7	0.7 to 1.2	1.06	3 to 5	8 to 12	10.6	35 GHz 94 GHz
5	1.39	2.76	1.67	1.40	0.17	0.01	0.02	0.001
10	1.46	3.00	1.87	1.56	0.19	0.02	0.02	0.001
30	1.59	3.60	2.14	2.04	0.21	0.03	0.03	0.001
50	1.89	3.66	2.67	2.28	0.19	0.03	0.03	0.001
70	2.40	3.18	2.57	2.28	0.19	0.03	0.05	0.001
90	5.72	2.15	2.14	2.03	0.27	0.06	0.08	0.001
95	10.49	1.81	1.98	1.93	0.31	0.07	0.09	0.001

*Yield factor is discussed in par. 2-7.2.

HC concentration on the battlefield depends on the firing rate and weather conditions. An illustration of HC integrated path length after a firing of four rounds, in neutral atmospheric conditions, is shown in Fig. 4-3.

HC smoke is a good visual screener, a marginal screener in the 3-5 μm band, poor in the 8-12 μm band, and ineffective at mmw wavelengths.

4-2.3 DIESEL AND FOG OIL SMOKE

US Army oil smokes are dispensed by vaporizing vehicle engine diesel fuel or specially supplied fog oil. The resulting oil droplet aerosol is neither exothermic nor hygroscopic; thus it has no thermally induced buoyancy and stays closer to the ground than HC or WP screeners.

Oil smokes, unlike WP and HC smokes, are produced at a constant rate. Production ends only when the oil has been used up or the engine or generator has stopped. A representative plot of the fog oil concentration created by four fog oil generators vs time is shown in Fig. 4-4. The fluctuations in concentration indicate the effect of local meteorological conditions.

Oil smokes are effective screeners only at visible and near IR wavelengths.

4-2.4 DEVELOPMENTAL SMOKES

Inventory smokes provide good attenuation in the visible and near IR regions, have marginal effectiveness in the thermal bands, and are ineffective at mmw wavelengths. Army research and development programs are investigating the development of smokes with better multispectral screening capabilities (Ref. 1). The design considerations for effective screening materials are discussed in Ref. 8. Information on developmental and candidate smokes is contained in Refs. 9 and 10.

4-2.5 THREAT SMOKES

Smokes of the Warsaw Pact Countries include phosphorus smokes, pyrotechnic smokes (Yershov composi-
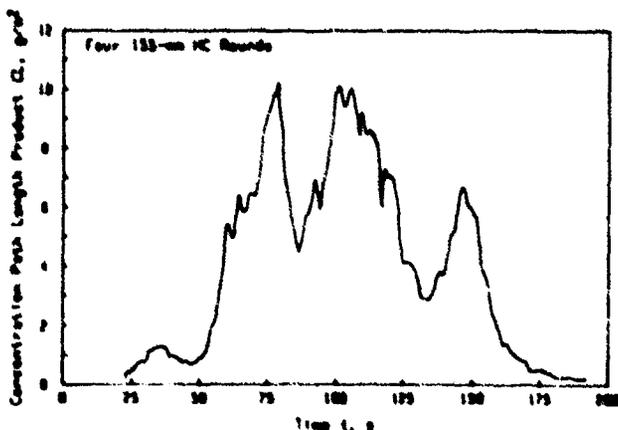
Figure 4-3. Integrated HC Smoke Concentration vs Time (Ref. 7)
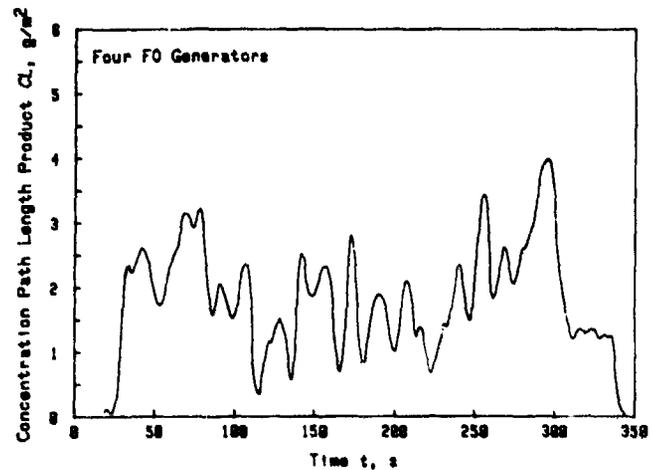
Figure 4-4. Integrated Fog Oil Concentration vs Time (Ref. 7)

tion), and diesel oil smokes. The mass extinction coefficients for these smokes are shown in Fig. 4-1. Information on other threat smokes is not available on an unclassified basis but is included in Ref. 11. System designers should consult CRDC and the Foreign Science and Technology Center (FSTC) for characterizations of threat smokes in their system spectral band.

4-3 MUNITION EXPLOSIONS

As discussed in par. 2-5.2, munition explosions are characterized by three phases. In the impact phase, dust and large chunks of debris are hurled aloft, a hot dust-and-fire ball several meters across is formed, and a cooler dust skirt 6-10 m wide and 1-3 m high* develops. In the rise phase, the dust-and-fire ball expands and rises rapidly, the large debris settle out, and the dust skirt diffuses slowly. Finally, in the drift and dissipation phase, the cloud, blown by the wind, dissipates.

The impact phase lasts only a few seconds, but during that period there is sufficient debris aloft to interrupt mmw LOS. The heat and bright light from the explosion and fireball may saturate visual and thermal sensors. In the rise phase and the drift and dissipation phase thermal radiance may still be important. In the drift and dissipation phase, the airborne dust may still block visible and thermal transmittance, but mmw systems are unaffected.

4-3.1 DUST AND DEBRIS

Fig. 4-5 illustrates the variation in transmittance through the cloud with time as the cloud is generated and slowly dissipates. The irregular structure again indicates turbulent mixing in the dust cloud. Realistic obscurant levels for an HE munition barrage can be developed from the artillery usage example in par.

*These dimensions apply to 155-mm munitions.
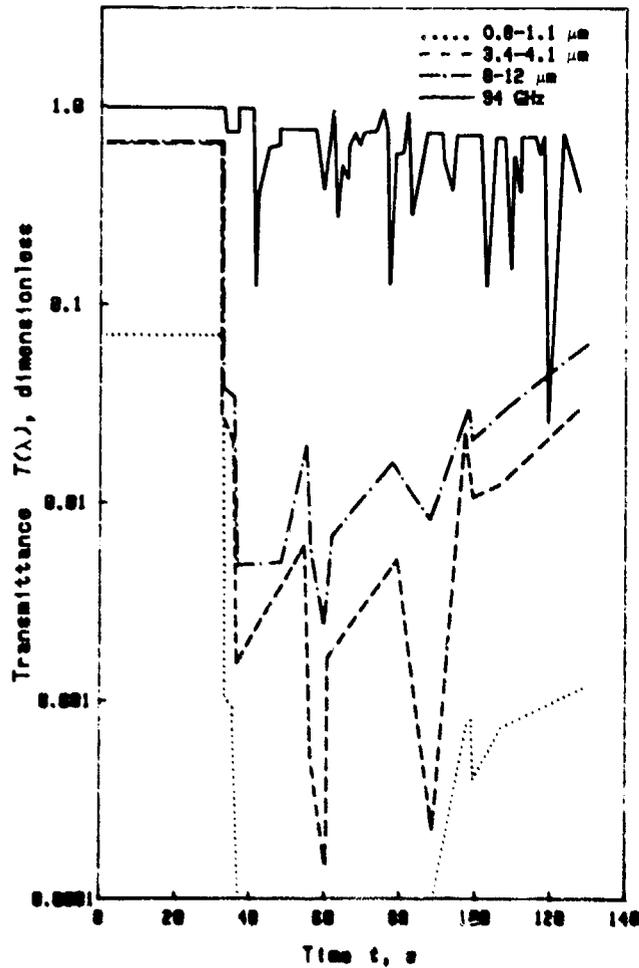
Figure 4-5. Near IR, Thermal, and Millimeter Wave Transmittance After an HE Explosion (Ref. 12)

4-7.1. Mass extinction coefficients for both large and small dust particles are included in Table 4-6. Transmittance $T_d(\lambda)$ through dust is calculated from the CL product of the obscurant and the spectral mass extinction coefficient $\alpha_d(\lambda)$ for the spectral band of interest.

$$T_d(\lambda) = e^{\alpha_d\lambda CL}, \text{ dimensionless} \quad (4\text{-}3)$$

where

$\alpha_d(\lambda) =$ dust mass extinction coefficient for any wavelength λ, m^2 g.

HE-generated dust may degrade visible, near IR, and thermal sensor performance. The debris lofted in the impact phase may break the mmw sensor LOS for 2 to 4 s; the residual dust does not significantly degrade mmw transmittance. Two-way attenuations of 10 dBm and backscatter of -10 dBm at 94 GHz have been observed on the centerline of 105-mm HE explosions. The attenuation drops rapidly with distance from the impact point and is negligible for lines of sight 15-20 m off the centerline (Ref. 13).

4-3.2 GASEOUS EMISSIONS AND HEAT

Extremely high temperatures develop in the HE-munition fireball in the period immediately after impact. Temperatures in the fireball may reach above 1500 K, drop to 350-400 K after only two seconds, and fall to ambient temperature in about five seconds. Cloud temperature data vs time, for three events reduced from the Battlefield-Induced Contamination Test (BICT) III, are shown in Table 4-7. Figs. 4-6 and 4-7 show hot spot radius r and cloud centroid height, respectively, for the same events.

The gaseous emissions from munitions explosions include CO_2, CO, CH_4, H_2O, H_2, N_2, NH_3, HCN, and HF. These gases are generally not significant obscurants simply because they occur when severe obscuration is present due to lofted dirt and debris, and thermal effects. However, particulate carbon, a by-product of some explosions, is a factor in obscuration for short periods of time after the detonation (Ref. 15).

4-4 GUN-FIRING OR LAUNCHER-ASSOCIATED OBSCURATION

Obscuration associated with the firing of guns or howitzers or with missile or rocket launches may degrade the performance of sensors on the platform. Obscuration is caused by muzzle flash radiance effects, the attenuation of signal radiation by the rocket plume, and by dust and debris raised by the launch or gun firing shock wave.

TABLE 4-6. MASS EXTINCTION COEFFICIENT $\alpha_d(\lambda)$ FOR HE DUST (Ref. 3)

	Mass Extinction Coefficient $\alpha_d(\lambda)$, m^2 g						
	Wavelength λ, μm						
Obscurant	0.4 to 0.7	0.7 to 1.2	1.06	3 to 5	8 to 12	10.6	35 GHz 94 GHz
HE dust, small	0.32	0.29	0.26	0.27	0.26	0.21	0.001
HE dust, large	0.04	0.04	0.04	0.04	0.04	0.04	0.001

TABLE 4-7 HE-GENERATED DUST CLOUD TEMPERATURE vs TIME
(Ref. 14)

Event HE2* Clay Soil			Event HE3 Wet Sand			Event HE9 Wet Soil		
Time t, s	Temperature T, K	Radius r, m	Time t, s	Temperature T, K	Radius r, m	Time t, s	Temperature T, K	Radius r, m
0.010	1750	2.9	—	—	—	—	—	—
0.110	1365	2.6	—	—	—	—	—	—
0.210	1000	2.4	0.20	650+	2.3	0.34	650+	3.5
0.310	865	2.3	0.50	605	2.6	0.50	630	3.5
—	—	—	0.90	495	2.9	0.81	470	3.8
2.21	354	4.0	1.94	375	2.2	1.71	430	3.5
3.11	329	3.9	3.04	330	2.5	2.71	345	3.4
4.5	300	5.4	4.55	315	3.0	4.75	301	7.8
5.95	298	6.9	5.95	305	4.4	—	—	—

* All events were for a 4.5-kg fill.

† Instrument saturated; actual value was higher.
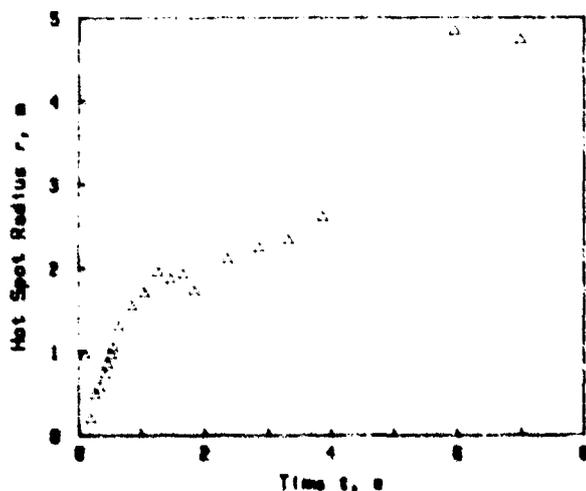
Figure 4-6. HE-Generated Dust Cloud Hot Spot Radius vs Time (Ref. 14)
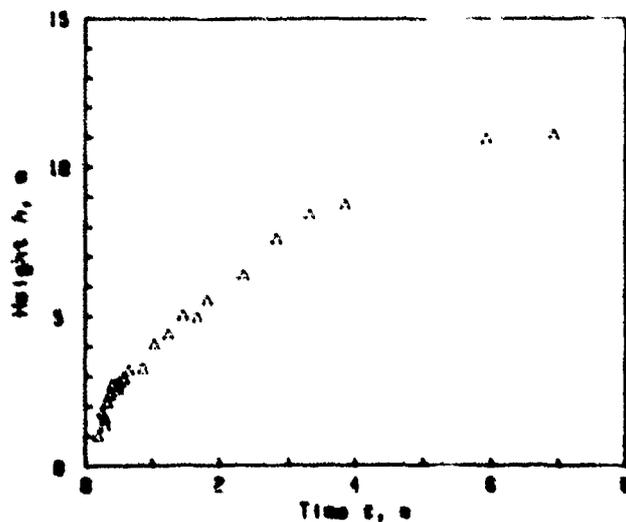
Figure 4-7. HE-Generated Dust Cloud Centroid Height vs Time (Ref. 14)

4-4.1 MUZZLE FLASH

The muzzle flash created by the firing of a projectile from an artillery weapon is apparent in the visible, near IR, and thermal spectral bands. It is a short-duration phenomenon on the order of 125 ms; peak radiation is seen at about 20-25 ms after the blast, and the peak value decays by one-half at 45-50 ms after the blast (Ref. 16). The effect is short-term detector saturation for a sensor looking at the muzzle flash. Fig. 4-8 shows the apparent muzzle flash signature of an M-68 105-mm gun in the 4.35-4.70 μm (red spike) missile band; the data were taken 750 m from the gun.

The peak apparent muzzle flash signatures in the 3-5 μm band exceeded 4 × 10⁴ W·sr (Ref. 16). Muzzle flash signatures in the 8-12 μm region show the same time dependence but are significantly lower in magnitude
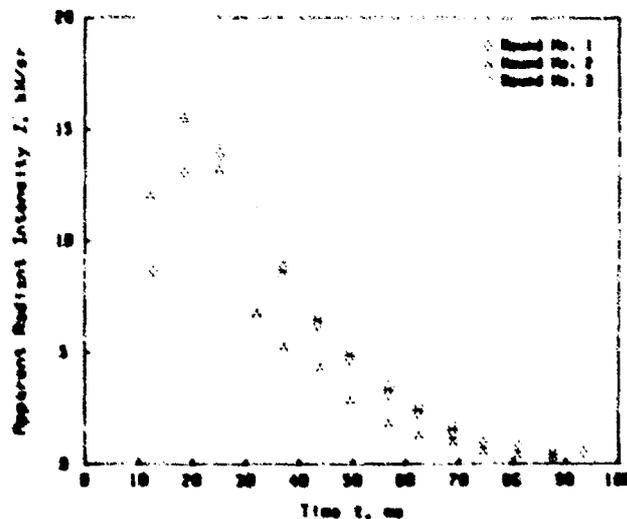
Figure 4-8. Apparent Radiant Intensity of an M-68 105-mm Gun in the 4.35 to 4.70 μm Spectral Band (Ref. 16)

(by one-fifth to one-half the peak radiance) because the muzzle gases, primarily CO_2 and hot H_2O, are less efficient radiators in the thermal band.

4-4.2 ROCKET PLUME

Rocket plumes can temporarily obscure visual and thermal sensors for periods of several seconds. More detailed measurement data are contained in the classified literature (see Ref. 17).

4-4.3 DUST AND DEBRIS

Dust and debris raised by the shock wave from a missile or rocket launch or gun firing can temporarily obscure the LOS of a sensor mounted on the weapon platform, particularly if the soil is dry or loose and not secured by a vegetative cover. The obscuration may last for several seconds. An LOS interruption may slow the artillery firing rate or cause the gunner to temporarily lose track on a target.

4-5 VEHICULAR FACTORS

Military vehicles can cause obscuration. This paragraph describes vehicle-induced obscurants, including dust raised by the movement of tracked or wheeled vehicles, snow and dust lofted by helicopter downwash, and vehicular gaseous and particulate emissions.

Estimated mass extinction coefficients for vehicle-generated obscurants—vehicular dust and helicopter-lofted snow—are given in Table 4-8. Transmittance $T_s(\lambda)$ through vehicle-generated obscurants is calculated using mass extinction coefficients from Table 4-8 and concentration path length products (CL) obtained from pars. 4-5.1 and 4-7.3 for dust raised by tracked or wheeled vehicles or from par. 4-5.2 for helicopter-lofted snow and dust. For vehicular dust $T_s(\lambda)$ is calculated by using Eq. 4-4. For helicopter-lofted snow

$$T_s(\lambda) = e^{-\alpha_s'(\lambda) \cdot CL}, \text{ dimensionless} \quad (4\text{-}4)$$

where

$\alpha_s'(\lambda)$ = mass extinction coefficient for lofted snow for any wavelength λ, m^2/g.

4-5.1 DUST (TRACKED AND WHEELED VEHICLES)

Dust loading into the atmosphere by tracked and wheeled vehicles is determined by the amount of vegetative cover, the soil type and wetness, and the vehicle mass and speed. On dirt roads (representing the limiting case), the amount of dust raised by a vehicle is roughly linear with velocity, and scales linearly with the percent of silt in the soil. For example, in dry soil with about 65% silt content, an armored personnel carrier (APC) will raise about 2.3* kg of dust per mph of vehicle speed per mile covered. An M60 tank will raise about 4.4* kg of dust per mph of vehicle speed per mile covered (Ref. 19). Representative concentrations and CL values for dust raised by movement of columns of tanks, trucks, and APCs can be obtained from the vehicular dust example in par. 4-7.3. Transmittance through dust is calculated using these CL values in Eq. 4-4 with extinction coefficients from Table 4-8.

4-5.2 HELICOPTER DOWNWASH (LOFTED SNOW AND LOFTED DUST)

Dust and snow lofted by helicopter downwash will reduce transmittance or break the LOS in the visible, thermal, and mmw spectral bands. Because of the turbulence caused by the downwash, the amount of obscurant in the sensor LOS will change rapidly to show some periods of nearly total obscuration and others of essentially no obscuration. This effect is illustrated in Fig. 4-9, which shows visible and 8-12 μm transmittance through lofted snow, measured during the SNOW-ONE-A field test.

The amount of dust or snow lofted by helicopter downwash will depend on the helicopter weight, rotor diameter, height, and velocity, and on the soil type, wetness, and vegetative cover. For wind speeds above a certain threshold value, particles begin to bounce along

*These values apply for wind speeds from 5 to 25 mph

TABLE 4-8. MASS EXTINCTION COEFFICIENTS $\alpha_s(\lambda)$ $\alpha_s'(\lambda)$ FOR VEHICLE-GENERATED OBSCURANTS (Refs. 3, 5, and 18)

| Obscurant	Mass Extinction Coefficient $\alpha_s(\lambda)$ and $\alpha_s'(\lambda)$, m^2/g						
	Wavelength λ, μm						
	0.4 to 0.7	0.7 to 1.2	1.06	3 to 5	8 to 12	10.6	35 GHz 94 GHz
Vehicular Dust	0.32	0.30	0.29	0.27	0.25	0.25	0.001*
Lofted Snow	0.05	0.05	0.05	0.04	0.05	0.05	0.005-0.1

*Or lower
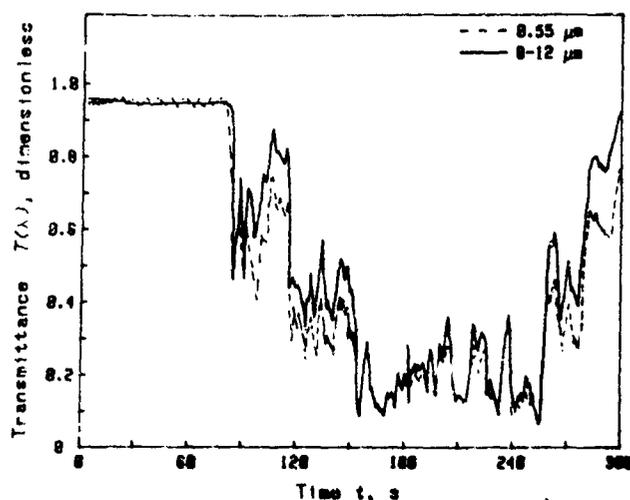
Figure 4-9. Transmittance Through Snow Lofted by Helicopter Downwash (Ref. 20)

the surface in a mode called "saltation". At higher velocities the smaller particles rise into suspension. During take-off and landing the downwash is capable of lifting particles from the ground. During forward flight the penetration will vary considerably; as the forward velocity or altitude of the helicopter increases, the effect of downwash diminishes (Ref. 18).

Data on obscuration by helicopter-lofted snow is limited; this paragraph contains preliminary data and is based primarily on the SNOW-ONE-A and SNOW-TWO field tests (Refs. 20 and 21). Lofted snow concentrations from 0.2 g·m³ to 2.8 g·m³ were measured in these tests, and averaged about 1.5 g·m³; the particle size distribution peaked at a snow particle radius of 300 μm. These particle sizes are in the geometric optics scattering regime for visible and thermal wavelengths. However, transmittance data from the SNOW-ONE-A test showed better visible transmittance with a systematic difference of 10-20% between the visible and the IR. This difference is due to the narrower scattering angle for visual radiation—more thermal energy is scattered out of the field of view of the transmission. The mass

extinction coefficients for helicopter-lofted snow shown in Table 4-8 are based on these measurements. No appreciable mmw attenuation was noted at the SNOW-ONE-A test (Refs. 20 and 22).

Helicopter-lofted snow cloud dimensions depend on the helicopter (weight, rotor diameter, altitude, and forward speed) and on the characteristics of the snow ground cover. Dry, fresh snow will result in a much larger snow cloud than older, grainy snow. The SNOW-ONE-A and SNOW-TWO tests were performed on dry snow and thus probably indicate worst case obscuration. Dimensions of snow clouds produced by the UH1H helicopter in these tests ranged from 100 m (about 8 rotor diameters) when the helicopter was within 3 m of the ground to 0 m (no cloud) at heights above 50 m. Table 4-9 gives rules of thumb to estimate snow cloud transmittance as a function of helicopter altitude and rotor diameter. The estimated concentration path length product CL shown in Table 4-9 was calculated using Eq. 4-4. Values in Table 4-9 give a rule-of-thumb estimate of visible, near IR, and thermal transmittance through the helicopter-lofted snow.

Measured quantitative data on helicopter-lofted dust are limited. Measurements of dust lofted by an H-21 helicopter were made at Yuma, AZ, and Fort Benning, GA. In these tests, the concentrations at takeoff and landing reached 11.9 g·m³. The highest dust concentrations near a hovering helicopter were measured directly below the rotor blade overlap and the lowest were measured beneath the rotor blades. The peak values are shown in Table 4-10.

4-3.3 GASEOUS AND PARTICULATE EMISSIONS

Gaseous and particulate emissions from vehicle exhausts are minor in their effect on sensor performance. CO and CO_2 do absorb in the thermal bands, and carbon is an excellent broadband attenuator, but the mass loading of these obscurants is low enough that they have a significant effect only if the sensor LOS intersects the exhaust itself.

TABLE 4-9. ESTIMATED OBSCURATION FOR HELICOPTER-LOFTED SNOW*
(Ref. 18)

Helicopter Altitude (in rotor diameters D)	Approximate Transmittance T (vis, near IR, thermal), dimensionless	Approximate CL, g·m²
1 D	1.0	0
3 D	0.6	16
2 D	0.35	33
1 D	0.15	60

*SNOW-TWO preliminary data for UH1H helicopter hovering over dry snow

TABLE 4-10. DUST CONCENTRATION NEAR H-21 HELICOPTER (Ref. 23)

Hover Height, m	Dust Concentration, g/m³		
	Drop Zone, Yuma	Dust Course, Yuma	Drop Zone, Ft. Benning
0.3	3.7	4.6	5.5
3.0	5.5	5.1	5.2
25.0	1.6	4.1	0.9

4-6 BATTLEFIELD FIRES

Battlefield fires have three main effects on sensor performance—radiance (heat or light) of the fire itself, transmittance losses through the fire products (smoke and hot gases), and system degradation caused by the turbulent air around the fire.

4-6.1 FIRE PRODUCTS

Vegetative fire products include gases, primarily carbon dioxide and water vapor, and particulates including carbon, soot, metal oxides, and silicates. In an oxygen-deficient environment, carbon monoxide, nitrogen oxides, and hydrocarbons are also produced. Vehicular fire products include carbon dioxide, aldehydes, organic acids, nitrogen oxides, carbohydrates,

and particulates. Table 4-11 gives estimates of the gaseous and particulate components for vegetative and vehicle fires. For vegetative fires, mass loading is given as mass of gas or particulate matter generated by burning 1 kg of vegetative matter. Vehicular fire products are estimates of the mass of matter generated by burning one vehicle, including tires and fuel.

Carbon is the only fire product that is an important attenuator at all visual and thermal wavelengths. Extinction by gaseous components is generally not significant for broadband radiation, even for large fires with path-integrated concentrations CL of up to 15 g/m² of gaseous products (Ref. 25). However, absorption by hot hydrocarbons is important in the 3-5 μm region. In addition, laser radiation may be significantly attenuated by gaseous fire products if the laser wavelength coincides with a gas absorption line. Absorption by N_2O may be important in the 3.8-μm region. Absorption by CO_2 will clearly affect CO_2 laser performance.

Mass extinction coefficients $\alpha_s(\lambda)$ for the smoke formed by carbon and burning diesel fuel are given in Table 4-12. Transmittance $T_s(\lambda)$ through fire products is calculated using Eq. 4-2.

4-6.2 FIRE-INDUCED TURBULENCE

Fire-induced turbulence will cause laser beam spread and short-term beam centroid jitter. In imaging systems the effect of the turbulence is smearing of the target image. Calculations of turbulence effects on propaga-

TABLE 4-11. MASS LOADING FOR FIRE PRODUCTS (Ref. 24)

Vegetative Fires		Vehicle Fires	
Component	Emission, g/kg	Component	Emission, kg/vehicle
Carbon Dioxide	100-1730	Carbon Dioxide	1.1
Particulates	10-20	Particulates	0.9
Nitrogen Oxides	1-5	Nitrogen Oxides	0.05
Carbon Monoxide	10-250	Carbohydrates	0.23
Hydrocarbons	4-20	Aldehydes	0.09
Water Vapor	250-750	Organic Acids	0.1

Reprinted with permission of the Society of Photo-Optical Instrumentation Engineers (SPIE), Barbara W. Levitt, and Leonard S. Levitt. Copyright © by the Society of Photo-Optical Instrumentation Engineers.

TABLE 4-12. MASS EXTINCTION COEFFICIENTS FOR FIRE PRODUCTS (Refs. 3, 4, and 26)

Obscurant	Mass Extinction Coefficient $\alpha_s(\lambda)$, m²/g						
	Wavelength λ, μm						
	0.4 to 0.7	0.7 to 1.2	1.06	3 to 5	8 to 12	10.6	35 GHz 94 GHz
Carbon	1.50	1.46	1.42	0.75	0.32	0.30	0.001
Diesel Fuel	6.40	3.69	2.94	1.34	1.00	1.00	—

tion are fairly complex. General experimental results can, however, be used to give order of magnitude estimates of fire plume parameters and the atmospheric effects associated with these plumes.

For a vertical fire plume the plume centerline temperature above ambient δT_c is approximated by (Ref. 27)

$$\delta T_c = \delta T_s e^{-0.25 h_r} \text{ deg C} \qquad (4\text{-}5)$$

where

δT_s = source temperature above ambient, deg C

h_r = height above source expressed in source radii, dimensionless.

Because normal temperature variations in the atmosphere are of the order of several tenths of a degree, the equation predicts that the turbulence effects are significant to a height equal to roughly 50 times the fire radius.

Values of the index of refraction structure constant C_n^2 in fire plumes were found to vary from 10^{-9} m$^{-2/3}$ (at h_r = 1 to 10^{-11} m$^{-2/3}$ (at h_r = 16) as compared to atmospheric C_n^2 values of about 10^{-14} to 10^{-9} m$^{-2/3}$.

For the area close to the fire ($h_r < 6$), beam jitter was found to be in the range of 100 to 600 mrad about an aimpoint that was displaced by 1 to 4 mrad by the presence of the plume. If the propagation path is near the edge of the plume, plume wander could cause jitter with magnitude equal to the aimpoint displacement. These values are obtained using only the portion of the path from the plume to the target. Beam jitter caused by the atmosphere over the same path was in the range of 0.06-0.09 mrad.

In the same area of the plume, the beam spread was found to average 0.5 to 1.0 mrad (half angle) with a time variation of roughly 100%. It should be noted that the plume acts as an inhomogeneous lens which redistributes the energy within the spot, so intensities cannot be easily predicted.*

4-7 BATTLEFIELD OBSCURANT USAGE LEVELS

Representative combat environment examples are developed here to estimate general levels of combat-induced obscurants likely to occur in actual combat. To keep the problem manageable, only the effects of artillery-delivered HE rounds, WP rounds, screening smokes, and vehicular dust are considered. These are felt to be major contributors to combat-induced obscuration.

---

*Most of the data in par. 4 to 2 are for small laser beams about to roughly 2 to 3 orders of magnitude less than plume diameters and for plumes which obscure much about 1% of the propagation path.

Three examples are considered. The first details the dust obscuration due to an artillery barrage. The second example describes the potential obscuration due to artillery-delivered WP smoke rounds, smoke pots, and smoke generators. The third example deals with dust generated by truck, tank, and APC traffic. These examples were extracted from more comprehensive usage examples developed by the Smoke and Aerosol Working Group of the Joint Technical Coordination Group Munitions Effectiveness (JTCG ME) for the *Combat Environment Obscuration* Handbook (Ref. 15).

In each example, the data are presented as snapshots-in-time as the scenario develops. There are two formats: (1) downward-looking optical depth (OD) over an area several kilometers on a side and (2) concentration at a 2-m altitude.

Optical depth is defined as the negative of the natural logarithm of the visible transmittance.

$$OD = -\ln T(\text{vis}) = \alpha_d(\text{vis}) CL, \qquad (4\text{-}6)$$
dimensionless

Table 4-13 tabulates visual transmittance vs optical depth.

TABLE 4-13. OPTICAL DEPTH vs VISUAL TRANSMITTANCE

Optical Depth OD, dimensionless	Visual Transmittance $T(\text{vis})$, dimensionless
0.1	0.90
0.5	0.60
1.0	0.37
2.0	0.14
3.0	0.05

Downward-looking OD contours may be used to estimate near IR and thermal transmittance $T(\lambda)$ through the obscurant by

$$T(\lambda) = e^{-\alpha(\lambda) CL}, \text{ dimensionless} \qquad (4\text{-}7)$$

where

$\alpha(\lambda)$ = obscurant mass extinction coefficient for any wavelength λ, m^2/g.

$$CL = \frac{OD}{\alpha(\text{vis})}, \text{ dimensionless.} \qquad (4\text{-}8)$$

The values of $\alpha(\lambda)$ are contained in Table 4-2 ($\alpha_s(\lambda)$ for smokes), Table 4-6 ($\alpha_d(\lambda)$) for HE-generated dust), and Table 4-8 ($\alpha_d(\lambda)$ for vehicular dust).

The second obscurant format type is a plot of obscurant concentration at a 2-m altitude over the area con-

tained in the downward-looking *OD* plots. These illustrations permit estimates of obscurant concentration (and hence transmittance) over LOS through the obscurant.* For simplicity in comparing the *OD* and concentration plots, *CL* values (at 2-m altitude) have been indicated on the *OD* plots along the selected LOS.

4-7.1 ARTILLERY EXAMPLE

The HE dust combat example is a first-day deliberate attack against a prepared defense. The attacking force consists of seven 152-mm artillery battalions, three 130-mm artillery battalions, one 122-mm artillery battalion, and one multiple rocket launcher (MRL) unit. The attack occurs over a 5 x 7-km area during the late morning in autumn in Central Europe.**

Results are presented for a 2 x 5-km grid for two snapshot-in-time intervals during the first 30 min of

---

*CL over an LOS is estimated by drawing the LOS then summing the products of concentration and length through the obscurant along that LOS.

**This combat example is extracted from a more comprehensive engagement described in Ref. 15. The meteorological setting used in this example is based upon climatic estimates for Central Europe compiled in EOSAEL 82 (Ref. 3). The selected conditions are appropriate for early morning autumn, with Pasquill Stability C and a 5-m s (18-km h) wind.

preparatory fire. The obscuration is portrayed two ways: (1) vertical (path integrated) *OD* for downward-looking sensors and (2) obscurant concentration at the 2-m level, from which the integrated path concentration lengths for a horizontal LOS can be calculated. The obscurant under consideration is HE-produced dust from the artillery barrage. The wavelength-dependent mass extinction coefficients in Table 4-6 may be used to estimate reductions in transmittance for optical and IR b ⋯ of military interest.

The large-are ⋯ obscurant due to the preparatory fire barrage is displayed sequentially for two successive times in Figs. 4-10 and 4-12. Fig. 4-10 illustrates the impact area after the in⋯ial 5 min of fire; approximately 1000 rounds have impacted by this time. Fig. 4-12 illustrates the same area 25 min after the beginning of the attack when most of the fire is directed to the west of this grid; only scattered fire and residual dust are shown.

The *OD* is used to illustrate the extent and the amount of obscuration seen by a downward-looking observer. The mass concentration of the airborne dust at the 2-m level is portrayed in Figs. 4-11 and 4-13 for the same times as in the previous two figures. The obscuration illustrated here is due to the small mode dust, which is the component that remains airborne for long periods of time (minutes to hours).
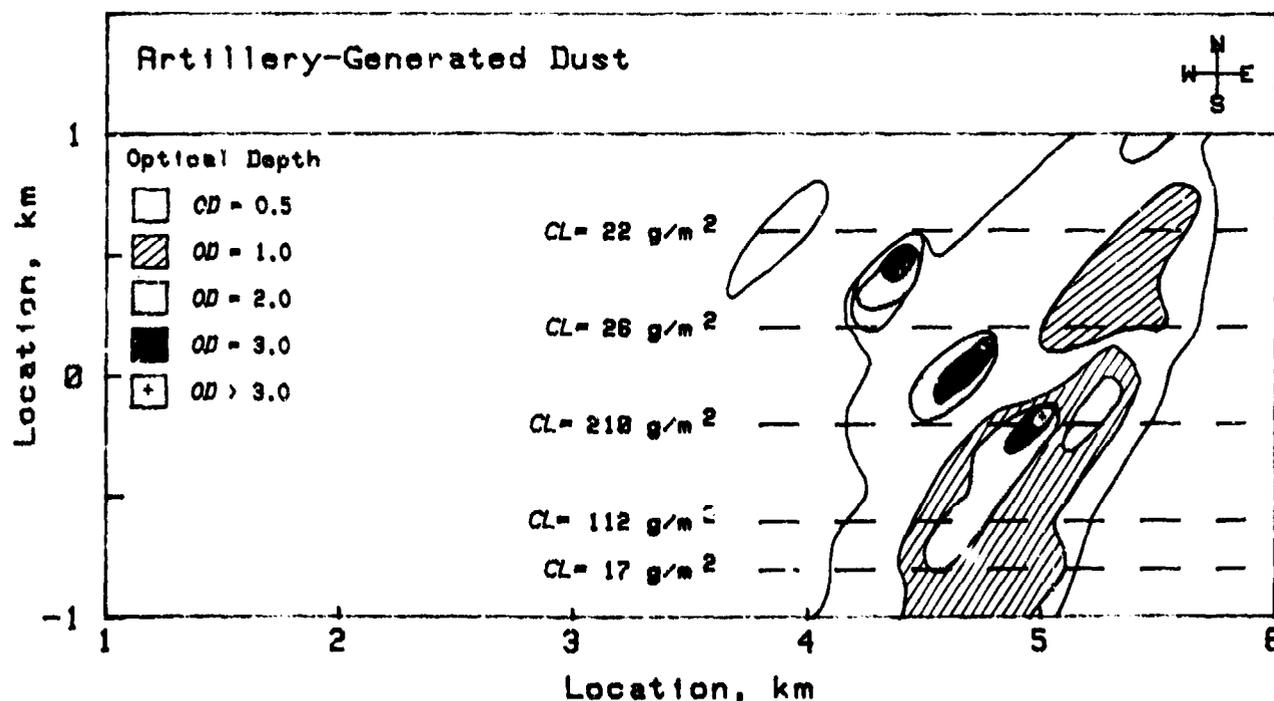

Figure 4-10. Downward-Looking Optical Depth of HE-Generated Dust
After Fifth Volley (Ref. 15)
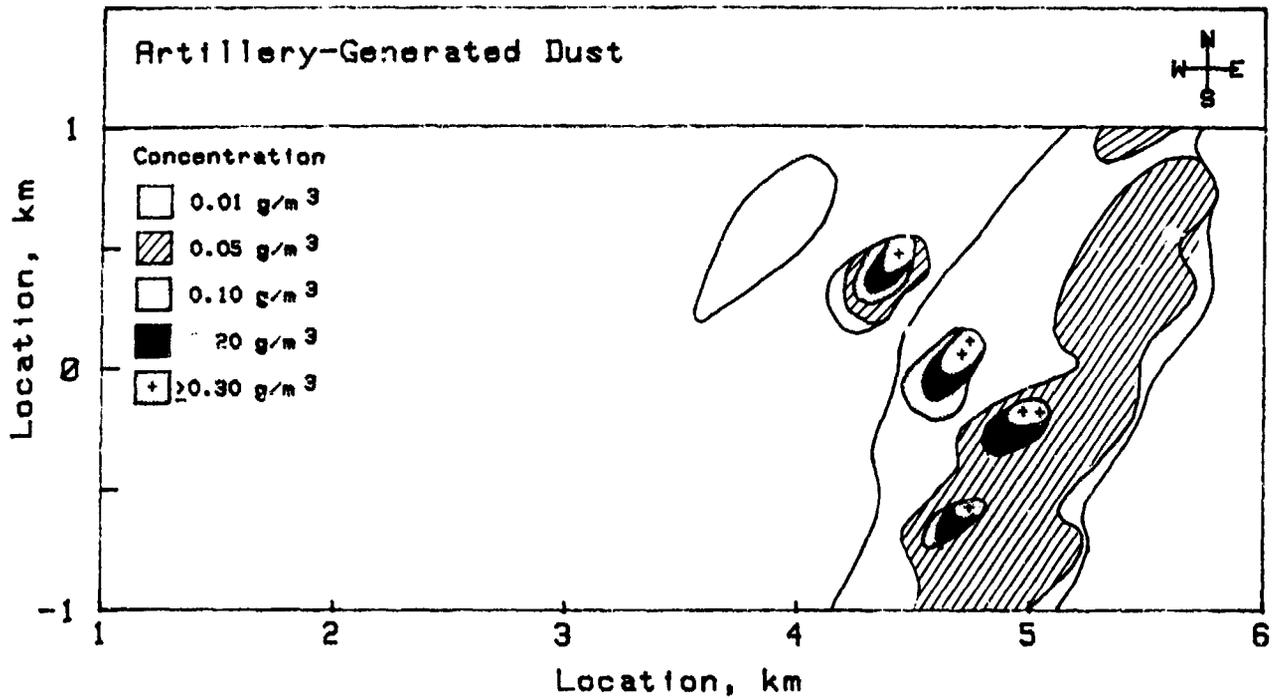
Figure 4-11. Concentration of HE-Generated Dust at 2-m Altitude After Fifth Volley (Ref. 15)
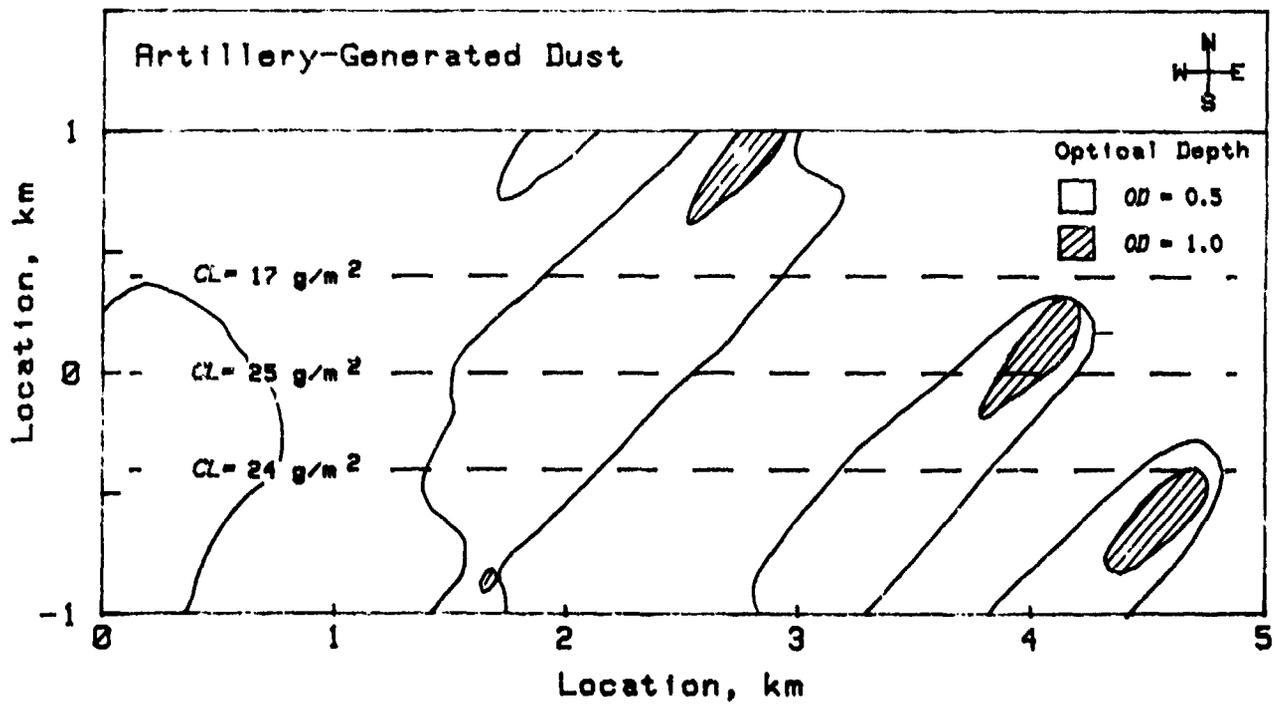
Figure 4-12. Downward-Looking Optical Depth of HE-Generated Dust
After Twenty-Fifth Volley (Ref. 15)
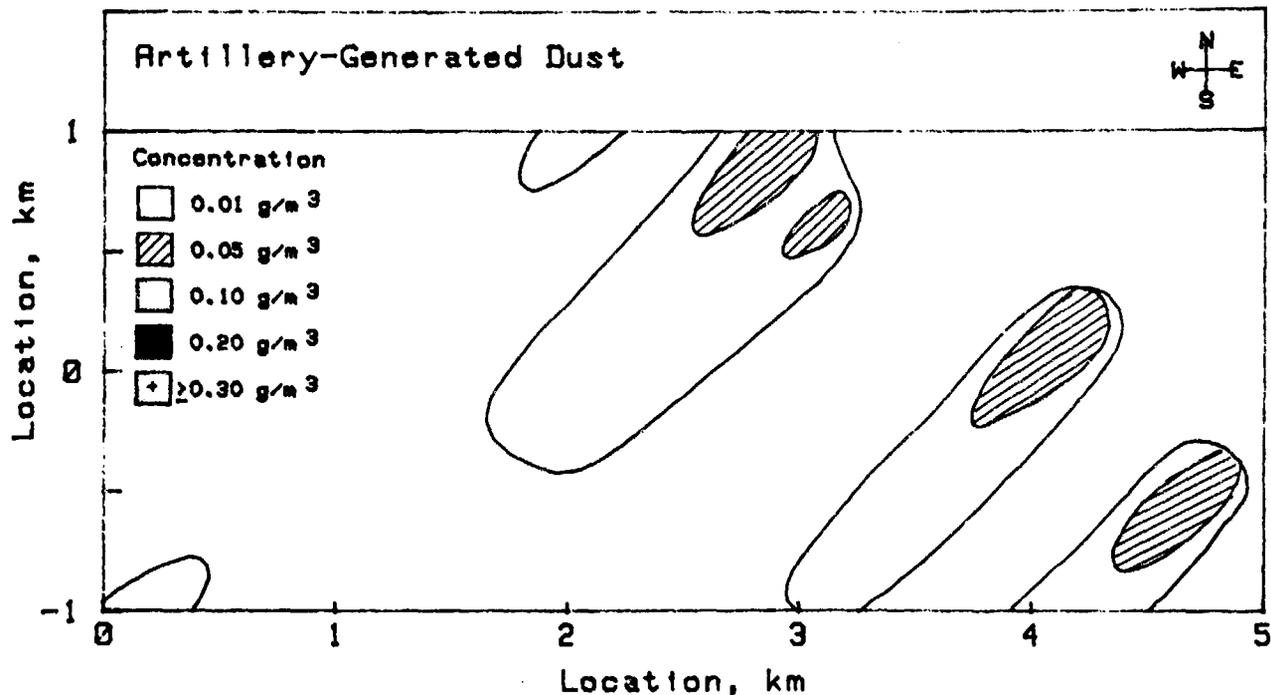
Figure 4-13. Concentration of HE-Generated Dust at 2-m Altitude After Twenty-Fifth Volley (Ref. 15)

4-7.2 SMOKE EXAMPLE

This combat example consists of the smoke used to cover the assault of a tank battalion and motorized rifle company, with supporting artillery and mortars, on a fixed defense.

The basic objective of screening smoke is to conceal from the enemy the true location and nature of actions of friendly troops. Such screening or camouflaging smokes are generated by VEESS, smoke pots, and smoke generators. Blinding smoke screens are generated in the vicinity of the adversary's position with indirect fire, such as mortars, rockets, or artillery, for the purpose of denying ground-level observation to the enemy.

The basic outline of the example is presented graphically in Fig. 4-14; there is amplifying information in Table 4-14.* The smoke example is laid out on a 2-km x 5-km grid and covers a period of 18 min with 4 separate smoke-producing events. The smoke is introduced at the right-hand (east) side of Fig. 4-14 and advances toward the left-hand (west) side at a quartering angle from upper right (northeast) to lower left (southwest). The smoke events are initiated sequentially from right to left (east to west).

The sequence of smoke events portrayed in Fig. 4-14 and Table 4-14 are displayed graphically in time sequence in Figs. 4-15 to 4-22.

Figs. 4-15 through 4-17 give an overview of the smoke example from H−9 min (5 min after the initiation of

*This example is a subset of the Soviet training example developed in Ref. 15.

Event 1) to H+4 min (the end of Events 3 and 4). The perspective is one of a viewer looking down on the field of battle. OD is used to give the viewer an indication of where the smoke is placed, its subsequent drift, and its relative thickness. The larger the OD, the smaller the transmittance, and consequently the more attenuation the smoke would provide for a downward-looking sensor.

Fig. 4-15 illustrates the large area of coverage due to the TMS-65 smoke generators (fog oil). Fig. 4-16 shows smoke from the DM-11 smoke pots (anthracene smoke) and residual smoke from the TMS-65 generators. Fig. 4-17 demonstrates the coverage due to mortar- and howitzer-delivered white phosphorus smoke rounds.

Figs. 4-18 through 4-21 show selected small-scale plots of smoke concentration at a 2-m altitude for four of the events shown in Fig. 4-14: (1) TMS oil smoke from Event 1 at Time H−9 min, (2) DM-11 smoke from Event 2 at Time H−3 min, (3) phosphorus smoke from WP munitions, Event 3, at Time H+4 min, and (4) phosphorus smoke from PWP munitions, Event 4, at Time H+4 min. Smoke concentration from a VEESS unit is shown in Fig. 4-22 for comparison. These figures may be used to estimate the amount of smoke along any LOS through the smoke by multiplying the smoke concentration along the path by the path length to obtain concentration path length product CL. Transmittance through the smoke may be calculated using these CL values in Eq. 4-2 and the mass extinction coefficients $\alpha_s(\lambda)$ obtained from Table 4-2.

TABLE 4-14. SMOKE EXAMPLE OVERVIEW (Ref. 15)

Major Smoke Events	Smoke Used; Method of Disposition	Timing of Smoke Event	Rate of Dispersion	Effect of Smoke Screen	Action of Participating Units
1	Smoke oil* 2 TMS-65 smoke generators (100 kg vehicle) 1.5 km front	H−14 min to H−9 min (5 min)	200 kg min unit; vehicle speed = 9 km h	Camouflaging smoke screen across 1.5 km front up to 400 m in height	Deployment of attacking troops assault
2	Anthracene 240 DM-11 smoke pots (1.8 kg pot) 2.0 km front	H−9 min to H−3 min (6 min)	12 min burn time (5-7 min coverage); 25 m separation (group of 3 pots)	Favorable wind direction results in blinding of defensive weapon emplacements	As smoke dissipates, entire firepower of attacking battalion concentrated on defending force
3	WP bulk* 6 120-mm mortars (1.9 kg WP round) 500 m front	H+2 min to H+4 min (2 min)	1 round 24 s tube; nominal 150 m impact area per volley	Blinding of defensive Antitank guided missiles (ATGMs)	Defensive ATGMs neutralized
4	WP (PWP)** 18 122-mm howitzers (72 smoke rounds) (3.6 kg WP round) 500 m front	H+2 min to H+4 min (2 min)	2 rounds min gun; nominal 150 m impact area per volley	Blinding of defensive ATGMs	

*Fog Oil
*White phosphorus, bulk-filled munition
**White phosphorus, plasticized
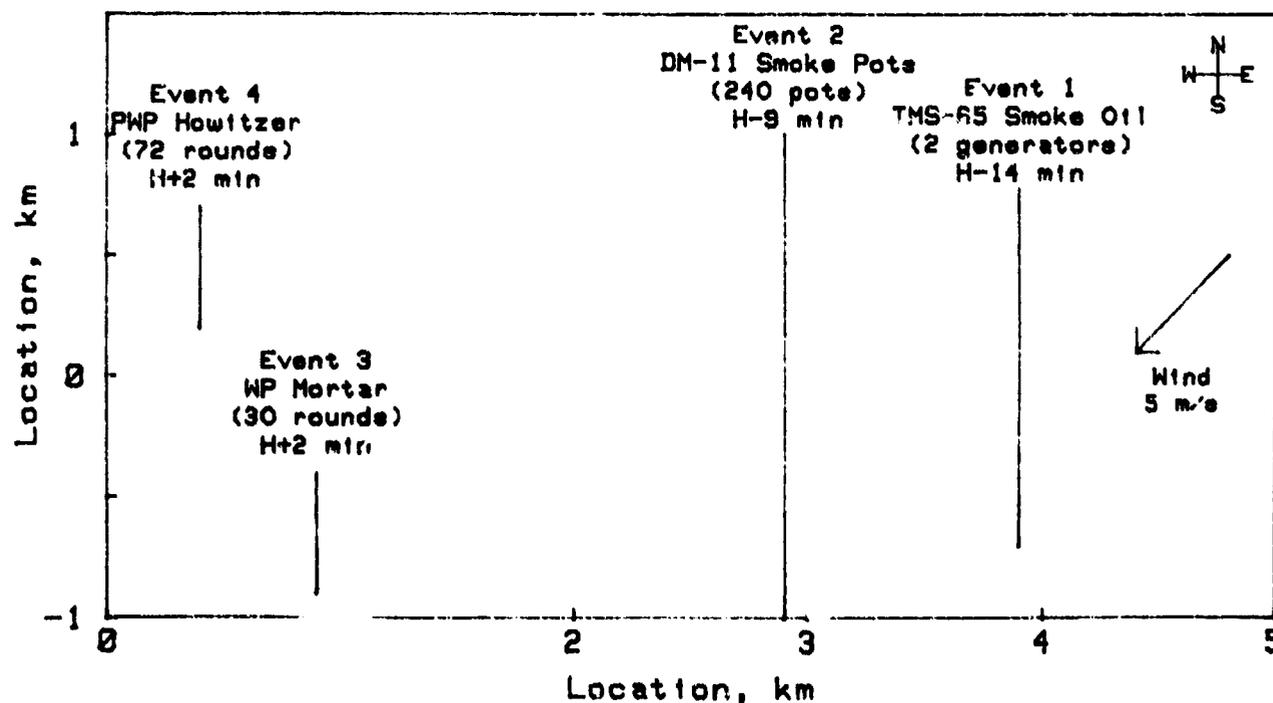
Figure 4-14. Smoke Example Overview
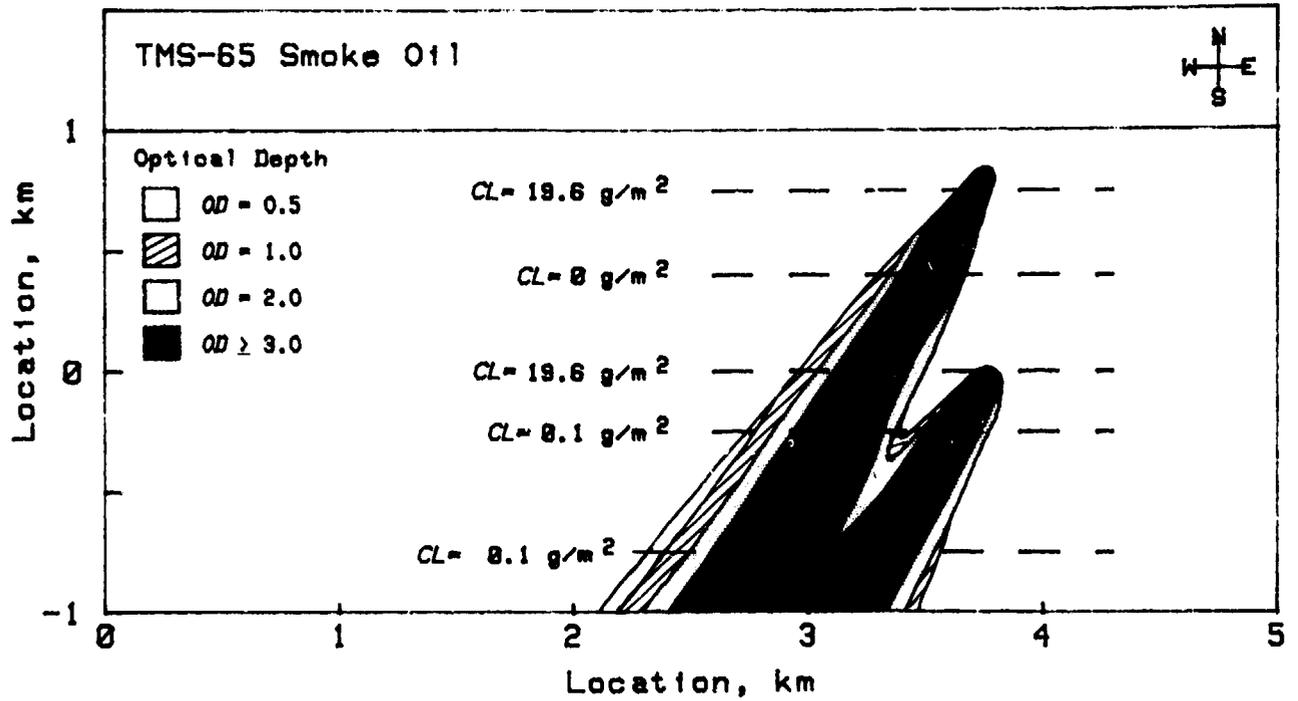
Figure 4-15. Downward-Looking Optical Depth of TMS Smoke at Time H−9 Min (Ref. 15)
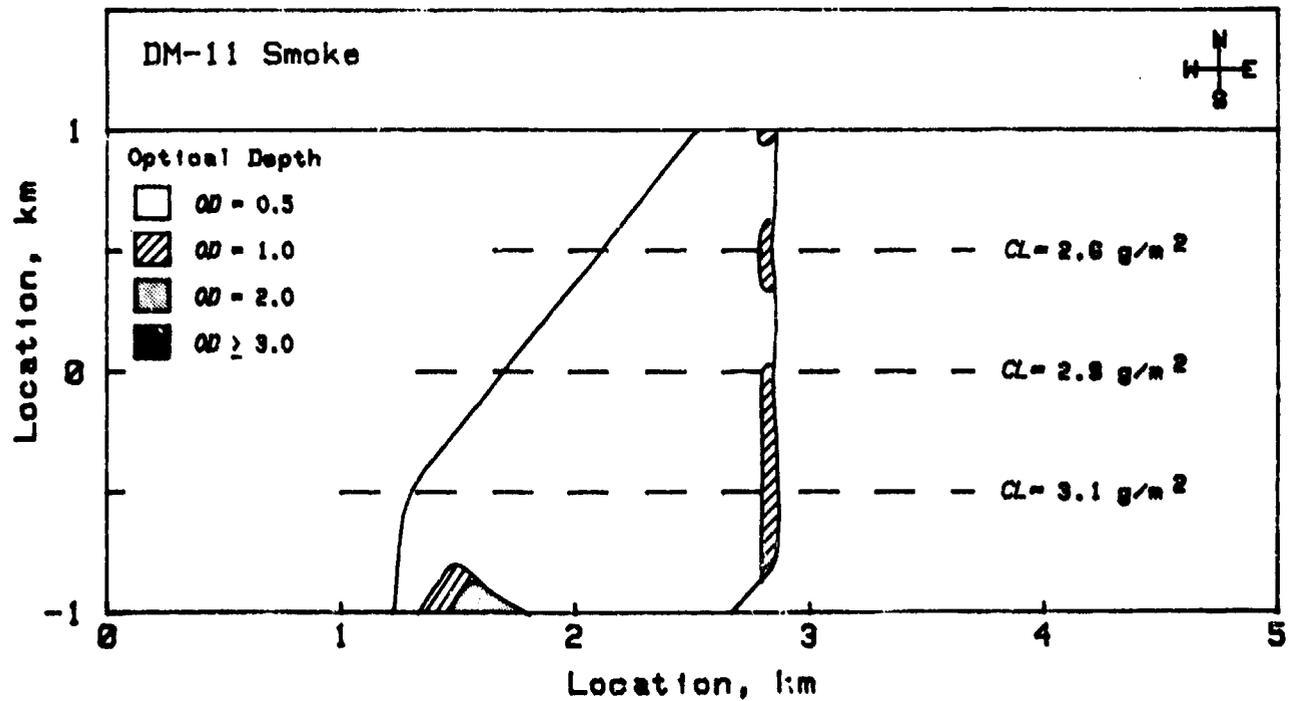
Figure 4-16. Downward-Looking Optical Depth of DM-11 Smoke at Time H−3 Min (Ref. 15)
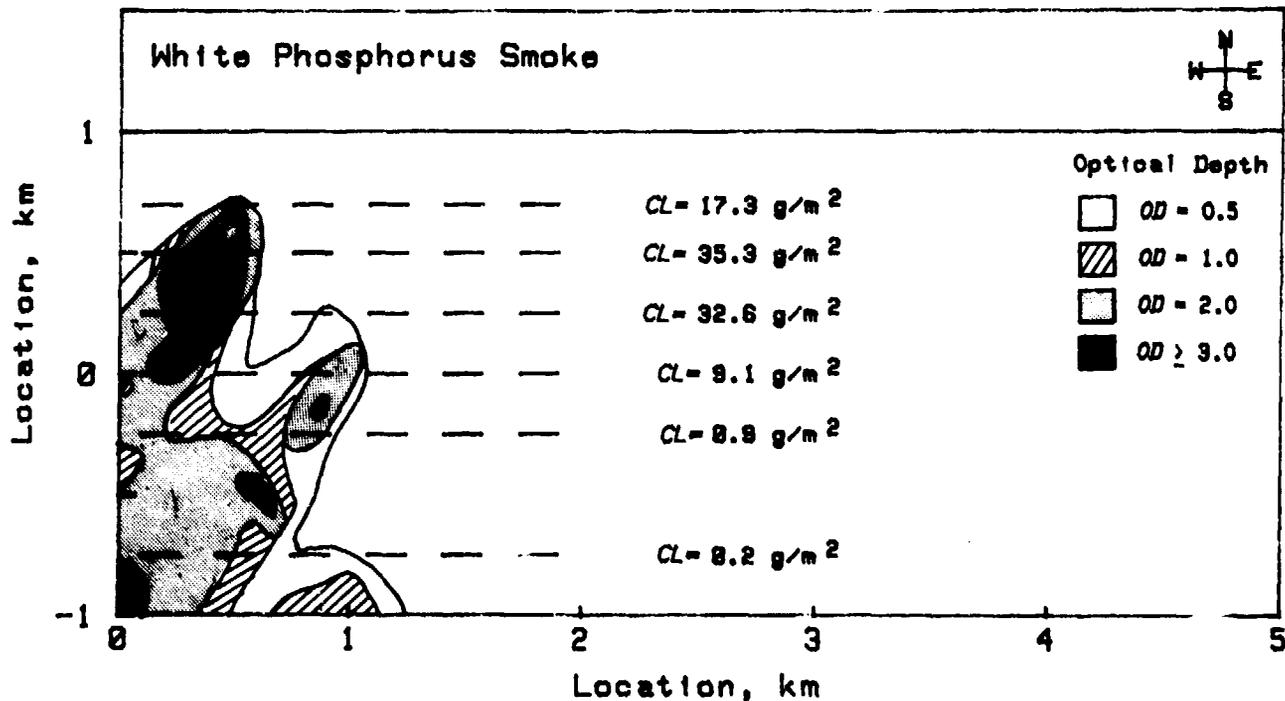
Figure 4-17. Downward-Looking Optical Depth of Phosphorus Smoke at Time H+4 Min
(Ref. 15)
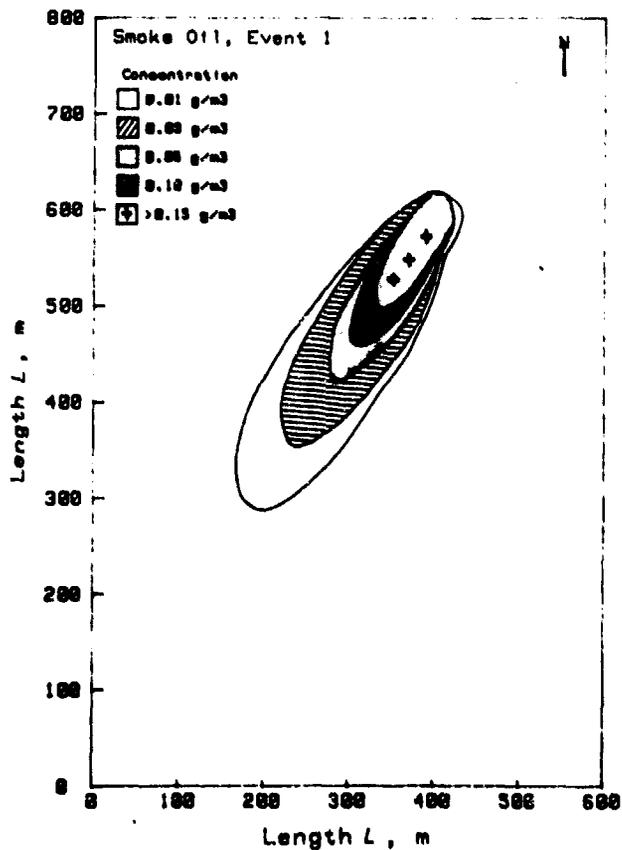
Figure 4-18. Concentration of TMS Oil Smoke
at a 2-m Altitude at Time H—9 min
(Ref. 15)
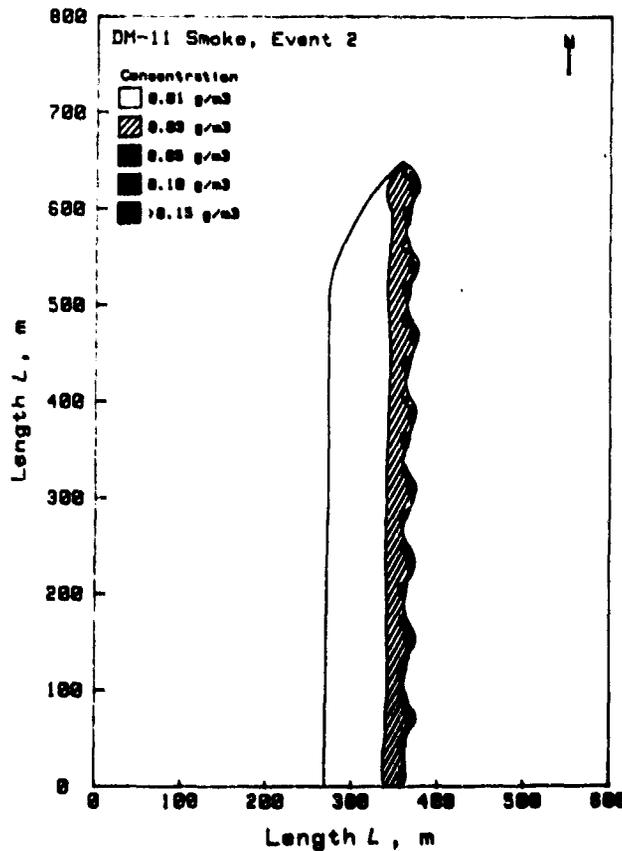
Figure 4-19. Concentration of DM-11 Smoke
at a 2-m Altitude at Time H—3 Min
(Ref. 15)
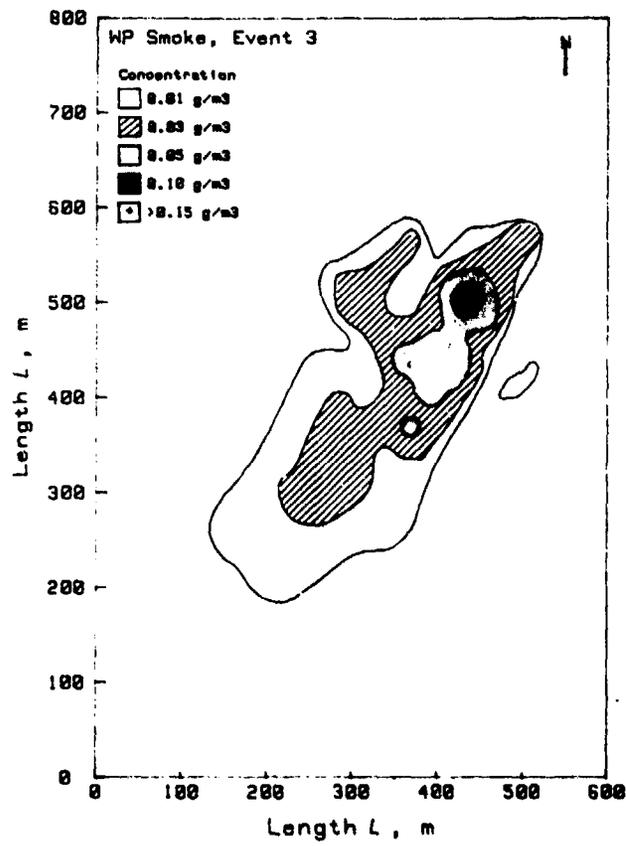
Figure 4-20. Concentration of Phosphorus
Smoke from WP Munitions at a 2-m Altitude
at Time H+4 Min (Ref. 15)
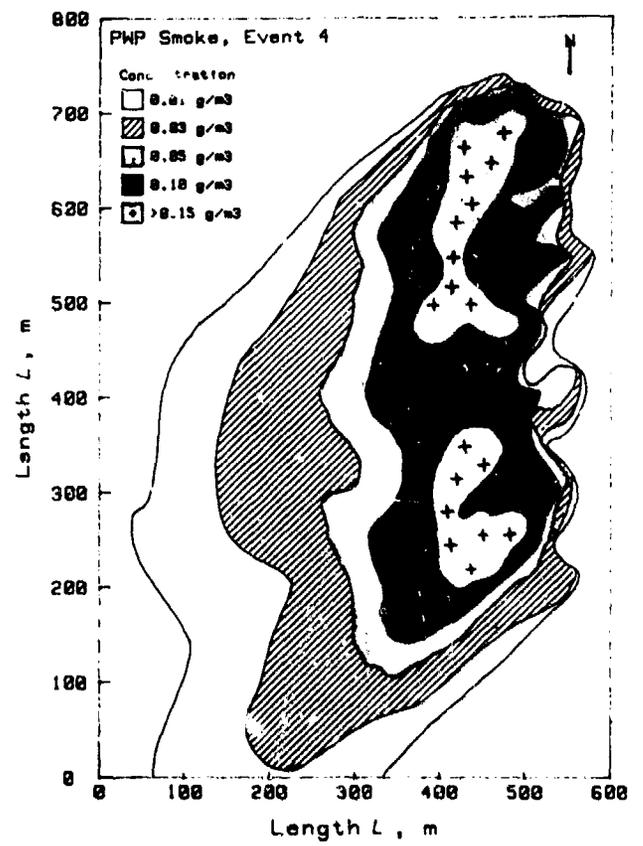
Figure 4-21. Concentration of Phosphorus
Smoke from PWP Munitions at a 2-m Altitude
at Time H+4 Min (Ref. 15)
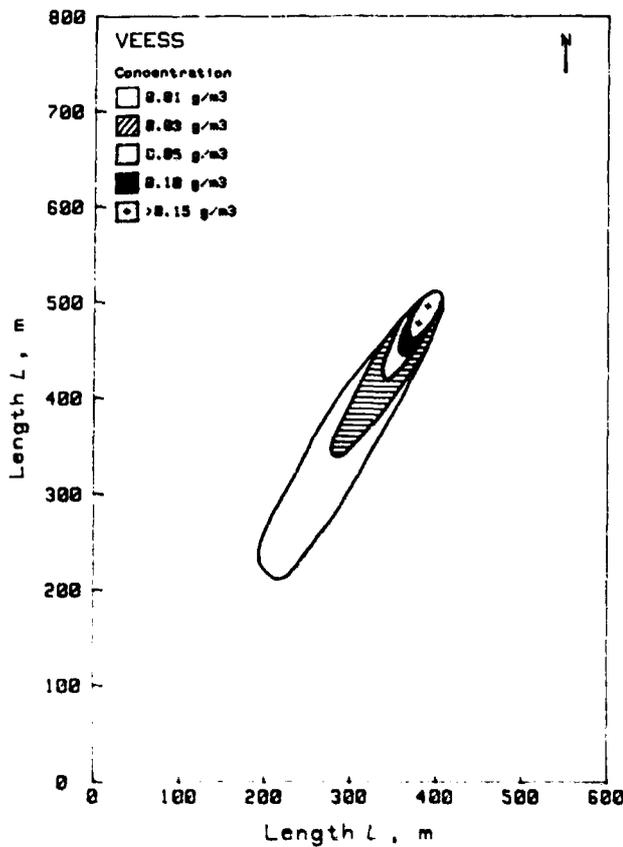
Figure 4-22. Concentration of Smoke from VEESS at a 2-m Altitude

Figure 4-23. Concentration of Dust at a 2-m Altitude from Motorized Rifle Battalion in Column Formation

4-7.3 VEHICULAR DUST EXAMPLE

The vehicular dust combat example illustrates the dust raised by the movement of a motorized rifle battalion. The battalion has three companies, each of which has four tanks and 10 BMPs.* In this illustration, the companies approach from the east in column formation and then deploy into wedge and line formation to attack. Separation between columns is about 500 m, and vehicles within the columns are about 50 m apart and move at 3 to 5 m/s. As the companies group to attack, the north and south companies form line formations with a north-south line of tanks followed by a line of BMPs. The center company forms a wedge—a north-south line of tanks followed by two lines of BMPs. The line formations are about 500 m wide (north-south) and 300 m long (east-west); the wedge is about 100 m wide and 150 m long.

_____

*BMPs, like tanks, are tracked vehicles.

Fig. 4-23 illustrates dust concentration at a 2-m altitude for the companies as they just start the transition from the column to the attack formation. CL products of dust are indicated for selected lines through the dust clouds. Fig. 4-24 illustrates dust concentration for the attack formation. These dust concentrations may be used in Eq. 4-3 to estimate obscuration due to vehicle-generated dust. Downward-looking optical depths of vehicular dust are not included because the OD values are very low; obscuration of downward-looking sensors by vehicular dust is not significant.

Figs. 4-23 and 4-24 show dust raised by vehicular movement over dry, unvegetated terrain with about 10% silt content in the soil. If the ground is wet or covered with dense vegetation, no significant amount of dust will be raised. If the soil is very silty, the dust concentrations will be higher than those shown.
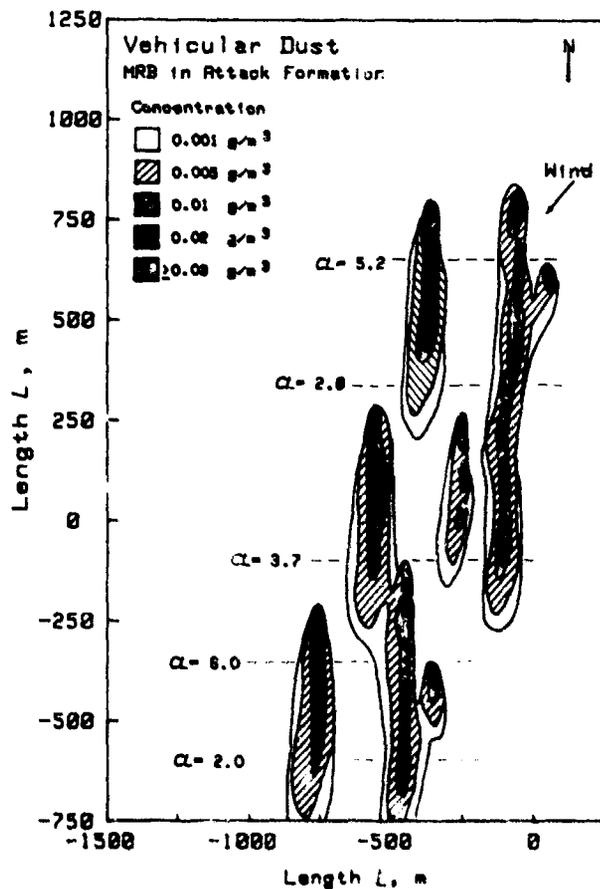
Figure 4-24. Concentration of Dust at a 2-m Altitude from Motorized Rifle Battalion in Attack Formation

REFERENCES

1. J. Vervier, "Smoke Obscurant Technology" (U), *Proc. Smoke Symposium III*, Program Manager Smoke Obscurants, Aberdeen Proving Ground, MD, 1979, (THIS DOCUMENT IS CLASSIFIED CONFIDENTIAL).

2. M. E. Milham and D. H. Anderson, *Obscuration Sciences Smoke Data Compendium: Standard Smokes (Draft)*, ARCSL-SP-82021, US Army Chemical Systems Laboratory, Aberdeen Proving Ground, MD, 1983.

3. Louis D. Duncan, et al., *EOSAEL 82*, ASL-TR-0122, US Army Atmospheric Sciences Laboratory, White Sands Missile Range, NM, 1982.

4. M. V. Maddix, et al., *A Survey of Extinction Coefficients Available for Various Transient Aerosols and Selection of Extinction Coefficients for BELDWSS Modeling of Transient Aerosols*, Special Report RG-82-1, US Army Missile Command, Redstone Arsenal, AL, 1982.

5. D. W. Hoock and R. A. Sutherland, *Modeling the*

6. W. Stump, *Calibrated Thermal Imagery Measurements from Battlefield Induced Contamination Test (BICT)*, Internal Data Report, US Army Night Vision and Electro-Optics Laboratory, Fort Belvoir, VA, 1981.

7. Marvin D. Smith and William W. Jones, "Characteristics of Filtered Smoke Data With Associated Empirical Relationship", *Proc. Smoke Obscurants Symposium VII, Vol. 1*, Project Manager Smoke Obscurants, Aberdeen Proving Ground, MD, 1983.

8. Gerald C. Holst and Janon F. Embury, *Design Criteria for Smokes and Obscurants*, ARCSL-TR-82024, US Army Chemical Systems Laboratory, Aberdeen Proving Ground, MD, 1982.

9. M. J. Heyl, *Obscuration Sciences Smoke Data Compendium: Experimental Smokes (U)*, ARCSL-SP-82020, US Army Chemical Systems Laboratory, Aberdeen Proving Ground, MD, 1983, (THIS DOCUMENT IS CLASSIFIED CONFIDENTIAL).

10. M. J. Heyl, *Obscuration Sciences Smoke Data Compendium: Candidate Smokes (Draft) (U)*, ARCSL-SP-82017, US Army Chemical Systems Laboratory, Aberdeen Proving Ground, MD, 1983, (THIS DOCUMENT IS CLASSIFIED CONFIDENTIAL).

11. A. L. Turetsky, et al., *Obscuration Sciences Smoke Data Compendium: Foreign Smokes (U)*, ARCSL-SP-82023, US Army Chemical Systems Laboratory, Aberdeen Proving Ground, MD, 1982, (THIS DOCUMENT IS CLASSIFIED CONFIDENTIAL).

12. L. P. Obert, J. T. Wood, and C. J. Nash, *Visionics Handbook of EO Sensor Performance, Volume I (Natural European Environment) (U)*, US Army Night Vision and Electro-Optics Laboratory, Fort Belvoir, VA, 1981, (THIS DOCUMENT IS CLASSIFIED CONFIDENTIAL).

13. Bruce W. Kennedy, Ed., *Dusty Infrared Test-II (DIRT-II) Program*, ASL-TR-0058, US Army Atmospheric Sciences Laboratory, White Sands Missile Range, NM, 1980.

14. Brian K. Matise, et al., *BICT-III III: Dust Data Reduction Data Report*, ASL-DR-81-0001, US Army Atmospheric Sciences Laboratory, White Sands Missile Range, NM, 1983.

15. *Combat Environment Obscuration Handbook (Draft)*, Smoke and Aerosol Working Group, Joint Technical Coordination Group Munitions Effectiveness, Aberdeen Proving Ground, MD, 1981.

16. Charles R. Caudill, Jr., "Infrared Measurements of

a 105 mm Gunblast", (THIS PAPER IS UNCLAS-
SIFIED), *Proc. IRIS Symposium on IR Counter-
measures*, Environmental Research Institute of
Michigan, Ann Arbor, MI, 1980, (THIS DOCU-
MENT IS CLASSIFIED CONFIDENTIAL.)

17. Charles R. Cundiff, Jr. "Launch Cloud Interfer-
ence With Electro-Optical Systems" (U), *Proc.
IRIS Symposium on IR Countermeasures*, Envir-
onmental Research Institute of Michigan, Ann
Arbor, MI, 1983, (THIS DOCUMENT IS CLASSI-
FIED SECRET—NOFORN.)

18. John F. Ebersole, *Estimates of Helicopter-Down-
wash-Produced Obscuration Factors*, Creative Op-
tics, Inc., Bedford, MA, 1984.

19. Donald W. Hoock, *DOT Test Analysis—Derived
Dust Production Rates for Tracked Vehicles*, US
Army Atmospheric Sciences Laboratory, White
Sands Missile Range, NM, 1983.

20. G. W. Aitken, Ed., *SNOW-ONE-A Data Report*,
CRREL-TR-82-8, US Army Cold Regions Research
and Engineering Laboratory, Hanover, NH, 1982.

21. R. K. Redfield, W. M. Farmer, and J. F. Ebersole,
*SNOW-TWO Smoke Week II Field Experiment
Plan*, US Army Cold Regions Research and Engi-
neering Laboratory, Hanover, NH, 1983.

22. J. F. Ebersole, *Data Report for Helicopter Snow
Obscuration Sub-Test at the SNOW-TWO Field
Experiment (Draft)*, Creative Optics, Inc., Bedford,
MA, 1984.

23. AMCP 706-117, Engineering Design Handbook,
*Environmental Series, Part Three, Induced Envir-
onmental Factors*, 1976.

24. Barbara W. Levitt and Leonard S. Levitt, "Atmo-
spheric Mass Loading of Fire Products", *Optical
Engineering* 21, 118-51 (1982).

25. Raj K. Khanna and Herman L. Ammon, *Optical
Properties of Vehicular and Vegetative Fire Prod-
ucts*, Dept. of Chemistry, University of Maryland,
College Park, MD, 1983.

26. Charles W. Bruce and N. M. Richardson, "Millime-
ter Wave Gas Aerosol Spectrophone and Applica-
tion to Diesel Smoke", *Applied Optics* 23, 13
(1984).

27. D. Bruce and D. Larson, "The Fitte Model—
Modifications and Sensitivity Studies", *Proc.
EOSAEL Workshop*, US Army Atmospheric
Sciences Laboratory, White Sands Missile Range,
NM, 1983.

BIBLIOGRAPHY

G. W. Aitken, Ed., *SNOW-ONE-A Data Report*, CRREL-
TR-82-8, US Army Cold Regions Research and
Engineering Laboratory, Hanover, NH, 1982.

M. J. Heyl, *Obscuration Sciences Smoke Data Com-
pendium: Experimental Smokes* (U), ARCSL-SP-
82020, US Army Chemical Systems Laboratory,
Aberdeen Proving Ground, MD, 1983, (THIS DOCU-
MENT IS CLASSIFIED CONFIDENTIAL).

M. J. Heyl, *Obscuration Sciences Smoke Data Com-
pendium: Candidate Smokes (Draft)* (U), ARCSL-
SP-82017, US Army Chemical Systems Laboratory,
Aberdeen Proving Ground, MD, 1983, (THIS DOCU-
MENT IS CLASSIFIED CONFIDENTIAL).

Gerald C. Holst and Janon F. Embury, *Design Criteria
for Smokes and Obscurants*, ARCSL-TR-82024, US
Army Chemical Systems Laboratory, Aberdeen Prov-
ing Ground, MD, 1982.

Donald W. Hoock, *DOT Test Analysis—Derived Dust
Production Rates for Tracked Vehicles*, US Army
Atmospheric Sciences Laboratory, White Sands Mis-
sile Range, NM, 1983.

D. W. Hoock and R. A. Sutherland, *Modeling the
Complex Dirty Battlefield*, US Army Atmospheric
Sciences Laboratory, White Sands Missile Range,
NM, 1983.

Marvin D. Kays, et al., *Qualitative Description of Ob-
scuration Factors in Central Europe*, ASL Mono-
graph No. 1, US Army Atmospheric Sciences Labor-
atory, White Sands Missile Range, NM, 1980.

Bruce W. Kennedy, Ed., *Dusty Infrared Test-II (DIRT-
II) Program*, ASL-TR-0058, US Army Atmospheric
Sciences Laboratory, White Sands Missile Range,
NM, 1980.

Raj K. Khanna and Herman L. Ammon, *Optical Prop-
erties of Vehicular and Vegetative Fire Products*,
Dept. of Chemistry, University of Maryland, College
Park, MD, 1983.

M. V. Maddix, et al., *A Survey of Extinction Coeffi-
cients Available for Various Transient Aerosols and
Selection of Extinction Coefficients for BELDWSS
Modeling of Transient Aerosols*, Special Report RG-
82-1, US Army Missile Command, Redstone Arsenal,
AL, 1982.

Brian K. Matise, et al., *BICT-III/IR Dust Data Reduc-
tion Data Report*, ASL-DR-84-001, US Army At-
mospheric Sciences Laboratory, White Sands Missile
Range, NM, 1983.

M. E. Milham and D. H. Anderson, *Obscuration Scien-
ces Smoke Data Compendium: Standard Smokes
(Draft)*, ARCSL-SP-82024, US Army Chemical Sys-
tems Laboratory, Aberdeen Proving Ground, MD,
1983.

D. Bruce Turner, "A Diffusion Model for an Urban Area", *Journal of Applied Meteorology*, 83-91 (February 1964).

A. L. Turetsky, et al., *Obscuration Sciences Smoke Data Compendium: Foreign Smokes* (U), AKCSL-SP-82023, US Army Chemical Systems Laboratory, Aberdeen Proving Ground, MD, 1982, (THIS DOCUMENT IS CLASSIFIED CONFIDENTIAL).

Combat Environment Obscuration Handbook (Draft), Smoke and Aerosol Working Group, Joint Technical Coordination Group Munitions Effectiveness, Aberdeen Proving Ground, MD, 1984.

Smoke, An Obscuration Primer, 61 JTCG/ME-77-13, Joint Technical Coordination Group Munitions Effectiveness, Aberdeen Proving Ground, MD, 1978.

AMCP 706-117, *Engineering Design Handbook, Environmental Series, Part Three, Induced Environmental Factors*, 1976.

TRADOC Pamphlet 525-3, *Employment of Smoke*, 1980.

Other Data Sources

In addition to the documents mentioned, the proceedings of relevant symposia are excellent data sources. These include

1. FOSAEL Workshop, sponsored by the US Army Atmospheric Sciences Laboratory, White Sands Missile Range, NM.

2. IRIS Symposium on Infrared Countermeasures and IRIS Symposium on Infrared Imaging Systems, conducted for the Office of Naval Research by Environmental Research Institute of Michigan, Ann Arbor, MI.

3. Smoke Obscurants Symposium, sponsored the Program Manager, Smoke Obscurants, Aberdeen Proving Ground, MD.

4. Snow Symposium, sponsored by the Cold Regions Research and Engineering Laboratory, Hanover, NH.

CHAPTER 5
OBSCURATION FACTORS AND SYSTEM DESIGN

This chapter explains the measures used to calculate the performance of imaging and nonimaging systems. It discusses how naturally occurring obscurants and battlefield-induced contaminants degrade or defeat sensor performance, and it provides sensor defeat mechanism tables indicating the potential severity of the defeat mechanism on different sensor classes. Example problems show explicitly how to calculate obscurant effects on different sensor classes and sensor designs.

5-0 LIST OF SYMBOLS

A_r = receiver effective aperture area, km^2

A_t = target area, m^2

C = concentration of obscurant, g/m^3

C_o = target contrast, dimensionless

C = apparent target contrast at sensor, dimensionless

CL = concentration path length product, g/m^2

c = speed of light, km/s

FAR = false alarm rate, s^{-1}

FAR_p = per pulse false alarm rate, dimensionless

h = target height, m

I_n = current at peak noise, A

I_s = current at peak signal, A

I_t = current threshold, A

L = path length of obscurant, m

M = target-to-beam ratio, dimensionless

MDT = minimum detectable temperature difference, K

MRC = minimum resolvable contrast, dimensionless

MRT = minimum resolvable temperature, K

MTF = modulation transfer function, dimensionless

NEP = detector noise equivalent power, W

NET = noise equivalent temperature, K

n = Johnson criterion for the task, dimensionless

n_r = number of cycles resolved across the target, dimensionless

P = probability of task accomplishment, dimensionless

P_d = probability of detection, dimensionless

P_{fa} = probability of false alarm, dimensionless

P_r = received signal power, W

P_t = peak transmitter power, W

R = range, km

R_m = maximum design range, km

SNR = signal-to-noise ratio, dimensionless

SNR_v = signal-to-noise ratio of voltages, dimensionless

T_r = receiver optics transmittance, dimensionless

T_t = transmitter optics transmittance, dimensionless

$T(\lambda)$ = transmittance, dimensionless

$T_c(\lambda)$ = atmospheric contrast transmittance, dimensionless

ΔT = target thermal signature, K

$\Delta T'$ = apparent target thermal signature at sensor, K

t = time interval between laser pulse and radiation signal, s

t_d = detector on-time, s

V = visibility, km

δ = half-angle laser beam divergence, mrad

θ = angle between target and beam, deg

κ = spatial frequency, cycles/mrad

κ_t = target spatial frequency, cycles/mrad

ρ_t = target reflectance, dimensionless

τ = laser pulse width, s or ns

ϕ = target angular size, mrad

5-1 INTRODUCTION

This chapter covers three major topics: (1) the sensor performance measures used to evaluate imaging and nonimaging, passive and active sensors, (2) the mechanisms by which sensor performance is impaired by naturally occurring atmospheric constituents and battlefield-induced contaminants, and (3) the calculation of obscurant effects on sensor performance.

The system performance measures are described in par. 5-2. Electro-optical (EO) and millimeter wave (mmw) sensor defeat mechanisms are described in par. 5-3, which also includes tables correlating the defeat mechanisms with natural or battlefield-induced obscurants in the visible and near infrared (IR), thermal, and

mmw spectral regions. The tables also indicate the potential impact of the obscurant on sensor performance. The illustrative examples in par. 5-4 lead the user through calculations of obscurant effects on sensor performance by using material developed in Chapters 3 and 4 and the sensor performance measures presented in par. 5-2.

5-2 SYSTEM PERFORMANCE MEASURES

This paragraph describes measures of system performance for passive imaging systems, passive nonimaging systems, and active nonimaging systems. It addresses three basic levels of performance: laboratory performance, one-on-one field performance, and sensor effectiveness. Laboratory performance is a measure of how well the system operates in the absence of environmental effects and may include such measures as system resolution (for imagers) or system sensitivity and noise level (for nonimaging systems). The resolution of a system describes the ability of a system to reproduce details in the scene image. The sensitivity of the system describes the ability of the system to detect low contrast targets. Subjective resolution is a performance measure that includes the effect of the human observer using the system.

One-on-one field performance calculations translate laboratory performance measures into an operational environment. They indicate how well the system will perform against a specified target in a specified environment and include the effects of the atmosphere. Measures of field performance include target detection range at a specified probability of detection P_d, the time required to acquire a target, and the false alarm rate, which indicates how many nontarget objects are falsely identified as targets. One-on-one sensor effectiveness, as used in this handbook, is a measure of how often or what percent of the time the system will perform at a specified field performance level in a specified location. It includes the effect of expected variations in atmospheric conditions and the sensitivity of target signatures to these variations. It does not include such engineering measures as system reliability rate or mean time between failure. Measures of the battlefield effectiveness of a system in one-on-many or many-on-many scenarios are beyond the scope of this engineering design handbook. Performance measures for passive imaging sensors, passive nonimaging sensors, and active nonimaging sensors are listed in Table 5-1 and described in pars. 5-2.1, 5-2.2, and 5-2.3, respectively.

This handbook does not include active imaging systems. Active system imagers will differ from passive imagers in four respects: (1) the active system target signature is determined by the reflectance of the target at the illumination wavelength, (2) the image may con-

TABLE 5-1. SENSOR PERFORMANCE MEASURES

Sensor	Laboratory Performance	Field Performance
Passive Imager	MRT* MRC* MDT*	P_d at fixed range Range at fixed P_d Time to detect
Passive Nonimager	SNR FAR	P_d Range FAR
Active Nonimager	SNR FAR	P_d Range FAR

*Defined in pars. 5-2.1, 5-2.2, and 5-2.3

tain the speckle characteristic of coherent illumination, (3) there are no shadows, and (4) the night imagery is usually equivalent to the daytime imagery. Natural atmospheric aerosols and battlefield-induced aerosols will scatter energy back into the active system receiver; with aerosols, backscatter is the primary cause of active system performance degradation. The effects of molecular absorption and scattering on active laser or mmw imagers resemble atmospheric effects on active nonimaging systems, but the effect is more severe because of the requirement for two-way transmittance of the illuminator radiation.

5-2.1 PASSIVE IMAGING SYSTEMS

The laboratory performance measures for passive imaging systems relate system resolution and system sensitivity. System resolution is given by the system modulation transfer function MTF, which is a set of values describing the effectiveness with which the system reproduces the contrast of a high-contrast bar target as a function of the angular spacing of the bars. The angular bar spacing is usually expressed in terms of cycles per mrad. A cycle is one line pair (one black bar and one white bar); a mrad is the angle subtended by a one-meter target at a distance of one km. Fig. 5-1 shows the MTF curve for a thermal imaging system with a resolution limit* of 0.17 mrad.

The subjective resolution of an imaging system is a laboratory measurement of the lowest temperature or contrast difference between a bar pattern and the background that is resolvable by a human observer using the device. It includes the system MTF, the human eye response curve, and the MTF of any system display. These threshold contrasts or temperature differences

___
*Certain thermal imagers are limited in resolution by the detector size. The resolution limit of these systems is the angle subtended by the detector.
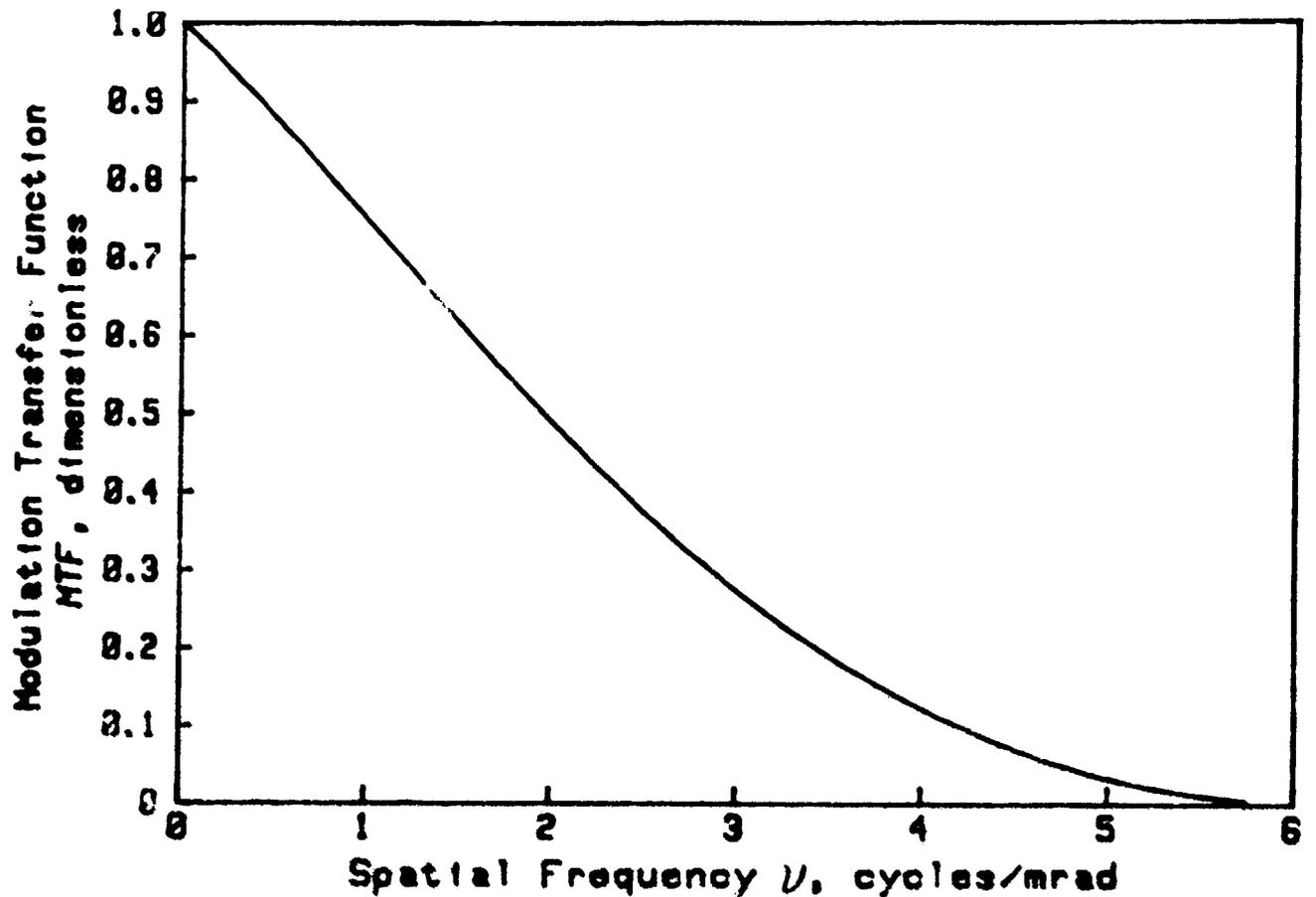
Figure 5-1. Modulation Transfer Function vs Spatial Frequency
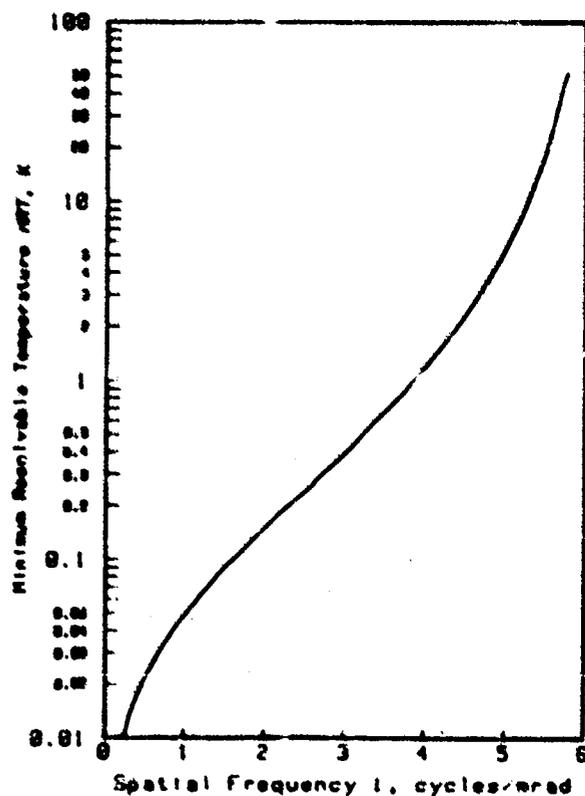
Figure 5-2. Thermal Imager _MRT_ Curve

are functions of the bar pattern spatial frequency. The minimum resolvable temperature difference _MRT_ curve, used for a thermal imager, is thus a plot of the bar pattern spatial frequency vs the minimum temperature difference resolvable at that spatial frequency. Fig. 5-2 shows the _MRT_ curve for the 0.17 mrad thermal imager shown in Fig. 5-1.

Another measure of FLIR* system performance is minimum detectable temperature difference _MDT_. _MDT_ is a subjective measure of the minimum temperature difference required to detect a circular spot on the display as a function of the angular subtense of the spot. It is a measure of the limiting hot-spot detection range of the system.

The minimum resolvable contrast _MRC_ curve, used for light level sensitive systems, is a plot of bar pattern contrast vs resolvable spatial frequency at a specified light level. A set of _MRC_ curves, one per light level, is used to describe eye, day sight, television, and image intensifier (I²) performance. Fig. 5-3 shows the eye _MRC_ curve under daylight conditions.

---

*Forward-looking infrared (FLIR) systems are thermal imaging systems developed for use in aircraft, the acronym FLIR is often used to indicate any thermal imaging system.
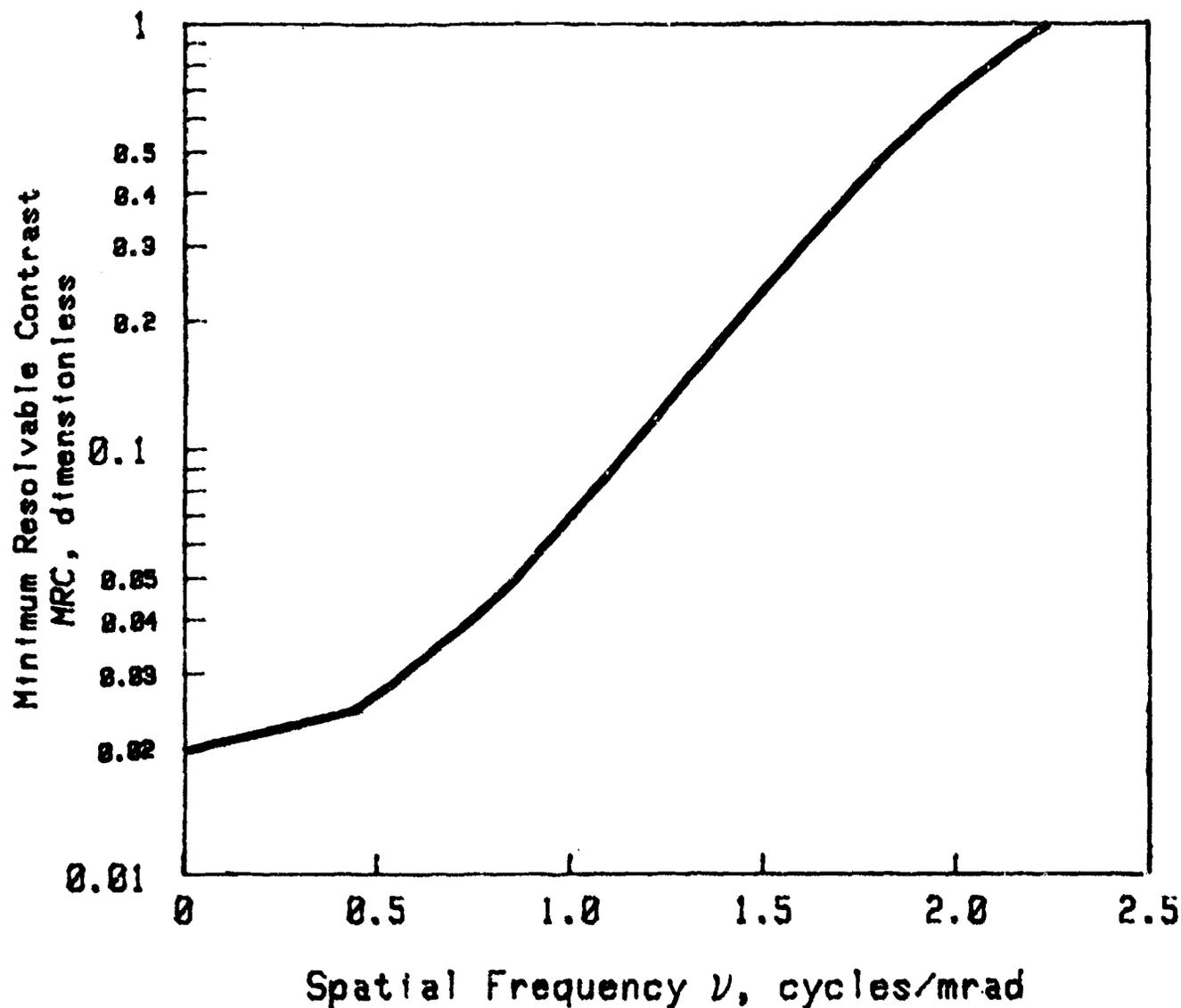
Figure 5-3. Eye *MRC* Curve, Daylight (Ref. 1)

The subjective resolution curves—*MRT*, *MDT*, or *MRC*—may be used to determine the system resolution under field conditions. This system resolution is translated to field performance using a set of experimental rules known as the Johnson criteria and a probability measure, the target transfer probability curve. The Johnson criteria and the target transfer probability curve will be explained following a discussion of system resolution.

To relate the subjective resolution curves in Figs. 5-2 and 5-3 to system resolution in the field, two concepts must be discussed: target spatial frequency and apparent target signature.

The spatial frequency *ν* resolved by the system is defined in terms of the spatial frequency of a bar pattern expressed in units of cycles/mrad. A target at range *R* has an angular size *φ* given by

$$\phi = \frac{h}{R}, \text{ mrad} \qquad (5\text{-}1)$$

where

h = target height, m
R = range, km.

The target spatial frequency ν_t is the reciprocal of its angular size:

$$\nu_t = \frac{R}{h}, \text{ cycles/mrad.} \qquad (5\text{-}2)$$

By definition, the *MRT* curve for a thermal imager gives the minimum resolvable temperature difference (referenced to a 300-K background) required to resolve a bar pattern with spatial frequency *ν*. It can also be read directly to give the target thermal signature ΔT (again,

by definition, referenced to a 300-K background) required to resolve a target of spatial frequency ν_t.

Similarly, the MRC curve for a light-level sensitive system (visible, I^2, or television) gives the minimum contrast signature required to resolve a bar pattern of frequency ν. The target contrast C_o required to resolve a target of spatial frequency ν_t can be read directly from the system MRC curve.

The apparent target signature is defined as the amount of radiation from the target in the sensor spectral band at the sensor aperture. It includes the effect of atmospheric extinction. The apparent target thermal signature $\Delta T'$ at a thermal imager can be obtained by multiplying the target thermal signature ΔT by the atmospheric transmittance $T(\lambda)$ in the sensor spectral band:

$$\Delta T' = T(\lambda)\Delta T , \text{ K} \qquad (5\text{-}3)$$

where

$\Delta T'$ = apparent target thermal signature at sensor, K

ΔT = target thermal signature, K.

Thus the MRT curve for a thermal imager can be used to determine the spatial frequency resolvable at a given $\Delta T'$ by simply equating the MRT to the apparent thermal target signature $\Delta T'$ and reading from the curve the spatial frequency ν the system can resolve at the MRT value.

The target thermal signature used in Eq. 5-3 may be obtained from measured values or analytical models. In the absence of such data, the target signature values from Table 5-2 may be used. The ΔT values in Table 5-2 are average 8-12 μm tank thermal signatures and 3-5 μm man thermal signatures for four seasons and three times of day (early morning, afternoon, and night.)

For light-level sensitive systems (visible, I^2, and television), the apparent target signature is the apparent contrast C_o' of the target (in the sensor spectral band) at the sensor aperture. It can be obtained using the contrast transmittance equation

$$C_o' = C_o \, T_c(\lambda) \quad , \text{dimensionless} \quad (5\text{-}4)$$

where

C_o = target contrast signature, dimensionless

$T_c(\lambda)$ = atmospheric contrast transmittance, dimensionless.

The MRC curve for a light-level sensitive system can be used to determine the spatial frequency resolvable at a given C_o' by equating the MRC at the appropriate light level to the apparent target contrast signature C_o' and then reading the spatial frequency ν the system can resolve at that light level.

TABLE 5-2. AVERAGE SEASONAL THERMAL SIGNATURES (Ref. 1)

Thermal Imaging Systems (8-12 μm)

Central European Environment

Signature of Exercised Tank Target, Front View

Season	Cloud Condition	ΔT, K		
		Early Morning	Afternoon	Night
Spring	Clear	1.0	2.6	1.4
	Overcast	0.5	0.9	0.5
Summer	Clear	1.2	3.5	2.2
	Overcast	0.5	1.3	0.8
Fall	Clear	1.0	2.6	1.4
	Overcast	0.5	0.9	0.5
Winter	Clear	0.9	1.8	0.9
	Overcast	0.4	0.6	0.4

Hand-Held Thermal Viewer (3-5.5 μm)

Target Signature, Man Target

Season	ΔT, K		
	Early Morning	Afternoon	Night
Spring	4.0	4.9	4.5
Summer	5.7	8.1	6.5
Fall	4.0	4.9	4.5
Winter	3.3	3.0	3.5

The target contrast signatures used in Eq. 5-4 may also be derived from measurements or analytical models. Tables 5-3 and 5-4 give values of target contrast signatures, which may be used to estimate the target contrast. Table 5-3 gives average tank contrast signatures in the I^2 band (0.4-0.9 μm) against dirt and grass backgrounds at three ambient nighttime illumination levels. Table 5-4 gives average daylight tank signatures in the visible band (0.4-0.7 μm) with dirt and grass backgrounds.

A critical number for imaging system calculations is the number of cycles n_t the system can resolve across the target. It is the ratio of the system resolution ν at the apparent target signature $\Delta T'$ or C_o' to the target spatial frequency ν_t at the sensor

$$n_t = \nu/\nu_t, \text{ dimensionless.} \qquad (5\text{-}5)$$

The value of n_t decreases with increasing range to the target because of changes in the target angular size and

TABLE 5-3. AVERAGE SEASONAL TARGET CONTRAST
SIGNATURES C_o FOR IMAGE INTENSIFIERS (Ref. 1)

Image Intensifier Systems (0.4-0.9 μm)

Target-to-Background Contrast Signatures

Tank Target, Front View

Sensor	Background	Season	Light Level		
			Full Moon	1/4 Moon	No Moon
Starlight Scope	Green Grass	All	0.21	0.22	0.29
Crew Served Sight	Dead Grass	All	0.42	0.40	0.37
M35/M36 Periscope	Dirt Road	All	0.61	0.60	0.57
NV Goggles	Green Grass	All	0.26	0.28	0.34
	Dead Grass	All	0.40	0.38	0.36
	Dirt Road	All	0.60	0.59	0.57

TABLE 5-4. AVERAGE TARGET SIGNATURES C_o FOR DAY SIGHTS (Ref. 1)

Eye And Day Sights (0.4-0.7 μm)

Contrast Signature of Tank Target, Front View

Sensor	Background	Season	Time of Day	
			Early Morning	Afternoon
Eye	Green Grass	All	0.03	0.03
Day Sights	Dead Grass	All	0.44	0.44
	Dirt Road	All	0.61	0.61

apparent signature. The target angular size becomes smaller with increasing range, which increases the target spatial frequency ν_t. The atmospheric attenuation of the target signature is greater at longer ranges, which reduces the apparent target signature, which thus reduces ν.

The experimentally derived Johnson criteria are used to relate system resolution to field performance. The Johnson criteria specify the number of cycles n that the system must resolve across the target in order to perform a target detection or discrimination task with 50% probability (Ref. 1).

The levels of performance specified by the Johnson criteria are detection, recognition, classification, and identification. These terms have precise meanings. Detection is the ability to distinguish that an artifact within the field of view is of military interest. Classification is the ability to distinguish a target by general type, e.g., as a tracked vehicle instead of a wheeled vehicle. Recognition is the ability to discriminate between two targets of similar type. For example, recognition would allow the observer to distinguish

between two types of tracked vehicles—i.e., armored personnel carrier (APC) vs tank. Identification is the ability to discriminate the exact model of a target. For example, identification would allow the observer to distinguish a T-62 from a T-72 tank.

The Johnson criteria for visible, IR, and thermal imaging systems are shown in Table 5-5. The Johnson criterion for recognition for a thermal system, for example, is 4 cycles. This means that for half of the observers to recognize a target through a thermal imaging system, the imager must resolve 4 cycles across the target. To identify the target, the imager must resolve 8 cycles across the target.

To summarize, the Johnson criterion n gives the number of cycles that must be resolved across the target to accomplish a task at the 50% probability level. The number of cycles n_t resolved by the system across a specified target is determined from the system MRT or MRC curve, the apparent target signature, and the target spatial frequency (size and the range to the target). If n equals n_t, the probability of accomplishing the task is 50%.

TABLE 5-5. JOHNSON CRITERIA n FOR TASK ACCOMPLISHMENT, 50% PROBABILITY LEVEL (Ref. 2)

Probability of Accomplishing Task	Number of Cycles Resolved Across Target Critical Dimension			
	Detection	Classification	Recognition	Identification
Thermal Sensors, Tank Target 0.50	1.00	2.00	4.00	8.00
Hand-Held Thermal Viewer, Man Target 0.50	1.50	1.50	1.50	—
Day Sights and Image Intensifiers, Tank Target 0.50	1.00	2.00	3.00	6.00
Image Intensifiers, Man Target 0.50	1.00	1.00	1.00	—

The process is illustrated by the nomogram in Fig. 5-4, used for estimating system performance for the crew served weapon sight, a passive I² system, against a tank target. The target signature C_o (upper left scale) is multiplied by the atmospheric contrast transmittance $T_c(\lambda)$ to obtain the apparent contrast $C'_o(\lambda)$ at the sensor. The subjective resolution curve is used to determine the spatial frequency ν resolvable at the apparent contrast. For this I² system in moonlight conditions, the system can resolve a spatial frequency ν of about 2.7 cycles mrad if the apparent target contrast at the sensor is 0.48. The target detection, recognition, and identification scales at the bottom of the chart yield task performance range at the 50% probability level. For the case illustrated, the I² system can detect a tank at about 5.8 km and recognize it at about 1.9 km. The range scales on Fig. 5-4 are generated by calculating target spatial frequency ν, as a function of range for a 2.2 m tank target and applying the Johnson criteria in Table 5-4 to determine the number of cycles n required to perform a task at that range.

For a given target and atmosphere, the probability of accomplishing the task is determined from the Johnson criterion n for the task and the number of cycles n_i resolved across the target under the input conditions by using an experimentally derived relationship called the target transfer probability curve. The target transfer probability of accomplishing the task is essentially 100%. If n_i / n equals 1.0, the probability is 50%, as required by the Johnson criteria.

The data in Fig. 5-5 may also be used to set probability levels. If a probability of 80% is required, for instance, the value of the Johnson criterion is multi-

plied by a factor of 1.4; the value of n_i / n corresponds to 80% detection probability.

5-2.2 PASSIVE NONIMAGING SYSTEMS

Passive nonimaging systems detect targets based on the intensity of the received radiation in the sensor spectral band, or, for multispectral systems, by comparison of the radiant intensity in two or more spectral bands. These sensors are usually designed for detection of hot targets such as aircraft engines or for terminal target detection and tracking at short ranges.

Laboratory performance measures for passive imagers are based on the system sensitivity (primarily detector response), the system noise characteristics, and the ability of the system to filter out background noise. The measure of system field performance is the probability of target detection as a function of range at a specified FAR. This performance measure accounts for both the number of correct detections and the number of times a nontarget is classed as a target.

The system FAR is a design parameter used to set the detector threshold and is based on expected detector and background noise statistics. Target detection probability is affected by the threshold setting; those targets with energy levels below the threshold generally will not be detected. Fig. 5-6 shows probability densities for the noise and the signal and also indicates the region in which signal and noise currents overlap. As the threshold is raised, more of the noise falls below the threshold and will not be detected, which reduces the probability of false alarm. The price of this reduced false alarm rate is that some of the lower target signals will also fall below the threshold; this reduces the probability of
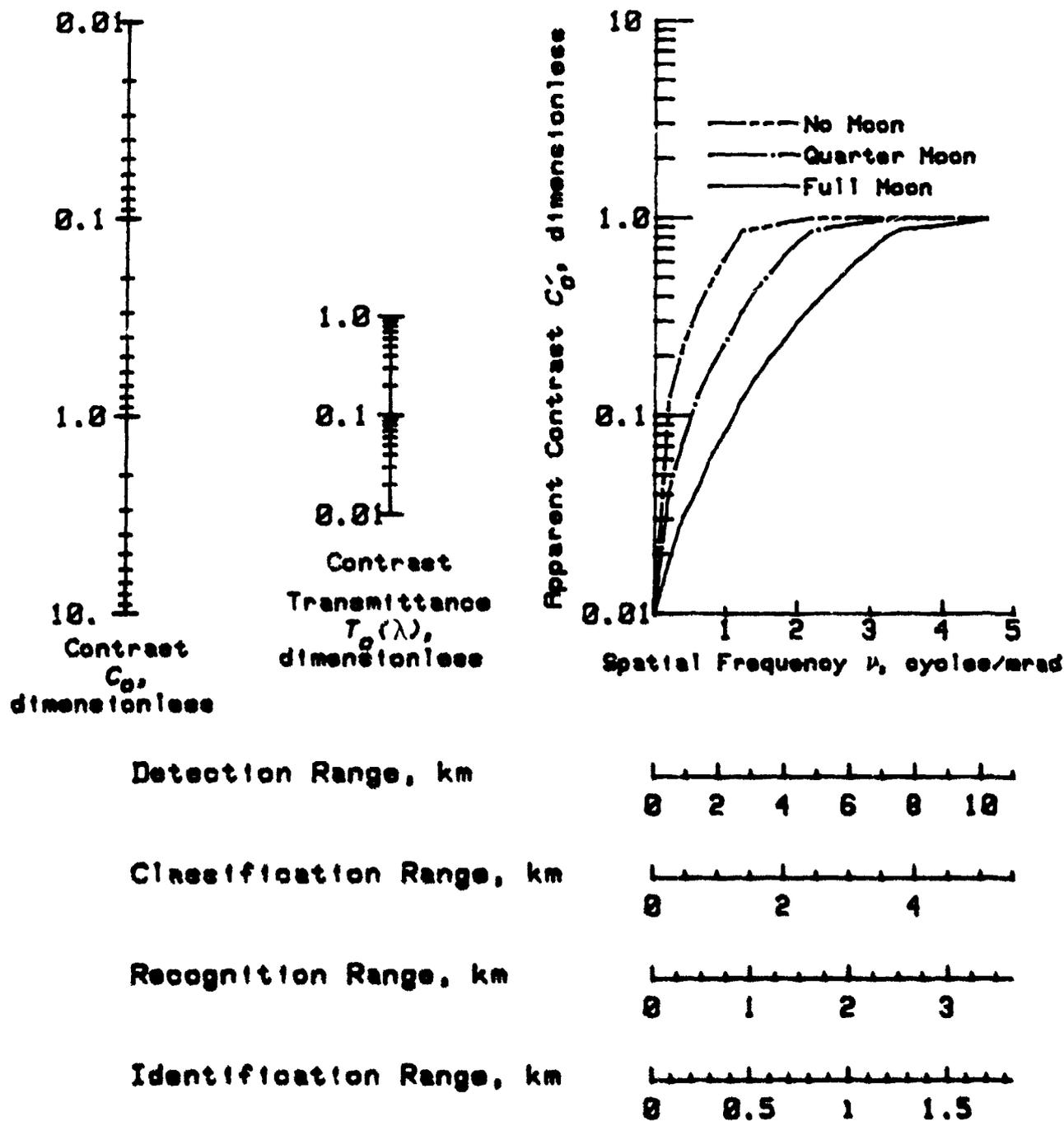
Figure 5-4. Crew Served Weapon Sight Performance Nomogram (Ref. 1)

detection. Conversely, decreasing the threshold increases the probability of detecting low target signals, but it also increases the false alarm rate. To better discriminate the target from the background, passive sensors may use multispectral comparisons, estimates of target angular extent (pulse width seen by a scanned detection), and scan-to-scan correlation.

For a simple threshold detector, the SNR will depend on the target signal in the spectral band, the system noise equivalent power NEP or noise equivalent temperature NET, the detector sensitivity, and the atmospheric transmittance of the signal. Fig. 5-7 shows detection probability vs root mean square (rms) voltage SNR for four probabilities of false alarm.

5-3.3 ACTIVE NONIMAGING SYSTEMS

The signal source for an active system is the illuminator energy. This energy is reflected by the target and thus is attenuated by a two-way path through the atmosphere. The target signature is the target reflec-
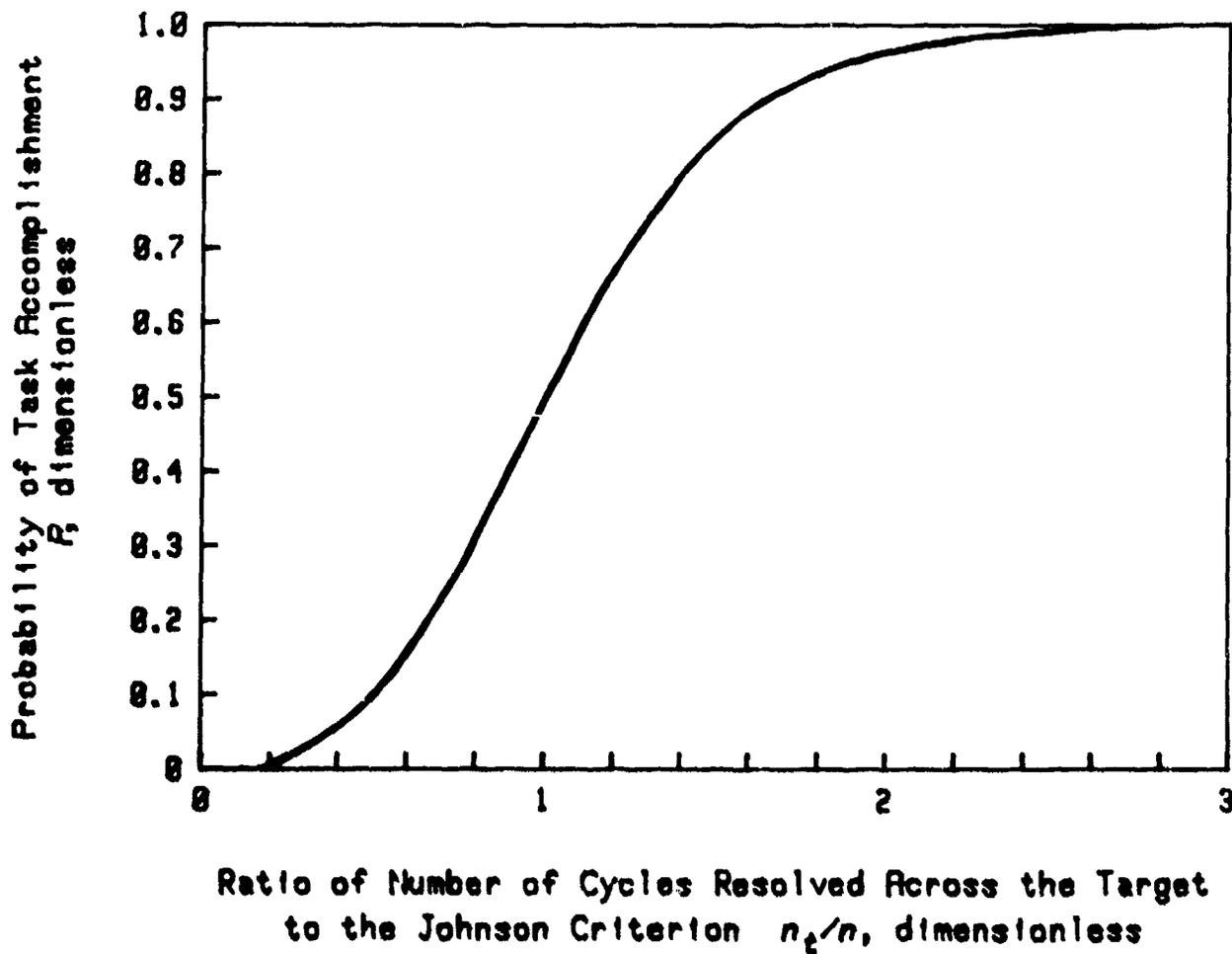
Figure 5-5. Probability vs Resolution Requirement (Ref. 2)

tance at the illuminator wavelength. These systems may be target detection systems, designators, or range finders. Active nonimaging systems include (1) the laser or mmw illuminator, which is a short pulse length, high peak power source, (2) the detector, which may be spectrally filtered to receive energy only at the illuminator wavelength or frequency, and (3) the associated signal processing electronics. Range information is obtained from the time required for a pulse to reach the target and be reflected back to the system detector. To reduce backscatter from the atmosphere near the source, the system may be range gated to accept only pulses falling within a given time (range) window. Spatial resolution of active nonimaging systems is limited by the divergence of the output beam, so the illuminated area increases with the square of the range. Range resolution is determined primarily by the pulse length. For threshold detection systems (noncoherent detection), the signal and noise are filtered by a matched filter with a bandwidth inversely proportional to the output pulse length to reduce the noise current at frequencies that do not correspond to the signal pulse.

The system threshold is set according to the design specification for FAR. The FAR is specified in terms of system on-time, so the threshold setting for a given FAR depends on both pulse width and maximum target range. Target detection probability is determined from the peak target signal to rms noise current ratio. Raising the system threshold to reduce the FAR will also reduce the target detection probability when the target return is weak or severely attenuated.

For an active system the target surface roughness will determine the specularity (glint) of the return signal, which leads to different detection probabilities for targets of different surface characteristics. Fig. 5-8 shows the detection probability curves for active energy detection and heterodyne systems with specular or well resolved targets, and Fig. 5-9 shows the detection probability for these systems against rough targets. Both sets of curves assume a FAR of 10^{-4}. Fig. 5-10 shows detection probability vs SNR as a function of FAR for signal detection in white noise using matched filtering of the input signal.
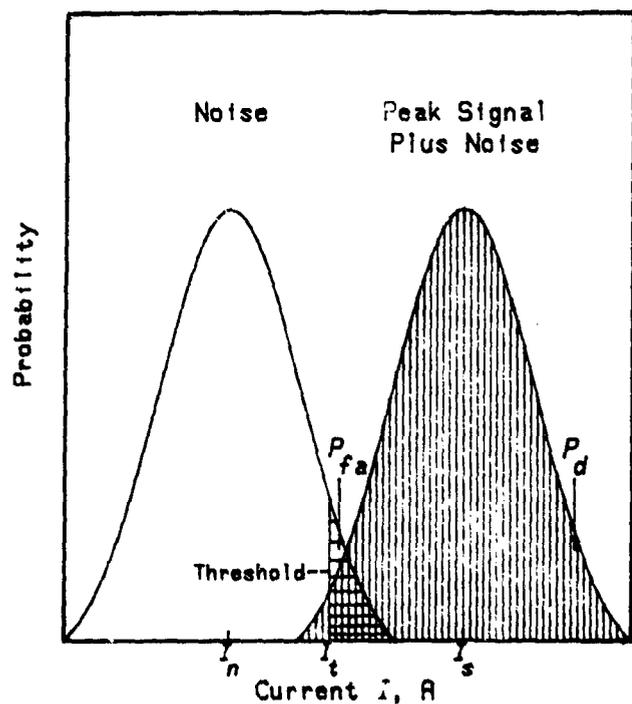
Reprinted with permission of RCA Corporation, New Products Division, Lancaster, PA 17604-3140, USA.

Figure 5-6. Probability of Detection P_d, Probability of False Alarm P_{fa}, and Current Threshold I_t (Ref. 3)
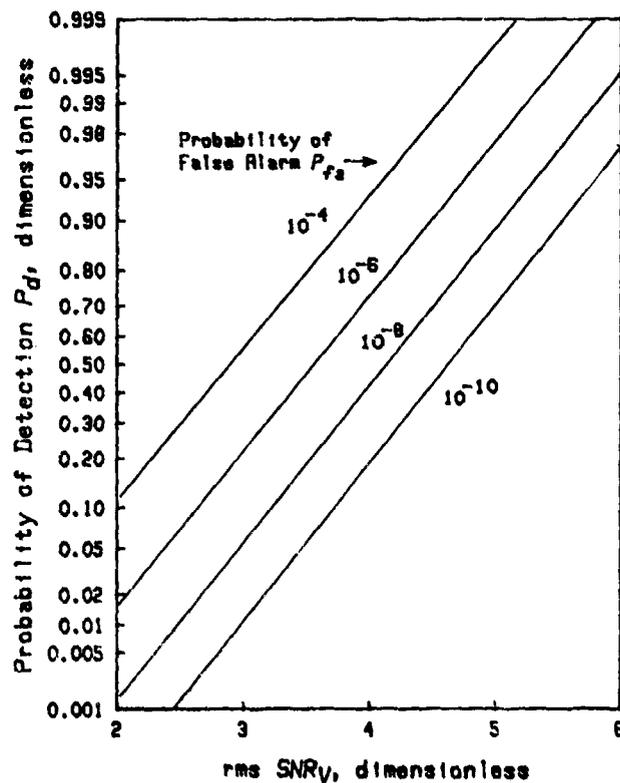
Figure 5-7. Probability of Detection vs rms Voltage SNR (Ref. 4)
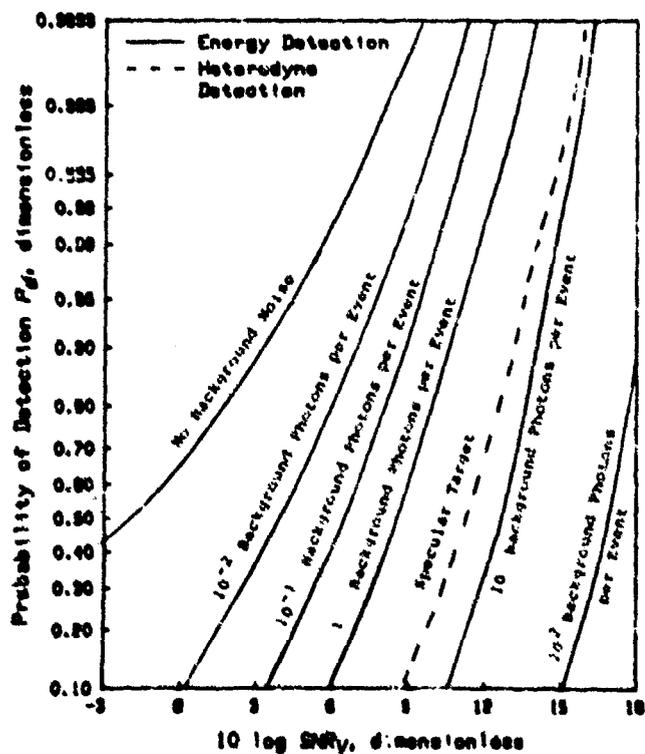
Figure 5-8. Probabilities of Detection for Active Systems With a Specular or Well-Resolved Rough Target (Ref. 4)
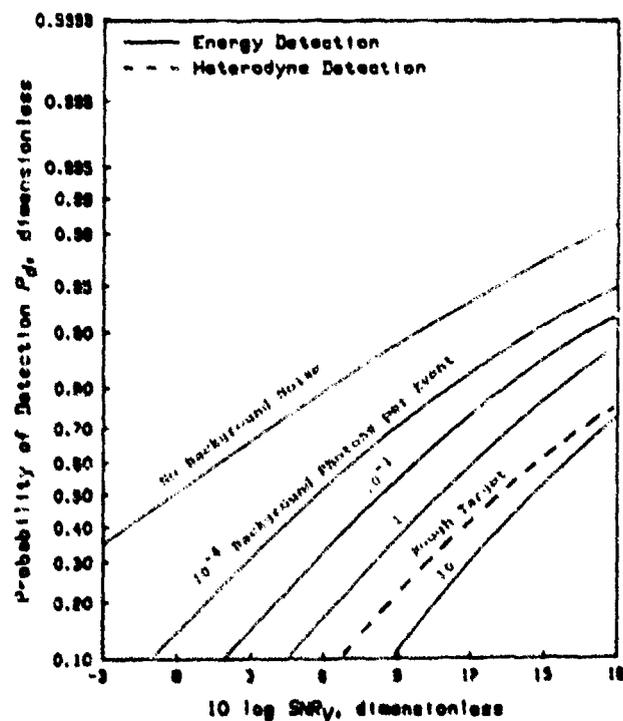
Figure 5-9. Probabilities of Detection for Active Systems With Rough Targets (Ref. 4)

Figure 5-10. Probability of Detection vs Signal-to-Noise Ratio as a Function of False Alarm Rate (Ref. 3)

Active system calculations will be illustrated for a laser range finder. The laser range finder is used to determine the range to a target that has been detected by an imaging system (eye, day sight, I² system, or thermal imager). The target is illuminated by the laser source, and the energy reflected by the target into the laser receiver is detected. The range R to the target is determined by the time interval t between the laser pulse and the return signal:

$$t = \frac{2R}{c}, \quad s \qquad (5\text{-}6)$$

where

c = speed of light, km/s.

Range finders may use pulsed lasers or continuous wave (CW) lasers. Pulsed laser systems use threshold detectors with matched filtering of the input signal. CW laser range finders use heterodyne detection. Both types of systems use spectral filters to eliminate energy that is not at the laser wavelength.

The geometry for the pulsed laser range finder is shown in Fig. 5-11. The laser pulse propagates through the atmosphere to the target, is reflected by the target, and propagates back to the laser range finder (LRF) to be detected by the LRF receiver.

Equations in this paragraph are developed for a pulsed LRF with matched filter detection, such as the Nd:YAG LRF currently used in Army systems. The equation for the received signal power P_s at the LRF detector is

$$P_s = [P_t T_t][T(\lambda)]$$
$$[M \rho \cos\theta][T(\lambda)][T_o A_r/(\pi R^2)], W \qquad (5\text{-}7)$$
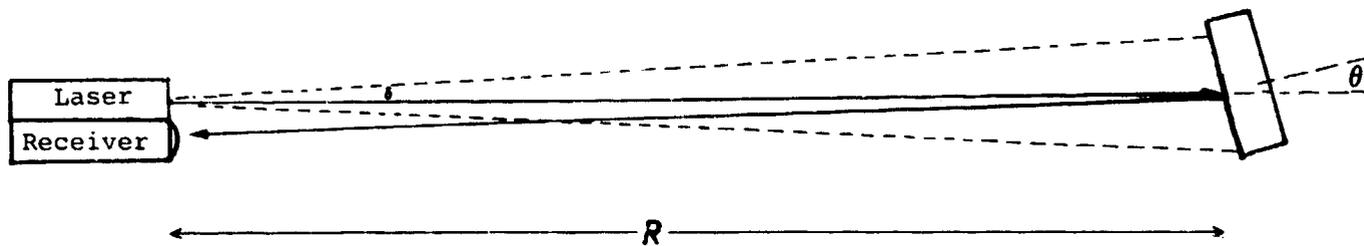
Figure 5-11. Laser Range Finder Geometry

where

P_t = peak transmitter power, W

T_t = transmitter optics transmittance, dimension-
less

M = target-to-beam ratio, dimensionless

ρ_t = target reflectance, dimensionless

θ = angle between target and beam, deg

T_r = receiver optics transmittance, dimension-
less

A_r = receiver effective aperture area, km².

Brackets are included in Eq. 5-7 to separate out the terms for transmitter power, propagation of the laser radiation to the target, diffuse reflection of the laser radiation by the target, propagation from the target to the receiver, and interception of the reflected signal at the laser receiver. The factor M is the ratio of the target area to the area illuminated by the laser and accounts for underfilling the target at short ranges and overfilling the target at long ranges:

$$M = A_t \ (\pi R^2 \delta^2) \quad , \text{dimensionless} \quad (5\text{-}8)$$

where

δ = half-angle laser beam divergence, mrad

A_t = target area, m².

M must be equal to or less than 1.0.

The LRF signal to noise ratio SNR is

$$SNR = \frac{P_s}{NEP} \quad , \text{dimensionless} \quad (5\text{-}9)$$

where

NEP = detector noise equivalent power, W.

Eqs. 5-7 and 5-9 illustrate the $T(\lambda)^2$ dependence of SNR. The effect of the atmosphere on pulse detection probability is more complex. The single pulse probability of detection P_d for the LRF is determined by the SNR and the FAR specification for the system. FAR is specified based on detector on-time t_d, which in turn is determined by the maximum design range for the LRF

$$t_d = \frac{2R_m}{c} \quad , \text{s} \quad (5\text{-}10)$$

where

R_m = maximum design range, km.

FAR is calculated from the per pulse false alarm rate FAR_p and the detector on-time

$$FAR = \frac{FAR_p}{t_d}, \text{s}^{-1}. \quad (5\text{-}11)$$

Fig. 5-10 shows detection probability vs SNR as a function of the product of pulse width τ and FAR. For example, for an LRF with a laser pulse width τ of 10^{-8} s and a FAR specification of 0.01 per pulse over a design range R_m of 15 km, the probability of detection P_d can be determined. Substitution in Eq. 5-10 gives

$$t_d = \frac{2 \times 15}{3 \times 10^5} = 10^{-4} \text{ s}.$$

With this value of t_d substitution in Eq. 5-11 gives

$$FAR = (0.01) \ (10^{-4}) = 10^2 \text{s}^{-1}$$

and

$$\tau FAR = (10^{-8})(10^2) = 10^{-6}.$$

From Fig. 5-10, if $\tau FAR = 10^{-6}$, then an SNR of 5 yields a detection probability P_d of 0.50.

5-3 EO AND MILLIMETER WAVE SYSTEM DEFEAT MECHANISMS

Atmospheric obscurants and battlefield-induced contaminants degrade and may defeat EO and mmw system performance. The sensor defeat mechanisms include loss of transmittance, change in contrast, the introduction of false targets, change in ambient illumination, and turbulence-induced system performance degradation. How these effects degrade or defeat sensor performance is the topic of this paragraph. Par. 5-3.6 contains

defeat mechanism tables, quick summary guides that indicate whether a particular obscurant may have a negligible, minor, or potentially major effect on the performance of a given sensor class.

5-3.1 LOSS OF TRANSMITTANCE

The attenuation of passive target radiation or target contrast by the atmosphere reduces the apparent target signature and results in lower spatial resolution for passive imaging systems and lower detection probability for passive imaging and nonimaging systems. For active systems signal-to-noise ratio and detection probability are reduced. Also for these systems the effect of obscurants is more severe because the illuminator radiation must traverse the path to the target, be reflected from the target, and again be attenuated by the intervening atmosphere.

5-3.2 CHANGE IN CONTRAST

Atmospheric constituents may change the apparent contrast of a target in three ways in addition to causing transmittance losses. Ambient light may be scattered into the sensor field of view (FOV), illuminator energy may be backscattered into the sensor FOV, and the actual target signature may be changed.

Scattering of ambient illumination into the sensor affects primarily visible and near IR systems, i.e., those systems that are sensitive to light level. Multiple scattering of target radiation into the sensor FOV by dense obscurants may also reduce the resolution of visible, near IR, and thermal sensors.

Scattering of active illuminator energy causes two problems. Energy backscattered into the receiver increases the apparent ambient noise level at the illuminator wavelength and may increase the FAR or, for range finders, cause false range readings. If the illuminator energy is forward-scattered into the receiver FOV by multiple scattering from a dense obscurant, the temporal pulse width will be stretched. This pulse shape deformation may cause an LRF target range return to be rejected or may destroy the pulse coding on a designator signal, which reduces the probability of missile lock-on or causes a missile tracking on the designator signal to break lock.

The target signature may be changed by a change in emitted energy, which affects passive thermal systems, or by a change in target reflectance characteristics, which affects light-level dependent systems and active systems. Rain, snow, and wet fogs change target signatures in all spectral bands. In the thermal band the cooling washes out differences in target and background signatures and turns the scene a generally featureless gray. Actively heated elements, such as tank treads and the engine on an exercised tank, will stand out better in this uncluttered scene. Passive visual and

near IR systems have poorer resolution when the light level is reduced. Surface wetting also makes the target reflection of active radiation more specular (glinty). This changes the spatial distribution of the return signal and causes a wide range in target reflectance signals, some of which may saturate a laser receiver although others are low enough to remain undetected.

5-3.3 FALSE TARGETS

Obscurants may appear as false targets to imaging and nonimaging passive sensors, and to active systems, or they may increase the level of clutter (target-like objects), which makes target discrimination a more difficult and time-consuming process. Hot spots in exothermic smokes, high explosive (HE) munition fireballs, muzzle flash, and burning vegetation or vehicles will appear as potential targets to thermal systems, whereas very hot spots may saturate the sensor. The radiance associated with these phenomena will degrade or defeat visual and near IR imagers through clutter introduction and sensor saturation. Bright lights and I² sensor saturation (and the concurrent green flash) at night will cause the human observer to suffer a temporary loss of visual night adaptation.

Backscattering of active system radiation from a dense obscurant may cause a false target detection or a false range reading.

5-3.4 CHANGE IN AMBIENT ILLUMINATION

Natural atmospheric phenomena—clouds, the phase of the moon, precipitation, the time of day, and time of year—all affect the ambient illumination and thus change the performance (spatial resolution) available from light-level dependent visual and I² systems. Reductions in solar insolation due to cloud cover, shorter days, or lower sun angle, reduce the passive thermal signatures of unexercised vehicles.

5-3.5 TURBULENCE

Atmospheric turbulence affects system performance because local fluctuations in atmospheric temperature cause changes in the index of refraction of the air. Temperature effects are strongest at visible and thermal wavelengths. Localized humidity fluctuations affect mmw radiation. Turbulence effects are most severe at visible wavelengths and are most pronounced for active systems because they degrade optical wave front quality, which causes beam spread, beam breakup, and scintillation (time-dependent spatial intensity fluctuations) in the transmitted and received illuminator energy. Turbulence-induced beam steering causes beam centroid wander and a loss of range accuracy and track accuracy. For imaging systems, turbulence may cause

some loss of resolution or blurring; this effect can be viewed as an atmospheric *MTF* degradation.

5-3.6 POLARIZATION

Scattering of radiation by dense media results in polarization changes. For randomly polarized radiation, such as reflected ambient radiation, these changes are not important. However, for polarized active sources, such as some laser and mmw systems, polarization effects may be used as a target discriminant. For these sensors an atmospheric-induced change in polarization characteristics of the illuminator radiation can reduce *SNR*, increase the *FAR*, and thus reduce range performance or target detection probability.

5-3.7 DEFEAT MECHANISM TABLES

This paragraph contains a tabular presentation of the potential effects of natural obscurants and battlefield-induced contaminants on sensor performance. The effects are summarized visually in Fig. 5-12. Tables 5-6 through 5-10 show the sensor defeat mechanism associated with each obscurant for a particular sensor class. The tables indicate the origin and potential severity of each defeat mechanism for active and passive visual, near IR and thermal systems, and active mmw systems.

5-4 ILLUSTRATIVE PROBLEMS

The sample problems in this paragraph illustrate the use of the system performance measures described in this chapter to calculate obscurant effects on system performance. The climatic data from Chapter 3 and battlefield usage examples from Chapter 4 are used to define environmental conditions; the quantitative data and equations from these chapters are used to calculate the effects of these environmental conditions on sensor performance.

The specification of a sensor performance problem includes (1) system, (2) weather conditions or obscured atmospheric conditions, (3) target and background, and (4) task to be performed. The information required to solve the problem includes

1. System:
    a. Sensor and spectral band
    b. Performance measure (subjective performance curve for imaging systems or *SNR* for nonimaging systems)

2. Atmosphere
    a. Natural atmospheric conditions
    b. Battlefield-induced contaminant, type and *CL*

3. Target and Background.
    a. Target dimensions
    b. Target-to-background signature (target thermal signature ΔT for thermal imagers, target contrast

signature C_0 for day sights and F systems, or target reflectance ρ_t for laser systems)

4. Task:
    a. Type of task, i.e., detection or identification
    b. Range of probability requirement.

Steps in the solution are

1. Determine atmospheric transmittance.

2. Determine target signal at the sensor.

3. Determine sensor performance requirement — i.e., *SNR* or resolution.

4. Determine sensor performance from sensor performance requirement and apparent target signal.

The 10 examples in this paragraph illustrate the use of material in this handbook to calculate the effect of obscurants on sensor performance. The first three problems are calculations of sensor performance for a day sight (par. 5-4.1), thermal sensor (par. 5-4.2), and laser range finder (par. 5-4.3) in the natural atmosphere and in the natural atmosphere with smoke added. These problems are solved in detail to illustrate complete systems calculations. In the fourth example (par. 5-4.4), the effects of turbulence on a laser system are calculated. The remainder of the examples illustrate how to determine atmospheric transmittance in obscurants by using the combat examples in par. 4-7. In these example problems (pars. 5-4.5 to 5-4.10), the calculations are limited to the determination of atmospheric transmittance through the obscurant in the system spectral bands.

5-4.1 DAY SIGHT IN CLEAR ATMOSPHERE AND SMOKE (CL=1)

PROBLEM. Calculation of the performance of a day sight in an atmosphere to which smoke has been added. This problem illustrates the severe degradation of day sights by inventory smokes.

5-4.1.1 Conditions

1. System
    a. Day sight, 0.4-0.7 µm, unity magnification
    b. *MRC* curve for eye (Fig. 5-3)

2. Atmosphere
    a. Clear winter afternoon, visibility $V = 15$ km
    b. Added fog oil (FO) smoke, $CL = 1$ g m⁻²
    c. Added white phosphorus (WP) smoke, $CL = 1$ g m⁻²

3. Target
    a. Tank, height $h = 2.4$ m
    b. Target contrast signature $C_0 = 0.61$

4. Task
    a. Target recognition at range $R = 0.5$ km in natural atmosphere
    b. Target recognition at range $R = 0.5$ km in atmosphere with FO smoke
    c. Target recognition at range $R = 0.5$ km in atmosphere with WP smoke

Contrast

Glare

Attenuation

(A) Eye, Day Sights, and Image Intensifiers

Contrast

Emission
Attenuation

(B) Thermal Imagers

Target Reflectance

Backscatter

Attenuation

Laser and Detector
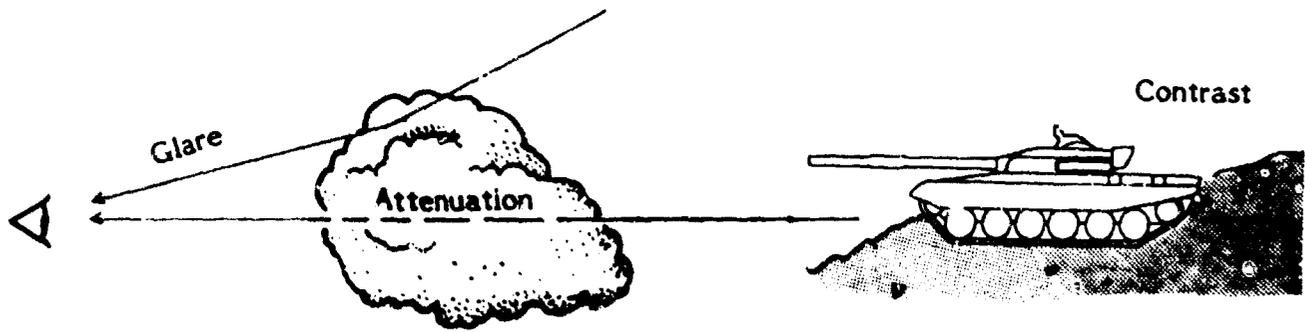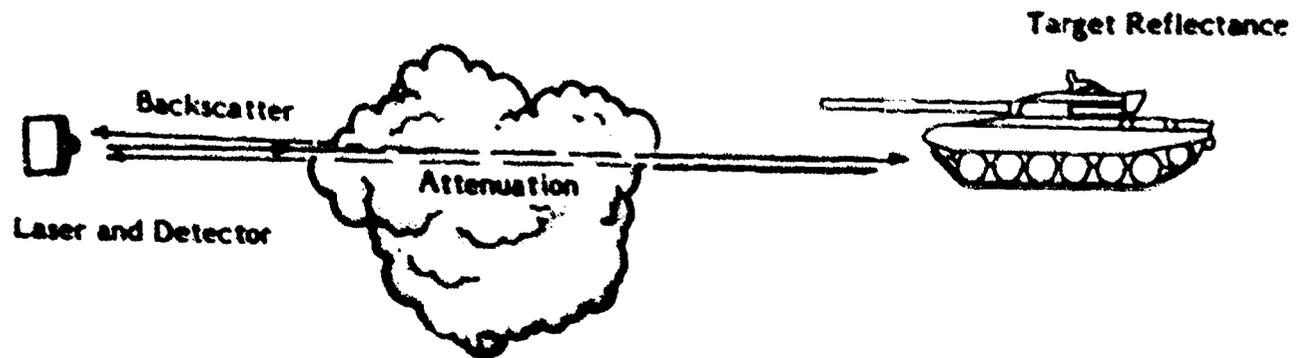
(C) Laser Range Finder

Figure 5-12. Obscurant Effects on System Performance

Target Thermal Signature

Missile

Emission (Path Radiance)

Attenuation

(D) Passive Homing

Flare Tracker

Attenuation

Missile

Eye
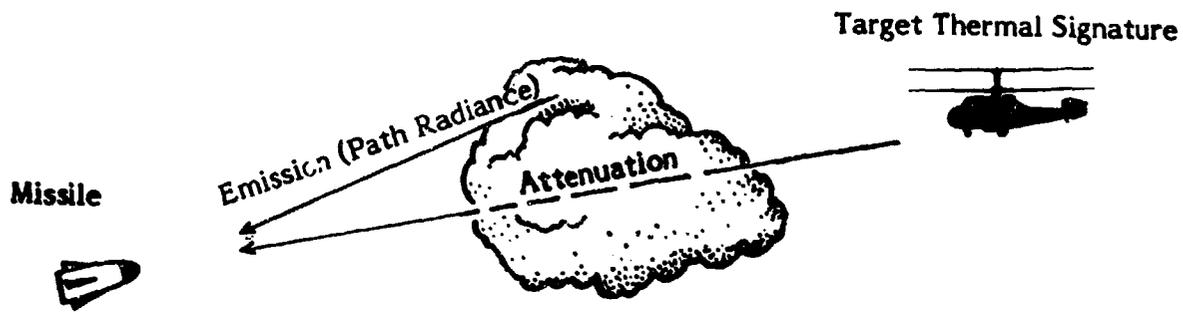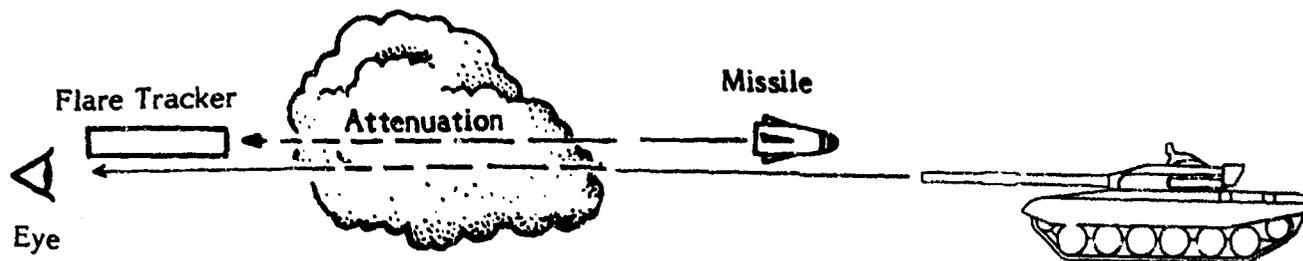
(E) Command Line of Sight Guidance

Missile

Multiple Scattering

Backscatter

Target Reflectance

Laser Designator

Attenuation
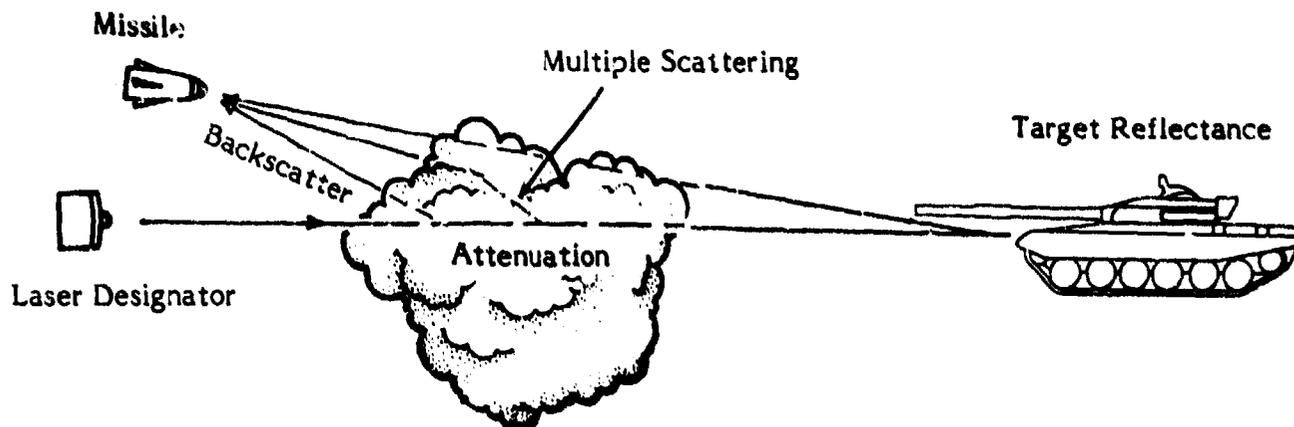
(F) Semi-Active Laser Guidance

Figure 5-12. (cont'd)
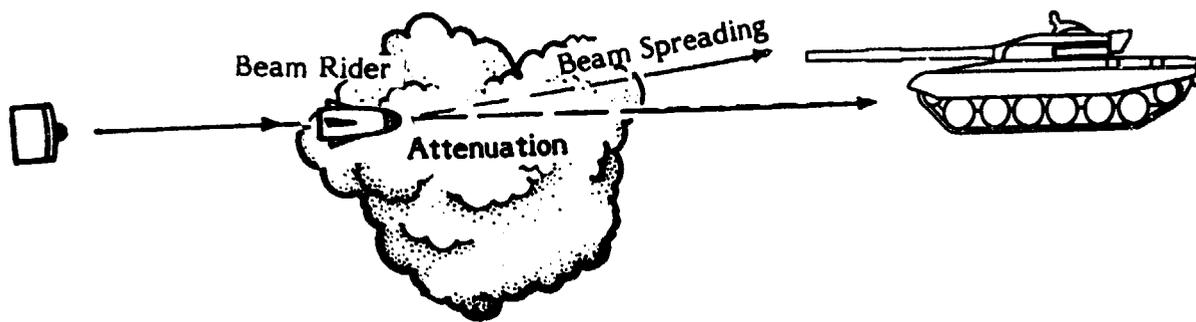
(G) Beam Rider

Figure 5-12. (cont'd)

5-4.1.2 Determine Probability of Target Recognition in Natural Atmosphere

1. Determine atmospheric transmittance:
   Atmospheric transmittance using Eq. 3-1 is

$$T(\lambda) = T_m(\lambda)T_a(\lambda)T_s(\lambda)T_d(\lambda), \text{ dimensionless}$$

where, in the absence of smoke and dust, the smoke transmittance term $T_s(\lambda)$ and the dust transmittance term $T_d(\lambda)$ are equal to 1.0.

The molecular transmittance term, from Eq. 3-3, is

$$T_m(\lambda) = e^{-\gamma_m(\lambda)R} \text{ , dimensionless.}$$

The aerosol transmittance term, from Eq. 3-4, is

$$T_a(\lambda) = e^{-\gamma_a(\lambda)R} \text{ , dimensionless.}$$

From par. 3-2.1.1, $\gamma_m(0.4\text{-}0.7) = 0.02$, and from par. 3-2.2.1, $\gamma_a(0.4\text{-}0.7) = 3.912$ V. Using $V = 15$ km and $R = 0.5$ km, as defined in the problem statement,

$$T(0.4\text{-}0.7\mu m) = e^{-(0.02)(0.5)}e^{-(3.912/15)(-5)}$$
$$= 0.87.$$

2. Determine apparent target signature at sensor. The apparent contrast is given by Eq. 2-11 as

$$C_a' = C_o\left[1 - \frac{L_{sb}}{L_{tb}}(1 - T(\lambda)^{-1})\right]^{-1} \text{ , dimensionless.}$$

The inherent contrast C_o is 0.61, from the statement of the problem, and the sky-to-ground ratio, L_{sb}/L_{tb} is taken to be 1.4 if the guidance in Table 2-4 for clear (desert) conditions is used. Therefore

$$C_a' = 0.61[1 - 1.4[1 - (1.0/0.87)]]^{-1}$$
$$= 0.50.$$

3. Determine sensor resolution requirement:
   From Table 5-5, the requirement for recognition is that a day sight resolve $n = 3$ cycles across the target. The number of cycles n_t the system can resolve across the target is, from Eq. 5-5,

$$n_t = \nu/\nu_t \text{ , dimensionless}$$

where the system resolution ν at the target apparent temperature is determined from the system MRC curve, and the target spatial frequency ν_t is found from the target height h and range R using Eq. 5-2:

$$\nu_t = R/h \text{ , cycles/mrad.}$$

In this case, for a 2.4-m target at 0.5 km,

$$\nu_t = \frac{0.5}{2.4} = 0.21 \text{ cycles/mrad.}$$

Thus from Eq. 5-5, the day sight must resolve a spatial frequency ν of at least (0.21×3) or 0.63 cycles/mrad to recognize the target (at the 50% probability level) at 0.5 km.

4. Determine sensor performance:
   Sensor resolution is determined from the apparent contrast C_a' calculated in Step 2 using the sensor MRC curve in Fig. 5-3. For a contrast of 0.50, the system can resolve a spatial frequency ν of about 1.8 cycles/mrad.

The number of cycles resolved across the target is, from Eq. 5-5,

$$n_t = \frac{1.8}{0.21} = 8.6 \text{ cycles.}$$

The probability of accomplishing the task is determined from the target transfer probability curve in Fig. 5-5. In this case

TABLE 5-6. SENSOR DEFEAT MECHANISMS FOR PASSIVE VISIBLE AND NEAR IR SYSTEMS

Observed Effect / Defeat Mechanisms**	Clear Air	Low Humidity	High Humidity	Haze	Cloud Cover	Turbulence	Fog	Rain	Snow Light	Snow Heavy	HE Artillery Light	HE Artillery Heavy	Smoke* Short-Term	Smoke* Long-Term	HC (CL=1)	HC (CL=5)	FO (CL=1)	FO (CL=5)	WP (CL=1)	WP (CL=5)	Vehicle Traffic	Fires
Transmittance Reduction																						
Signal Loss	—	—	—	2	—	—	2	2	1	2	1	2	2	2	2	2	2	2	2	2	1	2
Scattering of Ambient Illumination																						
Contrast Loss	—	—	—	2	—	—	2	—	1	1	1	2	1	—	2	2	2	2	2	2	—	—
Increased Noise	—	—	—	2	—	—	2	—	1	1	1	2	1	—	2	2	2	2	2	2	—	—
Scattering of Target Signal																						
Signal Loss	—	—	—	2	—	—	2	—	1	2	1	2	2	1	2	2	2	2	2	2	1	2
Resolution Loss	—	—	—	2	—	—	1	—	—	1	—	1	—	—	1	1	1	1	1	1	—	1
Scattering of Illuminator Energy																						
Signal Loss	—	—	—	—	—	—	—	—	—	—	—	—	—	—	—	—	—	—	—	—	—	—
Increased Noise	—	—	—	—	—	—	—	—	—	—	—	—	—	—	—	—	—	—	—	—	—	—
Pulse Stretching	—	—	—	—	—	—	—	—	—	—	—	—	—	—	—	—	—	—	—	—	—	—
False Returns	—	—	—	—	—	—	—	—	—	—	—	—	—	—	—	—	—	—	—	—	—	—
Centroid Shift	—	—	—	—	—	—	—	—	—	—	—	—	—	—	—	—	—	—	—	—	—	—
Obscurant Radiance																						
Increased Noise	—	—	—	—	—	—	—	—	—	—	—	—	—	—	2	2	—	—	2	2	—	2
Decreased Contrast	—	—	—	—	—	—	—	—	—	—	—	—	—	—	2	2	—	—	2	2	—	2
False Targets	—	—	—	—	—	—	—	—	—	—	—	—	—	—	—	—	—	—	—	—	—	—
Sensor Blinding	—	—	—	—	—	—	—	—	—	—	—	—	2	—	2	2	—	—	2	2	—	2
Reduced Target Signature	2	—	—	2	2	1	2	—	2	2	1	2	2	—	—	—	—	—	—	2	—	—

*HC = hexachloroethane smoke; CL = concentration path length product, g·m²
FO = fog oil smoke
WP = phosphorus smoke

** __ = N/A or Never a Problem
1 = Possible Minor Effect
2 = Possible Major Effect

TABLE 5-7. SENSOR DEFEAT MECHANISMS FOR PASSIVE THERMAL SYSTEMS

Obscurant Effect / Defeat Mechanism**	Clear Air	Low Humidity	High Humidity	Haze	Cloud Cover	Turbulence	Fog	Rain Light	Rain Heavy	Snow Light	Snow Heavy	HE Artillery Short-Term	HE Artillery Long-Term	Smoke* HC (CL=1)	HC (CL=5)	FO (CL=1)	FO (CL=5)	WP (CL=1)	WP (CL=5)	Vehicle Traffic	Fires
Transmittance Reduction																					
Signal Loss	—	—	2	2	2	—	2	—	2	—	2	2	—	—	2	—	—	—	2	—	2
Scattering of Ambient Illumination																					
Contrast Loss	—	—	—	—	—	—	—	—	—	—	—	—	—	—	—	—	—	—	—	—	—
Increased Noise	—	—	—	—	—	—	—	—	—	—	—	—	—	—	—	—	—	—	—	—	—
Scattering of Target Signal																					
Signal Loss	—	—	—	—	—	—	2	—	2	—	2	2	—	—	—	—	—	—	—	—	—
Resolution Loss	—	—	—	—	—	—	2	—	—	—	—	—	—	—	—	—	—	—	—	—	—
Scattering of Illuminator Energy																					
Signal Loss	—	—	—	—	—	—	—	—	—	—	—	—	—	—	—	—	—	—	—	—	—
Increased Noise	—	—	—	—	—	—	—	—	—	—	—	—	—	—	—	—	—	—	—	—	—
Pulse Stretching	—	—	—	—	—	—	—	—	—	—	—	—	—	—	—	—	—	—	—	—	—
False Return	—	—	—	—	—	—	—	—	—	—	—	—	—	—	—	—	—	—	—	—	—
Obscurant Radiance																					
Increased Noise	—	—	1	—	—	—	—	—	—	—	—	2	—	—	1	—	—	—	1	—	2
Decreased Contrast	—	—	1	—	—	—	—	—	—	—	—	2	—	—	1	—	—	—	1	—	2
False Targets	—	—	—	—	—	—	—	—	—	—	—	2	—	—	—	—	—	2	2	—	2
Sensor Blinding (short-term)	—	—	—	—	—	—	—	1	2	—	2	2	—	2	2	—	—	2	2	—	2
Reduced Target Signature	—	—	—	2	2	—	2	2	2	—	2	—	—	—	2	—	—	—	—	—	—

*HC = hexachloroethane smoke; CL = concentration path length product, g/m²
FO = fog oil smoke
WP = phosphorus smoke

**__ = N/A or Never a Problem
1 = Possible Minor Effect
2 = Possible Major Effect

TABLE 5-8. SENSOR DEFEAT MECHANISMS FOR ACTIVE VISIBLE AND NEAR IR SYSTEMS

Obscurant Effect / Defeat Mechanism**	Clear Air	Low Humidity	High Humidity	Haze	Cloud Cover	Turbulence	Fog	Rain	Snow Light	Snow Heavy	HE Artillery Light	HE Artillery Heavy	Short-Term	Long-Term	HC (CL=1)	HC (CL=5)	FO (CL=1)	FO (CL=5)	WP (CL=1)	WP (CL=5)	Vehicle Traffic	Fires
Transmittance Reduction																						
Signal Loss	—	—	—	2	2	2	2		1	2	1	2	2	2	2	2	2	2	2	2	1	2
Scattering of Ambient Illumination																						
Contrast Loss																						
Increased Noise																						
Scattering of Target Signal																						
Signal Loss				2		2	2			2		2	2	—	2	2	2	2	2	2	1	2
Resolution Loss				1		2	1		1	1			1	—	1				1	1	1	2
Scattering of Illumination Energy																						
Signal Loss						2	2			1		2	2	1	2	2	2	2	2	2		1
Increased Noise						1	2			1		2	2		2	2	2	2	2	2		
Pulse Stretching						1	2			1		2	1		2	2	2	2	2	2		
False Returns							2			1			1	1	2	2	2	2	2	2		
Obscurant Radiance																						
Increased Noise																						
Decreased Contrast																						
False Targets																						
Sensor Blinding (obscuration)																						
Reduced Target Signature							2			2	2	2					1					

*HC = hexachloroethane smoke; CL = concentration path length product, g·m⁻²

FO = fog oil smoke

WP = phosphorus smoke

** — = N.A or Never a Problem
1 = Possible Minor Effect
2 = Possible Major Effect

TABLE 5-9. SENSOR DEFEAT MECHANISMS FOR ACTIVE THERMAL SYSTEMS

Obscurant Effect Defeat Mechanism**	Clear Air	Low Humidity	High Humidity	Haze	Cloud Cover	Turbulence	Fog	Rain	Snow Light	Snow Heavy	HE Artillery Light	HE Artillery Heavy	Smoke* Short-Term	Smoke* Long-Term	HC (CL=1)	HC (CL=5)	FO (CL=1)	FO (CL=5)	WP (CL=1)	WP (CL=5)	Vehicle Traffic	Fires
Transmittance Reduction — Signal Loss	—	—	2	2	—	—	2	—	1	2	1	2	2	—	1	2	—	1	1	2	1	2
Scattering of Ambient Illumination — Contrast Loss	—	—	—	—	—	—	—	—	—	—	—	—	—	—	—	—	—	—	—	—	—	—
Increased Noise	—	—	—	—	—	—	—	—	—	—	—	—	—	—	—	—	—	—	—	—	—	—
Scattering of Target Signal — Signal Loss	—	—	—	—	—	—	2	1	1	2	1	2	2	1	—	—	—	—	—	—	1	2
Resolution Loss	—	—	—	—	—	—	1	—	—	1	1	2	2	1	—	—	—	—	—	—	—	1
Scattering of Illumination Energy — Signal Loss	—	—	—	1	—	—	2	—	1	2	1	2	2	1	—	—	—	—	—	—	—	—
Increased Noise	—	—	—	1	—	—	2	—	1	2	1	2	2	—	—	—	—	—	—	—	—	1
Pulse Stretching	—	—	—	—	—	—	2	—	—	1	1	2	2	—	—	—	—	—	—	—	—	—
False Returns	—	—	—	—	—	—	2	—	—	—	—	—	2	—	—	—	—	—	—	—	—	—
Obscurant Radiance — Increased Noise	—	—	—	—	—	—	—	—	—	—	—	—	—	—	—	—	—	—	—	—	—	—
Decreased Contrast	—	—	—	—	—	—	—	—	—	—	—	—	—	—	—	—	—	—	—	—	—	—
False Targets	—	—	—	—	—	—	—	—	—	—	—	—	—	—	—	—	—	—	—	—	—	—
Sensor Blinding (short-term)	—	—	—	—	—	—	—	—	—	—	—	—	—	—	—	—	—	—	—	—	—	—
Reduced Target Signature	—	—	—	—	—	—	2	—	2	2	2	2	—	—	—	—	—	—	—	—	—	—

*HC = hexachloroethane smoke. (CL = concentration path length product, g·m⁻²)
FO = fog oil smoke
WP = phosphorus smoke

**... = N/A or Never a Problem
1 = Possible Minor Effect
2 = Possible Major Effect

TABLE 5-10. SENSOR DEFEAT MECHANISMS FOR ACTIVE MILLIMETER WAVE SYSTEMS

Obscurant Effect / Defeat Mechanism**	Clear Air	Low Humidity	High Humidity	Haze	Cloud (Cover)	Turbulence	Fog	Rain Light	Rain Heavy	Snow Light	Snow Heavy	HE Artillery Light	HE Artillery Heavy	Smoke* Short-Term	Smoke* Long-Term	HC (CL=1)	HC (CL=5)	FO (CL=1)	FO (CL=5)	WP (CL=1)	WP (CL=5)	Vehicle Traffic	Fires
Transmittance Reduction																							
Signal Loss	—	—	—	—	—	1	1			2	2	1	2		2	—						—	2
Saturation of Ambient Illumination																							
Contrast Loss	—	—	—	—	—	—	—	—	—	—	—	—	—	—	—	—	—	—	—	—	—	—	—
Increased Noise	—	—	—	—	—	—	—	—	—	—	—	—	—	—	—	—	—	—	—	—	—	—	—
Saturation of Target Signal																							
Signal Loss	—	—	—	—	—	—	—	1	1	—	2	2	2		2	—							2
Resolution Loss	—	—	—	—	—	1	—	—	1	—	—	2	2		—	—							1
Saturation of Illumination Energy																							
Signal Loss	—	—	—	—	—	—	2	2	2	2	2	2	2		2	—							2
Increased Noise	—	—	—	—	—	—	2	—	—	2	2	2	2		1	—							—
Pulse Stretching	—	—	—	—	—	—	—	—	—	—	—	—	—		—	1							—
False Returns	—	—	—	—	—	—	—	—	—	—	—	—	—		2	—							—
Obscurant Radiance																							
Increased Noise	—	—	—	—	—	—	—	—	—	—	—	—	—	—	—	—	—	—	—	—	—	—	—
Decreased Contrast	—	—	—	—	—	—	—	—	—	—	—	—	—	—	—	—	—	—	—	—	—	—	—
False Target	—	—	—	—	—	—	—	—	—	—	—	—	—	—	—	—	—	—	—	—	—	—	—
Sensor Blinding (direct source)	—	—	—	—	—	—	—	—	—	—	—	—	—	—	—	—	—	—	—	—	—	—	—
Reduced Target Signature	2	2	2	1	1	1	2	2	2	2	2	2	2	—	—	—	—	—	—	—	—	—	—

**_ = N/A or Never a Problem
1 = Possible Minor Effect
2 = Possible Major Effect

*HC = hexachloroethane smoke; CL = concentration path length product, g·m³
FO = fog oil smoke
WP = phosphorus smoke

$$\frac{n_t}{n} = \frac{8.6}{3} = 2.9$$

which yields a probability of about 98% of recognizing the target.

5-4.1.3 Determine Probability of Target Recognition in Atmosphere With FO Smoke

1. Determine atmospheric transmittance:
From Eq. 3-1,

$$T(\lambda) = T_m(\lambda)T_a(\lambda)T_s(\lambda)T_d(\lambda), \text{dimensionless}$$

where $T_m(\lambda)$ and $T_a(\lambda)$ were determined in par. 5-4.1.2 and $T_d(\lambda) = 1.0$.

The smoke transmittance term $T_s(\lambda)$ is calculated using Eq. 4-2,

$$T_s(\lambda) = e^{-\alpha_s(\lambda)CL} \quad, \text{dimensionless.}$$

In this example, $CL = 1$ g m². From Table 4-2, the smoke mass extinction coefficient $\alpha_s(\lambda) = 6.85$ m² g at visible wavelengths. Therefore,

$$T(0.4\text{-}0.7 \ \mu m) =$$
$$e^{-(0.02)(0.5)}e^{-(3.912/15)(0.5)}$$
$$e^{-(6.85)(1)}(1.0) = 9.2 \times 10^{-4}.$$

2. Determine apparent target signature at the sensor. Apparent contrast C_a' may again be calculated using Eq. 2-11. However C_a' is less than 9×10^{-4} (the value of the atmospheric transmittance $T(\lambda)$, and for this contrast value the eye resolution is zero as indicated in Fig. 5-3. Therefore, the probability of recognizing the target through the smoke is zero.

5-4.1.4 Determine Probability of Target Recognition in Atmosphere With WP Smoke

1. Determine atmospheric transmittance. Atmospheric transmittance is determined as in pars. 5-4.1.3 except that the value of the smoke extinction coefficient $\alpha_s(\lambda)$ is different for WP than it is for FO. Because WP is hygroscopic, the value for $\alpha_s(\lambda)$ depends on relative humidity. From Table 4-3, $\alpha_s(0.4\text{-}0.7\mu m) = 1.08$ at 30% RH and 3.76 at 80% RH in the visible spectral band. By interpolation, $\alpha_s(0.4\text{-}0.7\mu m) = 3.92$ at 10% RH, i.e., the conditions for this problem. Then, for a CL of 1 g m² of WP,

$$T_s(0.4\text{-}0.7\mu m) = e^{-\alpha_s(0.4\text{-}0.7\mu m)CL}$$
$$= e^{-(3.92 \times 1.0)} \quad, \text{dimensionless}$$
$$= 0.020.$$

Therefore,

$$T(0.4\text{-}0.7 \ \mu m) = e^{-(0.2)(0.5)}e^{-(3.912/15)(0.5)}$$
$$e^{-(3.92)(1.0)}(1.0)$$
$$= 0.017.$$

2. Determine apparent target signature at the sensor. Apparent contrast C_a' may be calculated using Eq. 2-11. However, the value of C_a' will be below 0.02, which is the value of $T(\lambda)$. Thus the apparent target contrast is below the contrast threshold of the eye, as indicated in Fig. 5-3. The sensor user will not detect (or recognize) the target under these conditions.

5-4.1.5 Summary: Smoke Effects on Day Sight Performance

The unity magnification day sight in this problem can easily resolve the tank target; the probability of recognizing the target at 0.5 km in the specified natural atmosphere is 98%. However, moderate levels of smokes have a severe effect on day sight performance. If WP or FO smoke are present in a CL of 1 g m², the day sight user cannot detect (much less recognize) the tank at 0.5 km.

5-4.2 THERMAL IMAGER IN CLEAR ATMOSPHERE AND SMOKE ($CL=1$)

PROBLEM: Calculation of the performance of a thermal imager in an atmosphere to which a smoke has been added. This problem illustrates the negligible effect of FO smoke and moderate effect of WP smoke on thermal sight performance. The atmospheric conditions and target used in this problem are the same as those used in par. 5-4.1; however, the atmospheric transmittance and target signature will be different because of the different spectral bands of the sensors.

5-4.2.1 Conditions

1. System:
   a. Thermal imager, 8-12 μm
   b. MRT curve in Fig. 5-2
2. Atmosphere:
   a. Clear winter afternoon, 10% RH, 10°C, visibility $V = 15$ km
   b. Added fog oil smoke, $CL = 1$ g m²
   c. Added WP smoke, $CL = 1$ g m²
3. Target:
   a. Tank, height $h = 2.4$ m
   b. Target thermal signature $\Delta T = 1.8$ K
4. Task:
   a. Target recognition at range $R = 0.5$ km in atmosphere
   b. Target recognition at range $R = 0.5$ km in atmosphere with FO smoke

c. Target recognition at range $R = 0.5$ km in atmosphere with WP smoke.

5-4.2.2 Determine Probability of Target Recognition in Natural Atmosphere

1. Determine atmospheric transmittance:

Again, Eq. 3-1 is used to calculate transmittance:

$$T(\lambda) = T_m(\lambda)T_a(\lambda)T_s(\lambda)T_d(\lambda) \quad \text{,dimensionless}$$

but for this example the transmittance terms must be determined for the 8-12 μm spectral band.

From Table 3-2, the molecular transmittance term $T_m(8\text{-}12\mu m) = 0.92$ at 1.0 km. It is estimated to be about 0.96 at 0.5 km.

The aerosol transmittance is given by Eq. 3-4,

$$T_a(\lambda) = e^{-\gamma_a(\lambda)R}, \quad \text{dimensionless}$$

where, from Table 3-4, $\gamma_a(8\text{-}12\mu m)$ is 0.02, which gives

$$T_a(8\text{-}12\mu m) = e^{(-0.02)(0.5)}$$
$$= 0.99.$$

Therefore, in the absence of dust or smoke,

$$T(8\text{-}12\mu m) = (0.96)e^{-(0.2)(0.5)}(1.0)(1.0)$$
$$= 0.95.$$

2. Determine apparent target signature at sensor. From Eq. 5-3, the apparent target thermal signature $\Delta T'$ is

$$\Delta T' = T(\lambda)\Delta T, \text{ K}$$

where ΔT is given as 1.8 K, and $T(\lambda)$ was calculated to be 0.95 in Step 1. Therefore,

$$\Delta T' = (0.95)(1.8) = 1.7 \text{ K}.$$

3. Determine sensor resolution requirement. From Table 5-5, the Johnson criterion n is 4 cycles resolved across the target for recognition using a thermal imager. The number of cycles n_t the sensor can resolve across the target is given by Eq. 5-5,

$$n_t = \nu/\nu_t, \text{ cycles}$$

where ν_t for the tank at 0.5 km is 0.21 cycles/mrad, as determined in par. 5-4.1.1.

4. Determine sensor performance:

Sensor resolution is determined from the apparent thermal signature $\Delta T'$ calculated in Step 2 and the MRT curve in Fig. 5-2. For a $\Delta T'$ of 1.7 K, the thermal

imager can resolve a spatial frequency ν of about 4.3 cycles/mrad. Therefore, the number n_t of cycles resolved across the target is

$$n_t = \frac{4.3}{0.21} = 20 \text{ cycles}.$$

The probability of recognizing the target is found from the target transfer probability curve in Fig. 5-5. In this case

$$\frac{n_t}{n} = \frac{20}{4} = 5.0.$$

Therefore, from Fig. 5-5, the target recognition probability at 0.5 km is 100%.

5-4.2.3 Determine Probability of Target Recognition in Natural Atmosphere With FO Smoke

1. Determine atmospheric transmittance. From Eq. 3-1,

$$T(\lambda) = T_m(\lambda)T_a(\lambda)T_s(\lambda)T_d(\lambda) \quad \text{,dimensionless}$$

where $T_m(\lambda)$ and $T_a(\lambda)$ were determined in par. 5-4.2.2, and $T_d(\lambda) = 1.0$. The smoke transmittance term $T_s(\lambda)$ is calculated from Eq. 4-2

$$T_s(\lambda) = e^{-\alpha_s(\lambda)Cl}, \quad \text{dimensionless}$$

where $Cl = 1$ g/m². From Table 4-2, $\alpha_s(\lambda) = 0.02$ for FO in the 8-12μm band. Therefore,

$$T_s(8\text{-}12\mu m) = e^{-(0.02)(1.0)} = 0.98$$

and

$$T(8\text{-}12\mu m) = (0.96)e^{-(0.02)(0.5)}e^{-(0.02)(1.0)}(1.0)$$
$$= 0.93.$$

2. Determine apparent target signature. From Eq. 5-3, the apparent target signature $\Delta T'$ is

$$\Delta T' = T(\lambda)\Delta T, \text{ K}$$
$$= (0.93)(1.8)$$
$$= 1.7 \text{ K}.$$

3. Determine sensor resolution requirement. The Johnson criterion n is 4 cycles, and ν_t is 0.21 cycles/mrad, as discussed in par. 5-4.2.2.

4. Determine sensor performance. From Fig. 5-2,

the sensor resolution ν for an apparent target signature $\Delta T'$ of 1.7 K is about 4.3 cycles/mrad. Therefore,

$$n_t = \frac{\nu}{\nu_t} = \frac{4.3}{0.21} = 20 \text{ cycles.}$$

For recognition using the Johnson criterion $n = 4$ cycles:

$$\frac{n_t}{n} = \frac{20}{4} = 5.0.$$

Again, from Fig. 5-5, the probability of recognizing the target is 100%.

5-4.2.4 Determine Probability of Target Recognition in Natural Atmosphere With WP SMOKE

1. Determine atmospheric transmittance. Atmospheric transmittance is determined as in par. 5-4.2.3, except that the value of the smoke extinction coefficient $\alpha_s(\lambda)$ is different for WP than it is for FO. Table 4-3 gives $\alpha_s(\lambda) = 0.38$ for WP in the 8-12μm band at 50% RH, and $\alpha_s(\lambda) = 0.38$ at 30% RH. By interpolation $\alpha_s(\lambda) = 0.38$ at 40% RH, the conditions for this problem. Then, for a CL of 1 g m^2 of WP,

$$T_s(8\text{-}12\mu m) = e^{-\alpha_s(8\text{-}12\mu m)CL} \text{, dimensionless}$$
$$= e^{-(0.38)(1.0)}$$
$$= 0.74$$

and

$$T(8\text{-}12\mu m) = (0.96)e^{-(0.02)(0.5)}e^{-(0.38)(1.0)}(1.0)$$
$$= 0.65.$$

2. Determine apparent target signature. Under these conditions,

$$\Delta T' = T(8\text{-}12\mu m)\Delta T, \text{ dimensionless}$$
$$= (0.65)(1.8)$$
$$= 1.2 \text{ K.}$$

3. Determine sensor resolution requirement. The Johnson criterion n is 4 cycles, and ν_t is 0.21 cycles/mrad, as discussed in par. 5-4.2.2.

4. Determine sensor performance. From Fig. 5-2, the sensor resolution for an apparent target signature $\Delta T'$ of 1.2 K is about 4.0 cycles/mrad. Therefore,

$$n_t = \frac{\nu}{\nu_t} = \frac{4.0}{0.21}$$
$$= 19 \text{ cycles.}$$

For recognition

$$\frac{n_t}{n} = \frac{19}{4} = 4.8.$$

Again, from Fig. 5-5, the probability of recognizing the target is 100%.

5-4.2.5 Summary: Smoke Effects on Thermal Sight Performance

The performance of the thermal sight was calculated for the same atmosphere as the day sight in par. 5-4.1. The performance of the thermal sight in recognizing the tank target at 0.5 km in the clear atmosphere was equivalent to the day sight performance. However, neither FO smoke or WP smoke with a CL of 1 g m^2 affected the performance of the thermal sight. The WP smoke did, however, reduce thermal transmittance by about 25%. In higher concentrations or in conditions of marginal clear air thermal sensor performance, the WP smoke will degrade thermal sensor performance.

5-4.3 Nd: YAG LRF IN HAZY ATMOSPHERE AND WP SMOKE ($CL=1$)

PROBLEM: Calculation of the performance of an LRF in an atmosphere to which a smoke has been added. This problem illustrates the reduction in range performance of an Nd:YAG LRF by WP smoke.

5-4.3.1 Conditions

1. System:
   a. Nd: YAG LRF, 1.06 μm
   b. System specification
(1) Pulse width	8 ns
(2) Peak transmitter power P_t	5×10^6 W
(3) Optics transmittance T_oT_r	0.6
(4) Receiver diameter	0.07 m
(5) Receiver FOV	0.5 mrad
(6) Half-angle laser beam divergence δ	0.25 mrad
(7) Detector noise equivalent power NEP	6.5×10^{-8} W

   c. False alarm rate FAR equal to 150 s^{-1}
2. Atmosphere:
   a. 70% RH, 10°C, visibility $V = 5$ km
   b. Added WP smoke, $CL = 1$ g m^2
3. Target:
   a. Tank, 2.4 × 3.4 m
   b. Tank target reflectance $\rho_t = 0.3$ at 1.06 μm
4. Task:
   a. LRF range performance and SNR in natural atmosphere
   b. LRF range performance and SNR in atmosphere with WP smoke.

5-4.3.2 Determine *SNR* and 90% Detection Range in Natural Atmosphere

1. Determine atmospheric transmittance:
From Eq. 3-1, atmospheric transmittance $T(\lambda)$ is

$$T(\lambda) = T_m(\lambda)T_a(\lambda)T_s(\lambda)T_d(\lambda) \quad \text{,dimensionless.}$$

From par. 3-2.1.2, molecular absorption is negligible at 1.06 μm, so $T_m(1.06\mu m) = 1.0$. The aerosol transmittance term $T_a(\lambda)$, from Eq. 3-4, is

$$T_a(\lambda) = e^{-\gamma_a(\lambda)R} \quad \text{, dimensionless.}$$

From Eq. 3-6,

$$\gamma_a(\lambda) = 10^{[-0.136 + 1.16 \log(3.912 \cdot V)]} \text{, km}^{-1}.$$

For visibility V of 5 km,

$$\gamma_a(1.06\mu m) = 10^{[-0.136 + 1.16 \log(3.912 \cdot 5)]}$$
$$= 0.55 \text{ km}^{-1}.$$

Thus in the absence of dust and smoke, $T_s(1.06) = 1$ and $T_d(1.06) = 1$, and since $T_m(1.06) = 1$, transmittance $T(1.06 \mu m)$ from the LRF to the target is

$$T(1.06 \mu m) = (1.0)e^{-(0.55)R}(1.0)(1.0) = e^{-0.55R}.$$

2. Determine target signal at the sensor.
From Eq. 5-7, the received signal power P_s is

$$P_s = (P_t T_t)[T(\lambda)](M \rho_t \cos\theta)[T(\lambda)](T_o A_r / \pi R^2) \quad \text{, W.}$$

The receiver area A_r, calculated from the receiver optics diameter and converted from m² to km² is

$$A_r = \frac{\pi(0.07)^2}{4} \times 10^{-6} \quad \text{, km}^2$$
$$= 3.8 \times 10^{-9} \text{ km}^2.$$

From Eq. 5-8, the coverage factor M is

$$M = \frac{A_t}{\pi R^2 \delta} \quad \text{, dimensionless}$$

where the target area A_t is determined from the target dimensions:

$$M = \frac{(2.4)(5.4)}{\pi R^2 (0.25)^2} = \frac{41.6}{R^2}$$

The value of M cannot exceed 1.0 (i.e., the target cannot reflect more energy than is incident on it). Therefore, M has two values that depend on range to the target:

(1) R equal to or less than 6.45 km
$$M = 1$$
(2) R greater than 6.45 km
$$M = \frac{41.6}{R^2}$$

With these expressions, the target signal P_s at the receiver is

$$P_s = (5 \times 10^6)(0.6)(e^{-0.55R})$$
$$(M)(0.3)(1.0)(e^{-0.55R})(3.9 \times 10^{-9}/\pi R^2) \quad \text{, W}$$

$$= \frac{1.1 M e^{-2(0.55)R}}{R^2} \times 10^{-3} \quad \text{, W.}$$

(1) For R equal to or less than 6.45 km, $M = 1$ and

$$P_s = \frac{1.1 \times 10^{-3} e^{-1.1R}}{R^2} \quad \text{, W.}$$

(2) For R greater than 6.45 km, $M = 41.6 \ R^2$ and

$$P_s = \frac{4.65 \times 10^{-2} e^{-1.1R}}{R^4} \quad \text{, W.}$$

3. Determine sensor *SNR* requirement. Fig. 5-10 gives detection probability P_d vs *SNR* as a function of the product of τ and *FAR*. For this LRF,

$$\tau FAR = (8 \times 10^{-8} s)(150 \, s^{-1}) = 1.2 \times 10^{-5}.$$

This value falls between the curves for $\tau FAR = 10^{-4}$ and 10^{-5}. From an eyeball estimate of the intersection of these curves with the 90% detection probability curve, the required *SNR* is 6.25.

4. Determine sensor performance.
From Eq. 5-9, the LRF signal-to-noise ratio *SNR* is

$$SNR = \frac{P_s}{NEP}, \text{ dimensionless.}$$

Therefore, substituting for P_s and *NEP* gives
(1) For R equal to or less than 6.45 km

$$SNR = \frac{1.1 \times 10^{-3} e^{-1.1R}}{6.5 \times 10^{-9} R^2}$$

$$= \frac{1.7 \times 10^5 e^{-1.1R}}{R^2}$$

(2). For R greater than 6.45 km

$$SNR = \frac{4.65 \times 10^{-2}e^{-1.1R}}{6.5 \times 10^{-9}R^4}$$

$$= \frac{7.2 \times 10^6 e^{-1.1R}}{R^4}$$

To determine the 90% detection range, solve this expression for R when $SNR = 6.25$. The solution requires trial iterations of R, but it yields a range $R = 6.0$ km.

5-4.3.3 Determine SNR and 90% Detection Range in Atmosphere With WP Smoke

1. Determine atmospheric transmittance. From Eq. 3-1, transmittance $T(\lambda)$ is,

$$T(\lambda) = T_m(\lambda)T_a(\lambda)T_s(\lambda)T_d(\lambda), \text{dimensionless.}$$

In the absence of dust, $T_d(\lambda) = 1$. From par. 5-4.3.2,

$$T_m(1.06\mu m) = 1.0$$
$$T_m(1.06\mu m) = e^{-0.55 R}$$

From Eq. 4-2,

$$T_s(\lambda) = e^{-\alpha_s(\lambda)CL}, \text{dimensionless.}$$

From Table 4-3, the value of $\alpha_s(\lambda)$ at 1.06 µm for WP is 1.66 m² g at 70% RH. Therefore, for WP smoke with a CL of 1 g m² of WP,

$$T_s(1.06\mu m) = e^{(-1.66 \times 1.0)}$$
$$= e^{(-1.66)}.$$

Substituting in Eq. 3-1, the transmittance between the sensor and the target is

$$T(1.06\mu m) = (1.0 e^{-0.55R}e^{-1.66})(1.0)$$
$$= e^{-0.55R}e^{-1.66}$$
$$= 0.19 e^{-0.55R}$$

2. Determine target signal at the sensor. The signal P_s at the sensor is the same as calculated in par. 5-4.3.2, except the value of $T(1.06)$ has changed because of the addition of WP smoke. Substituting in Eq. 5-7 gives

(1) For R equal to or less than 6.45 km, $M = 1$ and

$$P_s = \frac{4.03 \times 10^{-5}e^{-1.1R}}{R^2}, \text{W.}$$

(2) For R greater than 6.45 km, M depends on range and

$$P_s = \frac{1.68 \times 10^{-3}e^{-1.1R}}{R^4}, \text{W.}$$

3. Determine sensor SNR requirement. The required SNR is 6.25, as calculated in par. 5-4.4.2.

4. Determine sensor performance. From Eq. 5-9,

$$SNR = \frac{P_s}{NEP}$$

It is evident from the calculation in par. 5-4.3.2 that performance range in this atmosphere will be less than 6.45 km. Therefore, only the expression for SNR where R is less than 6.45 km is required:

$$SNR = \frac{4.03 \times 10^{-5}e^{-1.1R}}{6.5 \times 10^{-9}R^2}$$

$$= \frac{6.20 \times 10^3 e^{-1.1R}}{R^2}$$

To determine performance range for 90% detection probability, set $SNR = 6.25$ and solve, by iteration, for R. This yields a 90% detection probability at range $R = 3.8$ km.

5-4.3.4 Summary: Smoke Effects on Nd: YAG LRF Performance

Smokes significantly degrade the performance of near IR laser systems such as the 1.06µm Nd:YAG LRF in this example. The introduction of 1 g m² of WP smoke into the atmosphere between the LRF and the target reduced LRF performance range from 6.0 to 3.8 km. The effects of FO and HC smokes are more severe, because these smokes are much better attenuators of visible and near IR radiation than WP is.

5-4.4 LASER OPERATION IN TURBULENCE

PROBLEM: Calculate the effect of naturally occurring turbulence on laser system operation. This problem illustrates the increase in beam diameter and reduction in on-axis irradiance as a laser beam is propagated through a turbulent atmosphere.

5-4.4.1 Conditions

1. System:
   a. Nd:YAG laser, 1.06µm
   b. Specification:
      (1) Beam divergence   diffraction limited

(2) Aperture diameter D 0.07m

(3) Pulse with τ 8 ns

2. Atmosphere:

   a. Natural atmosphere specified in par. 5-4.3.1

   b. Mild turbulence; index of refraction structure constant $C_n^2 = 10^{-14} \text{m}^{-2/3}$

3. Task. Laser performance in turbulent atmosphere.

5-4.4.2 Calculate On-Axis Irradiance and Beam Size at Range R in Turbulent Atmosphere

1. Determine atmospheric transmittance:

Atmospheric transmittance is not affected by turbulence. From par. 5-4.3.2, for the specified atmosphere,

$$T(\lambda) = e^{-0.55 R}, \quad \text{dimensionless.}$$

2. Determine signal at target:

The total power at range R is unchanged by the turbulent atmosphere. However, the spatial distribution of the energy is changed. In the turbulent atmosphere the peak irradiance on the target is reduced by the beam spread. In addition, beam wander and intensity fluctuations (scintillation) will change the magnitude of the irradiance at any point in the target plane from pulse to pulse.

The Strehl ratio is the ratio of the average on-axis irradiance with turbulence to average on-axis irradiance without turbulence. For single pulses, the short-term Strehl ratio S_s is used (Eq. 3-22 or 3-23). The choice between Eq. 3-22 and Eq. 3-23 depends on the ratio of the effective laser aperture diameters D to the coherence length r_o. From Eq. 3-24.

$$r_o = 0.3325(10^{-5}\lambda)^{6/5}(10^6 C_n^2 R)^{-3/5}, \text{ m.}$$

In the example,

$$r_o = 0.3325(1.06 \times 10^{-5})^{6/5}(6 \times 10^{-14} \times 10^6 R)^{-3/5}$$
$$= 3.03 \times 10^{-2} R^{-3/5}, \text{m.}$$

For the specified laser aperture of 0.07 m,

$$\frac{D}{r_o} = \frac{0.07}{0.0303} R^{3/5} = 2.31 R^{3/5}.$$

Therefore, $D/r_o > 3$ if $R \geq 1.5$ km, and so Eq. 3-23 is used to find the short-term Strehl ratio S_{s2} at ranges of 1.6 km or longer.

$$S_{s2} =$$
$$[1 + (D/r_o)^2 - 1.18(D/r_o)^{5/3}]^{-1}, \text{dimensionless.}$$

Substituting for D/r_o yields

$$S_{s2} = [1 + (2.31 R^{3/5})^2 - 1.18(2.31R^{3/5})^{5/3}]^{-1}$$
$$= (1 + 5.34R^{6/5} - 4.76 R)^{-1}.$$

At 6 km, $S_{s2} = 0.055$, which corresponds to a reduction in average (short-term), on-axis irradiance to 5.5% of the original value. The beam radius in the presence of turbulence is increased by a factor of $S_{s2}^{-1/2}$ over the diffraction-limited beam radius (see par. 3-2.6). At 6 km $S_{s2}^{-1/2}$ is about 4.3 for this atmosphere, so the beam diameter increases by a factor of 4.3. The beam area at 6 km is about 18 times larger in the turbulent atmosphere than it is in the diffraction-limited beam area.

5-4.4.3 Summary: Effects of Turbulence on LRF

Turbulence effects can limit LRF performance. The effects are more severe at 1.06 μm than they are at 10.6 μm because of the dependence of the coherence length r_o on λ as shown in Eq. 3-24. For the Nd:YAG LRF in this problem, mild turbulence increased the beam area by a factor of 18 at 6 km and reduced on-axis irradiance to less than 6% of the original (no turbulence) value.

5-4.5 ARTILLERY EXAMPLE, THERMAL SENSOR AND WIRE-GUIDED MISSILE

PROBLEM. Calculate the effect of an artillery barrage on transmittance for a wire-guided missile with xenon beacon and 8-12 μm thermal imager. This problem explains the use of the artillery example while illustrating the dependence of system performance on both spectral band and line of sight.

5-4.5.1 Conditions

1. System:

   a. Thermal imager, 8-12 μm, for target acquisition and track

   b. Xenon beacon on missile tracked by 3-5 μm missile tracker

2. Atmosphere:

   a. Winter afternoon, 10% RH, 10°C, visibility $V = 5$ km.

   b. Artillery barrage, represented by Figs. 4-10 and 4-11

3. Location:

   a. Sensor: (1, -0.8 km) coordinates, Figs. 4-10 and 4-11

   b. Target: (6, -0.7 km) coordinates, Figs. 4-10 and 4-11

   c. Missile: moves from target acquisition sensor (launcher) to target

4. Task:

   a. Thermal imager: detect target signal (8-12 μm)

   b. Missile tracker: detect missile signal (3-5 μm).

5-4.5.2 Determine Atmospheric Transmittance

1. Determine transmittance for thermal imager:

For the thermal imager, 8-12 μm transmittance is calculated along a 5-km path from (1, -0.8) to (6, -0.8) coordinates. From Eq. 3-1

$$T(\lambda) = T_m(\lambda)T_a(\lambda)T_s(\lambda)T_d(\lambda), \text{ dimensionless.}$$

From Table 3-2, for a 5-km path at 10°C and 40% RH, the 8-12 μm molecular transmittance $T_m(\lambda)$ is

$$T_m(8\text{-}12 \ \mu\text{m}) = 0.77.$$

From Eq. 3-4,

$$T_d(\lambda) = e^{-\gamma_d(\lambda)R} \text{, dimensionless.}$$

From Table 3-4, if visibility V = 5 km, $\gamma_d(8\text{-}12)$ is 0.07. At a range of 5 km,

$$T_d(8\text{-}12 \ \mu\text{m}) = e^{-(0.07)(5)} = 0.70.$$

Transmittance through the natural atmosphere, excluding obscurants, is thus

$$T(8\text{-}12 \ \mu\text{m}) = (0.70)(0.77) = 0.54.$$

From Eq. 4-3

$$T_d(\lambda) = e^{-\alpha_d(\lambda)CL} \text{, dimensionless.}$$

From Fig. 4-10, the dust concentration path length product CL integrated along the LOS from (1, -0.8 km) to (6, -0.8 km) is 17.0 g·m⁻². From Table 4-6, $\alpha_d(8\text{-}12 \ \mu\text{m})$ is 0.26 m²·g⁻¹. Then,

$$T_d(8\text{-}12 \ \mu\text{m}) = e^{-(0.26)(17.0)} = 0.012.$$

In the absence of smoke,

$$T_s(\lambda) = 1.$$

The 8-12 μm transmittance through the 5-km path is, therefore,

$$T(8\text{-}12 \ \mu\text{m}) = (0.77)(0.70)(1.0)(0.012)$$
$$= 0.0065.$$

2. Determine transmittance for the missile tracker

The missile tracker on the launcher has a 3-5μm detector, which tracks the missile plume or a xenon beacon on the missile; this depends on the system design. Transmittance is calculated over the path from the missile to the launcher. The path length will

increase from 0 to 5 km as the missile is launched and approaches the target. In addition, the amount of dust in the path will change, as shown in Fig. 4-11. For illustration, transmittance is calculated here for the full 5-km path. Again, from Eq. 3-1,

$$T(\lambda) = T_m(\lambda)T_a(\lambda)T_s(\lambda)T_d(\lambda), \text{ dimensionless.}$$

From Table 3-1, for the specified atmosphere (visibility V = 5 km, 10°C, 40% RH), 3-5 μm molecular transmittance over a 5-km path is

$$T_m(3\text{-}5 \ \mu\text{m}) = 0.46.$$

From Eq. 3-4

$$T_d(\lambda) = e^{-\gamma_d(\lambda)R}$$

where, from Table 3-4, $\gamma_d(3\text{-}5)$ = 0.11 km⁻¹ if visibility V = 5 km. Thus

$$T_d(3\text{-}5 \ \mu\text{m}) = e^{-(0.11)(5)} = 0.58.$$

Transmittance through the natural atmosphere, excluding obscurants, is thus

$$T(3\text{-}5 \ \mu\text{m}) = (0.46)(0.58) = 0.27.$$

Since there is no smoke,

$$T_s(\lambda) = 1.0.$$

The transmittance $T_d(\lambda)$ through dust is again calculated using Eq. 4-3:

$$T_d(\lambda) = e^{-\alpha_d(\lambda)CL}$$

where the CL product of dust was determined to be 17.0 g·m⁻². From Table 4-6, $\alpha_d(3\text{-}5 \ \mu\text{m})$ = 0.27 m²·g⁻¹ for munition-generated dust. Thus,

$$T_d(3\text{-}5 \ \mu\text{m}) = e^{-(0.27)(17.0)} = 0.010.$$

Substituting in Eq. 3-1 gives

$$T(3\text{-}5 \ \mu\text{m}) = (0.46)e^{-(0.11)(5)}(1.0)e^{-(0.27)(17.0)}$$
$$= 0.0027.$$

For paths shorter than the full 5-km path length, transmittance will be higher.

5-4.5.3 Summary: Artillery Example, Thermal Sensor and Wire-Guided Missile

If a weapon system has sensors operating in two different spectral bands, the atmosphere will almost

always affect the two sensors differently. Differences in location of the sensors relative to the target will affect their relative performance. In this example, natural atmospheric transmittance over the 5-km path differs by a factor of 2 for the 3-5 μm missile detector and the 8-12 μm thermal imager: 0.27 in the 3-5 μm band and 0.54 in the 8-12 μm band. Transmittance through the dust is about 0.01 in both bands. However, as the missile moves from the sensor to the target, transmittance over the line of sight (LOS) from the beacon to the thermal imager goes from 1.0 (at the imager) to about 0.003. A temporary blocking of the thermal imager LOS to the target could result in erroneous guidance to the missile and thus a miss even if there is very high transmittance on the missile-to-beacon LOS. Note that in the 3-5 μm band, the extinction coefficients for HE dust (Table 4-6), fog oil, diesel oil, and phosphorus (Table 4-2) are all between 0.25 and 0.29 m^2/g, whereas for HC it is a bit lower, 0.19 m^2/g. These obscurants will have very similar effects on 3-5 μm transmittance for equal CL products of obscurant. In the 8-12 μm band HE dust and WP have extinction coefficients of 0.26 and 0.38 m^2/g and will have similar effects on transmittance. The 8-12 μm extinction coefficients for other inventory smokes are much lower (Table 4-2); therefore, these obscurants—FO, HC, WP, and anthracene—will generally have negligible effects on 8-12 μm sensor performance.

5-4.6 ARTILLERY EXAMPLE, LASER DESIGNATOR

PROBLEM: Calculate transmittance for laser designation in artillery-generated dust. Two wavelengths must be considered in laser designation; the human eye for target location and the laser wavelength for designation and tracking. In addition, the designator and tracker are not collocated so both path length and obscuration may be different for the two systems.

5-4.6.1 Conditions

1. Laser designator and weapon system (see Fig. 2-5):
    a. Human eye, 0.4-0.7 μm
    b. Laser designator, 1.06μm (active)
    c. Laser spot tracker, 1.06 μm (passive)
2. Atmosphere:
    a. Central Europe, spring morning
    b. Artillery engagement, represented by Figs. 4-12 and 4-13
3. Locations:
    a. Designator system (eye and designator laser): (4, 1 km) coordinates
    b. Laser spot tracker (on weapon): (3, 0 km) coordinates
    c. Target: (5, 0 km) coordinates

4. Task:
    a. Designator system: acquire target visually and designate with 1.06 μm laser
    b. Laser spot tracker: track 1.06μm laser signal reflected from target.

5-4.6.2 Determine Atmospheric Transmittance for Visual Target Acquisition

From Fig. 4-13, there is a clear LOS from the designator to the target. The range R is 1.4 km. Average weather for a spring morning in the European highlands is found in Table 3-12. Visibility V has a mean value of 9.6 km for the 3 A.M. to 9 A.M. time period, and absolute humidity ρ averages 5.8 g/m^3.

Eq. 3-1 gives transmittance $T(\lambda)$:

$$T(\lambda) = T_m(\lambda)T_a(\lambda)T_s(\lambda)T_d(\lambda) \text{, dimensionless.}$$

In the visual and near IR spectral bands, $T_m(\lambda)$ is found using Eq. 3-3:

$$T_m(\lambda) = e^{-\gamma_m(\lambda)R} \text{, dimensionless.}$$

where, from par. 3-2.1.1, $\gamma_m(0.4-0.7) = 0.02\,\text{km}^{-1}$. Thus

$$T_m(0.4\text{-}0.7 \ \mu m) = e^{-(0.02)(1.4)} = 0.97.$$

Similarly, $T_a(\lambda)$ is found using Eq. 3-4:

$$T_a(\lambda) = e^{-\gamma_a(\lambda)R}$$

where $\gamma_a(0.4-0.7)$ is given by Eq. 3-5:

$$\gamma_a(0.4\text{-}0.7) = 3.912/V, \ \text{km}^{-1}.$$

Thus

$$T_a(0.4\text{-}0.7 \ \mu m) = e^{-(3.912/V)R}$$

$$= e^{-(3.912/9.6)(1.4)} = 0.57.$$

Since there are no obscurants such as smokes or dust in the LOS

$$T_s(\lambda) = 1.0 \text{ and } T_d(\lambda) = 1.0.$$

Substituting in Eq 3-1 gives

$$T(0.4\text{-}0.7 \ \mu m) =$$
$$e^{-(0.02)(1.4)}e^{-(3.912/9.6)(1.4)}(1.0)(1.0)$$
$$= 0.55.$$

5-4.6.3 Determine Atmospheric Transmittance for Laser Designator

The 1.06-μm designator radiation propagates from the designator to the target and is reflected off the target. The path from the designator to the target is the same (unobstructed) LOS for which visual transmittance was calculated in par. 5-4.6.2. The 2-km path from the target to the spot tracker contains munition-generated dust. Transmittance is calculated using Eq. 3-1 (see par. 5-4.6.2). $T_m(\lambda)$ and $T_a(\lambda)$ are calculated for the entire path length (2 km + 1.4 km); $T_d(\lambda)$ is calculated only over the obscured portion. From par. 3-2.1.2

$$T_m(1.06) = 1.$$

The near IR aerosol extinction is calculated using Eq. 3-4, with $\gamma_a(\lambda)$ given by Eq. 3-6 when visibility V is greater than 0.6 km:

$$\gamma_a(1.06) = 10^{-0.136 + 1.16 \log (3.912/V)} \text{ km}^{-1}$$
$$= 0.26 \text{ km}^{-1}.$$

$$T_a(1.06) = e^{-\gamma_a(\lambda)H}$$
$$= e^{-(0.26)(1.4 + 2)}$$
$$= 0.41.$$

Transmittance $T_d(\lambda)$ through the dust is determined from Eq. 4-3

$$T_d(\lambda) = e^{-\alpha_d(\lambda)CL}.$$

From Table 4-6,

$$\alpha_d(1.06) = 0.26.$$

The concentration path length product CL of dust in the path is scaled from the dust concentration plot from Fig. 4-13. On the path between the target and the laser tracker, (5, 0 km) to (3, 0 km), approximately 600 m is obscured by dust. There is about 250 m of dust with a concentration of 0.01 g/m³ and 350 m with a concentration of 0.05 g/m³. This gives an integrated dust concentration path length product:

$$CL = (0.01)(250) + (0.05)(350)$$
$$= 20 \text{ g/m}^2.$$

Thus

$$T_d(1.06 \ \mu\text{m}) = e^{-(0.26 \times 20)} = 0.0055.$$

Since $T_s(\lambda) = 1.0$ substituting in Eq. 3-1 gives

$$T(1.06) = (1.0)e^{-(0.26)(1.4 + 2)}(1.0)e^{-(0.26)(2.0)}$$
$$= 0.0027.$$

5-4.6.4 Summary: Artillery Example, Laser Designator

In this problem, weapon system effectiveness depends on performance in two spectral bands (eye and laser) over two atmospheric paths. The forward observer has an unobscured LOS to the target. The designator laser energy propagates along the unobstructed LOS to the target and then is reflected through munition-generated dust toward the tracker. The target can be located and designated by the observer, but the laser spot tracker may not be able to acquire the target because of the dust. Obscuration along the designator—target LOS would affect target location and designation.

Note, however, that in the visible and near IR spectral bands, dust (Table 4-6) has an extinction coefficient of about 0.3 m²/g; it is much less effective as an obscurant (given similar concentrations) than inventory smokes, which have extinction coefficients of 3.66 to 5.85 m²/g in the visible band and 1.77 to 4.59 at near IR wavelengths (see Table 4-2).

5-4.7 ARTILLERY EXAMPLE, MILLIMETER WAVE SYSTEM

PROBLEM: Calculate the effect of dust on downward-looking, passive mmw terminal guidance. This problem illustrates the negligible effect of dust on mmw radiation.

5-4.7.1 Conditions

1. System. Munition with 94 GHz passive terminal guidance
    2. Atmosphere:
        a. European highlands, winter afternoon
        b. Artillery-generated dust, represented by Fig. 4-10
    3. Sensor location:
        a. (5, -0.1 km) coordinates, Fig. 4-10
        b. Sensor altitude, 50 m
    4. Task. Downward-looking terminal target acquisition and guidance.

5-4.7.2 Determine Atmospheric Transmittance

1. Transmittance $T(\lambda)$ is given by Eq. 3-1

$$T(\lambda) = T_m(\lambda)T_a(\lambda)T_s(\lambda)T_d(\lambda).$$

At 94 GHz, from Eq. 3-3

$$T_m(\lambda) = e^{-\gamma_m(\lambda)R}$$

where γ_m(94 GHz) is dependent on absolute humidity ρ as shown in Table 3-3. Weather data for the European highlands are given in Table 3-12. In the winter, average absolute humidity is about 4.7 g m³. At this humidity, Table 3-3 gives γ_m(94 GHz) as approximately 0.063 km⁻¹. Thus

$$T_m(94 \text{ GHz}) = e^{-(0.063)(0.050)} = 1.0.$$

From par. 3-2.2.4, mmw radiation is not attenuated by haze. Therefore,

$$T_d(94 \text{ GHz}) = 1.0.$$

The mmw sensor was placed at a position where the downward-looking optical depth OD of dust varies from greater than 3.0 to about 1.0. The dust concentration must be determined in order to calculate 94 GHz transmittance. From Eq. 4-6,

$$OD = \ln T(0.4\text{-}0.7 \ \mu m)$$
$$= \alpha_d(0.4\text{-}0.7 \ \mu m)CL.$$

Table 4-6 gives α_d(0.4-0.7 μm) as 0.32 m² g. Therefore, these OD values correspond to dust CL products of about 3 to 10 g m². Millimeter wave transmittance $T_d(\lambda)$ through dust is calculated from Eq. 4-3, with α_d(94 GHz) equal to 0.001 g m² (from Table 4-6). For a CL of 10 g m² of dust

$$T_d(\lambda) = e^{-\alpha_d(\lambda)}$$
$$= e^{-(0.001 \times 10)}$$
$$= 0.99.$$

If the CL were 100 g m², the dust transmittance term would be

$$T_d(94 \text{ GHz}) = 0.90.$$

Clearly, a very high concentration of dust is required to defeat the 94 GHz sensor in clear weather (if the system design is viable in the dust-free environment).

5-4.7.3 Summary: Artillery Example, Millimeter Wave System

Munition-generated dust is not an effective obscurant for mmw systems. A CL of 100 g m² reduces 94 GHz transmittance to 0.90. Inspection of Table 4-2 shows that inventory smokes are equally ineffective against mmw systems.

5-4.8 OBSCURING SMOKE EXAMPLE, LASER GUIDANCE

PROBLEM: Determine effect of smoke on missile system with CO_2 laser guidance and TV or thermal imager target acquisition. This problem illustrates the effect of smoke on sensors that operate in different spectral bands but may be part of the same weapon system. Natural atmospheric transmittance effects have been covered in the previous examples; they are not treated in this example.

5-4.8.1 Conditions

1. System:
   a. Thermal imager, 8-12 μm, for target location and tracking
   b. Missile plume tracker, 3-5 μm, for initial missile tracking
   c. CO_2 laser, 10.6 μm, for missile guidance
   d. TV, 0.7-1.1 μm, as alternate for target location and tracking

2. Atmosphere:
   a. Natural atmosphere ignored for this illustration; $T_m(\lambda) = T_d(\lambda) = 1$.
   b. Phosphorus smoke from WP mun ... ns illustrated in Fig. 4-21
   c. Relative humidity $RH = 50\%$

3. Location (see Fig. 4-21):
   a. Target at (400, 75 m) coordinates
   b. Sensor at (130, 75 m) coordinates (smoke has just blown across sensor).

5-4.8.2 Determine Atmospheric Transmittance

Transmittance $T_s(\lambda)$ through smoke is given by Eq. 4-2:

$$T_s(\lambda) = e^{-\alpha_s(\lambda)CL}.$$

Values for $\alpha_s(\lambda)$ at 50% RH are given in Table 4-2. The CL of phosphorus in the path must be determined from Fig. 4-21.

To estimate the CL along any path through the obscurant, note the concentration contours. Using a ruler, measure the path length l, for each concentration C. The total CL is the sum of the concentration path length product for each of the dust contours in the LOS. For this example, as noted on Fig. 4-21, the total CL along the target to sensor LOS is

$$CL = (50 \text{ m})(0.01 \text{ g m}^{-1}) +$$
$$(190 \text{ m})(0.03 \text{ g m}^{-1}) + (30 \text{ m})(0.01 \text{ g m}^{-1})$$
$$= 6.5 \text{ g m}^2.$$

From Table 4-2

$$\alpha_s(0.7\text{-}1.1) = 1.77 \text{ m}^2/\text{g}$$
$$\alpha_s(3\text{-}5) = 0.29 \text{ m}^2/\text{g}$$
$$\alpha_s(8\text{-}12) = 0.38 \text{ m}^2/\text{g}$$
$$\alpha_s(10.6) = 0.38 \text{ m}^2/\text{g}.$$

Therefore, for the 8-12-μm thermal sight

$$T_s(8\text{-}12 \ \mu\text{m}) = e^{-(0.38)(6.5)}$$
$$= 0.085.$$

For the 3-5 μm sensor

$$T_s(3\text{-}5 \ \mu\text{m}) = e^{-(0.29)(6.5)}$$
$$= 0.15.$$

For the 10.6 μm laser

$$T_s(10.6 \ \mu\text{m}) = e^{-(0.38)(6.5)}$$
$$= 0.085.$$

For the (alternate) TV sight:

$$T_s(0.7\text{-}1.1) = e^{-(1.77)(6.5)}$$
$$= 1.0 \times 10^{-5}.$$

5-4.8.3 Summary: Obscuring Smoke Example, Laser Guidance

This example calculated transmittance through WP smoke for four different spectral bands that might form part of a weapon system using a CO_2 laser for missile guidance. Transmittance through the same amount of WP smoke (6.5 g/m²) varied from 1.0×10^{-5} for the TV sight to 0.085 for the CO_2 laser to 0.15 for the 3-5 μm sensor. The clear weak link in this example is the TV sensor if operation in WP smoke is required. The example illustrates that in a multispectral system, one critical sensor may not be able to see through the obscured atmosphere, even though the other systems have adequate signal.

5-4.9 VEHICULAR DUST EXAMPLE, LASER GUIDANCE

PROBLEM: Effect of vehicular dust on missile system with CO_2 laser guidance and TV or thermal imager target acquisition. System is the same as that in par. 5-4.8. This problem illustrates the effect of vehicular dust on sensors in different spectral bands by using the vehicular dust combat example from par. 4-7.3. Natural atmospheric transmittance is not calculated.

5-4.9.1 Conditions

1. System (same as par. 5-4.8.1):
   a. Thermal imager, 8-12 μm, for target location and tracking
   b. Missile plume tracker, 3-5 μm, for initial missile tracking
   c. CO_2 laser, 10.6 μm, for missile guidance
   d. TV, 0.7-1.1 μm, as alternate for target location and tracking
2. Atmosphere:
   a. Natural atmosphere ignored
   b. Vehicular dust from motorized rifle battalion in attack formation, illustrated in Fig. 4-24
3. Location (see Fig. 4-24):
   a. Target at $(+100, 325 \text{ m})$ coordinates
   b. Sensor at $(-500, 325 \text{ m})$ coordinates.

5-4.9.2 Determine Atmospheric Transmittance

Transmittance $T_d(\lambda)$ through vehicular dust is given by Eq. 4-3:

$$T_d(\lambda) = e^{-\alpha_d(\lambda)CL}.$$

Values for $\alpha_d(\lambda)$ for vehicular dust are given in Table 4-8. The CL of vehicular dust in the path is determined from Fig. 4-24. For the LOS selected in this example, the CL is indicated on Fig. 4-24 as 2.8 g·m². Transmittance will be calculated over the entire sensor to target LOS. From Table 4-8

$$\alpha_d(0.7\text{-}1.1) = 0.30 \text{ m}^2/\text{g}$$
$$\alpha_d(3\text{-}5) = 0.27 \text{ m}^2/\text{g}$$
$$\alpha_d(8\text{-}12) = 0.25 \text{ m}^2/\text{g}$$
$$\alpha_d(10.6) = 0.25 \text{ m}^2/\text{g}.$$

Therefore, for the 8-12 μm thermal sight

$$T_d(8\text{-}12) = e^{-(0.25)(2.8)} = 0.50.$$

For the 3-5 μm sensor

$$T_d(3\text{-}5) = e^{-(0.27)(2.8)} = 0.47.$$

For the 10.6 μm sensor

$$T_d(10.6) = e^{-(0.25)(2.8)} = 0.50.$$

For the alternate (0.7-1.2) TV sight

$$T_d(0.7\text{-}1.1) = e^{-(0.30)(2.8)} = 0.43.$$

5-4.9.3 Summary: Vehicular Dust Example, Laser Guidance

The extinction coefficient for vehicular dust is relatively flat in the visible and thermal bands; it varies from 0.32 m²/g in the visible band to 0.25 m²/g in the 8-12 μm band. For the amount of dust in this example, the effect will be small to moderate degradation in sensor performance.

5-4.10 PRECIPITATION EXAMPLE, LASER GUIDANCE

PROBLEM: Effect of rain on missile system with CO_2 laser guidance and TV or thermal imager target acquisition. System is the same as that in pars. 5-4.8 and 5-4.9. This problem illustrates the effect of rain on transmittance for different spectral bands.

5-4.10.1 Conditions

1. System (same as par. 5-4.8.1 and 5-4.8.2):
   a. Thermal imager, 8-12 μm for target location and tracking
   b. Missile plume tracker, 3-5 μm, for initial missile tracking
   c. CO_2 laser, 10.6 μm, for missile guidance
   d. TV, 0.7-1.1 μm, as alternate for target location and tracking
2. Atmosphere:
   a. Winter afternoon, light rain with rain rate $r = 2.5$ mm/h
   b. Relative humidity $RH = 90\%$, temperature $T = 10°C$.
3. Task. Calculate atmospheric transmittance over a 1-km path.

5-4.10.2 Determine Atmospheric Transmittance

1. Transmittance $T(\lambda)$ is given by Eq. 3-1

$$T(\lambda) = T_m(\lambda)T_a(\lambda)T_s(\lambda)T_d(\lambda)$$

where in the absence of dust and smoke $T_d(\lambda) = T_s(\lambda) = 1.0$. If it is raining or snowing, the aerosol extinction term $T_a(\lambda)$ is replaced by the precipitation transmittance term $T_p(\lambda)$. Therefore, in this case

$$T(\lambda) = T_m(\lambda)T_p(\lambda).$$

2. Determine the molecular transmittance term; use the conditions specified in par. 5-4.10.1.
   a. From Table 3-1, $T_m(3-5) = 0.59$.
   b. From Table 3-2, $T_m(8-12) = 0.83$.
   c. From par. 3-2.1, Eq. 3-3, for visible and near IR sensors

$$T_m(\lambda) = e^{-\gamma_m(\lambda)R}$$

From par. 3-2.1.2, $\gamma_m(0.7-1.1) = 0.03$ km⁻¹. Therefore,

$$T_m(0.7-1.1) = e^{-(0.03)(1.0)} = 0.97.$$

d. Values of $\gamma_m(\lambda)$ for the CO_2 laser line are given in Table 3-3, as a function of absolute humidity ρ. Absolute humidity ρ is calculated from relative humidity and temperature using information in Appendix B, Eq. B-1. Note that in this equation temperature is in Kelvins (Celsius temperature + 273) and RH is decimal.

$$\rho = \frac{1285\ RH}{T} \exp\left[5412\left(\frac{1}{273} - \frac{1}{T}\right)\right], \text{g/m}^3$$
$$= \frac{1285\ (0.4)}{283} \exp\left[5412\left(\frac{1}{273} - \frac{1}{283}\right)\right]$$
$$= 3.66 \text{ g/m}^3.$$

From Table 3-3, by interpolation, $\gamma_m(10.6\ \mu m) = 0.097$ km⁻¹. Then, using Eq. 3-3

$$T_m(10.6) = e^{-(0.097)(1.0)} = 0.91.$$

3. Determine the precipitation transmittance term $T_p(\lambda)$. From Eq. 3-12, for visible, near IR, and thermal systems

$$T_p(\lambda) = e^{-\gamma_p(\lambda)R}$$

where for widespread rain, from Eq. 3-14,

$$\gamma_{pw}(\text{vis, thermal}) = 0.36r^{0.61}, \text{ km}^{-1}$$
$$= 0.36\ (2.5)^{0.61}$$
$$= 0.64 \text{ km}^{-1}.$$

Therefore,

$$T_p(\lambda) = e^{-(0.64)(1.0)}$$
$$= 0.53.$$

4. Determine atmospheric transmittance by using values calculated for $T_m(\lambda)$ and $T_p(\lambda)$.
For the 3-5 μm sensor

$$T(3-5) = T_m(3-5\mu m)T_p(3-5\mu m)$$
$$= (0.59)e^{-(0.64)(1.0)}$$
$$= 0.31.$$

For the 8-12 μm sensor

$$T(8\text{-}12) = T_m(8\text{-}12\mu m)T_p(8\text{-}12\mu m)$$
$$= (0.83)e^{-(0.64)(1.0)}$$
$$= 0.44.$$

For the CO_2 laser

$$T(10.6) = T_m(10.6\mu m)T_p(10.6\mu m)$$
$$= e^{-(0.097)(1.0)}e^{-(0.64)(1.0)}$$
$$= 0.48.$$

For the TV sensor

$$T(0.7\text{-}1.1) = T_m(0.7\text{-}1.1\mu m)T_p(\text{near IR})$$
$$= e^{-(0.03)(1.0)}e^{-(0.64)(1.0)}$$
$$= 0.51.$$

5-4.10.3 Summary: Precipitation Example

This problem illustrates the calculation of transmittance through precipitation for near IR and thermal sensors. The transmittance through rain of visual, near IR, and thermal bands is calculated using the same expression for $T_p(\lambda)$, from Eq. 3-13 to Eq. 3-15. The determinant of overall transmittance in rain is therefore the molecular transmittance term $T_a(\lambda)$, so, in cold weather (low atmospheric water vapor content), thermal and visual transmittance through rain will not be significantly different. In warm weather (high atmospheric water vapor content), visual transmittance will be better. To calculate the effect of rain on sensor performance, one must also determine the effect of rain on target signature and, for day sights, I^2 sensors, and TV, or ambient light level.

REFERENCES

1. L. P. Obert and C. J. Nash, *The Visionics Handbook*, AIAA 21st Aerospace Sciences Meeting, Reno, NV, 1983.

2. J. A. Ratches, et al., *Night Vision Laboratory Static Performance Model for Thermal Viewing Systems*, ECOM-7043, US Army Night Vision and Electro-Optics Laboratory, Fort Belvoir, VA, 1975.

3. *RCA Electro-Optics Handbook*, RCA Corporation, Lancaster, PA, 1974.

4. W. Wolfe and G. Zissus, Eds., *The Infrared Handbook*, Environmental Research Institute of Michigan, Ann Arbor, MI, 1978.

BIBLIOGRAPHY

The references listed below are general texts, selected for breadth of coverage and clarity. For more detailed references on natural obscuration and battlefield-induced contaminants, refer also the the bibliographies in Chapters 3 and 4, respectively.

K. A. Brandt, et al., *Millimeter Wave Systems and Components*, ARSCL-CR-83008, ITT Research Institute, Chicago, IL, 1983.

Christopher Due and Lauren Peterson, *Optical-Mechanical, Active-Passive Imaging Systems*, Environmental Research Institute of Michigan, Ann Arbor, MI, 1982.

Louis D. Duncan, et al., *EOSAEL 82*, ASL-TR-0122, US Army Atmospheric Sciences Laboratory, White Sands Missile Range, NM, 1982.

Frederick Gebhardt, *Development of Turbulence Effects Models*, Science Applications, Inc., Ann Arbor, MI, 1980.

D. W. Hoock and R. A. Sutherland, *Modeling the Complex Dirty Battlefield*, US Army Atmospheric Sciences Laboratory, White Sands Missile Range, NM, 1985.

Gerald C. Holst and Janon F. Embury, *Design Criteria for Smokes and Obscurants*, ARSCL-TR-82024, US Army Chemical Systems Laboratory, Aberdeen, MD, 1982.

Marvin D. Kays, et al., *Qualitative Description of Obscuration Factors in Central Europe*, ASL Monograph No. 4, US Army Atmospheric Sciences Laboratory, White Sands Missile Range, NM, 1980.

Earl J. McCartney, *Optics of the Atmosphere*, John Wiley & Sons, New York, NY, 1976.

W. E. K. Middleton, *Vision Through the Atmosphere*, University of Toronto Press, Toronto, Canada, 1952.

Bruce Miers, *Geoserm Worldwide Data Base*, US Army Atmospheric Sciences Laboratory, White Sands Missile Range, NM, 1984.

W. R. Lawson, T. W. Cassidy, and J. A. Ratches, "A Search Model", *Proc. IRIS Infrared Imaging Symposium*, Environmental Research Institute of Michigan, Ann Arbor, MI, 1978.

J. M. Lloyd, *Thermal Imaging Systems*, Plenum Press, New York, NY, 1975.

L. P. Obert, J. T. Wood, and C. J. Nash, *Visionics Handbook of EO Sensor Performance, Volume 1 (Natural European Environment)* (U), US Army Night Vision and Electro-Optics Laboratory, Fort Belvoir, VA, 1981 (THIS DOCUMENT IS CLASSIFIED CONFIDENTIAL).

J. A. Ratches, et al., *Night Vision Laboratory Static Performance Model for Thermal Viewing Systems*, ECOM-7043, US Army Night Vision and Electro-Optics Laboratory, Fort Belvoir, VA, 1975.

William Wolfe and George Zissis, Eds., *The Infrared Handbook*, Environmental Research Institute of Michigan, Ann Arbor, MI, 1978.

William L. Wolfe, Ed., *Handbook of Military Infrared Technology*, Office of Naval Research, Washington, DC, 1965.

Combat Environment Obscuration Handbook (Draft), Smoke and Aerosol Working Group, Joint Technical Coordination Group Munition Effectiveness, Aberdeen Proving Ground, MD, 1984.

Electro-Optics Handbook, RCA Corporation, Lancaster, PA, 1974.

RCA Electro-Optics Handbook, RCA Commercial Engineering, Harrison, NJ, 1968.

GLOSSARY

A

Absolute humidity. The ratio of the mass of water vapor present in air to the volume occupied by the mixture of water vapor and air.

Active system. System which uses an illuminator (lamp source, laser, or mmw beam) to detect targets. The signal detected by an active system is the illuminator energy reflected by the target (and/or background).

Aerosol. Colloidal suspension of solid or liquid particles dispersed in a gas.

Aerosol extinction. The atmospheric attenuation of radiation due to scattering and absorption by suspended aerosol particles.

Air temperature. The temperature of the air as measured by a dry-bulb thermometer.

Apparent contrast. The target-to-background contrast seen by an observer or other sensor separated from the target scene by a contrast-degrading medium such as the atmosphere.

Atmospheric pressure, ground level. The force per unit area applied to the ground by the column of air above it.

Atmospheric transmittance. Ratio of received power to emitted power, defined over a specified path length through the atmosphere. Atmospheric transmittance depends on the wavelength of the radiation, the length of the atmospheric path, and the type and concentration of the atmospheric constituents.

Atmospheric window. A spectral band that is characterized by good atmospheric transmittance.

B

Beam rider. A missile for which the guidance system consists of standard reference signals transmitted in a radar beam that enable the missile to sense its location relative to the beam, correct its course, and thereby stay in the beam.

Burn rate. The rate of delivery of munition fill mass into the atmosphere.

C

Classification. The ability to distinguish a target by general type, e.g., as a tracked vehicle instead of a wheeled vehicle.

Clutter. Objects in the background scene that interfere with the ability of an observer to acquire and distinguish targets.

Concentration path length product (CL). The quantity of an obscurant along a line of sight, obtained by integrating the obscurant concentration along the path length.

Contrast. Target radiance minus background radiance divided by background radiance.

Contrast transmittance. The ratio of apparent contrast to inherent contrast. The contrast reduction is caused by light scattered into the sensor field of view by the atmosphere between the sensor and the target.

D

Day sight (direct view optics). Optical systems such as binoculars or day periscopes which only magnify an image. In a day sight, the human eye is the detector.

Detection. The ability to distinguish that an artifact within the field of view is of military interest. For thermal systems, detection may be either **MDT** detection or **MRT** detection.

Dew point. The temperature to which air at a given pressure and water vapor content (absolute humidity) must be cooled for saturation to occur.

E

Extinction. The removal of energy by scattering or absorption from radiation traversing a medium.

F

Field of view. The portion (angle) of the object scene that is included in the displayed imagery of an imaging system.

Fog. A visible aggregate of minute water particles suspended in the atmosphere at or near ground level.

Fog oil smoke. Oil droplet aerosol dispensed by vaporizing vehicle engine diesel fuel or specially supplied fog oil.

G

Geometric optics region. Particle size is large compared to the wavelength of the scattered radiation. Scattering efficiency is about 2.0 for geometric optics scattering.

H

Haze. Naturally occurring atmospheric aerosol, which may include dust particles, salt spray, or industrial pollutants. "Haze" is used to describe atmospheres with visibilities 1-2 km or greater.

Hexachloroethane smoke. A pyrotechnic smoke generated by the burning of the hexachloroethane (HC) composition of aluminum, zinc oxide, and hexachloroethane resulting in a hygroscopic zinc chloride aerosol.

Hygroscopic smoke. Smoke that hydrates by absorbing water from the atmosphere. The extinction coefficient of hygroscopic aerosol particles depends on relative humidity.

I

Identification. The ability to discriminate the exact model of a target, e.g., to distinguish a T-72 from a T-80 tank.

Image intensifier. An imaging device using an electron tube that reproduces on a fluorescent surface an image of a radiation pattern focused on its photosensitive surface. Image intensifiers are used at night to produce an image that is brighter to the eye than the original scene. They respond to 0.4-0.9 μm radiation (second generation) or 0.6-0.9 μm radiation (third generation.)

Index of refraction. The ratio of the speed of light in a vacuum to the speed of light of specified wavelength in a medium.

M

Mass extinction coefficient. A measure of the effectiveness of an obscurant in attenuating radiation.

Mie scattering. Scattering that occurs from particles with radii greater than 1/10 the size of the radiation wavelength, and for which Mie scattering theory must be used to calculate scattering efficiency.

Minimum detectable temperature (MDT). The MDT of a thermal device is the minimum temperature difference between a square (or circular) target and the background necessary for an observer to perceive the target through the thermal imager. It is a function of target angular size and represents the threshold detection capability of the system.

Minimum resolvable contrast (MRC). A parameter used in modeling the performance of image intensifiers, day sights, and the eye. MRC is the apparent contrast required to resolve a target of a given spatial frequency and is presented as a function of spatial frequency in units of cycles mm or cycles mrad.

Minimum resolvable temperature difference (MRT). The central parameter in the modeling of infrared imaging hardware performance. MRT is the minimum temperature difference required between a standard bar type pattern (4-bar, 7:1 aspect ratio) at which a trained observer with normal vision can distinguish the bar pattern as a four-bar pattern. It is plotted as a graph of minimum temperature difference (K or °C) normalized to 300 K versus spatial frequency (cycles mrad) in object space.

Modulation transfer function (MTF). The sine wave spatial frequency amplitude, which is a measure of the spatial frequency response of an imaging system. It is strictly defined as the modulus of the complex Fourier transform of the point spread function of the device.

Molecular extinction. The atmospheric attenuation of radiation due to absorption by or scattering from atmospheric molecules.

Monochromatic radiation. Spectrally narrow radiation (containing energy in a very limited wavelength region).

O

Optical depth. A measure of opacity to visible radiation. Optical depth is the negative of the logarithm of visual transmittance.

P

Particle size distribution. Number density or mass density of (aerosol) particles as a function of particle radius.

Pasquill category. A measure of the rate of vertical spread of an obscurant from the obscurant source. The atmosphere is characterized as unstable (Pasquill Category A or B), neutral (C or D), or unstable (E or F).

Passive system. System that does not use an illuminator as a signal source. Passive systems detect energy emitted by the target and background, or reflected ambient illumination.

Phosphorus smoke. Pyrotechnic smoke formed by burning elemental phosphorus in air, which results in a hygroscopic phosphoric acid aerosol.

R

Radian. Angle subtended by an arc of a circle equal in length to the radius of the circle. One radian equals $(180/\pi)$ deg.

Radiance. The total radiant flux per unit solid angle per unit projected area which emanates from a surface.

Rayleigh scattering. Scattering in which the particle size is small compared to the wavelength of the scattered radiation; Rayleigh scattering efficiency has a $(1/\lambda)^4$ dependence.

Relative humidity. The ratio of the actual water vapor pressure of the air to the water vapor pressure that would be obtained if the air were saturated with water vapor.

Resolvable cycles. The number of cycles which the average observer, using an imaging system, can discriminate 50% of the time under the set of conditions being considered.

S

Scattering. The removal of energy from a beam of radiation traversing a medium by reflection and refraction.

Scattering efficiency. The ratio of the effective scattering cross section of a particle to its geometric cross section.

Sky-to-ground ratio. The ratio of the radiance of the horizon sky to the inherent radiance of the background. Sky-to-ground ratio will depend on viewing angle, sun or moon angle, and environmental and atmospheric conditions.

Spatial frequency. The frequency (in cycles/mrad or cycles/mm) of an evenly spaced bar pattern or sinusoidal target pattern. One cycle is equivalent to two TV lines or one line pair.

T

Turbulence, mechanical. Local variations in wind speed and direction caused by variations in atmospheric temperature.

Turbulence, optical. Time-varying local fluctuations in the index of refraction of the atmosphere caused by localized differences in air temperature.

V

Visibility. The distance at which a human observer can just detect a high contrast ($C_o = 1$) target. Atmospheric transmittance is proportional to the logarithm of the visibility.

Volume extinction coefficient. A measure of the effectiveness of an obscurant. Volume extinction coefficient $\gamma(\lambda)$ is defined as

$$\gamma(\lambda) = \frac{1}{R}\frac{dI_s(\lambda,r)}{I_s(\lambda,r)}, \text{ km}^{-1}$$

where

R = path length, km

$dL(\lambda, r)$ = change in spectral radiance, W (m²sr)

$L(\lambda, r)$ = spectral radiance, W (m²sr)

λ = wavelength, μm.

W

Wire-guided missile. Missile that receives guidance signals through a wire connected from missile to launcher.

Y

Yield factor. Ratio of mass of obscurant aerosol to mass of obscurant fill material. Yield factor is used to account for the growth of hygroscopic aerosol particles in the atmosphere by absorption of atmospheric water vapor.

APPENDIX A
ATMOSPHERIC TRANSMITTANCE CALCULATION SUMMARY

The equations or table references required to determine transmittance are summarized in this appendix. The locations of the required data in the text are referenced by paragraph. Tables are also referenced if the data are tabulated.

A-0 LIST OF SYMBOLS

a,b = rain extinction parameters, dimensionless

CL = concentration path length product of obscurant, g/m^2

c,d = snow extinction parameters, dimensionless

R = path length, km

r = rain rate, mm/h

r_s = rain equivalent snow rate, mm/h

$T(\lambda)$ = transmittance, dimensionless

$T_a(\lambda)$ = atmospheric transmittance considering only aerosol extinction, dimensionless

$T_d(\lambda)$ = transmittance through HE dust or vehicular dust, dimensionless

$T_d'(\lambda)$ = transmittance through lofted snow, dimensionless

$T_m(\lambda)$ = atmospheric transmittance considering only molecular extinction, dimensionless

$T_p(\lambda)$ = atmospheric transmittance considering only precipitation, dimensionless

$T_s(\lambda)$ = transmittance through smoke, dimensionless

V = visibility, km

$\alpha(\lambda)$ = obscurant mass extinction coefficient, m^2/g

$\alpha_d(\lambda)$ = dust mass extinction coefficient for any wavelength λ, m^2/g

$\alpha_s(\lambda)$ = smoke mass extinction coefficient for any wavelength λ, m^2/g

$\gamma_a(\lambda)$ = aerosol volume extinction coefficient for any wavelength λ, km^{-1}

$\gamma_m(\lambda)$ = molecular volume extinction coefficient for any wavelength λ, km^{-1}

$\gamma_p(\lambda)$ = precipitation volume extinction coefficient for any wavelength λ, km^{-1}

$\gamma_{ps}(vis, near\ IR)$ = precipitation volume extinction coefficient for visible and near IR, km^{-1}

$\gamma_{ps}(mmw)$ = precipitation volume extinction coefficient for mmw, km^{-1}

A-1 TRANSMITTANCE CALCULATION SUMMARY

The transmittance $T(\lambda)$ is the product of the atmospheric molecular transmittance term $T_m(\lambda)$, the atmospheric aerosol extinction term $T_a(\lambda)$ or precipitation term $T_p(\lambda)$, and the dust transmittance $T_d(\lambda)$ or smoke transmittance $T_s(\lambda)$. In the absence of precipitation

$$T(\lambda) = T_m(\lambda)T_a(\lambda)T_s(\lambda)T_d(\lambda), \text{dimensionless.} \quad (A-1)$$

If it is raining or snowing,

$$T(\lambda) = T_m(\lambda)T_p(\lambda)T_s(\lambda)T_d(\lambda), \text{dimensionless.} \quad (A-2)$$

If there is no smoke,

$$T_s(\lambda) = 1, \text{dimensionless.}$$

If there is no dust,

$$T_d(\lambda) = 1, \text{dimensionless.}$$

A-1.1 MOLECULAR TRANSMITTANCE $T_m(\lambda)$

For visible, near IR, laser, and mmw wavelengths,

$$T_m(\lambda) = e^{-\gamma_m(\lambda)R}, \text{dimensionless} \quad (A-3)$$

where

R = pathlength, km

$\gamma_m(\lambda)$ = molecular volume extinction coefficient for any wavelength λ, km^{-1}.

References for molecular volume extinction coefficient $\gamma_m(\lambda)$ are

Visible (0.4-0.7μm)	par. 3-2.1.1
Near IR (0.7-1.1μm)	par. 3-2.1.2
Nd:YAG laser (1.06μm)	par. 3-2.1.2
CO$_2$ laser (10.591μm)	par. 3-2.1.4, Table 3-3
mmw (35 GHz, 94 GHz)	par. 3-2.1.4, Table 3-3.

For broadband thermal calculations, $T_m(\lambda)$ is tabulated. References for thermal transmittance $T_m(\lambda)$ are

Mid IR (3-5μm)	par. 3-2.1.3, Table 3-1
Far IR (8-12μm)	par. 3-2.1.3, Table 3-2.

A-1.2 AEROSOL TRANSMITTANCE $T_a(\lambda)$

The aerosol transmittance term $T_a(\lambda)$ through haze, fog, or clouds is

$$T_a(\lambda) = e^{-\gamma_a(\lambda)R}, \text{ dimensionless} \quad (A\text{-}4)$$

where

$\gamma_a(\lambda) =$ aerosol extinction coefficient for any wavelength λ, km^{-1}.

References for aerosol volume extinction coefficient $\gamma_a(\lambda)$ are

Visible (0.4-0.7μm)	par. 3-2.2.1
Near IR (0.7-1.1μm)	par. 3-2.2.2
Mid IR (3-5μm)	par. 3-2.2.3
Far IR (8-12μm)	par. 3-2.2.3
Nd:YAG laser (1.06μm)	par. 3-2.2.2
CO$_2$ laser (10.59μm)	par. 3-2.2.3
mmw (35 GHz, 94 GHz)	par. 3-2.2.4.

A-1.3 TRANSMITTANCE THROUGH PRECIPITATION $T_p(\lambda)$

The precipitation transmittance term $T_p(\lambda)$ is

$$T_p(\lambda) = e^{-\gamma_p(\lambda)R}, \text{ dimensionless} \quad (A\text{-}5)$$

where

$\gamma_p(\lambda) =$ precipitation volume extinction coefficient for any wavelength λ, km^{-1}.

A-1.3.1 Rain

The precipitation volume extinction coefficient $\gamma_p(\lambda)$ for rain depends on the rain rate r and the dimensionless constants a and b:

$$\gamma_p(\lambda) = ar^b, \text{ km}^{-1} \quad (A\text{-}6)$$

where

$r =$ rain rate, mm/h.

References for values of a and b are

Visible (0.4-0.7μm)	par. 3-2.3
Near IR (0.7-1.1μm)	par. 3-2.3
Mid IR (3-5μm)	par. 3-2.3
Far IR (8-12μm)	par. 3.2.3
Nd:YAG laser (1.06μm)	par. 3-2.3
CO$_2$ laser (10.59μm)	par. 3-2.3
mmw (35 GHz, 94 GHz)	par. 3-2.3.

A-1.3.2 Snow*

A-1.3.2.1 Visible, Near IR, Thermal, and Laser Wavelengths

In the visible, near IR and thermal bands, and for lasers, the precipitation volume extinction coefficient for snow γ_{ps} (vis, near IR) depends on visibility:

$$\gamma_{ps}(\text{vis, near IR}) = 3.912/V, \text{km}^{-1} \quad (A\text{-}7)$$

where

$V =$ visibility, km.

A-1.3.2.2 Millimeter Wavelengths

Th mmw precipitation volume extinction coefficient for snow γ_{ps}(mmw) depends on rain equivalent snow-rate r_s and dimensionless constants c and d:

$$\gamma_{ps}(\text{mmw}) = cr_s^d, \text{ km}^{-1} \quad (A\text{-}8)$$

where

$r_s =$ rain equivalent snow rate, mm/h.

Reference for values of c and d is

mmw(35 GHz, 94GHz)	par. 3-2.4.

A-1.4 DUST TRANSMITTANCE TERM $T_d(\lambda)$

The dust transmittance term $T_d(\lambda)$ is

$$T_d(\lambda) = e^{-\alpha_d(\lambda)CL}, \text{ dimensionless} \quad (A\text{-}9)$$

where

$\alpha_d(\lambda) =$ dust mass extinction coefficient for any wavelength λ, m^2/g

$CL =$ concentration path length product of obscurant, g/m^2.

References for values of $\alpha_d(\lambda)$ are

Naturally occuring dust (all wavelengths)	par. 3-2.5
Vehicular dust (all wavelengths)	par. 4-5
Helicopter-lofted dust (all wavelengths)	par. 4-5.2
Munition-generated dust (all wavelengths)	par. 4-3.1.

*Helicopter-lofted snow is treated in pars. 4-5 and 4-5.2.

References for representative values of CL are

Naturally occurring dust	par. 3-2.5
Vehicular dust	pars. 4-5.1, 4-7.3.
Helicopter-lofted dust	par. 4-5.2
Munition-generated dust	par. 4-7.1.

References for values of $\alpha_s(\lambda)$ are

Fog oil smoke (all wavelengths)	par. 4-2
HC smoke (all wavelengths)	par. 4-2, 4-2.2
Phosphorus smoke (all wavelengths)	par. 4-2, 4-2.1
Fire products (all wavelengths)	par. 4-6.1.

A-1.5 SMOKE TRANSMITTANCE TERM $T_s(\lambda)$

The smoke transmittance term $T_s(\lambda)$ is

$$T_s(\lambda) = e^{-\alpha(\lambda)CL}, \text{ dimensionless } (A\text{-}10)$$

where

$\alpha_s(\lambda)$ = smoke mass extinction coefficient for any wavelength λ, m^2/g.

References for values of CL are

Fog oil smoke	par. 4-7.2
HC smoke	par. 4-7.2
Phosphorus smoke	par. 4-7.2
Fire products	par. 4-6.1.

APPENDIX B
RELATIONSHIP OF RELATIVE HUMIDITY, ABSOLUTE HUMIDITY, AND DEW POINT

The water vapor content of the atmosphere may be given as relative humidity RH at temperature T, absolute humidity ρ, or dew point T_d. The equations in Chapter 3 of this handbook require either absolute humidity or relative humidity. The equations given in this appendix are empirical relationships for converting between absolute humidity and relative humidity or for determining either absolute humidity or relative humidity from dew point temperature.

B-O LIST OF SYMBOLS

RH = relative humidity (decimal), dimensionless

T = temperature, K

T_d = dew point temperature, K

ρ = absolute humidity, g/m³

B-1 EQUATIONS

1. Absolute humidity ρ from ambient temperature T and relative humidity RH is

$$\rho = \frac{1285\,RH}{T} \exp\left[5412\left(\frac{1}{273} - \frac{1}{T}\right)\right],\ g/m^3.$$
(B-1)

where

T = temperature, K

RH = relative humidity (decimal), dimensionless.

2. Absolute humidity ρ from dew point temperature T_d is

$$\rho = \frac{1285}{T} \exp\left[5412\left(\frac{1}{273} - \frac{1}{T_d}\right)\right],\ g/m^3.$$
(B-2)

3. Relative humidity (decimal) RH at temperature T from absolute humidity is

$$RH = \frac{\rho T}{1285} \exp\left[-5412\left(\frac{1}{273} - \frac{1}{T}\right)\right],$$
dimensionless. (B-3)

4. Relative humidity RH (decimal) at temperature T from dew point temperature T_d and ambient temperature T is

$$RH = \exp\left[5412\left(\frac{1}{T} - \frac{1}{T_d}\right)\right],\ \text{dimensionless.}$$
(B-4)

INDEX

INDEX cont'd

INSTRUCTIONS: In a continuing e⸱⸱rt to make our standardization documents better, the DoD provides this form for use in submitting comments and suggestions for improvements. All users of military standardization documents are invited to provide suggestions. This form may be detached, folded along the lines indicated, taped along the loose edge (DO NOT STAPLE), and mailed. In block 5, be as specific as possible about particular problem areas such as wording which required interpretation, was too rigid, restrictive, loose, ambiguous, or was incompatible, and give proposed wording changes which would alleviate the problems. Enter in block 6 any remarks not related to a specific paragraph of the document. If block 7 is filled out, an acknowledgement will be mailed to you within 30 days to let you know that your comments were received and are being considered.

NOTE: This form may not be used to request copies of documents, nor to request waivers, deviations, or clarification of specification requirements on current contracts. Comments submitted on this form do not constitute or imply authorization to waive any portion of the referenced document(s) or to amend contractual requirements.

(Fold along this line)

(Fold along this line)

DEPARTMENT OF THE ARMY

OFFICIAL BUSINESS
PENALTY FOR PRIVATE USE $300

BUSINESS REPLY MAIL
FIRST CLASS   PERMIT NO 12062   WASHINGTON D C

POSTAGE WILL BE PAID BY THE DEPARTMENT OF THE ARMY

Commander/Director
US Army Laboratory Command
Atmospheric Sciences Laboratory
ATTN: SLCAS-AR-A
White Sands Missile Range, NM 88002-5501

NO POSTAGE
NECESSARY
IF MAILED
IN THE
UNITED STATES

STANDARDIZATION DOCUMENT IMPROVEMENT PROPOSAL
(See Instructions – Reverse Side)

1. DOCUMENT NUMBER DOD-HDBK-178(ER)	2. DOCUMENT TITLE Quantitative Description of Obscuration Factors for Electro-Optical and Millimeter Wave Systems

3a. NAME OF SUBMITTING ORGANIZATION	4. TYPE OF ORGANIZATION (Mark one) ☐ VENDOR ☐ USER
b. ADDRESS (Street, City, State, ZIP Code)	☐ MANUFACTURER ☐ OTHER (Specify): _____

5. PROBLEM AREAS

a. Paragraph Number and Wording:

b. Recommended Wording:

c. Reason/Rationale for Recommendation:

6. REMARKS

7a. NAME OF SUBMITTER (Last, First, MI) – Optional	b. WORK TELEPHONE NUMBER (Include Area Code) – Optional
c. MAILING ADDRESS (Street, City, State, ZIP Code) – Optional	8. DATE OF SUBMISSION (YYMMDD)

DD FORM 1426 83 MAR   PREVIOUS EDITION IS OBSOLETE